

UNIVERSIDADE DE LISBOA
FACULDADE DE CIÊNCIAS



**Ciências
ULisboa**

**Impact of climate change and contamination in the oxidative stress response of
marine organisms**

“ Documento Definitivo ”

Doutoramento em Ciências do Mar

Ana Rita José Lopes

Tese orientada por:

Professor Doutor Rui Afonso Bairrão da Rosa

Professor Doutor Mário Emanuel Campos de Sousa Diniz

Documento especialmente elaborado para a obtenção do grau de doutor

2018



**Ciências
ULisboa**

**Impact of climate change and contamination in the oxidative stress response of
marine organisms**

Doutoramento em Ciências do Mar

Ana Rita José Lopes

Tese orientada por:

Professor Doutor Rui Afonso Bairrão da Rosa

Professor Doutor Mário Emanuel Campos de Sousa Diniz

Júri:

Presidente:

- Doutora Maria Manuela Coelho, Professora Catedrática e Presidente do Departamento de Biologia Animal, Faculdade de Ciências da Universidade de Lisboa

Vogais:

- Doutora Maria Helena Costa, Professora Catedrática, Faculdade de Ciências e Tecnologias da Universidade Nova de Lisboa
- Doutora Rosa de Fátima Lopes de Freitas, Investigadora Auxiliar, Departamento de Biologia Animal, Universidade de Aveiro
- Doutor António Manuel Barros Marques, Investigador Principal, Instituto Português do Mar e Atmosfera - IPMA
- Doutor Carlos Alexandre Sarabando Gravto, Professor Auxiliar, Faculdade de Ciências da Universidade de Lisboa
- Doutor Rui Afonso Bairrão da Rosa, Investigador FCT de nível de desenvolvimento, Faculdade de Ciências da Universidade de Lisboa (orientador)

Documento especialmente elaborado para a obtenção do grau de doutor

Fundação para a Ciência e Tecnologia (SFRH/BD/97070/2013)

“The Sea, once it casts its spell, holds one in its net of wonder forever”

- Jacques Yves Cousteau

*“Everybody is a genius. But if you judge a fish by its ability to climb a tree,
it will live its whole life believing that it is stupid.”*

- Albert Einstein

“Even Alice had to fall before she found her Wonderland”

- Unknown

*“A vida é curta demais para se acordar com arrependimentos.
Ama as pessoas que te tratam bem.
Esquece aquelas que não.
A vida coloca cada um no seu lugar. Tudo vai e vem por uma razão.
Se tens uma segunda oportunidade, agarra-a.
Ninguém disse que a vida seria fácil, só prometeu que iria valer a pena.
Vive, deixa viver e sê feliz.”*

- António Feio

Acknowledgments

“Hoje” sinto-me uma pessoa feliz, completa, mas sobretudo sortuda. Tenho do meu lado os melhores do mundo e sem os quais, cada um do seu jeito, esta etapa não teria sido vivida da mesma forma e intensidade. Mas mais importante ainda é saber que esta etapa também vocês a tomaram como vossa, sentindo as minhas frustrações e sorrindo a cada conquista. Por isso o meu maior obrigado a todos vós!

Quero agradecer em primeiro lugar às duas pessoas que me acompanharam neste meu percurso e me ajudaram a chegar onde estou hoje, os meus orientadores.

Obrigada Rui por me teres acolhido no laboratório em 2011, altura em que comecei o meu mestrado e esta aventura na minha segunda casa. Obrigada por me teres tornado na pessoa que sou hoje, pois nem só de sorrisos se faz o mundo. A Marisa Liz tem uma música que sumariza o meu sentimento no fim desta etapa *“Lembra-me das minhas fraquezas. E eu conto-te como as tornei nas minhas certezas”*. Hoje sei reconhecer a ter a capacidade de te agradecer por me pões à prova, pois cheguei aqui, consegui, cresci e tornei-me numa melhor profissional. Não costumo prezar um amigo pela forma como está sempre de acordo comigo, mas sim pela capacidade de me fazer ver onde errei. Por isso o meu mais sincero obrigada.

Ao Mário, obrigada por teres aceite o convite do Rui também em 2011 e me teres vindo a acompanhar desde aí. Obrigada por seres um professor e um colega de bancada excepcional, por ouvires as minhas frustrações e teres sempre uma palavra amiga de volta. Obrigada pela tua paciência e sobretudo pela tua calma e paz interior que sempre me ajudaram nos tempos mais difíceis. Nunca irei esquecer as conversas de laboratório, os risos e a amizade que se criou ao longo destes anos.

Agradeço também a Fundação para a Ciência e Tecnologia (FCT) pelo financiamento da minha bolsa (SFRH/BD/97070/2013) e também pelos projectos PTDC/AAG-GLO/1926/2014 e PTDC/AAG-GLO/3795/2014, liderados pelos Doutores Rui Rosa e Tiago Grilo, respectivamente, que financiaram o material necessário para o desenvolvimento desta dissertação.

Como não podia deixar de ser, quero agradecer à minha família do Laboratório Marítimo da Guia. Aos de passagem – Luana Mincarelli, Marta Morais, Lidia García, Meri Bilan, Eve

| Acknowledgments

Otjacques – e aos de sempre – Tiago Repolho, Marta Pimentel, Catarina Frazão, Eduardo Sampaio, Catarina Santos, José Paula, Miguel Baptista, Maria Rita, Francisco Carvalho, Francisco Borges, Érica Moura, Cláudia Pereira, Ricardo Cyrne, Inês Rosa, Gisela Dionísio, Ana Couto, Sofia Francisco, Vasco Pissara, Ricardo Lopes, Maria Paulo, Filipa Faleiro, Joana Portugal, Eduarda Pinto, Ana Luísa Maulvault, Patrícia Anacleto, Carolina Camacho, Vera Barbosa, Marta Santos.

Quero também agradecer aos de para sempre.

Em especial à Kuka, por me acompanhar nesta fase, foram quatro anos de luta, mas conseguimos, chegamos à nossa meta, parabéns para nós. Obrigada por toda a tua amizade, por lado-a-lado teres vivido toda esta fase com a mesma intensidade que eu. Foi extremamente reconfortante ter a minha pessoa, a minha colega de secretária a viver esta fase ao mesmo tempo que eu e contigo poder partilhar todas as frustrações e alegrias que só nós compreendíamos na altura. Obrigada!

À minha Cátia e ao meu Grilo. *“What is a friend? A single soul dwelling in two bodies”* (Aristotle). Neste caso três, obrigada por serem das pessoas mais fantásticas e fascinantes que conheço e tenho na minha vida, é um orgulho ser vossa amiga. Foram vocês uns dos maiores suportes nesta etapa, sem vocês e sem o vosso apoio incondicional sem dúvida que teria sido um percurso sem graça. Não consigo expressar o quanto são importantes para mim, quer a nível profissional quer a nível pessoal, são sem sombra de dúvida as minhas pessoas, aquelas que quero levar para o resto da minha vida. Aquelas que me irão perguntar há quanto tempo nos conhecemos e irei responder “it’s been 84 years” e “this is this”, porque é o que é, e é para sempre.

À minha espanhola preferida, a minha Sara, que sempre me conseguiu enviar todo o seu amor e amizade, em todas as alturas, que veio para ficar. Obrigada por me mostrares o teu lado doce, divertido e espontâneo. Obrigada por todos os sorrisos e abraços partilhados, nas despedidas e nas chegadas. Se um dia Madrid não vier a Portugal, Portugal vai a Madrid.

À minha família do 2765 – Ina, Vítor, Daniel, Anaísa, Flecha. É um privilégio enorme ter-vos na minha vida. Obrigada por me terem acolhido tão bem no vosso grupo e por me acompanharem nesta luta, por me questionarem sobre o que faço, mesmo quando não percebiam tão bem o que é que faço. Por me retirarem de casa nos meus dias loucos e me fazerem lembrar que existe mais do que trabalho e que quando se tem uma família e amigos assim como vocês o equilíbrio entre trabalho e amizade é fácil e tudo se torna melhor.

Aos que entraram na minha vida em momentos tão diferentes, mas que continuam e que não imaginam o quanto me mudaram. À minha Daniela, à minha Joana e ao meu André, obrigada. Os tempos de Peniche não voltam, mas a cada dia que passa construímos histórias e aventuras novas, que vou guardar sempre no meu coração. Ao Ricardo Durão, obrigada por teres entrado na minha vida numa das piores fases possíveis, sem fazeres a menor ideia ajudaste-me mais do que alguma vez imagínaste. Obrigada por seres o meu parceiro de treino, mas acima de tudo por seres esse amigo com um coração do tamanho do mundo, um amigo que vou preservar. À Lucy, Nuno, Vicente, Dora, Evin, Lena, Diogo, Martim por serem absolutamente únicos. É tão bom chegar à minha terra natal e ser inundada do vosso amor!

Quero agradecer aos meus tios de coração Arminda e Rui e às minhas pessoas Joana e Luis, a família de coração é aquela que temos o privilégio de escolher e eu não podia ter feito melhor escolha. Obrigada pelos jantares de sábado, por todas as gargalhadas e momentos. Obrigada Joana e Luis por partilharam comigo o vosso mundo, um mundo chamado Laura, o baguinho que se tornou na minha princesa. É um orgulho ser a “Miinha Ita”.

À minha Madrinha Lena, ao Tio Rui, à Cristina, à Maria e à Constança por todo o vosso apoio em todas as fases da minha vida. Por me mostrarem que há laços que não se quebram e por me fazerem ver que há palavras que não são precisas ser ditas para ser verdade. Também gosto muito de vocês e tenho muito orgulho em vocês.

À família que ganhei quando conheci o amor da minha vida. Obrigada Ana, Natacha e Carlos por todo o carinho e apoio. Por todos os mimos e por todos os jantares que reconfortaram o coração. Não podia estar mais feliz com a família que me calhou.

“Alice: How long is forever?”

White Rabbit: Sometimes, just one second.”

— Lewis Carroll, Alice in Wonderland

Por fim quero agradecer aqueles sem os quais não consigo passar um segundo na minha vida.

Em especial ao amor da minha vida. Obrigada Alex por seres a pessoa mais cativante, carinhosa e generosa do mundo e por ser eu a privilegiada da tua escolha. Obrigada pela tua compreensão, pela tua ajuda, mas acima de tudo por me fazeres crescer e querer ser uma pessoa melhor. Quero também agradecer ao meu Lucky - “Until one has loved an animal a part of one’s soul remains

| Acknowledgments

unawakened” (Anatole France) - por todos os mimos e por toda a companhia ao longo destes 5 anos. Vocês elevam a palavra família a um novo nível. Obrigada!

Por fim, quero agradecer aos mais importantes. Aos que me conhecem desde o dia zero. Ao enorme pilar familiar que tenho. Obrigada pai e mãe por fazerem de mim a pessoa que sou hoje, é a vocês que devo tudo. Obrigada por sempre me apoiarem nos momentos difíceis, e por mostrarem tanto orgulho nos momentos felizes. Obrigada por me ensinarem a lutar pelo que quero, contra tudo e todos, a levantar a cabeça e andar com orgulho. Quero também agradecer aos meus avós Luísa e Fernando. Obrigada pelo orgulho estampado nos vossos olhos e por todo o amor que sempre tiveram por mim. Quero agradecer em especial a ti avô, por seres um exemplo de garra, perseverança e luta, por enfrentares uma das piores batalhas de sempre com esperança no coração e por nunca teres desistido, nem nos dias mais difíceis. Ser tua neta é um dos maiores privilégios da minha vida.

Quero também agradecer em avanço a todas as pessoas que irão um dia ler esta dissertação, pois no fim do dia é com vocês que o meu “trabalho” está completo.

“Sharing knowledge is the most fundamental act of friendship.

Because it is a way you can give something without losing something”

- Richard Stallman

Contents

Abstract	1
Resumo	3
Resumo Alargado	5
List of Articles	9
List of Abbreviations and Units	11
List of Figures	15
List of Tables	21
Chapter 1. General Introduction	23
Global Climate Change – A high CO ₂ World.....	23
Ocean under High CO ₂	25
Ocean Warming.....	28
Ocean Acidification.....	30
Contamination under Climate change.....	31
Heavy metals - the mercury case.....	32
Biological responses.....	34
Oxidative stress under climate change.....	35
Protective mechanisms.....	36
Cellular damage	40
Conventional biomarkers and marine tree of life.....	41
General Objectives.....	44
References	47
Part One. Within- and Trans-Generational Effects Under Ocean Acidification	67
Chapter 2. Absence of cellular damage in tropical newly-hatched sharks (<i>Chiloscyllium plagiosum</i>) under ocean acidification conditions.....	69
Abstract	69
Materials and Methods	72
Results.....	79
Discussion	82
Acknowledgments.....	85
Competing of interests.....	85
Funding	85
References	86

Chapter 3. Transgenerational exposure to ocean acidification induces biochemical distress in a keystone amphipod species (<i>Gammarus locusta</i>)	93
Abstract	93
Material and methods	96
Results	103
Discussion.....	107
Acknowledgements.....	110
Conflict of Interest	110
References	111
Part Two. ¹¹⁹ Biochemical Responses Under a Multiple Stressor Environment	119
Chapter 4. Physiological resilience of a temperate soft coral to ocean warming and acidification	121
Abstract	121
Materials and Methods	124
Results	128
Acknowledgments.....	132
Competing of interests.....	132
References	133
Chapter 5. Encased in troubled waters: Oxidative damage in shark embryos under ocean warming and the protective role of the capsule against contamination.....	141
Abstract	141
Material and methods	144
Results	150
Discussion	156
Acknowledgments.....	160
Funding	160
Conflict of Interest	160
References.....	161
Chapter 6. Ocean acidification dampens physiological stress response to warming and contamination in a commercially-important fish (<i>Argyrosomus regius</i>).....	169
Abstract	169
Material and Methods.....	172
Results	179
Discussion	189
Conclusions	193
Acknowledgments.....	194
References	195
Chapter 7. General Discussion.....	205

Biochemical responses under a multi-stressor environment.....	205
Biochemical responses across taxa	209
Within- and trans-generational biochemical responses	211
Future Directions	212
References	214
Supplemental Material	219

Abstract

Atmospheric carbon dioxide (CO₂) levels are increasing at an unprecedented rate, changing the carbonate chemistry (in a process known as ocean acidification) and temperature of the world's ocean. Moreover, the simultaneous occurrence of highly toxic and persistent contaminants, such as mercury, will play a key role in further shaping the ecophysiology of marine organisms. Thus, the main goal of the present dissertation was to undertake the first comprehensive and comparative analysis of the biochemical strategies, namely antioxidant defense (both enzymatic and non-enzymatic antioxidants) and protein repair and removal mechanisms, of several marine organisms – from invertebrate (*Veretillum cynomorium* and *Gammarus locusta*) to vertebrate species (*Argyrosomus regius*, *Chiloscyllium plagiosum* and *Scyliorhinus canicula*) – encompassing different life-stages and life-strategies to the predicted climate-mediated changes. The findings provided in the present dissertation proved that organisms' responses were mostly underpinned by temperature (increasing lipid, protein and nucleic acid damage), that also culminated into increased mercury bioaccumulation and toxicity, while ocean acidification as a sole stressor usually played a minor role in defining species vulnerability (i.e. responsible for increased oxidative damage in the marine calcifying organisms *G. locusta*). Nonetheless when co-occurring with warming and contamination scenarios, acidification was usually responsible for the reduction of heavy metal accumulation and toxicity, as well as decreased warming and contamination-elicited oxidative stress. Additionally, organisms' responses were species-specific, and organisms that usually occupy more variable environments (e.g. daily changes in abiotic conditions) usually displayed greater responses towards environmental change than organisms inhabiting more stable environments. Furthermore, and assuming the relevance of transgenerational effects, it seems that the negative effects of OA are potentially being inherited by the offspring's, compromising the efficiency of future generations to endure the upcoming conditions.

Key-words: Ocean acidification, Warming, Mercury contamination, Biochemical defense mechanisms, Oxidative stress

Resumo

Os níveis de dióxido de carbono na atmosfera têm vindo a aumentar drasticamente, alterando a temperatura e a química dos oceanos, num processo designado de acidificação dos oceanos. Adicionalmente, a ocorrência simultânea de contaminantes tóxicos, tais como o mercúrio, irá desempenhar um papel fundamental na resposta fisiológicas dos organismos marinhos. Desta forma, o objetivo principal da presente dissertação foi o de realizar uma análise comparativa dos mecanismos de defesa (antioxidantes e mecanismos de reparação/eliminação de proteínas) em organismos marinhos – invertebrados (*Veretillum cynomorium*, *Gammarus locusta*) e vertebrados (*Argyrosomus regius*, *Chiloscyllium plagiosum*, *Scyliorhinus canicula*) - abrangendo diferentes estágios e estratégias de vida em relação às alterações ambientais globais previstas para o final deste século. Os resultados apresentados na presente dissertação provaram que a resposta dos organismos foi principalmente afetada pelo aumento da temperatura dos oceanos (traduzindo-se num aumento de dano lipídico, proteico e de DNA), culminando também numa maior bioacumulação e toxicidade do mercúrio, enquanto a acidificação dos oceanos, geralmente desempenhou um papel menos relevante relativamente à vulnerabilidade das espécies (sendo apenas responsável pelo aumento de dano oxidativo em organismos calcificadores, como foi o caso do *G. locusta*). No entanto, durante a exposição simultânea de fatores, a acidificação foi responsável pela redução da toxicidade e acumulação de metais pesados, bem como pela diminuição do stress oxidativo causado pelo aquecimento e contaminação do oceano. Por fim, a resposta dos organismos varia de espécies para espécie, e geralmente organismos que habitam em ambientes mais variáveis – mudanças diárias nas condições abióticas – conseguem responder de forma mais positiva às alterações climáticas que organismos que habitam ambientes mais estáveis. Além disso, e tendo em conta os efeitos parentais em resposta às alterações do oceano, parece que os efeitos negativos da acidificação dos oceanos irão potencialmente ser herdados pelos descendentes, comprometendo desta forma a sobrevivência das gerações futuras.

Palavras-chave: Acidificação dos oceanos, Aquecimento dos oceanos, Contaminação, Mecanismos de defesa, Stress oxidativo

Resumo Alargado

Desde a Revolução Industrial os níveis dióxido de carbono (CO₂) atmosférico têm vindo a aumentar, atingindo pela primeira vez na história da humanidade valores consistentemente acima dos 400 ppm. Para além disso, é esperado que as concentrações atmosféricas de CO₂ cheguem aos 1000 ppm até ao final deste século. Sendo um dos principais gases do efeito de estufa, este incremento – cerca de 80% nos últimos dois séculos – tem também intensificado a temperatura atmosférica e consequentemente o aumento da temperatura dos oceanos (i.e. 90% da temperatura atmosférica é absorvida pelo oceano). Desta forma, para a temperatura média da superfície dos oceanos, que tem vindo a aumentar a uma taxa de 0.1 °C por década, prevê-se um aquecimento adicional de 1–4 °C até 2100. Considerando que os oceanos são um dos maiores reservatórios naturais de CO₂ e que absorvem cerca de um terço das emissões antropogénicas, é esperado que a dissolução do CO₂ na água do mar leve ao aumento da quantidade de iões hidrogénio na água, que por sua vez irão reduzir o seu pH num processo designado de acidificação dos oceanos. Adicionalmente, esta alteração na química da água do mar irá também diminuir a concentração e saturação de iões carbonato de cálcio causando um impacto adicional sobretudo para espécies que sintetizam um exosqueleto calcário (i.e. corais, moluscos, crustáceos, etc). Aliado a estes fatores, a ocorrência simultânea de contaminantes tóxicos e extremamente persistentes, tais como metais pesados como o mercúrio, também irá desempenhar um papel fundamental na resposta fisiológicas dos organismos marinhos. Sendo compostos não degradáveis, os metais pesados são facilmente acumulados nos sedimentos marinhos ou em organismos marinhos, entrando na teia alimentar – bioacumulação – sendo transferidos para níveis tróficos mais elevados – biomagnificação.

É espetável que as futuras alterações climáticas afetem os vários níveis de organização biológica dos organismos marinhos – desde o nível moléculas ao organismo. Contudo, a crescente informação relacionada com este tópico tem deixado a componente molecular um pouco mais aquém. Nomeadamente no que diz respeito aos mecanismos de resposta dos organismos marinhos ao aumento das espécies reactivas ao oxigénio (ROS) que é esperado ocorrer quando expostos às condições supramencionadas. Os ROS são naturalmente formados durante os processos metabólicos (i.e. respiração e fotossíntese), mais concretamente durante o processo de redução do oxigénio para a produção de energia na cadeia de transporte de eletrões. Deste

processo resultam intermediários extremamente reativos (i.e. ROS) tais como o ião superóxido (O_2^-), peróxido de hidrogénio (H_2O_2) e o radical hidroxilo (HO^\bullet), com uma elevada capacidade de causar danos irreversíveis nos lípidos, proteínas e DNA dos organismos marinhos. Contudo, e em condições normais os organismos marinhos exibem mecanismos de defesa contra as ROS, tais como compostos enzimáticos (e.g. superóxido dismutase, catalase, glutathione peroxidase, etc) e não enzimáticos (e.g. vitaminas, ácido úrico e ascórbico, etc). Adicionalmente podem também exibir uma resposta secundária sustentada pela produção de proteínas de choque térmico (HSP), cujo papel principal é o de garantir a conformação e função proteica.

Desta forma o principal objetivo da presente dissertação foi o de integrar, pela primeira vez, uma análise comparativa das estratégias bioquímicas, incluindo os mecanismos de defesa antioxidante (enzimáticos e não enzimáticos) e de reparação/eliminação de proteínas dos organismos marinhos, abrangendo espécies invertebradas (*Veretillum cynomorium*, *Gammarus locusta*) e vertebradas (*Argyrosomus regius*, *Chiloscyllium plagiosum*, *Scyliorhinus canicula*), bem como diferentes estágios e estratégias de vida em relação às alterações climáticas esperadas até ao fim deste século. Assim, a presente dissertação foi dividida em duas partes: Parte 1 – com o objetivo de entender as defesas bioquímicas utilizadas pelos organismos marinhos face à acidificação dos oceanos, quer numa só geração quer a nível transgeracional (Capítulos 2 e 3, respectivamente); e a Parte 2 – onde se pretendeu fazer uma abordagem mais holística do sinergismo entre os diferentes fatores (i.e. aquecimento e/ou acidificação do oceano, e a exposição simultânea à contaminação por mercúrio (orgânico e inorgânico), Capítulos 4-6).

Os resultados apresentados na presente dissertação provaram que a resposta dos organismos marinhos foi principalmente estimulada pelo aumento da temperatura dos oceanos o que se traduziu num aumento de dano dos lípidos, proteínas e de DNA, resultando também num maior aumento da concentração de mercúrio nos tecidos dos organismos marinhos [especialmente no fígado (caso do metilmercúrio) e nas brânquias (caso do cloreto de mercúrio)], bem como numa maior toxicidade, especialmente do mercúrio inorgânico, que se traduziu numa elevada taxa de mortalidade em embriões do tubarão *S. canicula*. Relativamente à acidificação dos oceanos, esta desempenhou de uma forma geral um papel menos relevante relativamente à vulnerabilidade das espécies (sendo apenas responsável pelo aumento de dano oxidativo em organismos calcificadores, como foi o caso do anfípode *G. locusta*). No entanto, durante a exposição simultânea de fatores, a acidificação foi responsável pela redução da toxicidade e acumulação de metais pesados, bem como pela diminuição do stress oxidativo causado pelo

aquecimento e contaminação do oceano. Especificamente, os iões hidrogénio (H^+) resultantes da dissolução do CO_2 na água parecem contrabalançar o aumento de ROS causado pelo aumento da temperatura e pela contaminação do oceano, através da conversão de iões H^+ e HO^\bullet em água, eliminando os radicais livres e consequentemente levando a uma diminuição da atividade das enzimas de stress oxidativo, culminando desta forma num decréscimo do dano celular.

Relativamente às respostas a nível taxonómico, a presente dissertação demonstrou que a resposta dos organismos varia de espécie para espécie. Desta forma, organismos que habitam em ambientes mais variáveis (i.e. zona intertital de regiões temperadas e estuários) no que diz respeito às condições abióticas de temperatura, salinidade e oxigénio, respondem de forma positiva às alterações climáticas (i.e. aumento das respostas antioxidantes e de proteínas de stress térmico, de forma a evitar dano celular) do que organismos que habitam ambientes mais estáveis (e.g. zonas tropicais). Contudo, como em tudo existem exceções à regra, uma vez que tubarões recém eclodidos (*C. plagiosum*) parecem estar melhor preparados, ao possuir um sistema de defesa antioxidante evolutivamente mais ancestral, baseado em compostos não enzimáticos, como a ureia e o N-óxido de trimetilamina (TMAO), que parecem conferir um maior grau de proteção que os compostos enzimáticos (estudados em peixes teleósteos, evolutivamente mais recentes, contudo insuficientes para evitar dano celular). Mas uma vez mais, os mecanismos de resposta empregues variam de espécie para espécie e também consoante o seu estado de vida e o stress ao qual estão expostos. Assim, e apesar da acidificação dos oceanos não ter provocado dano oxidativo em *C. plagiosum*, o efeito combinado da temperatura e da contaminação numa outra espécie de tubarão (embriões de uma espécie temperada – *S. canicula*) foi responsável por 100% de mortalidade após 6 dias de exposição. Levando-nos a assumir que o aumento da temperatura, como já provado noutras espécies, leva ao aumento da toxicidade do mercúrio devido ao aumento da atividade metabólica, que leva a uma maior concentração e acumulação de mercúrio nos tecidos desta espécie.

Adicionalmente, organismos calcificadores demonstram ser mais afetados pela acidificação dos oceanos, uma vez que é esperado que os iões H^+ diminuam também o pH intracelular, afetando proteínas responsáveis pelo desempenho da célula. Além disso, e tendo em conta os efeitos parentais das alterações do oceano, parece que os efeitos negativos da acidificação dos oceanos em anfípodas da espécie *G. locusta*, irão potencialmente ser herdados pelos seus descendentes, comprometendo desta forma a sobrevivência das gerações futuras.

Desta forma, e como reforçado na presente dissertação, a contribuição das respostas bioquímicas ao longo da teia trófica é extremamente importante para podermos determinar corretamente quais as respostas individuais de cada organismo ao oceano do futuro, e para complementar os estudos já realizados relativamente às variações a nível fisiológico (i.e. metabolismo, reprodução, crescimento). Apenas assim poderemos determinarmos de forma correta os efeitos das mesmas na fenologia e distribuição das espécies, e determinar possíveis extinções. Por fim, consideramos que estudos relativos aos efeitos a nível trans- e multigeracional são extremamente importantes e que deveriam ser o foco num futuro próximo, uma vez que muitas vezes os efeitos das alterações climáticas não são visíveis numa só geração. Desta forma, determinar de que forma o condicionamento parental poderá afetar a descendência é extremamente importante para que se possa complementar a informação já existente.

List of Articles

This thesis comprises a total of five scientific papers, listed below, each corresponding to a chapter (2-4 and 6). Three of the articles are already published in peer-reviewed international journals, and one under review.

Chapter 2

Lopes AR, Sampaio E, Santos C, Couto A, Pegado MR, Diniz M, Munday PL, Rummer JL, Rosa R. Absence of cellular damage in tropical newly-hatched sharks (*Chiloscyllium plagiosum*) under ocean acidification conditions

Cell Stress and Chaperones (2018) (DOI: 10.1007/s12192-018-0892-3)

Chapter 3

Lopes AR, Borges F, Figueiredo C, Sampaio E, Diniz M, Rosa R, Grilo TF. Transgenerational exposure to ocean acidification induces biochemical distress in a keystone amphipod species (*Gammarus locusta*)

Submitted

Chapter 4

Lopes AR, Faleiro F, Rosa IC, Pimentel MS, Trübenbach K, Repolho T, Diniz M, Rosa R. Physiological resilience of a temperate soft coral to ocean warming and acidification

Cell Stress and Chaperones (2018) (DOI: 10.1007/s12192-018-0919-9)

Chapter 5

Lopes AR, Santos C, Diniz M, Rosa R. Encased in troubled waters: Oxidative damage in shark embryos under ocean warming and the protective role of the capsule against contamination

Submitted

Chapter 6

Sampaio E*, Lopes AR*, Francisco S, Paula JR, Pimentel M, Maulvault AL, Repolho T, Grilo TF, Pousão-Ferreira P, Marques A, Rosa R. Ocean acidification dampens physiological stress response to warming and contamination in a commercially-important fish (*Argyrosomus regius*)

Science of the Total Environment (2018) 618: 388-398 (Doi: 10.1016/j.scitotenv.2017.11.059)

* equally contributed

List of Abbreviations and Units

%	Percentage	CH ₃ Hg	Methylmercury
~	Approximately	CH ₄	Methane
>	Above	CO ₂	Carbon dioxide
±	Plus - minus	CO ₃ ⁻²	Carbonate ions
µatm	Micro atmosphere	CT	Total dissolved inorganic carbon
µL	Microliter		
µm	Micrometer	dw	Dry weight
µM	Micromolar	e ⁻	electron
µm	Micromole	e.g.	For example (from the Latin “ <i>exempli gratia</i> ”)
¹ O ₂	Singlet Oxygen		
4-HNE	4-hydroxynonenal	ELISA	Enzyme-linked immunosorbent assay
8-OHdG	8-hydroxy-2'-deoxyguanosine	ETC	Electron transport chain
AAS	Atomic absorption Spectrometry	etc	Etcetera
abs	Absorbance	εmM	Extinction coefficient
ABTS	2,2'-azino-bis(3-ethylbenzothiazoline-6-sulphonic acid)	F0	Parental/First generation
		F1	Offspring/Progeny
		Fe	Iron
		g	Relative centrifugal force
AChE	Acetylcholinesterase	GHG	Greenhouse gases
ANOVA	Analysis of variance	GLM	Generalized linear models
ATP	Adenosine triphosphate	GPx	Glutathione peroxidase
BSA	Bovine serum albumin	GR	Glutathione reductase
C ₂ H ₆ Hg	Dimethylmercury	GSH	Glutathione
C ₉ H ₁₂ O ₂	Cumene hydroperoxide	GSSG	Oxidized glutathione
Ca ²⁺	Calcium ions	GST	Glutathione S-Transferase
CaCO ₃	Calcium carbonate ions	h	Hour
CAT	Catalase	H ⁺	Hydrogen ions
CDNB	1-chloro-2,4-dinitrobenzene	H ₂ CO ₃	Carbonic acid

| List of Abbreviations and Units

H ₂ O	Water	min	Minutes
H ₂ O ₂	Hydrogen peroxide	mL	Milliliter
HCL	Hydrochloric acid	mM	Millimolar
HCO ₃ ⁻¹	Bicarbonate ions	N ₂ O	Nitrous oxide
Hg	Mercury	Na ₂ HPO ₄	Sodium phosphate
Hg ⁰	Elemental mercury	NaCl	Sodium chloride
HgCl ₂	Mercury chloride	NADP+	Nicotinamide adenine dinucleotide phosphate
Hg ^{II}	Inorganic mercury	NADPH	Dihydronicotinamide- adenine dinucleotide phosphate
HgT	Total mercury	NaOH	Sodium hydroxide
HO•	Hydroxyl radical	NBT	Nitro blue tetrazolium
HSC	Heat shock cognate	Nm	Nanometers
HSP	heat shock protein	nmol	Nanomole
HSR	Heat shock response	NO	Nitric oxide
i.g.	That is (from the Latin “ <i>id est</i> ”)	O ₂ ⁻	Superoxide ion
IPCC	Intergovernmental panel on climate change	O ₂	Oxygen
KCl	Potassium chloride	O ₃	Ozone
kDa	Kilodalton	OA	Ocean acidification
kg	Kilogram	°C	Degrees celsius
KH ₂ PO ₄	Potassium phosphate	OCLTT	Oxygen and capacity limited thermal tolerance concept
km	Kilometer	OMZ	Oxygen minimum zone
km ²	Square kilometer	OONO ⁻	Peroxynitrite
KOH	Potassium hydroxide	OW	Ocean warming
L	Litter	PBS	Phosphate buffered saline
LPO	Lipid peroxidation	pH	Power of hydrogen
m	Meter	pH _e	external pH
M	Molar	pH _i	internal pH
MDA	Malondialdehyde	pH _T	pH total scale
Me ₂ Hg	Dimethylmercury	ppm	Part per million
MeHg	Methylmercury		
mg	Milligram		

PUFA	Polyunsaturated fatty acid	T _d	Denaturation temperature
RNS	Reactive nitrogen species	TGP	Transgenerational plasticity
ROS	Reactive oxygen species	TMAO	Trimethylamine N-oxide
rpm	Revolutions per minute	T _{opt}	Optimum temperature
SOD	Superoxide dismutase	T _p	Pejus temperature
sp. or spp.	Specific epithet of species not identified. Single or several species within a genus	U	Units
SST	Sea surface temperature	Ub	Ubiquitin
TAC	Total antioxidant capacity	v/v	Volume/Volume
TBARS	Thiobarbituric acid reactive substances	ww	Wet weight
T _c	Critical temperature	XOD	Xanthine oxidase
		yr	Year
		Δ	Delta
		Ω	Saturation State

List of Figures

Chapter 1

Figure 1 – (a) Diagram of the greenhouse effect: greenhouse gases (CO_2 , N_2O , O_3 , CH_4) sources and the capture of solar heat, increasing atmospheric temperature; (b) Annual average CO_2 emissions, from 2014-present, data from Mauna Loa Observatory (NOAA 2018)

Figure 2 – (a) Projected changes in annual average surface temperature for 2081-2100, according to RCP2.6 and 8.5 (source: IPCC 2014); (b) Ocean acidification schematics of the fate of carbon dioxide (CO_2) as it dissolves in the seawater

Figure 3 – Schematics of the thermal window of oxygen and capacity limited thermal tolerance concept (OCLTT) of marine organisms. Optimum temperature (T_{opt}) correspond to the temperature which a specific performance (e.g. growth, reproduction) is maximal. Pejus temperatures (T_p) correspond to the first temperature threshold to which a specific animal has a time-limited tolerance. Critical temperatures (T_c) is the second temperature threshold, where O_2 availability becomes insufficient, demarks the beginning of the anaerobic metabolism. Denaturation temperature (T_d) is characterized by the onset of cell and protein damage. Full black curve represents the performance curve under normal conditions. Dashed grey curve represent the performance curve options under OA and/or hypoxic seawater (source: Pörtner et al. 2014, following Pörtner 2002; 2012; Pörtner and Farrell 2008)

Figure 4 – Schematic response of a marine organism to OA. Effects are mediated via diffusive CO_2 entry (black arrows) into the body and cell compartments, resulting in a rise in $p\text{CO}_2$ (highlighted in red), a drop in compartmental pH (highlighted in blue), and their effects (red arrows) on various processes (red text) in tissues and cellular compartments (source: Pörtner et al. 2014; after Pörtner 2008)

Figure 5 – Mercury (Hg) cycle: atmospheric and oceanic Hg sources; oxidation – reduction, methylation – demethylation and deposition processes of different Hg forms

[elemental Hg (Hg^0), inorganic Hg (Hg^{II}) and methylmercury (MeHg); bioaccumulation and biomagnification throughout the marine food chain.

Figure 6 – Routes of oxygen (O_2) metabolism in marine organisms and reactive oxygen species (ROS) formation. Electron transport chain (ETC) as an electron (e^-) source during the reduction of O_2 to produce adenosine triphosphate (ATP). One-electron reduction sequencing causing the formation of ROS, such as: superoxide ion (O_2^-), hydrogen peroxide (H_2O_2) and hydroxyl radical (OH^\bullet), with water (H_2O) as a final product. Four-electron reduction of O_2 to form H_2O (adapted from Lushchak 2011).

Figure 7 – Schematics of reactive oxygen species (ROS) action within the cell: electron stealing of a stable molecule, causing cell damage (left side); electron donation by an antioxidant, avoiding cell damage (right side).

Figure 8 – Schematics of the activity of superoxide dismutase (SOD), catalase (CAT) and glutathione peroxidase (GPx) against reactive oxygen species (ROS), and glutathione-S-transferase (GST) against xenobiotics.

Figure 9 – Lipid peroxidation of polyunsaturated fatty acids (PUFA)

Chapter 2

Figure 1 – Impact of high CO_2 exposure on levels of: (A) LPO, (B) Protein carbonyl, and (C) 8-OHdG levels in *C. plagiosum* tissues. The horizontal line within the box indicates the median, boundaries of the box indicate the 25th and 75th percentiles, and the whiskers indicate the highest and lowest values of the results. Different letters represent significant differences between tissues, while asterisks (*) represent significant differences within tissues. GLM analyses described in Supplemental Tables S2 and S5.

Figure 2 – Impact of high CO_2 exposure on levels of: (A) SOD, (B) CAT, (C) GPx, (D) Aconitase activities, and (E) TAC in *C. plagiosum* tissues. The horizontal line within the box indicates the median, boundaries of the box indicate the 25th and 75th percentiles, and the whiskers indicate the highest and lowest values of the results. Different letters represent significant differences between tissues, while asterisks (*) represent

significant differences within tissues. GLM analyses described in Supplemental Tables S3 and S6.

Figure 3 – Impact of high CO₂ exposure on protein repair and removal, namely: (A) HSP and (B) Ub levels in *C. plagiosum* tissues after 50 days exposure to high CO₂. The horizontal line within the box indicates the median, boundaries of the box indicate the 25th and 75th percentiles, and the whiskers indicate the highest and lowest values of the results. Different letters represent significant differences between tissues, while asterisks (*) represent significant differences within tissues. GLM analyses described in Supplemental Tables S4 and S7.

Chapter 3

Figure 1 – Diagram of the experimental design. Parental generation (F0): C – amphipods reared under control pCO₂ levels; H – amphipods reared under elevated pCO₂ levels. Offspring generation (F1): offspring reared under the same treatment as their progenitors (continuous line) [Control (C-C) or High CO₂ (H-H)]; or reared on the opposing treatment (dotted line) [High CO₂ – Control (H-C) or Control – High CO₂ (C-H)].

Figure 2 – Impact of high CO₂ exposure on: A) LPO (nmol mg⁻¹ total protein); and B) DNA damage (relative abs mg⁻¹ total protein) levels in *G. locusta* parents and offspring's. Values represent mean ± SD. Different letters represent significant differences between treatments identified by GLM analyses which are described in Supplemental Tables SII and SIII.

Figure 3 – Impact of high CO₂ exposure on: A) HSP (μg mg⁻¹ total protein); and B) Ub (μg mg⁻¹ total protein) levels in *G. locusta* parents and offspring's. Values represent mean ± SD. Different letters represent significant differences between treatments identified by GLM analyses which are described in Supplemental Tables SIV and SV.

Figure 4 – Impact of high CO₂ exposure on: A) SOD (% Inhibition min⁻¹ mg⁻¹ protein); B) CAT (nmol min⁻¹ mg⁻¹ total protein); C) GPx (nmol min⁻¹ mg⁻¹ total protein); D) GST (nmol min⁻¹ mg⁻¹ total protein) activities; and E) TAC (mM Trolox mg⁻¹ total protein) levels in *G. locusta* parents and offspring's. Values represent mean ± SD. Different

letters represent significant differences between treatments identified by GLM analyses which are described in Supplemental Tables SVI-SXI.

Chapter 4

Figure 1 – Antioxidant enzyme activities in *Veretillum cynomorium* under ocean warming and acidification conditions: (A) Catalase (CAT) and (B) Glutathione S-transferase (GST). Values represent mean \pm standard deviation.

Figure 2 – Lipid peroxidation (MDA - malondialdehyde) levels in *Veretillum cynomorium* under ocean warming and acidification conditions. Values represent mean \pm standard deviation.

Figure 3 – Heat shock protein (HSP70/HSC70) concentrations in *Veretillum cynomorium* under ocean warming and acidification conditions. Values represent mean \pm standard deviation.

Chapter 5

Figure 1 – Survival (%) of *S. canicula* exposed to different combinations of temperature and HgCl₂ contamination for 7 days. GLM analyses described in Supplemental Table SI.

Figure 2 – Total mercury (HgT) accumulation in *S. canicula* capsule. The horizontal line within the box indicates the median, boundaries of the box indicate the 25th and 75th percentiles, and the whiskers indicate the highest and lowest values of the results. Different letters represent significant differences between treatments. GLM analyses described in Supplemental Table SII.

Figure 3 – Total mercury (HgT) accumulation in *S. canicula* tissues. The horizontal line within the box indicates the median, boundaries of the box indicate the 25th and 75th percentiles, and the whiskers indicate the highest and lowest values of the results. Different letters represent significant differences between tissues, while asterisks (*) represent significant differences between contamination treatments. GLM analyses described in Supplemental Table SIII.

Figure 4 – Impact of HgCl₂ and warming exposure on levels of: A) Heat shock proteins (HSP) and B) Ubiquitin (Ub) in *S. canicula* tissues. The horizontal line within the box

indicates the median, boundaries of the box indicate the 25th and 75th percentiles, and the whiskers indicate the highest and lowest values of the results. Different letters represent significant differences between tissues, while asterisks (*) and cardinals (#) represent significant differences between contamination and temperatures, respectively. GLM analyses described in Supplemental Tables SIV and SV.

Figure 5 – Impact of HgCl_2 and warming exposure on levels of: A) Lipid peroxidation (LPO) and B) DNA damage levels in *S. canicula* tissues. The horizontal line within the box indicates the median, boundaries of the box indicate the 25th and 75th percentiles, and the whiskers indicate the highest and lowest values of the results. Different letters represent significant differences between tissues, while cardinals (#) represent significant differences between temperatures. GLM analyses described in Supplemental Tables SVI and SVII.

Figure 6 – Impact of HgCl_2 and warming exposure on: A) Superoxide dismutase (SOD), B) Catalase (CAT), C) Glutathione peroxidase (GPx), D) Glutathione S-Transferase (GST), E) Acetylcholinesterase (AChE) activities and F) Total antioxidant capacity (TAC) in *S. canicula* tissues. The horizontal line within the box indicates the median, boundaries of the box indicate the 25th and 75th percentiles, and the whiskers indicate the highest and lowest values of the results. Different letters represent significant differences between tissues, while asterisks (*) and cardinals (#) represent significant differences between contamination and temperatures, respectively. GLM analyses described in Supplemental Tables SVI-SXI.

Chapter 6

Figure 1 - Total mercury (HgT) accumulation (mean \pm SE) in *A. regius*: a) Differences among tissues (muscle, gills and liver); and shaped by interactions between temperature (19 and 23 °C) and CO_2 (400 and 1500 μatm) within b) muscle, c) gills and d) liver, respectively. Graphs were plotted according to significant factors yielded by GLM analysis described in Table 1 and 2, respectively.

Figure 2 - Malondialdehyde (MDA) build-up concentrations (mean \pm SE) in *A. regius* muscle driven by an interaction between MeHg contamination (Non-contaminated and

contaminated) and temperature (19 and 23 °C). Graphs were plotted according to significant factors yielded by GLM analysis described in Table 3 and 4, respectively.

Figure 3 - a) Catalase (CAT) enzyme activities (mean \pm SE) driven by MeHg contamination (Non-contaminated and Contaminated). b) Superoxide dismutase (SOD) activities (mean \pm SE) in *A. regius* muscle driven by an interaction temperature (19 and 23 °C) and CO₂ (400 and 1500 μ atm). Graphs were plotted according to significant factors yielded by GLM analysis described in Table 4.

Figure 4 - Glutathione S-Transferase (GST) activities (mean \pm SE) in *A. regius* muscle driven by: a) an interaction between temperature (19 and 23 °C) and CO₂ (400 and 1500 μ atm); and b) an interaction between MeHg contamination (Non-contaminated and contaminated) and CO₂ (400 and 1500 μ atm). Graphs were plotted according to significant factors yielded by GLM analysis (triple interaction) described in Table 4.

Figure 5 - Heat shock protein70 (Hsp70) concentrations (mean \pm SE) in *A. regius*: a) tissues; b) in the gills shaped by MeHg contamination (Non-contaminated and Contaminated) and CO₂ (400 and 1500 μ atm); in the c) muscle shaped by an interaction between temperature (19 and 23 °C) and CO₂ (400 and 1500 μ atm); and in the d) liver shaped by an interaction between MeHg contamination (Non-contaminated and Contaminated) and CO₂ (400 and 1500 μ atm). Graphs were plotted according to significant factors yielded by GLM analysis described in Table 5.

List of Tables

Chapter 3

Table I – Summary table of the oxidative damage (LPO and DNA), protein repair and removal mechanisms (HSP and Ub) and antioxidant response (SOD, CAT, GPx and GST activities and TAC) in *G. locusta* following within- and transgenerational exposure to ocean acidification

Chapter 6

Table I – GLM analysis of *A. regius* Fulton's K and total mercury (HgT) concentration in tissues (3 levels within contaminated treatments: liver, muscle and gills) exposed to MeHg contamination (2 levels: non-contaminated and contaminated) for 30 days. Model formula on top, family and respective model AIC in the bottom. Est – Estimates; Std Error – Standard Error. Bold values indicate $p < 0.05$. For more details please see the R script in Supplemental Data.

Table II – GLM analysis of total mercury concentration (HgT) within each sampled tissue (liver, muscle and gills) of *A. regius* exposed to MeHg for 30 days, under crossed treatments of temperature (T, 2 levels: 19 °C and 23 °C) and CO₂ (CO₂, 2 levels: 400 µatm and 1500 µatm). Model formula on top, family and respective model AIC in the bottom. Est – Estimates; Std Error – Standard Error. Bold values indicate $p < 0.05$. For more details please see the R script in Supplemental Data.

Table III – GLM analysis of malondialdehyde (MDA) build-up in *A. regius* after 30 days exposed to crossed treatments of MeHg contamination (MeHg, 2 levels, non-contaminated and contaminated) and temperature (T, 2 levels: 19 °C and 23 °C). Model formula on top, family and respective model AIC in the bottom. Est – Estimates; Std Error – Standard Error. Bold values indicate $p < 0.05$. For more details please see the R script in Supplemental Data.

Table IV – GLM analysis of oxidative stress response (CAT, SOD and GST) in *A. regius* after 30 days exposed to crossed treatments of MeHg exposure (MeHg, 2 levels: non-contaminated and contaminated), temperature (T, 2 levels: 19 °C and 23 °C) and

| List of Tables

CO₂ (CO₂, 2 levels: 400 µatm and 1500 µatm). Model formula on top, family and respective model AIC in the bottom. Est – Estimates; Std Error – Standard Error. Bold values indicate $p < 0.05$. For more details please see the R script in Supplemental Data.

Table V – GLM analysis of heat shock protein 70 (Hsp70) production in *A. regius* tissues (gills, muscle and liver) and, posteriorly within tissues, under crossed treatments of MeHg exposure (MeHg, 2 levels, non-contaminated and contaminated), temperature (T, 2 levels: 19 °C and 23 °C) and CO₂ (CO₂, 2 levels: 400 µatm and 1500 µatm). Model formula on top, family and respective model AIC in the bottom. Est – Estimates; Std Error – Standard Error. Bold values indicate $p < 0.05$. For more details please see the R script in Supplemental Data.

Chapter 7

Table I – Summary of the major finding in the present dissertation (n.a. – not available)

1 General Introduction

1.1. Global Climate Change – A high CO₂ World

“Climate change is no longer some far-off problem; it is happening here, it is happening now”

- Barack Obama

The 18th century was known in the history of mankind as the Era of change, where simple hand using tools were replaced by powered machinery and factories, nonetheless, this era of growth and expansion did not come without a cost (Allen 2010). With the Industrial Revolution, man began the burning of fossil fuels - coal, oil and natural gas - increasing the amount of greenhouse gases (GHG) emissions - carbon dioxide (CO₂), methane (CH₄), nitrous oxide (N₂O) and ozone (O₃) - into the atmosphere (IPCC 2014). This continuous emission of GHG is acting as a thick blanket around the Earth, absorbing the heat radiation resultant from the Sun, in a phenomenon known as the greenhouse effect, increasing the average global surface temperature (see Fig. 1a; Black and Weisel 2010). Additionally, increasing human pressures - habitat modification and pollution - started what years after we became to acknowledge as Climate Change¹.

Carbon dioxide (CO₂) emissions, one of the main GHG, that has been relatively stable during the 10,000 years preceding the Industrial Revolution, with levels ranging around 280 ppm, has increased 80% in the last two centuries, reaching for the first time in human history levels consistently above 400 ppm (see Fig. 1b; IPCC 2014; Lüthi et al. 2008). Furthermore, and unless anthropogenic CO₂ emissions are reduced, they are predicted to reach ~1000 ppm until the end of the century (Gattuso and Hansson 2011; Pörtner et al. 2014).

¹ The United Nations Framework Convention on Climate Change (UNFCCC) defined climate change has the direct and indirect causes of human activities, while climate variability refers to natural causes.

The CO₂ concentration in the Earth's atmosphere is naturally absorbed and emitted as part of the carbon cycle. In fact, CO₂ reaches the atmosphere through various “sources” and can be partly reabsorbed by “reservoirs” – oceans, lakes, rivers and plants (Pittock 2009). Nonetheless the unreasonable burning of fossil fuels and changes in the land use - deforestation, industrialization and urbanization - caused the atmospheric CO₂ concentration to rise above the Earth capacity (Black and Weisel 2010).

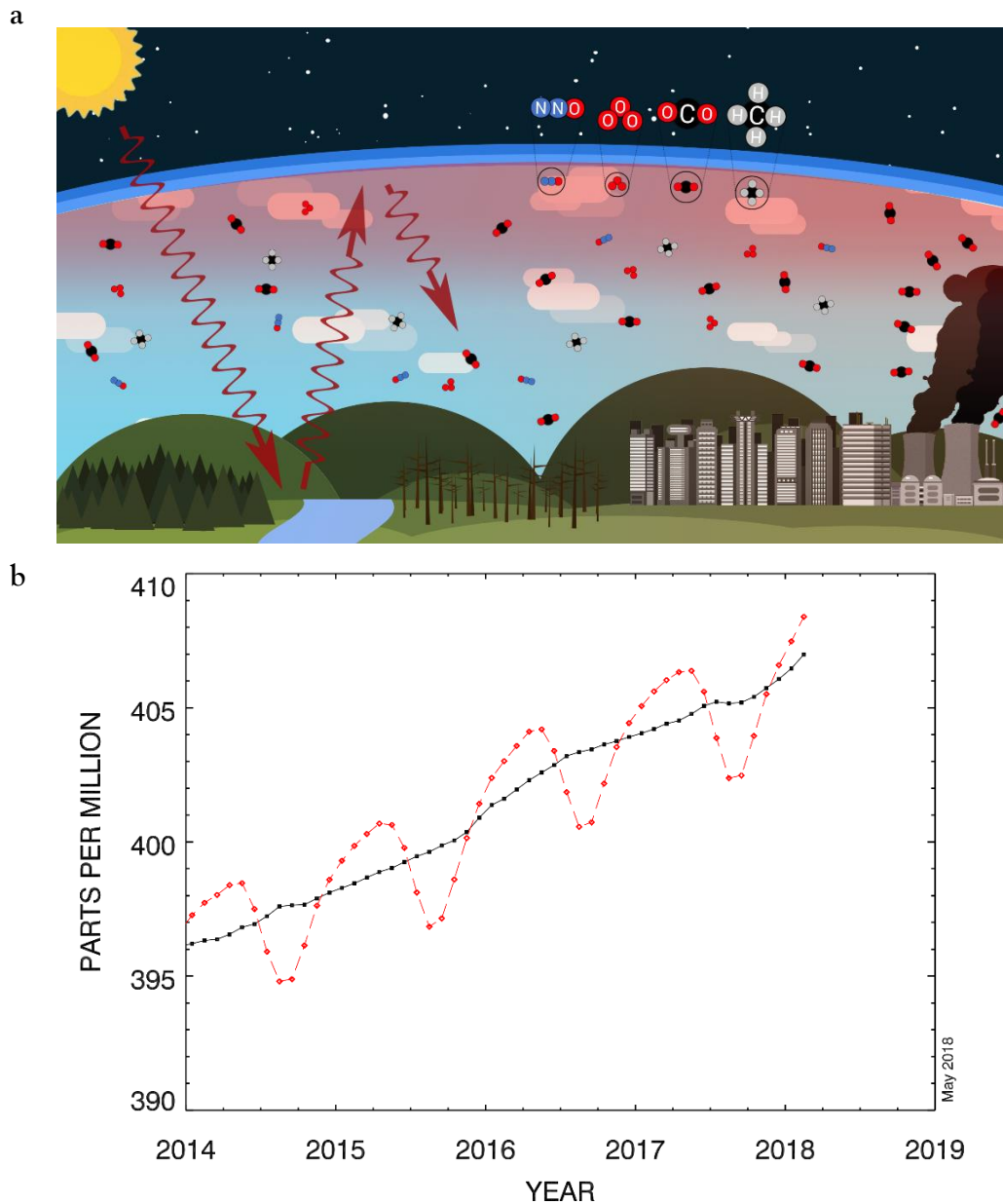


Figure 1 – (a) Diagram of the greenhouse effect: greenhouse gases (CO₂, N₂O, O₃, CH₄) sources and the capture of solar heat, increasing atmospheric temperature; (b) Annual average CO₂ emissions, from 2014-present, data from Mauna Loa Observatory (NOAA 2018)

With the Earth warmed by almost 2 °C since pre-industrial times, we are now witnessing sea-level rising, causing the flooding of coastal cities and changing weather patterns, which will culminate in stronger storms, and severe droughts, resulting in an additional 80,000 km² of grass and farmland turned into deserts each year (Black and Weisel 2010). In fact, the Earth is now warming so fast that it is believed that we are half-way to reach a tipping point. Additionally, future projections point out to a further 1.1-6.4 °C increment until 2100, as well as an increase in the severity and frequency of heat waves (Pörtner et al. 2014).

1.2. Ocean under High CO₂

The ocean is by far the most dominant feature of our planet, covering around 70% of the Earth's surface, and representing 97% of the Earth's total water content, it pertains 99% of the world's entire biosphere (Costello et al. 2015; Kaiser et al. 2005; Reid 2016). With almost 40% of the world entire population living near the coastal areas (within 60 km distance), the anthropogenic pressure in the world's ocean is extremely high (Kaiser et al. 2005).

Being one of the most efficient CO₂ “reservoir”, the ocean plays a key role in mitigating climate change, decreasing atmospheric CO₂ build-up by absorbing more than 25% of the current global anthropogenic CO₂ emissions (~10⁶ metric tons of CO₂ per hour), and storing more than 90% of the atmospheric heat content (Pörtner et al. 2014).

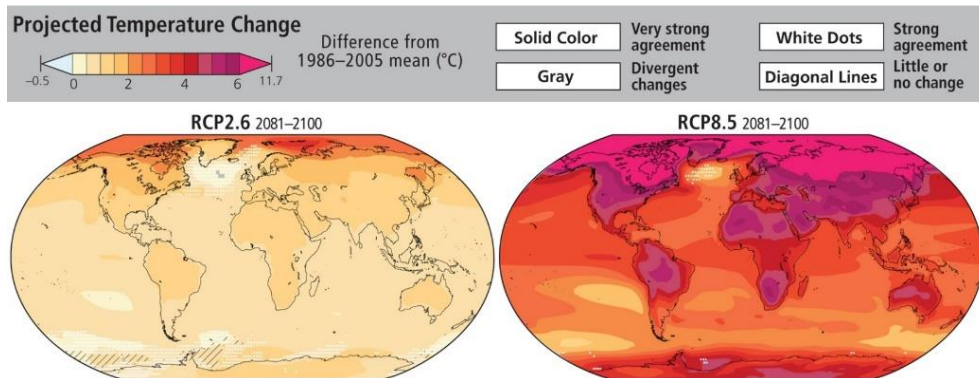
The rise in atmospheric CO₂ concentration and the greenhouse effect is also increasing average sea surface temperature (SST; Fig. 2a), which has risen by 0.1 °C per decade since pre-industrial times, and with predictions pointing out to a further 1-4 °C rise until 2100 (Collins et al. 2013; Rosa et al. 2014). Moreover, as CO₂ dissolves in the seawater, a chemical chain of reactions is expected to occur (see Fig. 2b). Firstly, carbonic acid (H₂CO₃) is produced and can be further dissociated into bicarbonate ions (HCO₃⁻), with the additional formation of hydrogen ions (H⁺), which will decrease the seawater pH, contributing to a process known as ocean acidification (OA) (Caldeira and Wickett, 2003; Doney et al., 2009; Zeebe and Ridgwell, 2011). Surface-ocean pH levels, that have been relatively stable for over 800 million of years, have dropped 0.1 units since pre-industrial times – representing a 30% increase in ocean acidity – and if anthropogenic CO₂ emissions continue to increase, it is forecast to a further 0.13-0.42 pH unit drop until the end

of this century (~100-150 % H^+ increase) (Caldeira and Wickett 2005; Gattuso and Hansson 2011; Pörtner et al. 2014).

Future ocean climate-related changes are expected to challenge marine organisms across all levels of biological organization - from molecular to organism level - affecting population, communities and ecosystems dynamics (Fabry et al. 2008; Harvey et al. 2013; Pörtner et al. 2005; Pörtner et al. 2004). Furthermore, these changes could affect species physiology, causing shifts in species distribution (Edwards and Richardson 2004; Harvey et al. 2013; Kroeker et al. 2013; Parmesan and Yohe 2003), ultimately leading to worldwide extinction events (Thomas et al. 2004). Nonetheless, we should bear in mind that the response towards climate change is species-specific, varying among taxonomic groups, trophic level and life stages (e.g. early life stages are more vulnerable than adults), and dependent upon the stressor to which they are exposed to (Byrne 2011; Dupont and Thorndyke 2009; Halpern et al. 2007).

Some of the major effects of ocean warming and acidification, known to date, on marine organisms are summarized below.

a



b

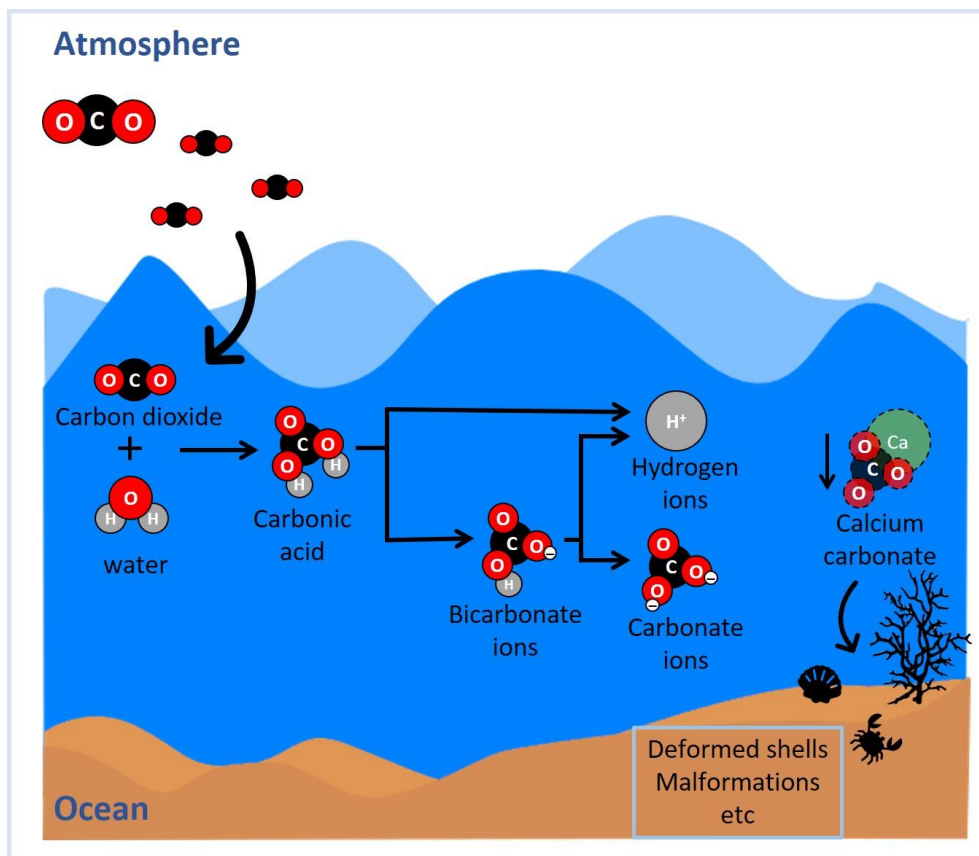


Figure 2 – (a) Projected changes in annual average surface temperature for 2081–2100, according to RCP2.6 and 8.5 (source: IPCC 2014); (b) Ocean acidification schematics of the fate of carbon dioxide (CO₂) as it dissolves in the seawater, and the consequences of decreased pH.

1.2.1. Ocean Warming

Temperature is a key factor known to influence marine organisms, especially marine ectotherm² performance and physiology. It determines species distribution, across latitudinal and depth ranges, and within the organisms' optimum thermal window, it can even benefit them, as slightly increases in temperature can provide more food sources and energy for biological and biochemical processes (e.g. growth, reproduction, etc.) (Pörtner et al. 2001; 2005). Nonetheless, OW is expected to reduce the amount of dissolved oxygen (O₂; already decreased at a rate of 0.1 to > 0.3 $\mu\text{mol kg}^{-1} \text{yr}^{-1}$) in the ocean, once O₂ solubility is temperature-dependent, therefore increasing ocean stratification and expansion of oxygen minimum zones (OMZs) (Reid 2016; Schmidtke et al. 2017; Stramma et al. 2010). This will limit the amount of O₂ that reaches deeper waters and threaten the survival of water-breathing marine organisms, reducing the nutrient availability, and consequently primary production (Pörtner 2001 ; Pörtner et al. 2000; Pörtner and Knust 2007). Additionally, and considering that marine organisms live and function within limited temperature ranges (T_{opt}), it is expected that beyond those limits (T_p - *pejus*), the metabolic demand and oxygen consumption increases, forcing aerobic organisms to adopt an anaerobic strategy. This may cause other downstream events, such as decreased growth and reproduction, and the activation of antioxidant and heat-shock defenses mechanisms to avoid cellular damage (see the oxygen and capacity limited thermal tolerance concept (OCLTT) in Fig. 3; Pörtner 2002; 2010; 2012; Pörtner and Farrell 2008; Pörtner and Knust 2007).

Furthermore, OW is also changing species' phenology³, which will shift organisms' spawning, migration and dispersal seasons, affecting reproduction and life cycle timing, ultimately driving prey-predator mismatches (Drinkwater et al. 2010; Magnan and Gattuso 2016). Temperature is also known to influence swimming performance and the activity rates of marine fishes, which will affect both predator avoidance and feeding success (Fuiman et al. 2005; 2006). As mentioned above, increases in SST changes species' geographical distribution, but when temperature suppresses species thermal limits, while some may move to an optimal thermal niche or expand their geographical range, others may withdrawal and even disappear (Eddy and Handy 2012; Perry et al. 2005). This will increase the invasion of alien⁴ species, that will compete

² Organisms' whose body temperature regulation depends on the surrounding environment

³ Timing of biological events

⁴ Non-native species

with native species for food and habitat, disrupting trophic interactions and community structure (Bellard et al. 2013).

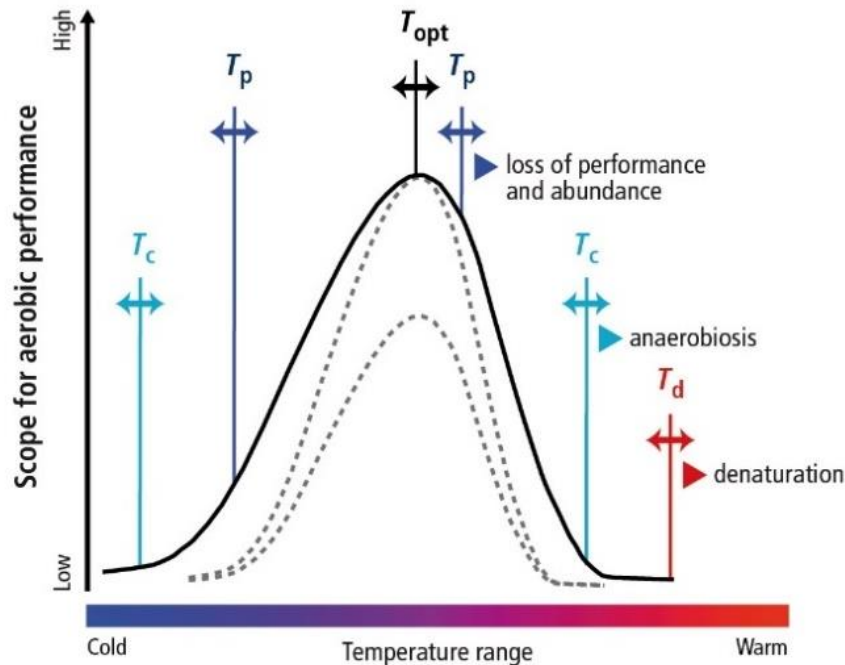


Figure 3 – Schematics of the thermal window of oxygen and capacity limited thermal tolerance concept (OCLTT) of marine organisms. Optimum temperature (T_{opt}) correspond to the temperature which a specific performance (e.g. growth, reproduction) is maximal. Pejus temperatures (T_p) correspond to the first temperature threshold to which a specific animal has a time-limited tolerance. Critical temperatures (T_c) is the second temperature threshold, where O_2 availability becomes insufficient, demarks the beginning of the anaerobic metabolism. Denaturation temperature (T_d) is characterized by the onset of cell and protein damage. Full black curve represents the performance curve under normal conditions. Dashed grey curve represent the performance curve options under OA and/or hypoxic seawater (source: Pörtner et al. 2014, following Pörtner 2002; 2012; Pörtner and Farrell 2008).

Warming is also threatening one of the most diverse ecosystems in our planet - coral reefs. As temperature rise the symbiosis between corals and zooxanthellae is disrupted, in a phenomenon known as coral bleaching (Glynn 1996). This disruption between the zooxanthellae and their host, which is primarily initiated with the overproduction of reactive oxygen species (ROS) in the symbiont photosystem II (Downs et al. 2002; Lesser 1997; Mydlarz et al. 2009), is one of the major threats to coral health, limiting their reproduction and causing coral death, ultimately culminating into habitat lost, decreased biodiversity and local extinction (Carpenter et al. 2008; Hoegh-Guldberg 1999; Hoegh-Guldberg et al. 2007).

1.2.2. Ocean Acidification

The consequences of decreasing seawater pH are extremely vast, and while some organisms are known to thrive under such conditions – primary producers using CO₂ as an inorganic carbon source – to others OA is known to have far-reaching consequences, ultimately leading to biodiversity loss, with repercussions at the community- and ecosystem-level (Cattano et al. 2018; Connell et al. 2018; 2013; Hernández-Hernández et al. 2018; Kroeker et al. 2010; Nagelkerken and Connell 2015).

Key calcifying organisms, such as mollusks, crustaceans, echinoderms and corals will be especially vulnerable under OA (Kroeker et al. 2010; Wittmann and Pörtner 2013). This is due to the fact that CO₂ is reducing the concentration of carbonate ions (CO₃²⁻), that will compete for calcium ions (Ca²⁺) with the highly reactive H⁺ ions. Consequently, this will decrease the concentration of calcium carbonate ions (CaCO₃), and the saturation state (Ω) of calcite, magnesium-calcite and aragonite minerals in seawater surface, the building blocks of marine organisms' shells and skeletons (see Fig.2b; Cao et al. 2007; Delille et al. 2005; Doney et al. 2009; Knoll and Fischer 2011).

Additionally, OA is also expected to induce changes in the acid-base balance of marine organisms (Fig. 4). As CO₂ increases, H⁺ ions are released and even though some marine organisms (i.e. fishes and crustaceans) have the ability to adjust their internal pH through active ion transport (i.e. HCO₃⁻ increase and/or H⁺ excretion), the assumption that such compensation will provide them a wide CO₂ tolerance could be overestimated (Heuer and Grosell 2014). In fact, increased acid-base regulation may have energetic costs, causing other downstream consequences, such as impaired growth (Baumann et al. 2012; Heuer and Grosell 2014), reduced metabolic performance (Rosa and Seibel 2008), decreased oxygen binding and delivery (Pörtner et al. 1998; Pörtner and Reipschläger 1996), altered behavior (i.e. prey-predator interaction, dispersal, settlement and habitat choice) (Clements and Hunt 2014; Dixon et al. 2010; Nagelkerken and Munday 2015), impaired protein function – causing oxidative stress and damage (discussed later on this chapter) (Dean 20010; Hu et al. 2011; Tomanek 2011) – ultimately increasing mortality (Baumann et al. 2012; Pörtner and Reipschläger 1996).

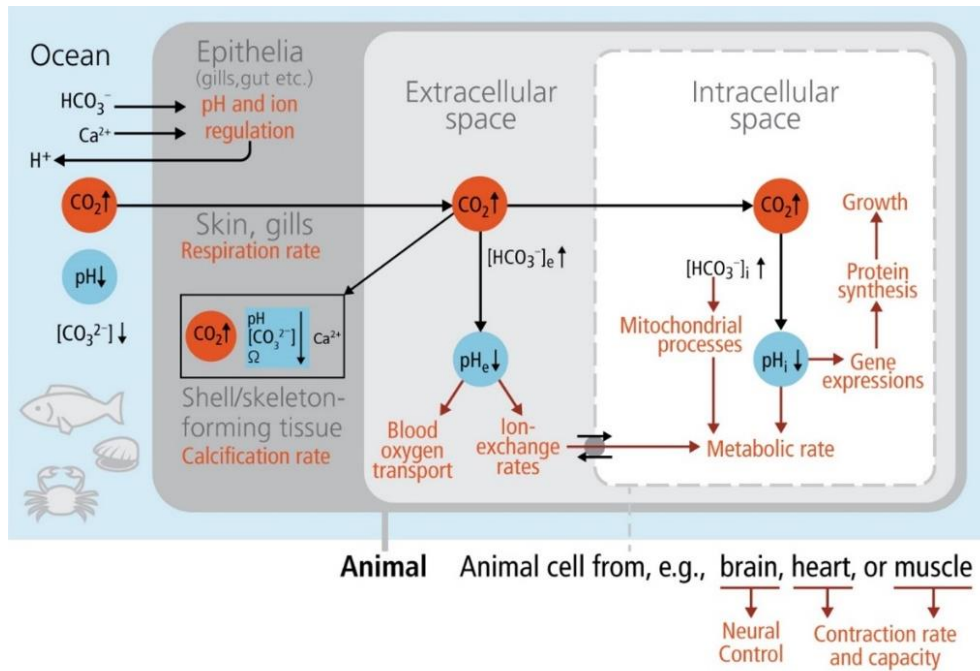


Figure 4 – Schematic response of a marine organism to OA. Effects are mediated via diffusive CO_2 entry (black arrows) into the body and cell compartments, resulting in a rise in $p\text{CO}_2$ (highlighted in red), a drop in compartmental pH (highlighted in blue), and their effects (red arrows) on various processes (red text) in tissues and cellular compartments (source: Pörtner et al. 2014, after Pörtner 2008)

1.3. Contamination under Climate change

Human activities are changing the marine environment, not only by inducing climate-related changes, such as OW and OA, but also through the boost of contamination. Anthropogenic activities, such as mining processes, chemical combustion, agriculture activities, medical wastes and sewage discharge, are increasing the load of pollutants – organic chemicals, litter, debris and heavy metals etc. – in aquatic systems, especially when considering coastal areas (Clarkson et al. 2003; He et al. 2005; Tchounwou et al. 2012). The increase of toxic chemicals into coastal areas can result in harmful effects on marine wildlife, ecosystem degradation, ultimately causing human poisoning (Fung et al. 2004; Ip et al. 2004; Morton and Blackmore 2001).

The major source of waste release to marine environments is due to domestic and industrial sewage discharges. Sewage encompasses a vast array of pathogens (e.g. *Salmonella spp.*, *Escherichia coli*, *Streptococcus sp.*, fungus and viruses) (Grillo et al. 2001; Islam and Tanaka 2004), which

decreases O₂ concentration in the seawater, due to bacterial activity, and increases nutrient levels, increasing algal blooms and consecutively toxin production (Bonsdorff et al. 1997; Hernandez et al. 1998; Islam and Tanaka 2004).

Additionally, pesticides resulting from agriculture activities contribute to almost 50 % of the total marine pollution. Due to its wide application in pest control and persistency in the environment (i.e. low degradability rate), pesticides release high levels of NH₄ and NO₃, being a major contributor to OA (Islam and Tanaka 2004). Pesticides are also known to have harmful effects on organisms'. At sublethal levels they cause neurotransmission disruption (Casida 2009) and interfere with pheromonal systems – reducing mating success (Park and Propper 2002). Furthermore, they also affect organisms' health, instigating cellular and molecular damage, ultimately leading to the death of the organism (Islam and Tanaka 2004).

1.3.1. Heavy metals - the mercury case

Heavy metals are naturally occurring constituents of the marine environment, and by-products of industrial processes. Metals are non-degradable and persistent in the environment, accumulating in sediments in the sea floor, or absorbed by marine organisms, entering the food chain – bioaccumulated by marine organisms – and transferred to higher trophic levels – biomagnified (Bryan and Darracott 1979; Rainbow and Luoma 2011; Wang et al. 2002). Furthermore, the ten most toxic heavy metals in marine environments are, in order of increasing toxicity: zinc, arsenic, chromium, copper, lead, selenium, nickel, silver, cadmium and mercury (Davies 1978).

Being one of the most hazardous heavy metals for all living organisms, mercury (Hg) is usually found in the natural environment in three different forms: elemental Hg (Hg⁰), inorganic Hg (Hg^{II}) and organic Hg [methylmercury (MeHg: CH₃Hg)] (see Fig. 5). As Hg^{II} reaches the seawater it can either be reduced into Hg⁰ and released to the atmosphere or methylated by bacteria into MeHg, increasing Hg bioavailability, bioaccumulation and biomagnification in marine food webs (Boening 2000; Braune et al. 2015; Jaishankar et al. 2014). The adverse effects of Hg on marine organisms depend on its speciation, the extent of exposure (frequency, quantity and duration) and individuals life stage (Clarkson and Magos 2006).

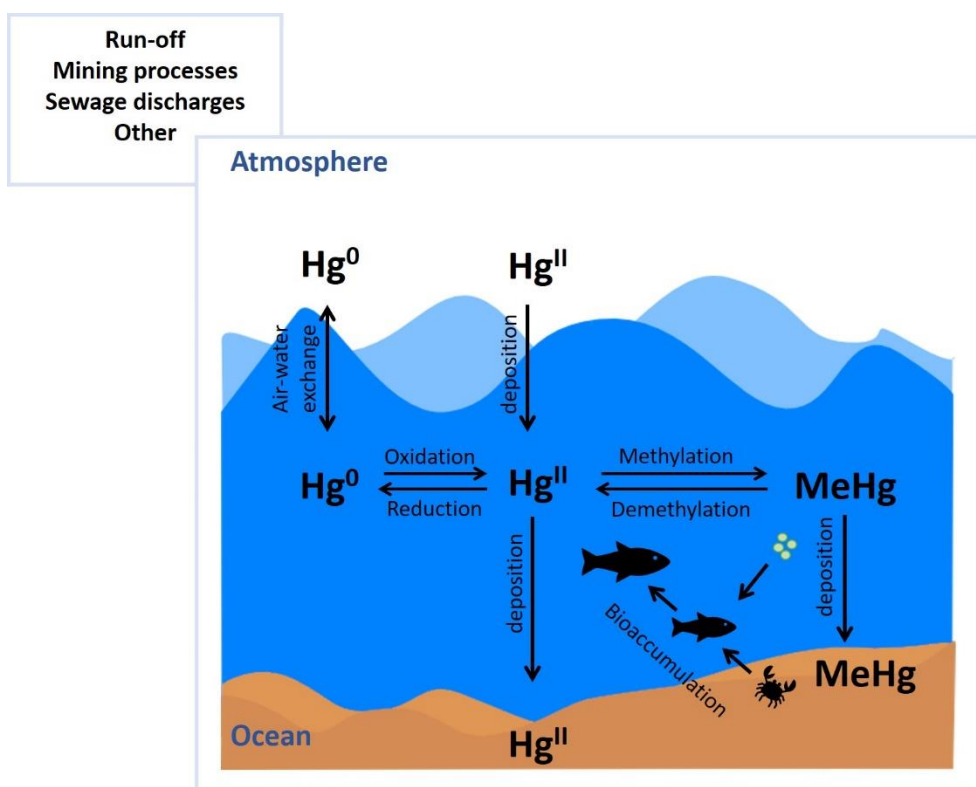


Figure 5 – Mercury (Hg) cycle: atmospheric and oceanic Hg sources; oxidation – reduction, methylation – demethylation and deposition processes of different Hg forms [elemental Hg (Hg^0), inorganic Hg (Hg^{II}) and methylmercury (MeHg)]; bioaccumulation and biomagnification throughout the marine food chain.

Specifically, Hg accumulation is known to be tissue-specific, accumulating preferentially in the gills – the main entrance into the body – and in lipid-rich organs such as the liver (Cairns et al. 1975; Jezierska and Witeska 2006). Furthermore, due to its high affinity for the thiol group of proteins, Hg effects on marine organisms can be extremely vast, including: i) organ function loss (Gonzalez et al. 2005); ii) accumulation of ROS in organisms' cells due to impaired antioxidant defense mechanisms, increasing the vulnerability towards oxidative stress and damage (Berntssen et al. 2003; Gonzalez et al. 2005; Mieiro et al. 2010; Tchounwou et al. 2012) and ultimately iii) death (Coccini et al. 2000). Additionally, Hg can also block ion channels or be transported along the central nervous system, causing neurotoxicity (Clarkson et al. 2003; Lüring 2015), and consequently impaired behavior patterns, such as predator avoidance (Berntssen et al. 2003; Boyd 2010; Sampaio et al. 2016; Sloman 2007).

1.3.2. Biological responses

Mercury cycle is likely to change with alterations in the physical environment, either by increases in temperature and/or changes in the carbon cycle. Nonetheless, there is still insufficient understanding on how climate change can affect Hg cycle and the consequences on marine organisms, which is of utmost importance if we ought to construct plausible predictive models of climate effects.

Warmer temperatures are expected to affect the frequency, magnitude and timing of Hg contamination. Specifically, increasing temperatures are known to increase Hg toxicity and accumulation (Holmstrup et al. 2010; Jones 1973). Due to the parallel increase of anaerobic bacterial activity with temperature, the methylation rate of Hg will also rise (e.g. by 37 % at 20 °C), increasing its concentration in the marine environment and consequently its bioaccumulation (Bodaly et al. 1993; Canário et al. 2007). Additionally, and as explained above, warming is expected to affect individuals' growth rates, which could in turn affect Hg accumulation. Specifically, species with low growth rates are expected to experience higher Hg concentration (Reist et al. 2006b; Simoneau et al. 2005). Moreover, temperature-induced metabolic stress is also expected to affect Hg accumulation/elimination rates (Dijkstra et al. 2013; Reist et al. 2006a). Temperature will also increase cell membrane fluidity, allowing Hg diffusion, while Hg will inactivate the antioxidative defense systems, increasing the amount of ROS and consequent peroxidation of lipid membranes (Holmstrup et al. 2010).

Ocean acidification is expected to affect the speciation of metals. Specifically, OA is expected to cause a pH-induced shift in Hg methylation. As pH decreases, dimethylmercury (Me_2Hg : $\text{C}_2\text{H}_6\text{Hg}$) shifts to MeHg , which is less volatile than the former and thus retained more efficiently in marine systems (i.e. water and sediments) and organisms (Fagerstrom and Jernelev 1972). Furthermore, the combination between OA and Hg contamination is expected to increase fish gill permeability (Drummond et al. 1974; Rodgers and Beamish 1983) and increased Hg concentration within tissues due to higher MeHg bioavailability (Miller and Akagi 1979).

Thus, it is expected that marine organisms already exposed to contamination by heavy metals could be under greater risk when climate change foreseen for the end of this century come into the big picture.

1.4. Oxidative stress under climate change

Aerobic metabolic processes (i.e. respiration and photosynthesis), which require molecular O_2 to produce energy (i.e. Adenosine triphosphate – ATP), inevitably lead to the formation of ROS, due to electron escape from the electron transport chain (ETC; Fig. 6) (Cadenas 1989; Lushchak 2011; Pamplona and Costantini 2011). The reduction of molecular O_2 to H_2O , produces reactive intermediates (i.e. ROS), such as the superoxide ion (O_2^-), hydrogen peroxide (H_2O_2) and hydroxyl radical (HO^\bullet) (Canesi 2015; Lesser 2006; Lushchak 2011; Sies 1993). Each one of them is intrinsically-linked and has the ability to enter in other reactions, with devastating consequences for all biological systems. For instance, O_2^- can either be reduced into H_2O_2 , which can occur spontaneously or via superoxide dismutase (SOD) activity, or react with reactive nitrogen species (RNS), such as nitric oxide (NO) to produce peroxynitrite ions ($OONO^-$) and HO^\bullet , responsible for protein, lipid and DNA modification (González et al. 2015). Furthermore, due to the lack of charge, H_2O_2 can easily pass across biological membranes, damaging cellular constituents outside its point of synthesis, ultimately triggering programmed cell death pathways (Lesser 2006). Additionally, H_2O_2 can also be further reduced into HO^\bullet , either by electron transfer or via Fenton reaction [conversion of iron (Fe) from ferrous (Fe(II)) to ferric (Fe(III)) form], the most damaging of ROS, due to its high reactivity with lipids, proteins and nucleic acids (González et al. 2015; Lesser 2006).

Under normal conditions, marine organisms display a powerful set of antioxidant mechanisms (i.e. enzymatic and non-enzymatic), as well as protein repair and removal mechanisms, to counterbalance ROS production and avoid oxidative stress⁵ and consequently damage (Lushchak 2011). Nonetheless, when exposed to stressful environments, such as increasing temperatures, decreasing pH and contamination, there is an overproduction of ROS (i.e. above the naturally occurring levels), and thus, the efficiency of their antioxidant systems may become compromised.

⁵ Imbalance between oxidants and antioxidants, in favor of the former

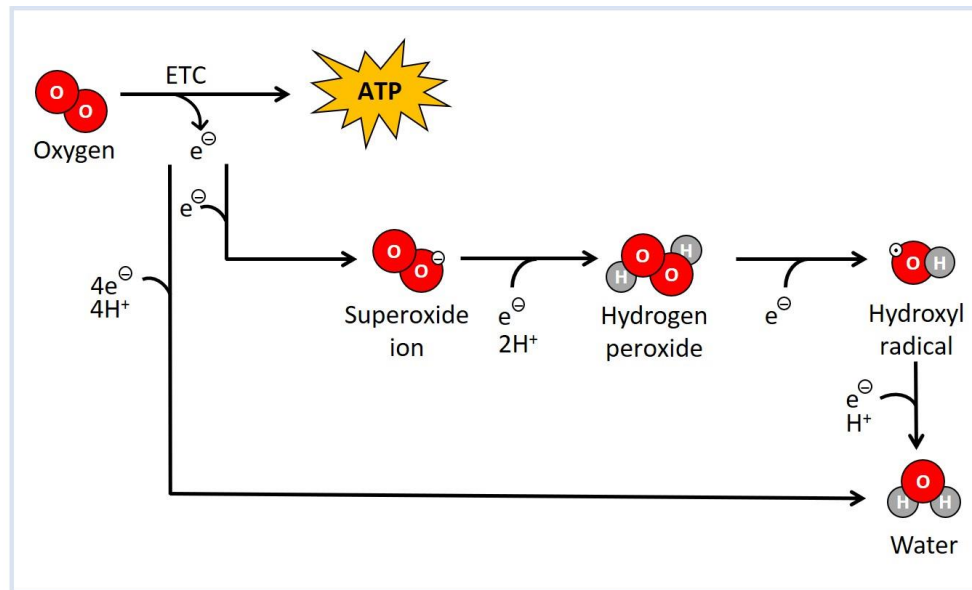


Figure 6 – Routes of oxygen (O₂) metabolism in marine organisms and reactive oxygen species (ROS) formation. Electron transport chain (ETC) as an electron (e⁻) source during the reduction of O₂ to produce adenosine triphosphate (ATP). One-electron reduction sequencing causing the formation of ROS, such as: superoxide ion (O₂⁻), hydrogen peroxide (H₂O₂) and hydroxyl radical (OH•), with water (H₂O) as a final product. Four-electron reduction of O₂ to form H₂O (adapted from Lushchak 2011).

1.4.1. Protective mechanisms

The increase in ROS will trigger organisms defense mechanisms - enzymatic and non-enzymatic antioxidants (Bartosz 2003). The term antioxidant refers to any substance that delays or inhibit the oxidation of biological molecules, by reacting with ROS (Halliwell and Gutteridge 2007). Specifically, ROS which have unpaired electrons steal an electron from a stable molecule, creating a new free radical (i.e. the oxidized molecule become a free radical itself), initiating a chemical chain reaction (each new free radical will react with stable molecules), and instigating oxidative stress (Fig. 7). Nonetheless, and to avoid oxidative damage, the antioxidant donates its free electrons to a ROS, ending the chain reaction (Gould 2003).

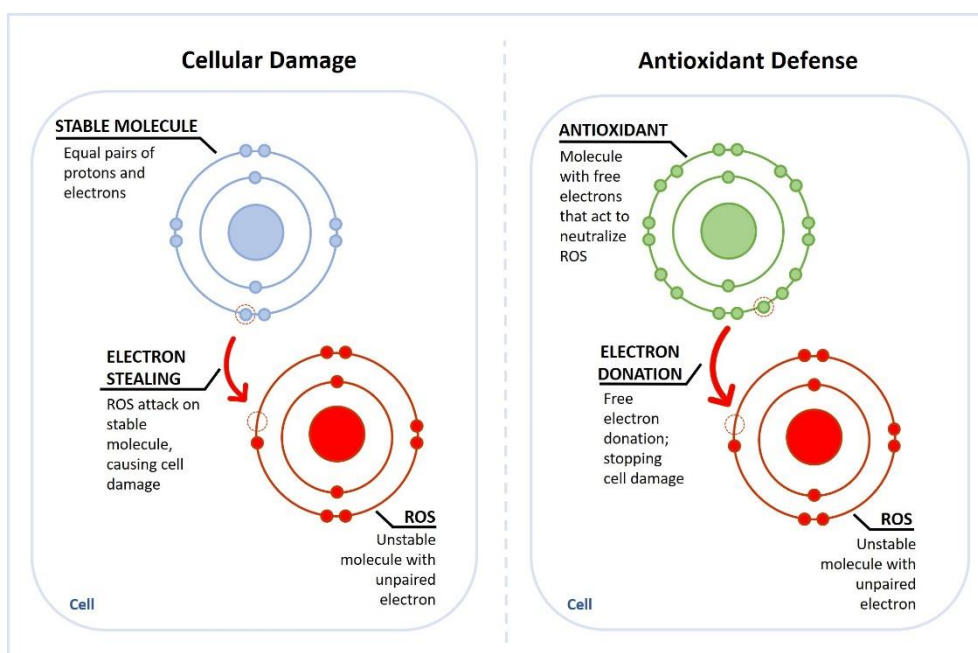


Figure 7 – Schematics of reactive oxygen species (ROS) action within the cell: electron stealing of a stable molecule, causing cell damage (left side); electron donation by an antioxidant, avoiding cell damage (right side).

Therefore, antioxidants are considered the first line of defense against oxidative stress, incorporating both low and high molecular mass antioxidants (Kappus 1987; Lesser 2006; Livingstone 2001). Low molecular mass antioxidants or non-enzymatic ROS scavengers include ascorbic acid (vitamin C), tocopherol (vitamin E), uric acid, carotenoids, flavonoids, alkaloids and glutathione (GSH, a by-product of the action of glutathione reductase (GR) that may also serve as a cofactor for glutathione-dependent antioxidant enzymes) (Asada 1987; Bartosz 2003; Cadenas 1989; Lesser 2006; Sies 1993). High molecular mass antioxidants consist of specific proteins (i.e. enzymatic antioxidants) that play a key role in the oxidative stress defense response, such as: (i) superoxide dismutase (SOD; EC 1.15.1.1), considered as the first enzyme acting against ROS, which converts O_2^- in H_2O_2 ; (ii) catalase (CAT; EC 1.11.1.6) that detoxify H_2O_2 , producing H_2O and O_2 ; (iii) glutathione peroxidase (GPx; EC 1.11.1.9), which uses the antioxidant GSH to eliminate H_2O_2 , producing H_2O and oxidized glutathione (GSSG); and (iv) glutathione-S-transferase (GST; EC 2.5.1.18), which play a key role in the second phase of the detoxification process, that in association with GSH enable the excretion of xenobiotics (see Fig. 8) (Lesser 2006; Sies 1993; Sies 1997; Wang et al. 2000). Additionally, high molecular mass

antioxidants are also represented by non-specific proteins, such as metallothionein and ferritin, that inhibit ROS damage through metal-binding (e.g. iron and copper) (Lushchak 2011).

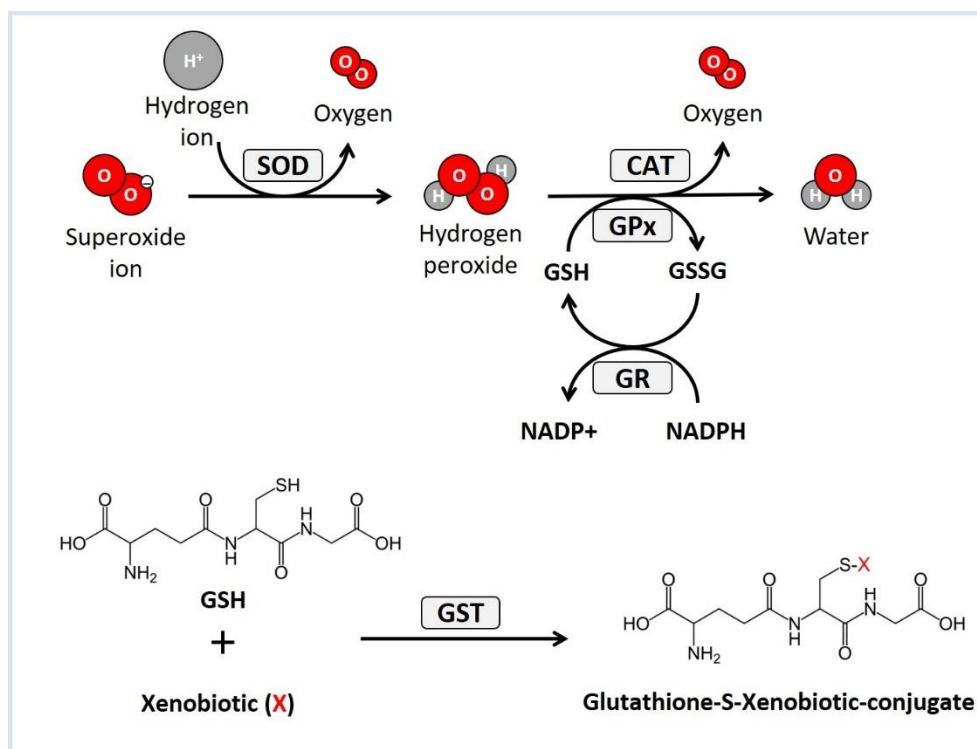


Figure 8 – Schematics of the activity of superoxide dismutase (SOD), catalase (CAT) and glutathione peroxidase (GPx) against reactive oxygen species (ROS), and glutathione S-transferase (GST) against xenobiotics.

Furthermore, marine organisms also display a powerful protein repair and removal mechanism. Protein activity is known to be temperature-dependent, additionally environmental stress, can also change protein stability (Alexandrov 1969; Hazel and Prosser 1974; Somero 1995). Therefore, when exposed to environmental disturbances, marine organisms harbor a heat shock response (HSR), which consists in the synthesis of molecular chaperones responsible for “house-keeping” functions in the cell - heat shock proteins (HSPs)⁶ (Sørensen et al. 2003). Specifically, HSPs are involved in processes such as (i) repair and refold of denatured proteins; (ii) prevention of further protein unfolding and aggregation; and (iii) removal of damaged or denatured proteins

⁶ Also called stress proteins, and their expression stress response, as they respond to other stresses besides temperature

(Feder and Hofmann 1999; Tomanek 2010). This highly conserved chaperones can be constitutively expressed (i.e. heat shock cognate (HSC)) or induced by a variety of stressors, that can either be intrinsic (i.e. aging and genetic stress – mutations) or extrinsic factors such as, temperature extremes, hypoxia, salinity and heavy metal contamination (for review see Sørensen et al. 2003).

Additionally, several families of HSPs have been classified, given their molecular weight in kilodalton (kDa), into six major families HSP100, HSP90, HSP70, HSP60 and HSP40 and small HSPs (sHSPs, molecular weight of 12-43 kDa) (Bakthisaran et al. 2015; Lindquist 1986; Sørensen et al. 2003). The most highly conserved and abundant HSP is the HSP70, found in both eukaryotes and prokaryotes. They have approximately 50% amino acid similarity between *Escherichia coli* and *Homo sapiens*, and approximately 70% between *Drosophila melanogaster* and *H. sapiens* (Lindquist 1986; Schlesinger 1990). They play a key-role in normal cell growth - assuring cell viability – and are involved in protein-protein interactions, such as protein transport from their site of synthesis until their final destination (Craig and Gross 1991; Lindquist 1986). Moreover, and as explained above, they are also involved in stress response mechanisms (i.e. protein repair and ROS scavenging).

When proteins are irreversibly damaged/denatured, they are degraded by intracellular proteases and permanently eliminated in a process known as ubiquitination (Hanna et al. 2007). Ubiquitin is one of the most physically stable sHSP (with 8.5 kDa), withstanding temperatures above 85°C and pH values between 1-13 units (Lenkinski et al. 1977). Ubiquitin have a main role in maintaining cellular homeostasis once it targets damaged proteins for degradation by the proteasome, rendering proteins into small polypeptides, and modulating protein-protein interactions (i.e. coordinating protein location and activating/inactivating proteins) (for reviews see Finley and Chau 1991; Hershko and Ciechanover 1992; Rechsteiner 1987).

It has been proposed that the HSR and ubiquitination mechanisms are complementary when dealing with environmental stress. Therefore, when HSPs fail to maintain functional protein conformation (i.e. preventing folding and aggregation), ubiquitin targets irreversibly damaged proteins and remove them through protease-targeting activity (Bond et al. 1988; Hanna et al. 2007; Sørensen et al. 2003).

1.4.2. Cellular damage

When the abovementioned physiological response fails to balance the antioxidant-prooxidant levels, ROS excess will instigate oxidative damage - lipid peroxidation, protein degradation and DNA strand breaks. Lipid peroxidation (LPO) is one of the most widespread mechanisms of cellular injury and is caused by the reaction of ROS (specifically HO[•]) with lipids (Sachdeva et al. 2014). Specifically, LPO consists in a three-phase process: (i) initiation; (ii) propagation; and (iii) termination. During the initiation phase, polyunsaturated fatty acids (PUFA) are oxidized by ROS, through carbon atoms attack near the double bonds, transforming the lipid molecule into a lipid radical. Moreover, the highly unstable lipid radical reacts with O₂, forming lipid peroxides, that in turn react with neighbor lipids in a radical chain reaction, propagating the lipid degradation process. Finally, the termination step occurs when lipid molecules are broken into LPO by-products such as malondialdehyde (MDA), 4-hydroxynonenal (4-HNE) and 4-hydroxy-2-alkenal, highly mutagenic and genotoxic substances (Henkel and Solomon 2018; Repetto et al. 2012; Sies et al. 1985).

Encompassing about 68% of total dry weight in cells and tissues, proteins are a major target for oxidative damage. Thus, protein damage occurs due to site-specific amino acid modifications (protein carbonylation), peptide chain fragmentation and increased susceptibility to degradation and removal (Davies 2003). Additionally, and taking into consideration that the organisms proteome⁷ is responsible for genome repair, replication and expression, it is expected that when affecting key proteins, environmental stress will, almost undeniably impair DNA structure, causing DNA damage (Gueranger et al. 2014; Krisko and Radman 2013). Furthermore, the direct interaction of ROS, will also react with DNA, causing single-strand breaks, base-pair mismatches, base modification/oxidation (8-oxoguanine), ultimately leading to mutations (Krisko and Radman 2013; Peacock et al. 2014).

⁷ Entire set of proteins that is expressed by a genome

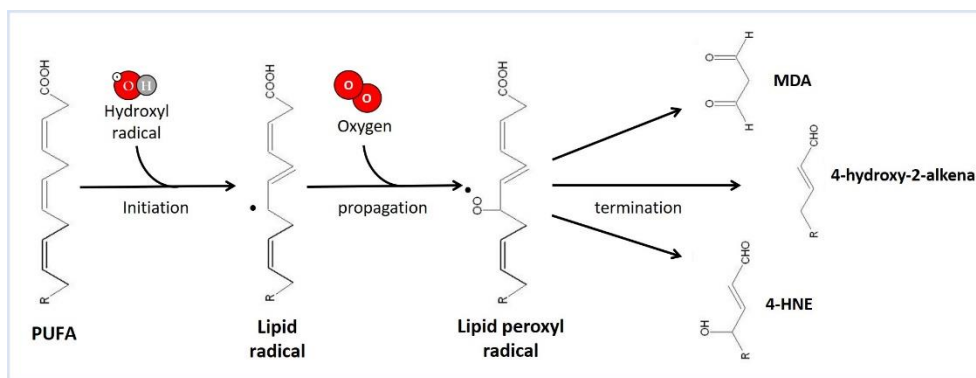


Figure 9 – Lipid peroxidation of polyunsaturated fatty acids (PUFA)

1.4.3. Conventional biomarkers and marine tree of life

Since the discovery of O_2 toxicity by Gerschman et al. (1956), the scientific knowledge on the effects of ROS increased dramatically, specifically due to its harmful effects on human health (i.e. cancer, cardiovascular and neurological diseases - Parkinson and Alzheimer's - and aging) (Hoeijmakers 2003; Pizzino et al. 2017). Furthermore, and once O_2 is a common feature of all living organisms (i.e. photosynthetic and air-breathing individuals), the toxic effects of ROS on marine life and their oxidative stress responses have also been under the spotlight of the scientific community. In fact, the google scholar search for “oxidative stress” and “marine” had a four-fold increase over the last 8 years (i.e. > 200.000 publication in 2018), when compared to Abele et al. (2012) in 2010 (50.000 publications).

Furthermore, from that bulk of the knowledge, hundreds of studies were conducted on the effects of climate change (i.e. OW and OA) on marine biota (e.g. Anacleto et al. 2014; Cardoso et al. 2017; Jesus et al. 2018; Pimentel et al. 2015; Rosa et al. 2012), whereas of those, more than 20 focuses on the combination of ocean warming and/or acidification with contamination (e.g. Coppola et al. 2017; Coppola et al. 2018; Freitas et al. 2017b; Maulvault et al. 2017; Moreira et al. 2016).

Owing to its responsiveness to various forms of stresses, the response of enzymatic (especially SOD, CAT and GST) and non-enzymatic antioxidants (e.g. GST), as well as the heat-shock response are considered widespread biomarkers for environmental change and toxicology (Boukadida et al. 2017; Priya et al. 2017; Zhou et al. 2010). Furthermore, and considering that their induction is, in most cases, more sensitive to environmental disturbances than the most

commonly used indices (e.g. fitness and reproduction), their usefulness as biomarkers is now widely recognized. Therefore, over the last few decades a considerable amount of scientific knowledge has accumulated on the physiological defense mechanisms of marine organisms as a means to avoid deleterious effects (i.e. oxidative damage, especially LPO).

The bulk of these studies have focused on the phylum Cnidaria, followed by Mollusca, Chordata, and Arthropoda. Cnidarian have been extensively studied, especially those that harbor zooxanthellae in their tissues (i.e. symbiotic corals). Specifically, climate change is expected to cause coral bleaching (Glynn 1996) due to the overproduction of ROS in the symbiont photosystem II (Downs et al. 2002; Lesser 1997; Mydlarz et al. 2009), disrupting the symbiosis between zooxanthellae and host, ultimately causing protein and DNA damage in the host (Downs et al. 2000; Lesser and Farrell 2004). Nevertheless, the bulk of these studies focused on reef-building coral species (e.g. Agostini et al. 2016; Downs et al. 2013; 2000; Griffin and Bhagooli 2004; Griffin et al. 2006), while studies on soft corals remain scarce (Madeira et al. 2015; Mydlarz and Jacobs 2006; Wiens et al. 2000).

Furthermore, the fact that mollusks, especially bivalves, have received tremendous attention is due to their economic value - human consumption – and to the fact that being sedentary organisms, with low mobility, they are more exposed to abiotic change and pollution, accumulating high levels of contaminants in their tissues, being useful sentinels to environmental disturbances (Anacleto et al. 2014; Freitas et al. 2015; Matozzo et al. 2013). In fact, exposure to OW and contamination conditions are expected to cause lipid peroxidation in *Mytillus galloprovincialis*, as increasing temperatures will also increase clams susceptibility towards contamination (Coppola et al. 2017; 2018; Freitas et al. 2017a; Nardi et al. 2017). Nonetheless we should bear in mind that the antioxidant response is species-specific and dependent upon the stressor to which organisms are exposed (Kumar et al. 2017; Matozzo et al. 2013; Sui et al. 2017). Thus, and while *M. galloprovincialis* seems to be at greater risk due to warming, *Crassostrea virginica* and *Mercenaria mercenaria* do not seem to be affected by the combination of warming and acidification (Matozzo et al. 2013). Furthermore, and if we consider that warming is also changing species distribution ranges, it is expected that native species will compete with invasive species for the same resources (i.e. habitat, food), with the latter displaying greater ability in maintaining their physiological functions over a wide range of temperatures. Thus, it is expected that invasive species will have better chances of survival as they adopt strategies to cope with increasing

temperatures (i.e. valve closure), which are efficient in avoiding oxidative stress - at least during short-term stressful events (Anacleto et al. 2014).

Furthermore, due to their high ecological relevance and importance as a food source for human consumption, fishes have also been the focus of considerable attention, especially the embryonic and juvenile stages. This is due to the fact that early life stages need to be particularly cautious in regulating their acid-base balance, to avoid other downstream consequences such as impaired growth (Skjærven et al. 2013). This is particularly true when exposed to climate-change related variables (i.e. OW and OA), once the upsurge of lipid damage and protein denaturation (i.e. increased HSP levels) seems to be a major cause of reduced growth and increased skeletal deformities, reducing larvae survival - compromising recruitment success (Madeira et al. 2017; Pimentel et al. 2015). Nonetheless, studies focusing Chordata phylum are assembled on bone fishes (i.e. class Actinopterygii), while cartilaginous fishes have received less attention (Rosa et al., 2016).

Lastly, it is worth noting that the majority of the studies conducted so far only focus on assessing the climate-related effects during an individual's lifetime (i.e. within-generation effects), ignoring the potential for evolutionary adaptation. In fact, to the best of our knowledge, only two studies were conducted to infer the trans- (Gibbin et al. 2017) and multi-generational (Chakravarti et al. 2017) ROS production on a marine polychaeta (i.e. *Ophryotrocha labronica*) and a dinoflagellate (i.e. *Symbiodinium spp.*), respectively. These studies are extremely important to measure the parental conditioning to global change – positive/negative carry-over effects in the offspring - and to infer the resilience of the future generations.

1.5. General Objectives

Acknowledging that the world's climate is changing at an unprecedented and faster rate than ever recorded in human history, with devastating effects on the world's ocean, it is of extreme importance to improve the scientific knowledge of those effects on marine organisms. Furthermore, and while physiological studies have been in the spotlight, studies on the biochemical pathways behind species tolerance have still some space for improvement. Therefore, the main goal of the present thesis was to undertake a comprehensive analysis of the biochemical mechanisms of marine organisms - invertebrate (*Veretillum cynomorium*, *Gammarus locusta*) and vertebrate species (*Argyrosomus regius*, *Chiloscyllium plagiosum*, *Scyliorhinus canicula*) - that may or may not allow them to cope with the conditions of the oceans of tomorrow.

Specifically, this thesis is divided in two parts:

- (i) part one - composed by two chapters, consisting on one scientific paper published in a peer-review international scientific journal and another currently under review. This part focus on the single- and trans-generational effects of ocean acidification alone.
- (ii) part two - composed by three chapters, consisting on two scientific papers published in peer-review international scientific journals and another in preparation. This part focuses on the combined effect of climate change-related variables and contamination. Even though single-stressor studies are of extreme importance to understand the role of a specific stressor, to accurately predict the effects of climate change, we ought to consider the interaction between stressors.

Furthermore, the specific objective of each chapter is presented below.

Part One: Within- and trans-generational effects under ocean acidification

Chapter 2

This chapter aimed to investigate sharks' ability to undergo oxidative stress under OA conditions. To that end, a comprehensive analysis of the oxidative stress-related responses comprising the activity of individual antioxidant enzymes and non-enzymatic molecules, as well as HSR and Ub levels and lipid, protein, and DNA damage levels were measured on recently-

hatched tropical sharks (whitespotted bamboo shark *C. plagiosum*) exposed to CO₂ levels predicted for 2100 ($p\text{CO}_2 \sim 900 \mu\text{atm}$). Ultimately, we discussed if the variety of physicochemical contexts experienced during shark evolution could allow these animals to successfully offset OA-induced oxidative stress.

Chapter 3

To fill the gap of knowledge on the transgenerational effects of OA on the biochemical defense mechanisms of the amphipod *G. locusta*, the aim of this study was to expose, for the first time, this amphipod to OA conditions predicted for the end of this century ($\Delta p\text{CO}_2 \sim 400\text{-}500 \mu\text{atm}$) for two generations (F0 and F1). In this context, we assessed the oxidative damage markers - lipid peroxidation and DNA damage - the HSP and Ub levels, as well as oxidative stress enzymes (SOD, CAT, GPx and GST) and total antioxidant capacity (TAC).

Part two: Biochemical responses under a multiple stressor environment

Chapter 4

The chapter 4 aimed to fill the gap of knowledge on the combined effects of temperature and acidification on soft corals. To that end the physiological mechanisms that may enable *V. cymnorum* to withstand future OW and OA conditions were investigated. Specifically, the antioxidant enzyme activities - GST and CAT - lipid peroxidation and heat shock response (HSP70/HSC70) were analysed.

Chapter 5

The aim of the chapter 5 study was to evaluate, for the first time, the accumulation of Hg in the shark *S. canicula* capsule and embryos (i.e. brain, gills, muscle, liver and stomach tissues) to determine the oxidative stress-related responses under mercury chloride (HgCl₂) contamination and warming conditions. Specifically, after 1-week exposure the oxidative damage markers - LPO and DNA damage - the oxidative stress enzymes - SOD, CAT, GPx, GST and AChE - as well as total antioxidant capacity and protein repair and removal mechanisms - HSP and Ub - were evaluated.

Chapter 6

Lastly, chapter 6 aimed to fill the gap of knowledge on the effects of the combination between climate-related stress conditions (i.e. OA and OW) and contamination (MeHg) on the commercially important fish *A. regius*. Therefore, after 30-day acclimation experiment under future ocean conditions, we investigated how interacting stressors modulate physiological impacts and elicited responses. To this end, we gauged how organ-dependent Hg accumulation (gills, liver and muscle) was modulated by warming and acidification and measured the direct consequences of isolated and combined stressor exposure at organism (survival rates and condition index) and cellular (lipid peroxidation, i.e. MDA) levels. Moreover, to provide a comprehensive depiction of the physiological state, the responses of antioxidant enzymatic - SOD, CAT and GST - and molecular chaperone - Hsp70 - machineries were also evaluated.

1.6. References

- Abele D, Vázquez-Medina JP, Zenteno-Savín T (2012) Introduction to oxidative stress in aquatic ecosystems. In: Abele D, Vázquez-Medina JP, Zenteno-Savín T (eds) Oxidative stress in aquatic ecosystems. Wiley-Blackwell, Oxford, pp 1-6
- Alexandrov VY (1969) Conformational flexibility of proteins, their resistance to proteinases and temperature conditions of life. *Currents in Modern Biology* 3:9-19
- Allen RC (2010) The British Industrial Revolution in Global Perspective. *Proceedings of the British Academy* 167:199-224
- Anacleto P, Maulvault AL, Lopes VM, Repolho T, Diniz M, Nunes ML, Marques A, Rosa R (2014) Ecophysiology of native and alien-invasive clams in an ocean warming context. *Comparative Biochemistry and Physiology, Part A: Molecular and Integrative Physiology* 175:28-37
- Asada K (1987) Production and scavenging of active oxygen in photosynthesis. *Photoinhibition* 227-287
- Bakthisaran R, Tangirala R, Rao CM (2015) Small heat shock proteins: Role in cellular functions and pathology. *Biochimica et Biophysica Acta - Proteins and Proteomics* 1854:291-319
- Bartosz G (2003) Total antioxidant capacity. In: Spiegel HE, Nowacki G, Hsiao K-J (eds). *Advances in clinical chemistry*, vol 37. Academic press, California, USA, pp 220-272
- Baumann H, Talmage SC, Gobler CJ (2012) Reduced early life growth and survival in a fish in direct response to increased carbon dioxide *Nature Climate Change* 2:38-41
- Bellard C, Thuiller W, Leroy B, Genovesi P, Bakkenes M, Courchamp F (2013) Will climate change promote future invasions? *Global Change Biology* 19:3740-3748
- Berntssen MHG, Aatland A, Handy RD (2003) Chronic dietary mercury exposure causes oxidative stress, brain lesions, and altered behaviour in Atlantic salmon (*Salmo salar*). *Aquatic Toxicology* 65 55-72
- Black BC, Weisel GJ (2010) *Global Warming*. Greenwood, Santa Brabara, California
- Bodaly RA, Rudd JWM, Fudge RJP, Kelly CA (1993) Mercury concentrations in fish related to size of remote Canadian shield lakes. *Canadian Journal of Fisheries and Aquatic Sciences* 50:980-987

- Boening DW (2000) Ecological effects, transport, and fate of mercury: a general review. *Chemosphere* 40:1335–1351
- Bond U, Agell N, Haas AL, Redman K, Schlesinger MJ (1988) Ubiquitin in stressed chicken embryo fibroblast. *Journal of Biological Chemistry* 263:2384–2388
- Bonsdorff E, Blomqvist EM, Mattila J, Norkko A (1997) Coastal eutrophication: causes, consequences and perspectives in the archipelago areas of the northern Baltic Sea. *Estuarine, Coastal and Shelf Science* 44:63–72
- Boukadida K, Cachot J, Clérandeaux C, Gourves P-Y, Banni M (2017) Early and efficient induction of antioxidant defense system in *Mytilus galloprovincialis* embryos exposed to metals and heat stress. *Ecotoxicology and Environmental Safety* 138:105–112
- Boyd RS (2010) Heavy metal pollutants and chemical ecology: exploring new frontiers. *Journal of Chemical Ecology* 36:46–58
- Braune B, Chételat J, Amyot M, Brown T, Clayden M, Evans M, Fisk A, Gaden A, Girard C, Hare A, Kirk J, Lehnher I, Letcher R, Loseto L, Macdonald R, Mann E, McMeans B, Muir D, O'Driscoll N, Poulain A, Reimer K, Stern G (2015) Mercury in the marine environment of the Canadian Arctic: Review of recent findings. *Science of the Total Environment* 509-510:67-90
- Bryan GW, Darracott A (1979) Bioaccumulation of marine pollutants. *Philosophical Transactions of the Royal Society B* 286:483-505
- Byrne M (2011) Impact of ocean warming and ocean acidification on marine invertebrate life history stages: vulnerability and potential for persistence in a changing ocean. *Oceanography Marine Biology* 49:1-42
- Cadenas E (1989) Biochemistry of oxygen toxicity. *Annual Reviews of Biochemistry* 58:79-110
- Cairns JJ, Heath AG, Parker BC (1975) The effects of temperature upon the toxicity of chemicals to aquatic organisms. *Hydrobiologia* 41:135-171
- Caldeira K, Wickett ME (2005) Ocean model predictions of chemistry changes from carbon dioxide emissions to the atmosphere and ocean. *Journal of Geophysical Research* 110:C09S04
- Canário J, Branco V, Vale C (2007) Seasonal variation of monomethylmercury concentrations in surface sediments of the Tagus Estuary (Portugal). *Environmental Pollution* 148:380–383

- Canesi L (2015) Pro-oxidant and antioxidant processes in aquatic invertebrates. *Annals of the New York Academy of Sciences* 1340:1-7
- Cao L, Caldeira K, Jain AK (2007) Effects of carbon dioxide and climate change on ocean acidification and carbonate mineral saturation. *Geophysical Research Letters* 34:L05607
- Cardoso PG, Grilo TF, Dionísio G, Aurélio M, Lopes AR, Pereira R, Pacheco M, Rosa R (2017) Short-term effects of increased temperature and lowered pH on a temperate grazer-seaweed interaction (*Littorina obtusata*/*Ascophyllum nodosum*). *Estuarine Coastal and Shelf Science* 197:35-44
- Carpenter KE, Abrar M, Aeby G, Aronson RB, Banks S, Bruckner A, Chiriboga A, Cortés J, Delbeek JC, Devantier L, Edgar GJ, Edwards AJ, Fenner D, Guzmán HM, Hoeksema BW, Hodgson G, Johan O, Licuanan WY, Livingstone SR, Lovell ER, Moore JA, Obura DO, Ochavillo D, Polidoro BA, Precht WF, Quibilan MC, Reboton C, Richards ZT, Rogers AD, Sanciangco J, Sheppard A, Sheppard C, Smith J, Stuart S, Turak E, Veron JE, Wallace C, Weil E, Wood E (2008) One-third of reef-building corals face elevated extinction risk from climate change and local impacts. *Science* 321:560-563
- Casida JE (2009) Pest toxicology: the primary mechanisms of pesticide action. *Chemical Research in Toxicology* 22:609-619
- Cattano C, Claudet J, Domenici P, Milazzo M (2018) Living in a high CO₂ world: a global meta-analysis shows multiple trait-mediated fish responses to ocean acidification. *Ecological Monographs*
- Chakravarti LJ, Beltran VH, van Oppen MJH (2017) Rapid thermal adaptation in photosymbionts of reef-building corals. *Global Change Biology* 23:4675-4688
- Clarkson TW, Magos L (2006) The toxicology of mercury and its chemical compounds. *Critical Reviews in Toxicology* 36:609-662
- Clarkson TW, Magos L, Myers GJ (2003) The toxicology of mercury – current exposures and clinical manifestations. *New England Journal of Medicine* 349:1731-1737
- Clements JC, Hunt HL (2014) Influence of sediment acidification and water flow on sediment acceptance and dispersal of juvenile soft-shell clams (*Mya arenaria* L.). *Journal of Experimental Marine Biology and Ecology* 453:62-69
- Coccini T, Randine G, Candura SM, Nappi RE, Prockop LD, Manzo L (2000) Low-level exposure to methylmercury modifies muscarinic cholinergic receptor binding

- characteristics in rat brain and lymphocytes: physiologic implications and new opportunities in biologic monitoring. *Environmental Health Perspectives* 108:29–33
- Collins M, Knutti R, Arblaster J, Dufresne J-L, Fichefet T, Friedlingstein P, Gao X, Gutowski WJ, Johns T, Krinner G, Shongwe M, Tebaldi C, Weaver AJ, Wehner M (2013) Long-term Climate Change: Projections, Commitments and Irreversibility. In: Stocker TF, Qin D, Plattner G-K, Tignor M, Allen SK, Boschung J, Nauels A, Xia Y, Bex V and Midgley PM (eds.). *Climate Change 2013: The Physical Science Basis. Contribution of Working Group I to the Fifth Assessment Report of the Intergovernmental Panel on Climate Change* Cambridge University Press, Cambridge, United Kingdom and New York, NY, USA
- Connell SD, Doubleday ZA, Foster NR, Hamlyn SB, Harley CDG, Helmuth B, Kelaher BP, Nagelkerken I, Rodgers KL, Sarà G, Russell BD (2018) The duality of ocean acidification as a resource and a stressor. *Ecology* 99:1005-1010
- Connell SD, Kroeker KJ, Fabricius KE, Kline DI, Russell BD (2013) The other ocean acidification problem: CO₂ as a resource among competitors for ecosystem dominance. *Philosophical Transactions of the Royal Society B* 368:20120442
- Coppola F, Almeida A, Henriques B, Soares AMVM, Figueira E, Pereira E, Freitas R (2017) Biochemical impacts of Hg in *Mytilus galloprovincialis* under present and predicted warming scenarios. *Science of the Total Environment* 601-602:1129-1138
- Coppola F, Almeida A, Henriques B, Soares AMVM, Figueira E, Pereira E, Freitas R (2018) Biochemical responses and accumulation patterns of *Mytilus galloprovincialis* exposed to thermal stress and Arsenic contamination. *Ecotoxicology and Environmental Safety* 147:954-962
- Costello MJ, Smith M, Fraczek W (2015) Correction to surface area and the seabed area, volume, depth, slope, and topographic variation for the world's Seas, Oceans, and Countries. *Environmental Science and Technology* 49:7071-7072
- Craig EA, Gross CA (1991) Is hsp70 the cellular thermometer? *Trends in Biochemical Sciences* 16:135-140
- Davies AG (1978) Pollution studies with marine plankton; Part II. Heavy metals. *Advances in Marine Biology* 15:381–508
- Davies MJ (2003) Singlet oxygen-mediated damage to proteins and its consequences. *Biochemical and Biophysical Research Communications* 305:761-770

- Dean JB (2010) Hypercapnia causes cellular oxidation and nitrosation in addition to acidosis: implications for CO₂ chemoreceptor function and dysfunction. *Journal of Applied Physiology* 108:1786-1795
- Delille B, Harlay J, Zondervan I, Jacquet S, Chou L, Wollast R, Bellerby RGJ, Frankignoulle M, Borges AV, Riebesell U, Gattuso J-P (2005) Response of primary production and calcification to changes of *p*CO₂ during experimental blooms of the coccolithophorid *Emiliania huxleyi*. *Global Biogeochemical Cycles* 19:GB2023
- Dijkstra JA, Buckman KL, Ward D, Evans DW, Dionne M, Chen CY (2013) Experimental and natural warming elevates mercury concentrations in estuarine fish. *PLoS One* 8:e58401
- Dixson DL, Munday PL, Jones GP (2010) Ocean acidification disrupts the innate ability of fish to detect predator olfactory cues. *Ecology Letters* 13:68-75
- Doney SC, Fabry VJ, Feely RA, Kleypas JA (2009) Ocean acidification: The other CO₂ problem. *Annual Review of Marine Science* 1:169-192
- Downs CA, Fauth JE, Halas JC, Dustan P, Bemiss J, Woodley CM (2002) Oxidative stress and seasonal coral bleaching. *Free Radical Biology and Medicine* 33:533-543
- Downs CA, Mueller E, Phillips S, Fauth JE, Woodley CM (2000) A molecular biomarker system for assessing the health of coral (*Montastraea faveolata*) during heat stress. *Marine Biotechnology* 2:533-544
- Drinkwater K, Hunt G, Lehodey P, Lluch-Cota S, Murphy EJ, Sakurai Y, Schwing F, Beaugrand G, Sundby S (2010) Climate forcing on marine ecosystems. In: Barange M, Field JG, Harris RP, Hofmann EE, Perry RI, Werner FE (eds) *Marine ecosystems and global change*. Oxford University Press, United Kingdom,
- Drummond RA, Olson GF, Batterman AR (1974) Cough response and uptake of mercury by brook trout, *Salvelinus fontinalis*, exposed to mercuric compounds at different hydrogen-ion concentrations *Transactions of the American Fisheries Society* 103:244-249
- Dupont S, Thorndyke MC (2009) Impact of CO₂-driven ocean acidification on invertebrates early life-history - What we know, what we need to know and what we can do. *Biogeosciences Discussions* 6:3109-3131
- Eddy FB, Handy RD (2012) Ecological and environmental physiology of fishes. In: Burggren W (ed) *Ecological and environmental physiology of fishes*. Oxford University Press, United Kingdom

- Edwards M, Richardson AJ (2004) Impact of climate change on marine pelagic phenology and trophic mismatch. *Nature* 430:881-884
- Fabry VJ, Seibel BA, Feely RA, Orr JC (2008) Impacts of ocean acidification on marine fauna and ecosystem processes. *ICES Journal Marine Science* 65:414-432
- Fagerstrom T, Jernelov A (1972) Some aspects of the quantitative ecology of mercury. *Water Research* 6:1193-1202
- Feder ME, Hofmann GE (1999) Heat-shock proteins, molecular chaperones, and the stress response: evolutionary and ecological physiology. *Annual Review of Physiology* 61:243-282
- Finley D, Chau V (1991) Ubiquitination. *Annual Review in Cell Biology* 7:26-69
- Freitas R, Almeida Â, Calisto V, Velez C, Moreira A, Schneider RJ, Esteves VI, Wrona FJ, Soares AM, Figueira E (2015) How life history influences the responses of the clam *Scrobicularia plana* to the combined impacts of carbamazepine and pH decrease. *Environmental Pollution* 202:205-214
- Freitas R, Coppola F, Henriques B, Wrona F, Figueira E, Pereira E, Soares AMVM (2017a) Does pre-exposure to warming conditions increase *Mytilus galloprovincialis* tolerance to Hg contamination? *Comparative Biochemistry and Physiology, Part C: Toxicology and Pharmacology* 203:1-11
- Freitas R, de Marchi L, Moreira A, Pestana JLT, Wrona FJ, Figueira E, Soares AMVM (2017b) Physiological and biochemical impacts induced by mercury pollution and seawater acidification in *Hediste diversicolor*. *Science of the Total Environment* 595:691-701
- Fuiman LA, Cowan JH, Smith ME, O'Neal JP (2005) Behavior and recruitment success in fish larvae: variation with growth rate and the batch effect. *Canadian Journal of Fisheries and Aquatic Sciences* 62:1337-1349
- Fuiman LA, Rose KA, Cowan JH, Smith EP (2006) Survival skills required for predator evasion by fish larvae and their relation to laboratory measures of performance. *Animal Behaviour* 71:1389-1399
- Fung CN, Lam JC, Zheng GJ, Connell DW, Monirith I, Tanabe S, Richardson BJ, Lam PK (2004) Mussel-based monitoring of trace metal and organic contaminants along the east coast of China using *Perna viridis* and *Mytilus edulis*. *Environmental Pollution* 127:203-216

- Gattuso J-P, Hansson L (2011) Ocean Acidification: background and history. In: Gattuso J-P, Hansson L (eds) Ocean Acidification. Oxford University Press, Oxford, New York, pp 1-17
- Gerschman R, Gilbert DL, Nye SW, Dwyer P, Fenn WO (1956) Oxygen poisoning and X-irradiation: a mechanism in common. *Science* 119:623-626
- Gibbin EM, Chakravarti LJ, Jarrold MD, Christen F, Turpin V, N'Siala GM, Blier PU, Calosi P (2017) Can multi-generational exposure to ocean warming and acidification lead to the adaptation of life history and physiology in a marine metazoan? *Journal of Experimental Biology* 220:551-563
- Glynn PW (1996) Coral reef bleaching: facts, hypotheses and implications. *Global Change Biology* 2:495-509
- Gonzalez P, Dominique Y, Massabuau JC, Boudou A, Bourdineaud JP (2005) Comparative effects of dietary methylmercury on gene expression in liver, skeletal muscle, and brain of the zebrafish (*Danio rerio*). *Environmental Science and Technology* 39:3972–3980
- González PM, Malanga G, Puntarulo S (2015) Cellular oxidant/antioxidant network: update on the environmental effects over marine organisms. *The Open Maine Biology Journal* 9:1-13
- Gould KS (2003) Free radicals, oxidative stress and antioxidants. *Abiotic Stresses/Free Radicals, Oxidative Stress and Antioxidants*:9–15
- Grillo V, Parsons ECM, Shrimpton JH (2001) A review of sewage pollution and cetaceans: a Scottish perspective. Paper presented at the Scientific Committee at the 53rd Meeting of the International Whaling Commission, London, 3–16 July 2001
- Gueranger Q, Li F, Peacock M, Larnicol-Fery A, Brem R, Macpherson P, Egly JM, Karran P (2014) Protein oxidation and DNA repair inhibition by 6-Thioguanine and UVA radiation. *Journal of Investigative Dermatology* 134:1408–1417
- Halliwell B, Gutteridge JMC (2007) Free radicals in biology and medicine. Oxford University Press, New York, USA
- Halpern BS, Selkoe KA, Micheli F, Kappel CV (2007) Evaluating and ranking the vulnerability of global marine ecosystems to anthropogenic threats. *Conservation Biology* 21:1301–1315
- Hanna J, Meides A, Zhang DP, Finley D (2007) A ubiquitin stress response induces altered proteasome composition. *Cell* 129:747–759

- Harvey BP, Gwynn-Jones D, Moore PJ (2013) Meta-analysis reveals complex marine biological responses to the interactive effects of ocean acidification and warming. *Ecology and Evolution* 3:1016–1030
- Hazel JR, Prosser CL (1974) Molecular mechanisms of temperature compensation in poikilotherms. *Physiological Reviews* 54:620–677
- He ZL, Yang XE, Stoffella PJ (2005) Trace elements in agroecosystems and impacts on the environment. *Journal of Trace Elements in Medicine and Biology* 19:125–140
- Henkel R, Solomon M (2018) Oxidative Stress. In: Zini A, Agarwal A (eds) *A Clinician's Guide to Sperm DNA and Chromatin Damage*. Springer International Publishing
- Hernández-Hernández N, Bach LT, Montero MF, Taucher J, Baños I, Guan W, Espósito M, Ludwig A, Achterberg EP, Riebsell U, Arítegui J (2018) High CO₂ under nutrient fertilization increases primary production and biomass in subtropical phytoplankton communities: a mesocosm approach. *Frontiers in Marine Science*
- Hernandez M, Robinson I, Aguilar A, González LM, López-Jurado LF, Reyero MI, Cacho E, Franco J, López-Rodas V, Costas E (1998) Did algal toxins cause monk seal mortality. *Nature* 393:28–29
- Hershko A, Ciechanover A (1992) The ubiquitin system for protein degradation. *Annual Review in Biochemistry* 61:761–807
- Heuer RM, Grosell M (2014) Physiological impacts of elevated carbon dioxide and ocean acidification on fish. *American Journal of Physiology - Regulatory, Integrative and Comparative Physiology* 307:R1061–R1084
- Hoegh-Guldberg O (1999) Climate change, coral bleaching and the future of the world's coral reefs. *Marine and freshwater research* 50:839–866
- Hoegh-Guldberg O, Mumby PJ, Hooten AJ, Steneck RS, Greenfield P, Gomez E, Harvell CD, Sale PF, Edwards AJ, Caldeira K, Knowlton N, Eakin CM, Iglesias-Prieto R, Muthiga N, Bradbury RH, Dubi A, Hatzioles ME (2007) Coral reefs under rapid climate change and ocean acidification. *Science* 318:1737–1742
- Hoeijmakers JHJ (2003) DNA damage, aging, and cancer. *New England Journal of Medicine* 361:1475–1485
- Holmstrup M, Bindesbol A-M, Oostingh GJ, Duschi A, Scheil V, Köhler HR, Loureiro S, Soares AMVM, Ferreira ALG, Kienie C, Gerhardt A, Laskowski R, Kramarz PE, Bayley M,

- Svendsen C, Spurgeon DJ (2010) Interactions between effects of environmental chemicals and natural stressors: A review. *Science of the Total Environment* 408:3746–3762
- Hu MY, Tseng Y-C, Stumpp M, Gutowska MA, Rainer Lucassen M, Melzner F (2011) Elevated seawater $p\text{CO}_2$ differentially affects branchial acid-base transporters over the course of development in the cephalopod *Sepia officinalis*. *American Journal of Physiology - Regulatory Integrative and Comparative Physiology* 300:R1100-R1114
- Ip CCM, Li XD, Zhang G, Farmer JG, Wai OWH, Li YS (2004) Over one hundred years of trace metal fluxes in the sediment of the Pearl River Estuary, South China. *Environmental Pollution* 132:157–172
- IPCC (2014) Impacts, Adaptation, and Vulnerability. Summaries, Frequently Asked Questions, and Cross-Chapter Boxes. A Contribution of Working Group II to the Fifth Assessment Report of the Intergovernmental Panel on Climate Change. World Meteorological Organization, Geneva, Switzerland
- Islam S, Tanaka M (2004) Impacts of pollution on coastal and marine ecosystems including coastal and marine fisheries and approach for management: a review and synthesis. *Marine Pollution Bulletin* 48:624-649
- Jaishankar M, Tseten T, Anbalagan N, Mathew BB, Beeregowda KN (2014) Toxicity, mechanism and health effects of some heavy metals. *Interdisciplinary Toxicology* 7:60-72
- Jesus TF, Rosa IC, Repolho T, Lopes AR, Pimentel MS, Almeida-Val VMF, Coelho MM, Rosa R (2018) Different ecophysiological responses of freshwater fish to warming and acidification. *Comparative Biochemistry and Physiology, Part A: Molecular and Integrative Physiology* 216:34-41
- Jeziarska B, Witeska M (2006) The metal uptake and accumulation in fish living in polluted waters. Paper presented at the Soil and Water Pollution Monitoring, Protection and Remediation, Dordrecht,
- Jones MB (1973) Influence of salinity and temperature on the toxicity of mercury to marine and brackish water isopods (Crustacea). *Estuarine and Coastal Marine Science* 1:425-431
- Kaiser MJ et al. (2005) Patterns in the marine environment. In: *Marine Ecology: processes, systems, and impacts*. 2nd edn. Oxford University Press, United States, pp 1-29
- Kappus H (1987) Oxidative stress in chemical toxicity. *Archives of Toxicology* 60:144–149

- Knoll AH, Fischer WW (2011) Skeletons and ocean chemistry: the long view. In: Gattuso J-P, Hansson L (eds) Ocean Acidification. Oxford University Press, Oxford, New York, pp 67–82
- Krisko A, Radman M (2013) Phenotypic and genetic consequences of protein damage. Plos Genetics 9:e1003810
- Kroeker KJ, Kordas RL, Crim R, Hendriks IE, Ramajo L, Singh GS, Duarte CM, Gattuso JP (2013) Impacts of ocean acidification on marine organisms: quantifying sensitivities and interaction with warming. Global change biology 19:1884–1896
- Kroeker KJ, Kordas RL, Crim RN, Singh GG (2010) Meta-analysis reveals negative yet variable effects of ocean acidification on marine organisms. Ecology Letters 13:1419–1434
- Kumar A, AbdElgawad H, Castellano I, Lorenti M, Delledonne M, Beemster GTS, Asard H, Buia MC, Palumbo A (2017) Physiological and biochemical analyses shed light on the response of *Sargassum vulgare* to ocean acidification at different time scales. Frontiers in Plant Science 8:570
- Lenkinski RE, Chen DM, Glickson JD, Goldstein G (1977) Nuclear magnetic resonance studies of the denaturation of ubiquitin. Biochimica et Biophysica Acta - Proteins and Proteomics 494:126–130
- Lesser MP (1997) Oxidative stress causes coral bleaching during exposure to elevated temperatures. Coral Reefs 16:187–192
- Lesser MP (2006) Oxidative stress in marine environments: biochemistry and physiological ecology. Annual Review of Physiology 68:253–278
- Lesser MP, Farrell JH (2004) Exposure to solar radiation increases damage to both host tissues and algal symbionts of corals during thermal stress. Coral Reefs 23:367–377
- Lindquist S (1986) The heat-shock response. Annual Review in Biochemistry 55:1151–1191
- Livingstone DR (2001) Contaminant-stimulated reactive oxygen species production and oxidative damage in aquatic organisms. Marine Pollution Bulletin 42:656–666
- Lürling M (2015) Infodisruption: pollutants interfering with the natural chemical information conveyance in aquatic systems In: Brönmark C, Hansson L-A (eds). Chemical Ecology in Aquatic Systems. pp 250–271
- Lushchak VI (2011) Environmentally induced oxidative stress in aquatic animals. Aquatic Toxicology 101:13–30

- Lüthi D, Le Floch M, Bereiter B, Blunier T, Barnola J-M (2008) High-resolution carbon dioxide concentration record 650,000–800,000 years before present. *Nature* 453:379–382
- Madeira C, Mendonça V, Leal MC, Flores AAV, Cabral HN, Diniz M, Vinagre C (2017) Thermal stress, thermal safety margins and acclimation capacity in tropical shallow waters – An experimental approach testing multiple end-points in two common fish. *Ecological Indicators* 81:146–158
- Magnan AK, Gattuso J-P (2016) The cascading effects of climate-related changes in the ocean. In: Laffoley D, Baxter JM (eds) *Explaining ocean warming: Causes, scale, effects and consequences*. IUCN, Gland, Switzerland, pp 47–54
- Matoo OB, Ivanina AV, Ullstad C, Beniash E, Sokolova IM (2013) Interactive effects of elevated temperature and CO₂ levels on metabolism and oxidative stress in two common marine bivalves (*Crassostrea virginica* and *Mercenaria mercenaria*). *Comparative Biochemistry and Physiology, Part A: Molecular and Integrative Physiology* 164:545–553
- Matozzo V, Chinellato A, Munari M, Bressan M, Marin MG (2013) Can the combination of decreased pH and increased temperature values induce oxidative stress in the clam *Chamelea gallina* and the mussel *Mytilus galloprovincialis*? *Marine Pollution Bulletin* 72:34–40
- Maulvault AL, Barbosa V, Alves R, Custódio A, Anacleto P, Repolho T, Pousão Ferreira P, Rosa R, Marques A, Diniz M (2017) Ecophysiological responses of juvenile seabass (*Dicentrarchus labrax*) exposed to increased temperature and dietary methylmercury. *Science of the Total Environment* 586:551–558
- Mieiro CL, Ahmad I, Pereira ME, Duarte AC, Pacheco M (2010) Antioxidant system breakdown in brain of feral golden grey mullet (*Liza aurata*) as an effect of mercury exposure. *Ecotoxicology* 19:1034–1045
- Miller DR, Akagi H (1979) pH affects mercury distribution, not methylation. *Ecotoxicology and Environmental Safety* 3:36–38
- Moreira A, Figueira E, Soares AMVM, Freitas R (2016) The effects of arsenic and seawater acidification on antioxidant and biomineralization responses in two closely related *Crassostrea* species. *Science of the Total Environment* 545:569–581
- Morton B, Blackmore G (2001) South China Sea. *Marine Pollution Bulletin* 42:1236–1263
- Mydlarz LD, Jacobs RS (2006) An inducible release of reactive oxygen radicals in four species of gorgonian corals. *Marine and Freshwater Behaviour and Physiology* 39:143–152

- Mydlarz LD, McGinty ES, Harvell D (2009) What are the physiological and immunological responses of coral to climate warming and disease? *Journal of Experimental Biology* 213:934-945
- Nagelkerken I, Connell SD (2015) Global alteration of ocean ecosystem functioning due to increasing human CO₂ emissions. *Proceedings of the National Academy of Sciences of the United States of America* 112:13272-13277
- Nagelkerken I, Munday PL (2015) Animal behaviour shapes the ecological effects of ocean acidification and warming: moving from individual to community-level responses. *Global Change Biology* 22:974-989
- Nardi A, Mincarelli LF, Benedetti M, Fattorini D, d'Errico G, Regoli F (2017) Indirect effects of climate changes on cadmium bioavailability and biological effects in the Mediterranean mussel *Mytilus galloprovincialis*. *Chemosphere* 169:493-502
- NOAA (2017) Trends in atmospheric carbon dioxide. Global Greenhouse Gas Reference Network
- Pamplona R, Costantini D (2011) Molecular and structural antioxidant defenses against oxidative stress in animals. *American Journal of Physiology - Regulatory Integrative and Comparative Physiology* 301:R843-R863
- Park D, Propper CR (2002) Endosulfan affects pheromonal detection and glands in the male red-spotted newt, *Notophthalmus viridescens*. *Bulletin of Environmental Contamination and Toxicology* 69:609-616
- Parmesan C, Yohe G (2003) A globally coherent fingerprint of climate change impacts across natural systems. *Nature* 421:37-42
- Peacock M, Brem R, Macpherson P, Karran P (2014) DNA repair inhibition by UVA photoactivated fluoroquinolones and vemurafenib. *Nucleic Acids Research* 42:13714-13722
- Perry AL, Low PJ, Ellis JR, Reynolds JD (2005) Climate change and distribution shifts in marine fishes. *Science* 308:1912-1915
- Pimentel MS, Faleiro F, Diniz M, Machado M, Pousão-Ferreira P, Peck MA, Pörtner H-O, Rosa R (2015) Oxidative stress and digestive enzyme activity of flatfish larvae in a changing ocean *PLoS ONE* 10:e0134082
- Pittock AB (2009) Climate change: the science, impacts and solutions. CSIRO, Oxford

- Pizzino G, Irrera N, Cucinotta M, Pallio G, Mannino F, Arcoraci V, Squadrito F, Altavilla D, Bitto A (2017) Oxidative stress: harms and benefits for human health. *Oxidative Medicine and Cellular Longevity* 2017:8416763
- Portner H-O (2001) Climate change and temperature dependent biogeography: oxygen limitation of thermal tolerance in animals *Naturwissenschaften* 88:137–146
- Pörtner H-O (2002) Climate variations and the physiological basis of temperature dependent biogeography: systemic to molecular hierarchy of thermal tolerance in animals. *Comparative Biochemistry and Physiology A: Molecular and Integrative Physiology* 132:739–761
- Pörtner H-O (2010) Oxygen-and capacity-limitation of thermal tolerance: a matrix for integrating climate-related stressor effects in marine ecosystems. *The Journal of Experimental Biology* 213:881–893
- Pörtner H-O (2012) Integrating climate-related stressor effects on marine organisms: unifying principles linking molecule to ecosystem-level changes. *Marine Ecology Progress Series* 470:273–290
- Portner H-O, Berdal B, Blust R, Brix O, Colosimo A, Wachter B, Giuliani A, Johansen T, Fisher T, Knust R, Nævdal G, Nedenes A, Nyhammer G, Sartoris FJ, Serendero I, Sirabella P, Thorkildsen S, Zakhartsev M (2001) Climate induced temperature effects on growth performance, fecundity and recruitment in marine fish: developing a hypothesis for cause and effect relationships in Atlantic cod (*Gadus morhua*) and common eelpout (*Zoarces viviparus*). *Continental Shelf Research* 21:1975–1997
- Pörtner H-O, Karl DM, Boyd PW, Cheung WWL, Lluich-Cota SE, Nojiri Y, Schmidt DN, Zavialov PO (2014) Ocean systems. In: Field CB, Barros VR, Dokken DJ, Mach KJ, Mastrandrea MD et al., editors. *Climate Change 2014: Impacts, Adaptation, and Vulnerability Part A: Global and Sectoral Aspects Contribution of Working Group II to the Fifth Assessment Report of the Intergovernmental Panel on Climate Change* Cambridge University Press:411–484
- Portner H-O, Storch D, Heilmayer O (2005) Constraints and trade-offs in climate-dependent adaptation: energy budgets and growth in a latitudinal cline *Scientia Marina* 69:271–285
- Portner H-O, van Dijk PLM, Hardewig I, Sommer A (2000) Levels of metabolic cold adaptation: tradeoffs in eurythermal and stenothermal ectotherms. In: Davison W, Howard-

- Williams C, Broady P (eds) Antarctic Ecosystems: Models for Wider Ecological Understanding. Caxton Press, Christchurch New Zealand, pp 109–122
- Pörtner H-O (2008) Ecosystem effects of ocean acidification in times of ocean warming: a physiologist's view. Marine Ecology Progress Series 373:203–217
- Pörtner H-O, Farrell AP (2008) Physiology and climate change Science 322:690–692
- Portner H-O, Knust R (2007) Climate change affects marine fishes through the oxygen limitation of thermal tolerance Science 315:95–97
- Pörtner H-O, Langenbuch M, Michaelidis B (2005) Synergistic effects of temperature extremes, hypoxia, and increases in CO₂ on marine animals: From Earth history to global change. Journal of Geophysical Research C - Oceans 110:C09S10
- Pörtner H-O, Langenbuch M, Reipschlager A (2004) Biological impact of elevated ocean CO₂ concentrations: Lessons from animal physiology and earth history. Journal of Oceanography 60:705–718
- Pörtner H-O, Reipschlager A, Heisler N (1998) Acid–base regulation, metabolism and energetics in *Sipunculus nudus* as a function of ambient carbon dioxide level. Journal of Experimental Biology 201:43–55
- Pörtner H-O, Reipschläger A (1996) Ocean disposal of anthropogenic CO₂: physiological effects on tolerant and intolerant animals. In: Ormerod B, Angel MV (eds) Ocean Storage of Carbon Dioxide. Workshop 2— Environmental Impact. IEA Greenhouse Gas R&D Programme, Cheltenham, UK, pp 57–81
- Priya RJ, Anand M, Maruthupandy M, Beevi AH (2017) Biomarker response of climate change-induced ocean acidification and hypercapnia studies on brachyuran crab *Portunus pelagicus*. Global Journal of Environmental Science and Management 3:165–176
- Rainbow PS, Luoma SN (2011) Metal toxicity, uptake and bioaccumulation in aquatic invertebrates—modelling zinc in crustaceans. Aquatic Toxicology 105:455–465
- Rechsteiner M (1987) Ubiquitin-mediated pathways for intracellular proteolysis. Annual Review in Cell Biology 3:1–30
- Reid PC (2016) Ocean warming: setting the scene. In: Laffoley D, Baxter JM (eds) Explaining ocean warming: Causes, scale, effects and consequences. IUCN, Gland, Switzerland, pp 17–45

- Reist JD, Wrona FJ, Prowse TD, Dempson JB, Power M, Köck G, Carmichael TJ, Sawatzky CD, Lehtonen H, Tallman RF (2006a) Effects of climate change and UV radiation on fisheries for Arctic freshwater and anadromous species. *AMBIO* 35:402–410
- Reist JD, Wrona FJ, Prowse TD, Power M, Dempson JB, Beamish RJ, King JR, Carmichael TJ, Sawatzky CD (2006b) General effects of climate change on Arctic fishes and fish populations *AMBIO* 35:370–380
- Repetto M, Semprine J, Boveris A (2012) Lipid Peroxidation: Chemical Mechanism, Biological Implications and Analytical Determination Lipid Peroxidation Angel Catala, IntechOpen
- Rodgers DW, Beamish FWH (1983) Water quality modifies uptake of waterborne methylmercury by rainbow trout, *Salmo gairdneri*. *Canadian Journal of Fisheries and Aquatic Sciences* 40:824–828
- Rosa R, Paula JR, Sampaio E, Pimentel M, Lopes AR, Baptista M, Guerreiro M, Santos C, Campos D, Almeida-Val VMF, Calado C, Diniz M, Repolho T (2016a) Neuro-oxidative damage and aerobic potential loss of sharks under elevated CO₂. *Marine Biology* 163:119
- Rosa R, Pimentel MS, Boavida-Portugal J, Teixeira T, Trübenbach K, Diniz M (2012) Ocean warming enhances malformations, premature hatching, metabolic suppression and oxidative stress in the early life stages of a keystone squid. *PLoS ONE* 7:e38282
- Rosa R, Seibel BA (2008) Synergistic effects of climate-related variables suggest future physiological impairment in a top oceanic predator. *Proceedings of the National Academy of Sciences* 105:20776–20780
- Rosa R, Trübenbach K, Pimentel MS, Boavida-Portugal J, Faleiro F, Baptista M, Dionísio G, Calado R, Pörtner HO, Repolho T (2014) Differential impacts of ocean acidification and warming on winter and summer progeny of a coastal squid (*Loligo vulgaris*). *The Journal of Experimental Biology* 217:518–525
- Sachdeva M, Karan M, Singh T, Dhingra S (2014) Oxidants and antioxidants in complementary and alternative medicine: a review. *Spatula* 4:1–16
- Sampaio E, Maulvault AL, Lopes VM, Paula JR, Barbosa V, Alves R, Pousão-Ferreira P, Repolho T, Marques A, Rosa R (2016) Habitat selection disruption and lateralization impairment of cryptic flatfish in a warm, acid, and contaminated ocean *Marine Biology* 163:217
- Schlesinger MJ (1990) Heat shock proteins. *Journal of Biological Chemistry* 265:12111–12114
- Schmidtko S, Stramma L, Visbeck M (2017) Decline in global oceanic oxygen content during the past five decades. *Nature* 542:335–339

- Sies H (1993) Strategies of antioxidant defense. *European Journal of Biochemistry* 215:213–219
- Sies H (1997) Oxidative stress: oxidants and antioxidants. *Experimental Physiology* 82:291–295
- Sies H, Cadenas E, Symons MCR, Scott G (1985) Oxidative stress: damage to intact cells and organs. *Physiological Transactions of the Royal Society* 311:617–631
- Simoneau M, Lucotte M, Garceau S, Laliberté D (2005) Fish growth rates modulate mercury concentrations in walleye (*Sander vitreus*) from eastern Canadian lakes. *Environmental Research* 98:73–82
- Skjærven KH, Penglase S, Olsvik PA, Hamre K (2013) Redox regulation in Atlantic cod (*Gadus morhua*) embryos developing under normal and heat-stressed conditions. *Free Radical Biology and Medicine* 57:29–38
- Sloman KA (2007) Effects of trace metals on salmonid fish: The role of social hierarchies. *Applied Animal Behaviour Science* 104:326–345 doi:10.1016/j.applanim.2006.09.003
- Somero GN (1995) Proteins and temperature *Annual Reviews of Physiology* 57:43–68
- Sørensen JG, Kristensen TN, Loeschcke V (2003) The evolutionary and ecological role of heat shock proteins. *Ecology Letters* 6:1025–1037
- Stramma L, Schmidtke S, Levin LA, Johnson GC (2010) Ocean oxygen minima expansions and their biological impacts. *Deep Sea Research Part I: Oceanographic Research Papers* 57:587–595
- Sui Y, Hu M, Shang Y, Wu F, Huang X, Dupont S, Storch D, Portner H-O, Li J, Lu W, Wang Y (2017) Antioxidant response of the hard shelled mussel *Mytilus coruscus* exposed to reduced pH and oxygen concentration. *Ecotoxicology and Environmental Safety* 137:94–102
- Tchounwou PB, Yedjou CG, Patlolla AK, Sutton DJ (2012) Heavy metal toxicity and the environment. In: Luch A (ed) *Molecular, Clinical and Environmental Toxicology* vol 101. Springer, Basel, pp 133–164
- Thomas CD, Cameron A, Green RE, Bakkenes M, Beaumont LJ, Collingham YC, Erasmus BF, De Siqueira MF, Grainger A, Hannah L, Hughes L, Huntley B, Van Jaarsveld AS, Midgley GF, Miles L, Ortega-Huerta MA, Peterson AT, Phillips OL, Williams SE (2004) Extinction risk from climate change. *Nature* 427:145–148
- Tomanek L (2010) Variation in the heat shock response and its implication for predicting the effect of global climate change on species' biogeographical distribution ranges and metabolic costs. *Journal of Experimental Biology* 213:971–979

- Tomanek L (2011) Environmental proteomics: changes in the proteome of marine organisms in response to environmental stress, pollutants, infection, symbiosis, and development. *Annual Review of Marine Science* 3:373–399
- Wang L, Groves MJ, Hepburn MD, Bowen DT (2000) Glutathione S-transferase enzyme expression in hematopoietic cell lines implies a differential protective role for T1 and A1 isoenzymes in erythroid and for M1 in lymphoid lineages. *Haematologica* 85: 573–579
- Wang W-X, Yan QL, Fan WH, Xu Y (2002) Bioavailability of sedimentary metals from a contaminated bay. *Marine Ecology Progress Series* 240:27–38
- Wiens M, Ammar MS, Nawar AH, Koziol C, Hassanein HM, Eisinger M, Müller IM, Müller WE (2000) Induction of heat-shock (stress) protein gene expression by selected natural and anthropogenic disturbances in the octocoral *Dendronephthya klunzingeri*. *Journal of Experimental Marine Biology and Ecology* 245:265–276
- Wittmann AC, Pörtner H-O (2013) Sensitivities of extant animal taxa to ocean acidification. *Nature Climate Change* 3:995–1001
- Zhou J, Wang L, Xin Y, Wang W-N, He W-Y, Wang A-L, Liu Y (2010) Effect of temperature on antioxidant enzyme gene expression and stress protein response in white shrimp, *Litopenaeus vannamei*. *Journal of Thermal Biology* 35:284–289

*“What is a scientist after all?
It is a curious man looking through a keyhole,
The keyhole of nature,
Trying to know what’s going on”*
- Jacques-Yves Cousteau

Part One

**Within- and Trans-Generational Effects Under Ocean
Acidification**

2 Absence of cellular damage in tropical newly-hatched sharks (*Chiloscyllium plagiosum*) under ocean acidification conditions

Ana R Lopes^{1,2}, Eduardo Sampaio¹, Catarina Santos¹, Ana Couto¹, Maria R Pegado¹, Mário Diniz², Philip L Munday³, Jodie L Rummer³, Rui Rosa¹

¹ MARE - Marine and Environmental Sciences Centre, Laboratório Marítimo da Guia, Faculdade de Ciências da Universidade de Lisboa, Avenida Nossa Senhora do Cabo 939, 2750-374 Cascais, Portugal

² UCIBIO, REQUIMTE, Departamento de Química, Faculdade de Ciências e Tecnologia, Universidade Nova de Lisboa, Quinta da Torre, 2829-516 Caparica, Portugal

³ ARC Centre of Excellence for Coral Reef Studies, James Cook University, Townsville, Queensland 4811, Australia

Published in: Cell Stress and Chaperones (Doi: 10.1007/s12192-018-0892-3)

Abstract

Sharks have maintained a key role in marine food webs for 400 million years and across varying physicochemical contexts, suggesting plasticity to environmental change. In this study, we investigated the biochemical effects of ocean acidification (OA) levels predicted for 2100 ($p\text{CO}_2 \sim 900 \mu\text{atm}$) on newly-hatched tropical whitespotted bamboo sharks (*Chiloscyllium plagiosum*). Specifically, we measured lipid, protein, and DNA damage levels, as well as changes in the activity of antioxidant enzymes and non-enzymatic ROS scavengers in juvenile sharks exposed to elevated CO_2 for 50 days following hatching. Moreover, we also assessed the secondary oxidative stress response, i.e. heat shock response and ubiquitin levels. Newly-hatched sharks appear to cope with OA-related stress through a range of tissue-specific biochemical strategies, specifically through the action of antioxidant enzymatic compounds. Our findings suggest that ROS-scavenging molecules, rather than complex enzymatic proteins, provide an effective defense mechanism in dealing with OA-elicited ROS formation. We argue that sharks' ancient antioxidant system, strongly based on non-enzymatic antioxidants (e.g. urea), may provide them with resilience towards OA, potentially beyond the tolerance of more recently-evolved species, i.e. teleost's. Nevertheless, previous research has provided evidence of detrimental effects of OA (interacting with other climate-related stressors) on some aspects of shark biology. Moreover, given that long-term acclimation and adaptive potential to rapid environmental changes are yet experimentally unaccounted for, future research is warranted to accurately predict shark physiological performance under future ocean conditions.

Key-words: Carbon dioxide, CO_2 , Elasmobranchs, Antioxidant systems, Heat shock response, Oxidative damage

Atmospheric carbon dioxide (CO₂) concentrations have risen above 400 ppm for the first time in over 800,000 years (Lüthi et al. 2008), and, unless anthropogenic CO₂ emissions are curtailed, are predicted to reach ~900 ppm by the end of the 21st century (Gattuso and Hansson 2011; Pörtner et al. 2014). Almost one third of the anthropogenically-originated CO₂ is absorbed by the oceans, which has already led to a 0.1 unit drop in seawater pH from the pre-industrial period to the present days (Gattuso and Hansson 2011; Pörtner et al. 2014). These changes in seawater chemistry are underpinned by a net increase of hydrogen (H⁺) and bicarbonate (HCO₃⁻) ions, and a decrease in carbonate ions (CO₃²⁻), a phenomenon known as ocean acidification (OA) (Caldeira and Wickett 2005; Ridgwell and Zeebe 2005; 2011). By 2100, assuming a “business-as-usual” scenario (~900 ppm CO₂), the continuous CO₂ uptake is expected to elicit a further 0.13-0.42 pH drop (Gattuso and Hansson 2011; Pörtner et al. 2014).

Marine biota can be negatively impacted by OA in numerous ways, including changes in calcification (Orr et al. 2005), development (Kroeker et al. 2010; Wittmann and Pörtner 2013), growth rates, behavior (Clements and Hunt 2014; Nagelkerken and Munday 2015), and mortality (Baumann et al. 2012; Stiasny et al. 2016; Sswat et al. 2018). Physiologically, OA disrupts the acid-base balance of marine organisms, and even though marine fishes are known to compensate for internal pH disturbances, the assumption that such compensation will confer broad CO₂ tolerance could be overestimated (Heuer and Grosell 2014a). In fact, greater acid-base regulation may have other downstream consequences, such as reduced metabolic performance, and concurrent alterations in protein activities and functions (Burnett 1997; Gattuso and Hansson 2011; Heuer and Grosell 2014b). Specifically, elevated CO₂ induces oxidative stress due to: a) the parallel increase of H⁺ ions (extra and intracellular acidosis); and b) the reaction of CO₂ with nitrogen reactive species, e.g. peroxynitrite; both of which contribute to an overproduction of reactive oxygen species (ROS) (Dean 2010; Feder and Hofmann 1999; Sampaio et al. 2018). Moreover, intracellular acidosis could also lead to the release of chelated transition metals (e.g. iron), which will in turn generate hydroxyl radicals through the Fenton reaction and potentially cause membrane-associated, protein, and DNA damage (Dean 2010; Hu et al. 2015; Sampaio et al. 2018; Stohs and Bagchi, 1995; Tomanek et al. 2011).

To cope with naturally occurring oxidative stress, marine organisms harbour a wide set of regulatory mechanisms, including enzymatic antioxidants, such as superoxide dismutase (SOD), catalase (CAT) and glutathione peroxidase (GPx) (Lesser 2006). Moreover, a complementary antioxidant defense mechanism is provided by the diffusion of low molecular weight ROS scavengers (e.g. ascorbic and uric acids, carotenoids, reduced glutathione, and amino acids) (Bartosz 2003). Prior studies have demonstrated that these compounds are particularly prevalent in chondrichthyans, suggesting that low molecular weight scavengers are the main antioxidant defense in opposition to the enzymatic machinery in teleosts (Rudneva 1997). In response to acute physical and chemical stressors, marine organisms also generate heat shock proteins (HSP) in order to repair and refold denatured proteins (Tomanek 2010; Tomanek et al. 2011). As a final line of defense, when HSPs fail to maintain functional protein conformation, ubiquitin targets irreversibly damaged proteins so they can be permanently eliminated (Bond et al. 1988; Hanna et al. 2007).

Recent studies show that the antioxidant defense system of teleost fishes under OA conditions sometimes fails to prevent oxidative damage, translating into chain-reactions in increased skeletal and tissue deformities and decreased metabolic, growth and survival rates in some species (Frommel et al. 2012; Pimentel et al. 2014; 2015; Silva et al. 2016; Stiasny et al. 2016). However, antioxidant defense responses to OA vary with ecological and life-history traits, such as life-stage, life-strategy and phylogeny (Doney et al. 2012; Hofmann et al. 2010). Sharks represent one of the oldest taxa of marine vertebrates, and have maintained an important role in the structure of marine food webs throughout their evolutionary history (Baum et al. 2003). Indeed, these cartilaginous fishes have survived over the last 400 million years (Lund and Grogan 2004), coping with changes in the seawater chemistry from above 3000 CO₂ ppm during the Devonian period to below 300 CO₂ ppm in the pre-industrial era (see Fig. 1 in Rummer and Munday 2016). But now the questions pertain to their acclimation to CO₂ concentrations consistently above 400 ppm levels (NOAA 2017) and increasing at a rate faster than ever recorded (Lüthi et al. 2008). Recent studies have shown that, although the performance of shark embryos appears mostly unaffected by OA-relevant conditions, there is evidence of OA-induced effects on the growth, metabolism, and behavior of later life stages of some species (see review in Rosa et al. 2017). For example, Pistevos et al. (2015) found significant changes in the Port Jackson shark behavior with elevated CO₂ levels. Similarly, Dixon et al. (2010) demonstrated that exposure to elevated CO₂ can significantly impair the feeding behavior of the smooth dogfish.

On the other hand, Heinrich et al. (2014; 2015) found no effect of near-future CO₂ levels on the respiratory physiology and behavior of the epaulette shark.

Considering previous results in other species and taking into account the variable outcomes reported for sharks, we aimed to investigate sharks' capacity to handle oxidative stress under OA conditions. Thus, here we investigated the oxidative stress-related responses of recently-hatched tropical sharks (whitespotted bamboo shark *Chiloscyllium plagiosum*) to OA conditions. After 50 days exposure to CO₂ levels predicted for 2100 under a “business-as-usual” scenario ($p\text{CO}_2 \sim 900 \mu\text{atm}$), we measured membrane-associated, protein, and DNA damage levels, as well as changes in the activity of individual antioxidant enzymes and non-enzymatic molecules, i.e. primary antioxidant defenses. Moreover, we gauged the secondary oxidative stress response, by quantifying heat shock response and ubiquitin levels. Ultimately, we discussed if the variety of physicochemical contexts experienced during shark evolution (Ridgwell and Zeebe 2005) could allow these animals to successfully offset OA-induced oxidative stress.

2.1. Materials and Methods

2.1.1. Ethics statement

Experimental procedures used in this research were in accordance with the requirements of Directive 2010/63/EU of the European Parliament and of the Council of 22 September 2010 on the protection of animals used for scientific purposes. They were reviewed and approved by the animal ethics committee ORBEA±Animal Welfare Body of FCUL (Statement 5/2016) and by the National Veterinary Medicines Directorate (DGAV).

2.1.2. Sharks acquisition and lab acclimation

Whitespotted bamboo shark eggs (*C. plagiosum*) were hand-collected by local fishers between June and July 2016 in the area of Lungsod Ng Cebu (Philippines; around 10°11'N 123°58'E) and transported to the Laboratório Marítimo da Guia aquaculture facilities (LMG, Cascais, Portugal) through a certified commercial supplier (TMC - Iberia). Upon arrival, eggs were suspended by strings in a 200L recirculating aquaculture system until hatching at average

ambient temperature (26°C) and $p\text{CO}_2$ (400 μatm). Contrary to our previous studies with a closely-related shark species (*C. punctatum*; Rosa et al. 2014; 2016a; 2016b), where we were able to expose shark embryos to high CO_2 levels from the beginning of the embryogenesis, *C. plagiosum* embryos arrived at our facilities in a more advanced developmental stage. As a result, exposure to elevated CO_2 only started after hatching. Each newly hatched shark ($n=10$) was transferred to individual opaque tanks (50 L) and randomly allocated to one of the experimental conditions: control ($\sim 390 \mu\text{atm CO}_2$, $n = 5$) or elevated CO_2 ($\sim 890 \mu\text{atm CO}_2$, $n = 5$) for 50 days, according to relevant levels expected for 2100 (Pörtner et al. 2014). Individual tanks were coupled within recirculation aquaculture systems (RAS) filled with 0.35 μm filtered (Harmsco, USA) and UV-irradiated (V2ecton 600, TMC Iberia, Portugal) natural seawater, pumped directly from the sea. Water quality in each RAS was ensured by biological (Ouriço®, Fernando Ribeiro Lda, Portugal), mechanical (Glass wool, Fernando Ribeiro Lda, Portugal), and physical filtration (V2 Skim Pro 450, TMC Iberia, Portugal), as well as an additional UV-irradiation (V2ecton 300, TMC Iberia, Portugal). Water quality was maintained by protein skimmers (Schuran, Jülich, Germany), wet-dry filters (BioBalls), and 30-W UV-sterilizers (TMC, Chorleywood, UK). Each RAS worked in a semi-closed system, with a continuous low-flow exchange system, allowing a daily 50% water exchange. Ammonia, nitrite and nitrate levels were daily monitored by means of colorimetric tests (Profi Test, Salifert, Holland) and kept within safe levels. The CO_2 level in each tank was controlled and maintained by continuously monitoring of seawater pH. A pH probe (GHL, Germany) in each tank was connected to an automated controller (Profilux 3.1, GHL, Germany) that adjusted pH values every two seconds. The appropriate seawater pH was achieved in each mixing tank ($n=5$), in which pH was downregulated by the injection of a certified CO_2 gas mixture (Air Liquid, Portugal), via solenoid valves (Etopi, Portugal), and upregulated by the injection of atmospheric air. Additionally, a daily manual monitoring of seawater pH (SevenGo pro SG8, Mettler Toledo) was performed to adjust system set-points, as necessary. Seawater carbonate system speciation (see Supplementary Table S1) was calculated weekly from total alkalinity (determined spectrophotometrically at a wavelength of 595 nm) according to Sarazin et al. (1999) and pH measurements, using pH total scale. Total dissolved inorganic carbon (CT), $p\text{CO}_2$, bicarbonate concentration and aragonite saturation levels were calculated using the CO2SYS software (Lewis and Wallace 1998), with dissociation constants from Mehrbach et al. (1973) as refitted by Dickson and Millero (1987). Temperature was regulated using electronic heaters. Temperature and salinity were monitored daily using a thermometer (TFX 430, WTW GmbH,

Germany) and a refractometer (V2, TMC Iberia, Portugal), respectively. The systems were illuminated with white fluorescent lamps in a 12 h: 12 h (light/dark) photoperiod. Sharks were fed daily to satiation with shrimp, kingfish, and squid. After the exposure period, organisms were sacrificed with MS222 and tissue samples were immediately frozen at -80°C until further analyses.

2.1.3. Biochemical Analyses

2.1.3.1. Preparation of tissue extracts

Muscle, liver and gills samples (n = 5 per treatment) were homogenized (Ultra-Turrax, Staufen, Germany) in 2 mL phosphate buffered saline solution (PBS, pH 7.4: 0.14 M NaCl, 2.7 mM KCl, 8.1 mM Na₂HPO₄ and 1.47 mM KH₂PO₄). Subsequently, homogenates were centrifuged (14000 x g for 20 min at 4°C) and the supernatant fraction transferred to new microtubes (1.5 mL) and frozen (-80°C) until further analyses. Each sample was run in triplicate (technical replicates), and the enzyme results were normalized to total protein content, as described by Bradford (1976).

2.1.3.2. Cellular, protein, and DNA damage

Lipid peroxidation (LPO), an indicator of cellular oxidative damage, was determined by malondialdehyde (MDA) quantification, a by-product of lipid damage, according to the thiobarbituric acid reactive substances (TBARS) assay (Uchiyama and Mihara 1978b). A total of 10 µL of the sample was added to 45 µL of monobasic sodium phosphate buffer (50 mM), followed by the addition of 12.5 µL of sodium dodecyl sulphate (8.1 %), 93.5 µL of trichloroacetic acid (20 %, pH 3.5), and 93.5 µL of thiobarbituric acid (1 %), to a 1 mL microtube. A volume of 50.5 µL of Milli-Q ultrapure water was added to this mixture, being subsequently mixed for 30 s and incubated in boiling water (100°C) for 10 min. The resulting mixture was placed on ice for 3 min to lower the temperature. Afterwards, 62.5 µL of Milli-Q ultrapure water and 312.5 µL of n-butanol pyridine (15:1 v/v) were added and microtubes centrifuged at 2000 x g for 5 min. The supernatant fraction (150 µL) was added to 96-well microplates, and absorbance was read at 532 nm in a microplate reader (Bio-Rad, Benchmark, USA). Malondialdehyde concentrations were calculated based on a calibration curve (0 - 0.3 µM) using MDA bis (dimethyl acetal) standards.

Protein carbonylation (i.e., protein modification and damage) was determined spectrophotometrically through an enzyme-linked immunosorbent assay (ELISA) method, according to Alamdari et al. (2005). Briefly, 50 μ L of each sample was added into the well and the plate let to incubate overnight at 4°C. Afterwards microplates were washed (3x) with PBS-TWEEN (0.1%) and incubated for 45 min at room temperature with 250 μ L of a 0.05 M DNPH solution (2,4-dinitrophenylhydrazin) adjusted to pH 6.2. After the incubation period, plates were washed with PBS-TWEEN: ethanol (5x, 1:1) and PBS-TWEEN (3x). Blocking solution (200 μ L BSA) was added, and after another incubation period (90 min at 37°C), microplates were washed with PBS-TWEEN (3x). Primary antibody (1 μ g/ml) was added into the wells (50 μ L: anti-DNP, Acris, USA), and microplates were allowed to incubate for another 90 min at 37°C. After another washing procedure (3x with PBS-TWEEN), 50 μ L of diluted (1 μ g/ml) secondary antibody (alkaline phosphatase-conjugated anti-mouse IgG, Fab specific, Sigma-Aldrich, USA) was added to each well, and microplates were incubated again for 90 min (37°C). After a final washing procedure, 100 μ L substrate solution (SIGMA FAST™ p-Nitrophenyl Phosphate Tablets, Sigma-Aldrich, USA) was added to each well and, after 30 min, the reaction was stopped by adding 50 μ L of sodium hydroxide (NaOH, 3 M). The absorbance was read at 405 nm in a microplate reader (Bio-Rad, Benchmark, USA).

8-hydroxy-2'-deoxyguanosine (8-OHdG), as a measure of DNA damage (i.e. DNA strand break or base mismatches), was assessed through an ELISA method, according to Maclouf et al. (1987) and Shen *et al.* (2007). Each sample (100 μ L) was added to each well in a 96 well microplate and allowed to incubate overnight at 4°C. After 24h, plates were washed (3x) with PBS-TWEEN and incubated for 90 min at room temperature with the blocking solution (200 μ L BSA). After another washing procedure (3x), microplates were incubated overnight with primary antibody (anti-OHdG, clone 15 A3, Sigma-Aldrich, Germany). On the subsequent day, microplates were washed to remove non-linked antibody and allowed to incubate for 90 min at 37°C with the secondary antibody (alkaline phosphatase-conjugated anti-mouse IgG, Fab specific, Sigma-Aldrich, USA). After a final washing procedure, plates were incubated at room temperature for 30 min with the substrate (SIGMA FAST™ p-Nitrophenyl Phosphate Tablets, Sigma-Aldrich, USA). Finally, the reaction was stopped by adding 100 μ L of 3M NaOH, and the absorbance was read at 405 nm (Bio-Rad, Benchmark, USA).

2.1.3.3. Antioxidant enzyme activities and total antioxidant capacity

Superoxide dismutase (SOD: EC 1.15.1.1) inhibition was determined based upon the method described by McCord and Fridovich (1969). Each sample (0.5 mL) was added to a polystyrene cuvette with 1.4 mL of reaction mix (deionized water, 23 mM potassium phosphate, 0.05 mM ethylenediaminetetraacetic acid, 0.005 mM cytochrome c, 0.02 mM xanthine, pH 7.8). Subsequently the reaction was initiated by adding 0.5 mL of xanthine oxidase. The absorbance was read during 15 min at 550 nm using a UV-Visible Spectrophotometer (Ultrospec 2100 pro, Amersham BioSciences, UK).

Catalase (CAT) activity was assessed based on the method described by Johansson and Borg (1988). Briefly, 20 μ L of each sample, 100 μ L of 100 mM potassium phosphate, and 30 μ L of methanol were added to a 96-well microplate, which was promptly shaken and incubated for 20 minutes. Afterwards, 30 μ L of potassium hydroxide (10 M KOH) and 30 μ L of purpald (34.2 mM in 0.5 M HCl) were added to each well, and the plate was shaken and incubated for another 10 minutes. Subsequently, 10 μ L of potassium metaperiodate (65.2 mM in 0.5 M KOH) was added to each well, and a final incubation was performed for 5 minutes. Enzymatic activity was measured spectrophotometrically at 540 nm, using a microplate reader (Bio-Rad, Benchmark, USA). Formaldehyde concentration of the samples was calculated based on a calibration curve (from 0 to 75 μ M formaldehyde), followed by the calculation of the CAT activity of each sample, where one unit of catalase is defined as the amount that will cause the formation of 1.0 nmol of formaldehyde per minute at 25°C. The results were expressed in relation to total protein content ($\text{nmol min}^{-1} \text{mg}^{-1} \text{protein}$).

Glutathione peroxidase (GPx: EC 1.11.1.9) activity was determined through an adaptation of the method described by Lawrence and Burk (1976) to 96 well microplates. Briefly, 20 μ L of each sample, 120 μ L of 50 mM phosphate buffer (pH 7.6), 50 μ L of co-substrate mixture (0.8 mM β -NADPH, 4 mM Glutathione, 4 U/mL glutathione reductase, and 4 mM sodium azide) and 20 μ L of 15 mM cumene hydroperoxide ($\text{C}_9\text{H}_{12}\text{O}_2$) were added to each well, and the absorbance was read every minute for 6 min at 340 nm (Bio-Rad, Benchmark, USA). The GPx activity was determined using the β -NADPH coefficient extinction, and results given in $\text{nmol min}^{-1} \text{mg}^{-1} \text{protein}$.

Aconitase (EC 4.2.1.3) activity was determined spectrophotometrically according to Morrison (1954) and adapted to 96 well microplates. Each sample (20 μ L) and 115 μ L of 100 mM Tris-HCL buffer, 20 μ L of 20 mM manganese sulphate, 10 μ L of 5.4 mM NADP⁺, 10 μ L of 143 U/mL Isocitric dehydrogenase enzyme (IsoDH) and 20 μ L of activation solution (100 mM Tris-HCl, 50 mM L-cystein and 1 mM ammonium ferrous sulphate, pH 7.4) were added to each well. Then, the reaction was initiated by adding of 10 μ L of 2 mM citric acid, and the absorbance was read at 340 nm each minute for 25 min (Bio-Rad, Benchmark, USA). Aconitase activity was achieved by measuring the formation of β -NADPH during the catalysis of Isocitrate to α -ketoglutarate.

Total antioxidant capacity (TAC) was determined according to Kambayashi et al. (2009). Briefly, a total of 10 μ L of each sample was added to each well in a 96 well microplate. Afterwards, 10 μ L of 90 μ M myoglobin, 150 μ L of 600 μ M ABTS [2,2'-azino-bis (3-ethylbenzothiazoline-6-sulphonic acid)], and 40 μ L of 500 μ M hydrogen peroxide were added to the wells, and the microplates were incubated at room temperature for 5 min. Absorbance was read at 410 nm (Bio-Rad, Benchmark, USA), and TAC was calculated from a calibration curve, based on a series of Trolox (0 – 0.3 mM).

2.1.3.4. Protein repair and removal mechanisms

Heat Shock Protein 70 (HSP70) content was assessed through an ELISA according to Njemini et al. (2005). Each sample (20 μ L) was diluted in 980 μ L phosphate-buffered saline (PBS). Afterwards, 100 μ L of each diluted sample was added to 96-well microplates (Microloan 600, Greiner, Germany) and incubated overnight at 4°C. After 24h, microplates were washed (3x) using PBS containing 0.05 % TWEEN 20. Afterwards, 100 μ L of blocking solution [1 % bovine serum albumin (BSA)] was added to each well, and microplates were incubated for 90 min at 37°C. Then, 50 μ L of primary antibody (5 μ g mL⁻¹ in 1% BSA: anti-HSP70/HSC70, Acris, USA) was added to each well. After another incubation period (overnight at 4°C), microplates were washed (3x) to remove non-linked antibodies. A second antibody [alkaline phosphatase-conjugated anti-mouse IgG (Fab specific, Sigma-Aldrich, USA)] was used by adding 50 μ L (1 μ g mL⁻¹) to each well, and then the microplate was incubated for 90 min at 37°C. After an additional washing procedure, 100 μ L of substrate (SIGMA FAST™ p-Nitrophenyl Phosphate Tablets,

Sigma-Aldrich, USA) was added to each well and incubated for 30 min at room temperature. Finally, 50 μL of stop solution (3 M NaOH) was added to each well.

Ubiquitin (Ub) content was assessed through an ELISA. Each sample (100 μL) was added to 96-well microplates (Microloan 600, Greiner, Germany) and incubated overnight at 4°C. After 24h, microplates were washed (3x) using PBS containing 0.05 % TWEEN 20. Afterwards, 100 μL of blocking solution [1 % bovine serum albumin (BSA)] was added to each well and microplates were then incubated for 90 min at 37°C. Consequently, 50 μL of primary antibody (P4D1, sc-8017, HRP conjugate, Santa Cruz, USA) was added to each well. After another incubation period (overnight at 4°C), microplates were washed (3x) to remove non-linked antibodies, and 100 μL of substrate (TMB/E, Temecula California, Merck Millipore) was added to each well and incubated for 30 min at room temperature. Afterwards, 100 μL of stop solution (1M HCL) was added to each well. Absorbances were read at 405 and 415 nm, respectively, using a microplate reader (Bio-Rad, Benchmark, USA). The HSP and Ub content were calculated from the calibration curve, based on serial dilutions of purified HSP70 active protein (0 - 2000 $\mu\text{g mL}^{-1}$, ACRIS, USA) and purified ubiquitin (0 - 1 $\mu\text{g mL}^{-1}$, UbpBio, E-1100, USA), respectively.

2.1.4. Statistical analyses

Generalized linear models (GLM) were used to infer significant differences between CO₂ treatments and across the tissues analyzed. All data followed a normal distribution, with the assumptions of homogeneity of variances and normality confirmed by visual inspection. In a first approach, tissue (three levels: muscle, liver, gills) was used as an explanative variable to find organ specific patterns for each specific dependent variable (Oxidative damage: LPO, Protein Carbonylation and 8-OHdG; Oxidative Stress: SOD, CAT, GPx, Aconitase and TAC; Protein repair and removal: HSP and Ub). Afterwards, CO₂ (two levels: Control and High CO₂) was used as an explanative variable, in order to scrutinize intra-tissues differences. All statistical analyses were performed using R Studio (R Development Core Team 2017).

2.2. Results

No mortalities occurred in either the control or elevated CO₂ treatment during the experiment. Lipid damage (i.e., LPO) exhibited significant differences among tissues, with lower levels in the gills and muscle when compared to the liver (both $p < 0.001$, GLM analysis in Table S2, Fig. 1A). However, no effects of elevated CO₂ were found within tissues ($p > 0.05$, GLM analysis in Table S5). Protein carbonylation levels also varied among tissues, with significantly lower values in the liver compared to muscle ($p < 0.05$, GLM analysis in Table S2, Fig. 1B). Moreover, elevated CO₂ decreased protein carbonylation in the gills ($p < 0.05$, GLM analysis in Table S5, Fig. 1B). Regarding DNA damage, the liver displayed significantly lower 8-OHdG levels than the other two tissues ($p < 0.001$, GLM analysis in Table S2, Fig. 1C). Furthermore, there was an increase in 8-OHdG levels in the liver with high CO₂ exposure ($p < 0.05$, GLM analysis in Table S5, Fig. 1C).

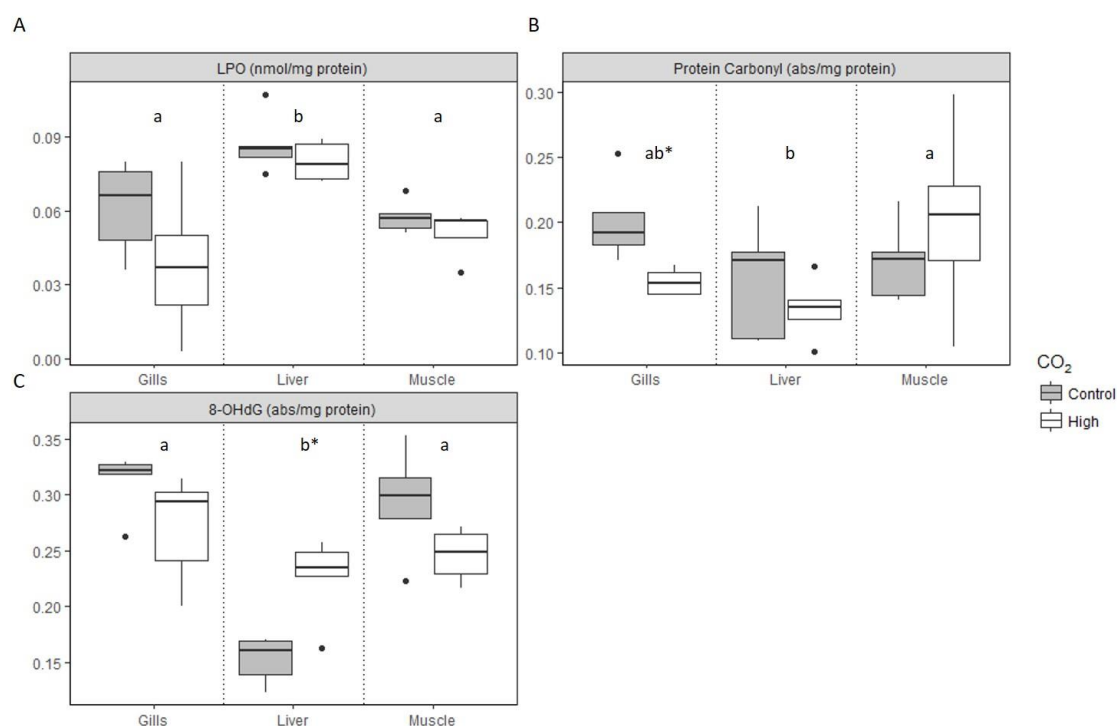


Figure 1 – Impact of high CO₂ exposure on levels of **A** LPO, **B** Protein carbonyl, and **C** 8-OHdG levels in *C. plagiolum* tissues. The horizontal line within the box indicates the median, boundaries of the box indicate the 25th and 75th percentiles, and the whiskers indicate the highest and lowest values of the results. Different letters represent significant differences between tissues, while asterisks (*) represent significant differences within tissues. GLM analyses described in Supplemental Tables S2 and S5.

Regarding the antioxidant enzymatic machinery, SOD activity did not exhibit any significant differences among tissues ($p > 0.05$, GLM analysis in Table S3). Within the tissues, elevated CO_2 resulted in a decrease in SOD activity in the liver ($p < 0.05$, GLM analysis in Table S6, Fig. 2A), but a two-fold increase in activity within the muscle ($p < 0.05$, GLM analysis in Table S6, Fig. 2A). CAT activity significantly varied among tissues, with lower levels detected in the gills when compared to the muscle and liver ($p < 0.001$ and $p < 0.05$, respectively, GLM analysis in Table S3, Fig. 2B). Within tissues, elevated CO_2 caused a decrease in CAT activity in the liver ($p < 0.05$, GLM analysis in Table S6, Fig. 2B). Elevated CO_2 also led to diminishing GPx activity in the liver ($p < 0.001$, GLM analysis in Table S6, Fig. 2C) and gills ($p < 0.05$, GLM analysis in Table S6, Fig. 2C) but an opposite trend was observed in the muscle ($p < 0.05$, GLM analysis in Table S6, Fig. 2C). Aconitase activity was significantly lower in the gills and liver when compared to the muscle (both $p < 0.001$, GLM analysis in Table S3, Fig. 2D). Elevated CO_2 also elicited a tissue-specific negative effect on aconitase activity in the gills ($p < 0.05$, GLM analysis in Table S6, Fig. 2D), whereas no changes were observed in the liver and muscle (both $p > 0.05$, GLM analysis in Table S6, Fig. 2D). With respect to the non-enzymatic antioxidant response, TAC levels were significantly higher in the gills when compared to the muscle ($p < 0.05$) and liver ($p < 0.001$, GLM analysis in Table S3, Fig. 2E). In addition, elevated CO_2 increased TAC levels in the muscle ($p < 0.05$, GLM analysis in Table S6, Fig. 2E).

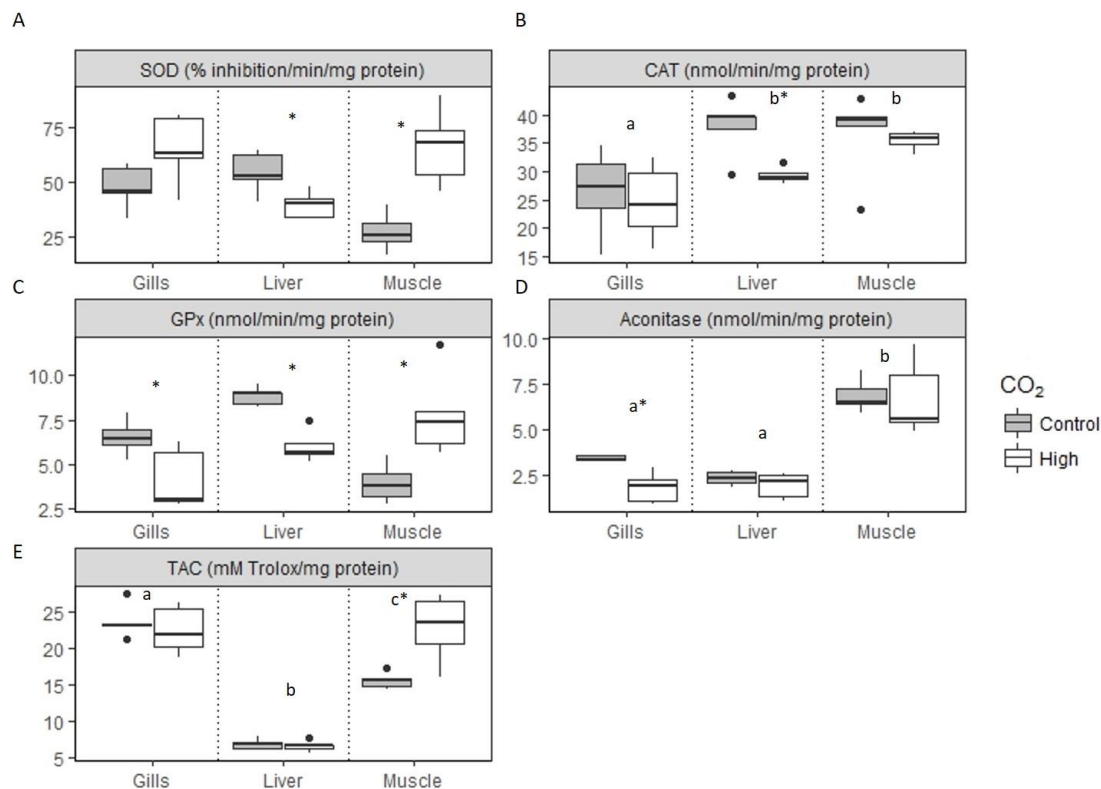


Figure 2 – Impact of high CO₂ exposure on levels of **A** SOD, **B** CAT, **C** GPx, **D** Aconitase activities, and **E** TAC in *C. plagiosum* tissues. The horizontal line within the box indicates the median, boundaries of the box indicate the 25th and 75th percentiles, and the whiskers indicate the highest and lowest values of the results. Different letters represent significant differences between tissues, while asterisks (*) represent significant differences within tissues. GLM analyses described in Supplemental Tables S3 and S6.

HSP levels were significantly higher in the gills and lower in the liver than in the muscle ($p < 0.001$, GLM analysis in Table S4, Fig. 3A). Elevated CO₂ reduced HSP levels in the gills ($p < 0.05$, GLM analysis in Table S7, Fig. 3A). Lastly, ubiquitination (Ub levels) was higher in the muscle when compared to the liver and gills (both $p < 0.05$, GLM analysis in Table S4, Fig. 3B). Elevated CO₂ increased Ub content within the gills ($p < 0.05$), while an opposite trend was observed in the liver ($p < 0.001$, GLM analysis in Table S7, Fig. 3B).

In summary, elevated CO₂ levels elicited macromolecular damage only in the form of increased 8-OHdG in the liver, while SOD, CAT and GPx activities decreased in the same tissue. In parallel, elevated CO₂ elicited an increase in SOD, GPx and TAC within the muscle, whereas

Aconitase decreased in the gills. Furthermore, HSP levels declined with elevated CO₂ in the gills, while Ub levels augmented. Lastly, Ub levels decreased within the liver.

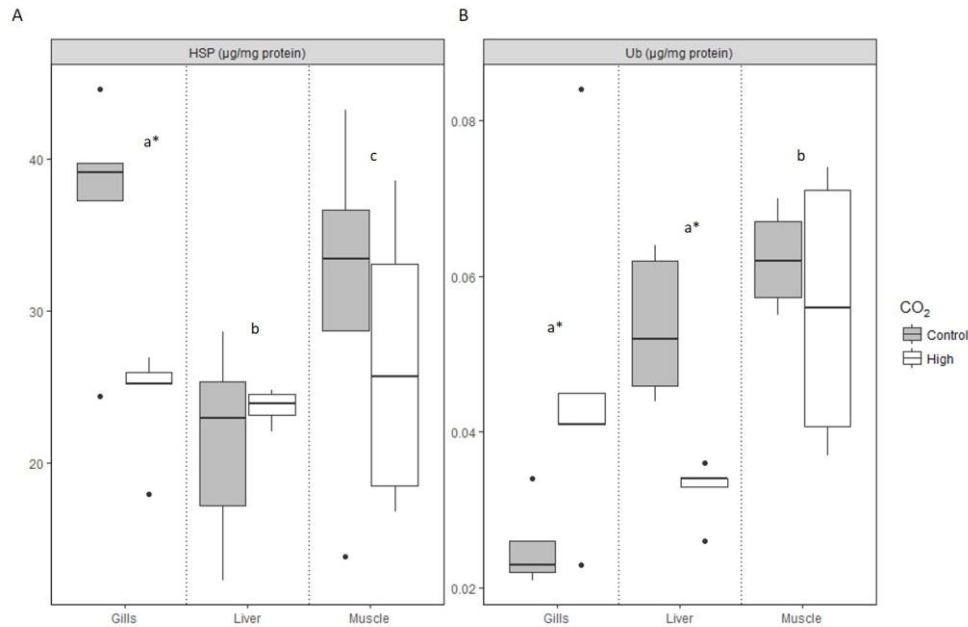


Figure 3 – Impact of high CO₂ exposure on protein repair and removal, namely **A** HSP and **B** Ub levels in *C. plagiosum* tissues after 50days exposure to high CO₂. The horizontal line within the box indicates the median, boundaries of the box indicate the 25th and 75th percentiles, and the whiskers indicate the highest and lowest values of the results. Different letters represent significant differences between tissues, while asterisks (*) represent significant differences within tissues. GLM analyses described in Supplemental TablesS4 and S7.

2.3. Discussion

In the present study, OA conditions expected for the end of this century did not result in significant oxidative damage in *C. plagiosum*, via lipid peroxidation (i.e., membrane-associated lipid damage) or protein carbonylation (i.e., oxidative modification of proteins). Our previous study with a closely-related shark species (*C. punctatum*) detected some detrimental effects (i.e. neuro-oxidative damage and MDA production in the muscle) on shark early development due to elevated CO₂ (Rosa et al. 2014; 2016a; 2016b). However, in those experiments, animals were exposed to elevated CO₂ during the entire embryonic development (> 200 days) and the pCO₂

levels used were substantially higher ($\sim 1500 \mu\text{atm}$) than the ones currently used. In contrast to the previous study, here we observed different tissue-specific biochemical responses of antioxidant enzymes in juvenile *C. plagiosum* exposed to elevated CO_2 for 50 days following hatching.

Specifically, we found that SOD, CAT and GPx decreased in the liver under elevated CO_2 , which translated into increasing DNA damage. It is also worth noting that DNA damage found within the liver was lower when compared with muscle and gills although, as a detoxifying organ (e.g. biotransformation of xenobiotics), the liver is naturally more prone to oxidative stress (Rudneva et al. 2014). Nevertheless, cells harbor an effective DNA repair mechanism, comprising specialized enzymes, to overhaul DNA strand breaks or base mismatches (Hoeijmakers, 2009; Sejersted et al. 2009). Furthermore, SOD and GPx activities, as well as non-enzymatic ROS scavengers, were upregulated in the muscle under elevated CO_2 conditions, successfully preventing any sort of damage. This increase in TAC levels may be linked to an upregulation of the naturally high urea levels that occur in sharks (Rudneva 1997). These molecules are known to be produced in the liver (via ammonium transformation) and retained by other tissues, playing a role both in osmoregulation and as a non-enzymatic complement to the antioxidant system, aiding in the prevention of oxidative damage (Rudneva 1997; Rudneva et al. 2014). Moreover, a significant pattern towards decreasing CAT, GPx, and aconitase levels was detected in the gills under elevated CO_2 conditions. When sharks experience high concentrations of hydrogen peroxide (H_2O_2), gill diffusion rates increase in order to remove excess ROS (López-Cruz et al. 2012). Thus, this decrease in H_2O_2 could lead to decreased antioxidant enzymatic response, as observed in the present study, i.e. decreased GPx and CAT levels (Filho and Boveris 1993; López-Cruz et al. 2012; Rudneva 1997). Gills are also known to accumulate high levels of urea (Wood et al., 2013), therefore naturally occurring levels may have been sufficient to prevent damage.

Regarding protein repair and elimination, significant differences between CO_2 treatments were found solely in the gills. Specifically, elevated CO_2 led to a decrease in HSP levels, while Ub levels increased. We reason that the heat shock response may have been insufficient in ensuring optimal protein function and conformation in this tissue, and therefore ubiquitin specifically targeted those proteins to be eliminated. Nevertheless, activation of these secondary antioxidant defenses rarely occurred, which may be attributed to the co-occurring high levels of Trimethylamine N-oxide (TMAO) in elasmobranchs (MacLellan et al. 2015). As a chemical

chaperone, TMAO is energetically less expensive than HSP (molecular chaperones) synthesis, acting therefore as a first line in protein repair and refolding (Kumar 2009).

Overall, our results suggest that recently hatched *C. plagiosum* can be resilient to OA-induced ROS that may be prevalent in a future ocean, as a consequence of CO₂ dissolution in seawater leading to chemical chain reactions (Dean 2010; Feder and Hofmann 1999; Sampaio et al. 2018), through multiple biochemical and physiological pathways. Long-lived species, such as most sharks, typically display comparatively lower ROS formation than shorter lived species, presumably to prevent constant detoxification and repairing actions, and insufficient energetic expenditure (Pamplona and Constantini 2011). Sharks also possess specialized compensatory mechanisms that prevent oxidative damage, e.g. direct diffusion of excess ROS through the gills (López-Cruz et al. 2012). Notwithstanding, resistance to oxidative stress in *C. plagiosum* seems to be strongly underpinned by the mainly molecular-based (i.e., urea, ascorbic acid) antioxidant system (Rudneva 1997), and its capacity to eradicate ROS and prevent cellular damage (Rudneva 1999).

The evolution of structure complexity in agents of the antioxidant system, from molecules to enzymatic proteins, can be associated with phylogenetic position in the tree of life (Rudneva 1997). In contrast to ancient cartilaginous fishes, relatively newly-evolved teleost fishes possess an enzyme-based antioxidant system (Filho and Boveris 1993; Solé et al. 2009). Thus, given the effects of elevated CO₂ found in some teleost fishes (Baumann et al. 2012; Pimentel et al. 2014; Stiasny et al. 2016), our findings could suggest that molecules, instead of complex enzymatic proteins, effectively deal with OA-elicited ROS formation in sharks. Mechanistically, as high CO₂-associated stress is attributed to increased H⁺ concentrations, we reason that it is likely that relatively unstable molecules (especially urea), are able to: i) incorporate H⁺ quickly, and/or ii) yield a neutralizing electron to ROS (highly reactive scavenger) (Wang et al. 1999). Moreover, beyond the naturally high concentrations of urea in shark fluids and tissues, serving as both the main molecular antioxidant agent and as an osmolyte (Rudneva et al. 2014), its synthesis is also energetically less costly than that of the protein analogues (Kumar 2009). Thus, paradoxically, shark species could be potentially more resilient to future ocean acidification conditions than more derived teleost fishes because of their conserved antioxidant systems based on non-enzymatic antioxidants.

It should also be taken into account that, beyond their inherent capacity to buffer ROS formation, sharks might be able to adapt in parallel to gradually increasing CO₂, before the latter

reaches the levels projected for the end of this century (Sunday et al. 2014). Further research is warranted to accurately predict shark physiological performance under future ocean conditions taking into account their adaptive potential over the timescale at which CO₂ is rising in the ocean.

2.4. Acknowledgments

We would like to thank Eduarda Pinto for the fundamental technical support during the preparation of the experimental setup and shark acclimation.

2.5. Competing of interests

The authors declare that there are no conflicts of interest.

2.6. Funding

The Portuguese Foundation for Science and Technology (FCT) supported this work through the project grant PTDC/AAG-GLO/1926/2014 and Programa Investigador FCT 2013 to R.R. FCT also supported this work through: i) the strategic project UID/MAR/04292/2013 granted to MARE, and ii) PhD grants to ARL (SFRH/BD/97070/2013), ES (SFRH/BD/131771/2017), CS (SFRH/BD/117890/2016), and MRP (SFRH/BD/111691/2015). Both PLM and JLR are supported by funding from the Australian Research Council (ARC) Centre of Excellence for Coral Reef Studies.

2.7. References

- Alamdari DH, Kostidou E, Paletas K, Sarigianni M, Konstas AG, Karapiperidou A, Koliakos G (2005) High sensitivity enzyme-linked immunosorbent assay (ELISA) method for measuring protein carbonyl in samples with low amounts of protein. *Free Radical Biology and Medicine* 39:1362-1367
- Bartosz G (2003) Total antioxidant capacity. In: Spiegel HE, Nowacki G, Hsiao K-J (eds) *Advances in clinical chemistry*, vol 37. Academic press, California, USA, pp 220-272
- Baum JK, Myers RA, Kehler DG, Worm B, Harley SJ, Doherty PA (2003) Collapse and conservation of shark populations in the Northwest Atlantic. *Science* 299:389-392
- Baumann H, Talmage SC, Gobler CJ (2012) Reduced early life growth and survival in a fish in direct response to increased carbon dioxide. *Nature Climate Change* 2:38-41
- Bond U, Agell N, Haas AL, Redman K, Schlesinger MJ (1988) Ubiquitin in stressed chicken embryo fibroblast. *Journal of Biological Chemistry* 263:2384-2388
- Bradford MM (1976) A rapid and sensitive method for the quantitation of microgram quantities of protein utilizing the principle of protein-dye binding. *Analytical biochemistry* 72:248-254
- Burnett LE (1997) The challenges of living in hypoxic and hypercapnic aquatic environments. *Integrative and Comparative Biology* 37:633-640
- Caldeira K, Wickett ME (2005) Ocean model predictions of chemistry changes from carbon dioxide emissions to the atmosphere and ocean. *Journal of Geophysical Research* 110:C09S04
- Clements JC, Hunt HL (2014) Influence of sediment acidification and water flow on sediment acceptance and dispersal of juvenile soft-shell clams (*Mya arenaria* L.). *Journal of Experimental Marine Biology and Ecology* 453:62-69
- Dahlke FT, Leo E, Mark FC, Pörtner H-O, Bickmeyer U, Frickenhaus S, Storch D (2016) Effects of ocean acidification increase embryonic sensitivity to thermal extremes in Atlantic cod, *Gadus morhua*. *Global Change Biology* 23:1499-1510
- Dean JB (2010) Hypercapnia causes cellular oxidation and nitrosation in addition to acidosis: implications for CO₂ chemoreceptor function and dysfunction. *Journal of Applied Physiology* 108:1786-1795

- Dickson A, Millero F (1987) A comparison of the equilibrium constants for the dissociation of carbonic acid in seawater media *Deep-Sea Research* 34:1733-1743
- Dixson DL, Munday PL, Jones GP (2010) Ocean acidification disrupts the innate ability of fish to detect predator olfactory cues *Ecology Letters* 13:68-75
- Doney SC, Ruckelshaus M, Duffy JE, Barry JP, Chan F, English CA, Galindo HM, Grebmeier JM, Hollowed AB, Knowlton N, Polovina J, Rabalais NN, Sydeman WJ, Talley LD (2012) Climate change impacts on marine ecosystems *Annual Review of Marine Science* 4:11-37
- Feder ME, Hofmann GE (1999) Heat-shock proteins, molecular chaperones, and the stress response: evolutionary and ecological physiology. *Annual Review of Physiology* 61: 243–282
- Filho DW, Boveris A (1993) Antioxidant defences in marine fish - II. Elasmobranchs *Comparative Biochemistry and Physiology C* 106:415-418
- Frommel AY, Maneja R, Lowe D, Pascoe CK, Geffen AJ, Folkvord A, Piatkowski U, Clemmesen C (2014) Organ damage in Atlantic herring larvae as a result of ocean acidification. *Ecological Applications* 24: 1131–1143
- Gattuso J-P, Hansson L (2011) Ocean Acidification: background and history. In: Gattuso J-P, Hansson L (eds) *Ocean Acidification*. Oxford University Press, Oxford, New York, pp 1-17
- Hanna J, Meides A, Zhang DP, Finley D (2007) A ubiquitin stress response induces altered proteasome composition. *Cell* 129:747-759
- Heuer RM, Grosell M (2014) Physiological impacts of elevated carbon dioxide and ocean acidification on fish. *American Journal of Physiology - Regulatory, Integrative and Comparative Physiology* 307:R1061-R1084
- Hoeijmakers JHJ (2009) DNA damage, aging and cancer. *The New England Journal of Medicine* 361 (15): 1475-1485
- Hofmann GE, Barry JP, Edmunds PJ, Gates RD, Hutchins DA, Klinger T, Sewell MA (2010) The effect of ocean acidification on calcifying organisms in marine ecosystems: an organism-to-ecosystem perspective. *Annual Review of Ecology, Evolution, and Systematics* 41:127-147

- Hu M, Li L, Sui Y, Li J, Wang Y, Lu W, Dupont S (2015) Effect of pH and temperature on antioxidant responses of the thick shell mussel *Mytilus coruscus*. *Fish and Shellfish Immunology* 46:573-583
- Johansson LH, Borg LA (1988) A spectrophotometric method for determination of catalase activity in small tissue samples. *Analytical Biochemistry* 174 (1): 331-336
- Kambayashi Y, Binh NT, Asakura HW, Hibino Y, Hitomi Y, Nakamura H, Ogino K (2009) Efficient assay for total antioxidant capacity in human plasma using a 96-well microplate. *Journal of Clinical Biochemistry and Nutrition* 44:46-51
- Kroeker KJ, Kordas RL, Crim RN, Singh GG (2010) Meta-analysis reveals negative yet variable effects of ocean acidification on marine organisms. *Ecology Letters* 13:1419–1434
- Kumar R (2009) Role of naturally occurring osmolytes in protein folding and stability. *Archives of Biochemistry and Biophysics* 49:1-6
- Lawrence RA, Burk RF (1976) Glutathione peroxidase activity in selenium-deficient rat liver. *Biochemical and Biophysical Research Communications* 71:952-958
- Lesser MP (2006) Oxidative stress in marine environments: biochemistry and physiological ecology. *Annual Review of Physiology* 68:253-278
- Lewis E, Wallace DWR (1998) CO2SYS-Program developed for the CO₂ system calculations. Report ORNL/CDIAC-105
- López-Cruz RI, Dafre AL, Filho DW (2012) Oxidative stress in sharks and rays. In: D. A, Vázquez-Medina JP, Zenteno-Savín T (eds). *Oxidative stress in aquatic ecosystems*. Wiley-Blackwell, Oxford, pp 157-163
- Lund R, Grogan ED (2004) The origin and relationships of early Chondrichthyes. In: Musick JA, Carrier JC, Heithaus MR (eds). *Biology of sharks and their relatives*. CRC Press Inc, pp 3-31
- Lüthi D, Le Floch M, Bereiter B, Blunier T, Barnola J-M (2008) High-resolution carbon dioxide concentration record 650,000-800,000 years before present. *Nature* 453:379-382
- MacLellan RJ, Tunnah L, Barnett D, Wright PA, MacCormack T, Currie S (2015) Chaperone roles for TMAO and HSP70 during hyposmotic stress in the spiny dogfish shark (*Squalus acanthias*). *Journal of Comparative Physiology B* 185:729-740
- Maclouf J, Grassi J, Pradelles P (1987) Development of enzyme-immunoassay techniques for measurement of eicosanoids. In: Walden TL, Hughes HN (eds) *Prostaglandin and Lipid Metabolism in Radiation Injury*. Springer, US, pp 355-364

- McCord JM, Fridovich I (1969) Superoxide dismutase an enzymic function for erythrocyte hemocuprein (hemocuprein). *Journal of Biological Chemistry* 244:6049-6055
- Mehrbach C, Culbertson C, Hawley J, Pytkowicz R (1973) Measurement of the apparent dissociation constants of carbonic acid in seawater at atmospheric pressure. *Limnology and Oceanography* 18:897-907
- Morrison J (1954) The activation of aconitase by ferrous ions and reducing agents. *Biochemical Journal* 58:685
- Nagelkerken I, Munday PL (2015) Animal behaviour shapes the ecological effects of ocean acidification and warming: moving from individual to community-level responses. *Global change biology* 22:974-989
- Njemini R, Lambert M, Demanet C, Mets T (2005) Heat Shock Protein 32 in human peripheral blood mononuclear cells: effect of aging and inflammation. *Journal of Clinical Immunology* 25:405-417
- NOAA (2017) Trends in atmospheric carbon dioxide. Global Greenhouse Gas Reference Network.
- Orr JC, Fabry VJ, Aumont O, Bopp L, Doney SC, Feely RA, Gnanadesikan A, Gruber N, Ishida A, Joos F, Key RM, Lindsay K, Maier-Reimer E, Matear R, Monfray P, Mouchet A, Najjar RG, Plattner G-K, Rodgers KB, Sabine CL, Sarmiento JL, Schlitzer R, Slater RD, Totterdell IJ, Weirig M-F, Yamanaka Y, Yool A (2005) Anthropogenic ocean acidification over the twenty-first century and its impact on calcifying organisms. *Nature* 437:681-686
- Pamplona R, Constantini D (2011) Molecular and structural antioxidant defenses against oxidative stress in animals. *American Journal of Physiology Regulatory, Integrative and Comparative Physiology* 301:R843-R863
- Pimentel M, Pegado MR, Repolho T, Rosa R (2014) Impact of ocean acidification in the metabolism and swimming behavior of the dolphinfish (*Coryphaena hippurus*) early larvae. *Marine Biology* 161:725-729
- Pimentel MS, Faleiro F, Diniz M, Machado J, Pousão-Ferreira P, Peck MA, Pörtner H-O, Rosa R (2015) Oxidative stress and digestive enzyme activity of flatfish larvae in a changing ocean. *PloS one* 10:e0134082
- Pistevos JC, Nagelkerken I, Rossi T, Olmos M, Connell SD (2015) Ocean acidification and global warming impair shark hunting behaviour and growth. *Scientific Reports* 5:16293

- Pörtner H-O, Karl DM, Cheung WWL, Lluch-Cota SE, Nojiri Y, Schmidt DN, Zavialov PO (2014). Ocean Systems. In Climate change 2014: Impacts, Adaptation and Vulnerabilities. Part A: Global and Sectorial Aspects Contribution of Working Group II to the Fifth Assessment Report of the Intergovernmental Panel on Climate Change (eds. CB Field VR Barros DJ Dokken KJ Mach MD Mastrandrea), pp. 411-484. Cambridge, United Kingdom and New York, USA
- Ridgwell A, Zeebe RE (2005) The role of the global carbonate cycle in the regulation and evolution of the Earth system. *Earth and Planetary Science Letters* 234:299-315
- Rosa R, Baptista M, Lopes VM, Pegado MR, Paula JR, Trübenbach K, Leal MC, Calado R, Repolho T (2014) Early-life exposure to climate change impairs tropical shark survival. *Proceedings of the Royal Society of London B: Biological Sciences* 281:20141738
- Rosa R, Paula JR, Sampaio E, Pimentel M, Lopes AR, Baptista M, Guerreiro M, Santos C, Campos D, Almeida-Val VMF, Calado C, Diniz M, Repolho T (2016a) Neuro-oxidative damage and aerobic potential loss of sharks under elevated CO₂. *Marine Biology* 163:119
- Rosa R, Pimentel M, Galan JG, Baptista M, Lopes VM, Couto A, Guerreiro M, Sampaio E, Castro J, Santos C, Calado C, Repolho T (2016b) Deficit in digestive capabilities of bamboo shark early stages under climate change. *Marine Biology* 163:1-5
- Rosa R, Rummer JL, Munday PL (2017) Biological responses of sharks to ocean acidification. *Biology Letters* 13:20160796
- Rosa R, Seibel BA (2008) Synergistic effects of climate-related variables suggest future physiological impairment in a top oceanic predator. *Proceedings of the National Academy of Sciences of the United States of America* 105:20776-20780
- Rudneva II (1997) Blood antioxidant system of black sea elasmobranch and teleosts. *Comparative Biochemistry and Physiology part C: Pharmacology, Toxicology and Endocrinology* 118:255-260
- Rudneva II (1999) Antioxidant system of Black Sea animals in early development. *Comparative Biochemistry and Physiology Part C: Pharmacology, Toxicology and Endocrinology* 122:265-271
- Rudneva II, Dorokhova II, Skuratovskaya EN, Kuz'minova NS (2014) Comparative studies of hepatic and blood biomarkers in three species of black sea elasmobranchs. *International Journal of Marine Science* 4:1-14

- Rummer JL, Munday PL (2016) Climate change and the evolution of reef fishes: past and future. *Fish and Fisheries* 18:22-39
- Sampaio E, Lopes AR, Francisco S, Paula JR, Pimentel M, Maulvault AL, Repolho T, Grilo TF, Pousão-Ferreira P, Marques A, Rosa R (2018) Ocean acidification dampens physiological stress response to warming and contamination in a commercially-important fish (*Argyrosomus regius*). *Science of the Total Environment* 618:388-398
- Sarazin G, Michard G, Prevot F (1999) A rapid and accurate spectroscopic method for alkalinity measurements in seawater samples. *Water Research* 33:290-294
- Sejersted Y, Aasland AL, Bjørås M, Eide L, Saugstad OD (2009). Accumulation of 8-Oxoguanine in liver DNA during hyperoxic resuscitation of newborn mice. *Pediatric Research* 66(5): 533-538
- Shen J, Deininger P, Hunt JD, Zhao H (2007) 8-Hydroxy-2'-deoxyguanosine (8-OH-dG) as a potential survival biomarker in patients with nonsmall-cell lung cancer. *Cancer* 109: 574-580
- Silva CSE, Novais SC, Lemos MFL, Mendes S, Oliveira AP, Gonçalves EJ, Faria AM (2016) Effects of ocean acidification on the swimming ability, development and biochemical responses of sand smelt larvae. *Science of the Total Environment* 563-564:89-98
- Solé M, Rodríguez S, Papiol V, Maynou F, Cartes JE (2009) Xenobiotic metabolism markers in marine fish with different trophic strategies and their relationship to ecological variables. *Comparative Biochemistry and Physiology, Part C* 149:83-89
- Stiasny MH, Mittermayer FH, Sswat M, Voss R, Jutfelt F, Chierici M, Puvanendran V, Mortensen A, Reusch TBH, Clemmesen C (2016) Ocean acidification effects on atlantic cod larval survival and recruitment to the fished population. *PloS one* 11:e0155448
- Stohs S, Bagchi D (1995) Mechanisms in the toxicity of metal ions. *Free Radical Biology and Medicine* 18(2): 321-336
- Sswat M, Stiasny MH, Jutfelt F, Riebesell U, Clemmesen C (2018) Growth performance and survival of larval Atlantic herring, under the combined effects of elevated temperatures and CO₂. *PLoS ONE* 13(1): e0191947
- Sunday JM, Calosi P, Dupont S, Munday PL, Stillman JH, Reusch TBH (2014) Evolution in an acidifying ocean. *Trends in Ecology & Evolution* 29:117-125

- Tiedke J, Cubuk C, Burmester T (2013) Environmental acidification triggers oxidative stress and enhances globin expression in zebrafish gills. *Biochemical and Biophysical Research Communications* 441:624-629
- Tomanek L (2010) Variation in the heat shock response and its implication for predicting the effect of global climate change on species' biogeographical distribution ranges and metabolic costs. *Journal of Experimental Biology* 213:971-979
- Tomanek L, Zuzow MJ, Ivanina AV, Beniash E, Sokolova IM (2011) Proteomic response to elevated $p\text{CO}_2$ level in eastern oysters, *Crassostrea virginica*: evidence for oxidative stress. *Journal of Experimental Biology* 214:1836-1844
- Uchiyama M, Mihara M (1978) Determination of malonaldehyde precursor in tissues by thiobarbituric acid test. *Analytical Biochemistry* 86:271-278
- Wang X, Wu L, Aouffen Mh, Mateescu M-A, Nadeau R, Wang R (1999) Novel cardiac protective effects of urea: from shark to rat. *British Journal of Pharmacology* 128:1477-1484
- Wittmann AC, Pörtner H-O (2013) Sensitivities of extant animal taxa to ocean acidification. *Nature Climate Change* 3:995-1001
- Wood CM, Liew HJ, Boeck GD, Walsh PJ (2013) A perfusion study of the handling of urea analogues by the gills of the dogfish shark (*Squalus acanthias*). *PeerJ* 1, e33
- Zeebe RE, Ridgwell A (2011) Past changes in ocean carbonate chemistry. In: Gattuso J-P, Hansson L (eds) *Ocean Acidification*. Oxford University Press, Oxford, New York, pp 21-37

3 Transgenerational exposure to ocean acidification induces biochemical distress in a keystone amphipod species (*Gammarus locusta*)

Ana R Lopes^{1,2}, Francisco Borges¹, Cátia Figueiredo¹, Eduardo Sampaio¹,
Tiago F Grilo¹, Mário Diniz², Rui Rosa¹

¹MARE- Marine Environmental Sciences Centre & Laboratório Marítimo da Guia, Faculdade de Ciências,
Universidade de Lisboa, Av. Nossa Senhora do Cabo 939, 2750-374 Cascais, Portugal

²UCIBIO, REQUIMTE, Departamento de Química, Faculdade de Ciências e Tecnologia, Universidade Nova de
Lisboa, Quinta da Torre, 2829-516 Caparica, Portugal

Abstract

Atmospheric carbon dioxide (CO₂) levels are increasing at the fastest rate ever recorded, causing higher CO₂ dissolution in the ocean, and leading to a process known as ocean acidification (OA). Unless anthropogenic CO₂ emissions are reduced, they are expected to reach ~900 ppm by the century's end, resulting in a 0.13-0.42 drop in the seawater pH levels. Since the transgenerational effects of high CO₂ in marine organisms are still poorly understood at lower levels of biological organization (namely at the biochemical level), here we reared a marine amphipod, *Gammarus locusta*, under control and high CO₂ conditions for two generations. We measured several stress-related biochemical endpoints: i) oxidative damage [lipid peroxidation (LPO) and DNA damage]; ii) protein repair and removal mechanisms [heat shock proteins (HSPs) and ubiquitin (Ub)]; as well as iii) antioxidant responses [superoxide dismutase (SOD), catalase (CAT), glutathione peroxidase (GPx) and glutathione S-transferase (GST)] and total antioxidant capacity (TAC). The present results support the premise that exposure to high CO₂ is expected to decrease survival rates in this species and cause within- and transgenerational oxidative damage. More specifically, the predicted upsurge of reactive oxygen and nitrogen species seemed to overwhelm amphipod antioxidant machinery, increasing antioxidant levels, nonetheless insufficient in circumventing protein damage within the parents. Additionally, negative effects of OA are potentially being inherited by the offspring, since the oxidative stress imposed in the parent's proteome is restricting the efficiency of the DNA repair mechanisms within the offspring's. Thus, we argue that a transgenerational exposure of *G. locusta* could further increase vulnerability to OA and may endanger the fitness and sustainability of natural populations.

Keywords: *Gammarus locusta*, Ocean acidification, transgenerational, oxidative stress, oxidative damage

Levels of carbon dioxide (CO₂) in the atmosphere are rising at an unprecedented and faster rate than ever recorded in human history (Lüthi et al., 2008). In parallel, CO₂ is being absorbed by the ocean resulting in drastic changes in the seawater carbonate system and contributing to a phenomenon known as ocean acidification (OA) (Caldeira and Wickett, 2003; Doney et al., 2009; Zeebe and Ridgwell, 2011). If anthropogenic CO₂ emissions continue unabated to increase – and are predicted to reach ~ 900 ppm by 2100 – this will elicit a further 0.13-0.42 pH drop (Gattuso and Hansson, 2011; Pörtner et al., 2014).

Studies addressing the impacts of OA on marine organisms have increased in the last decades to unveil the mechanisms that may or may not allow them to cope with elevated CO₂ (Kroeker et al., 2010; Orr et al., 2005). In general, as CO₂ increases, organisms may experience decreased growth rates (Baumann et al., 2012; Heuer and Grosell, 2014) and metabolism (Borges et al., 2018a; Rosa and Seibel, 2008), impaired oxygen binding (Pörtner and Reipschlöger, 1996), and ultimately, increased mortality (Baumann et al., 2012; Borges et al., 2018b; Pörtner and Reipschlöger, 1996).

Marine crustaceans can usually tolerate high CO₂ levels, due to their high hemolymph bicarbonate ions (HCO₃⁻) concentration (Pane and Barry, 2007; Pörtner et al., 2004), however, OA is expected to induce changes in their acid-base balance as intracellular acidosis could impair protein functions and cause oxidative stress (Burnett, 1997; Gattuso and Hansson, 2011; Heuer and Grosell, 2014). Specifically, the increasing availability of hydrogen ions (H⁺) with OA, as well as the reaction of CO₂ with peroxynitrite, a reactive nitrogen species (RNS), will in turn produce additional RNS, with a subsequent overproduction of reactive oxygen species [ROS, i.e. superoxide radicals (O₂⁻), hydrogen peroxides (H₂O₂), singlet oxygen (¹O₂) and hydroxyl radical (HO[•])], ultimately instigating oxidative damage (i.e. lipid, protein and DNA damage) (Dean, 2010; Feder and Hofmann, 1999; Hu et al., 2015; Sampaio et al., 2018; Tomanek et al., 2011). Nonetheless, to counteract oxidative stress, marine organisms bear effective enzymatic [i.e. superoxide dismutase (SOD), catalase (CAT), glutathione peroxidase (GPx) and glutathione s-transferase (GST)] and non-enzymatic (e.g. vitamins and amino acids) antioxidant mechanisms (Bartosz, 2003; Lesser, 2006). In addition, heat shock proteins (HSP) and ubiquitin (Ub) levels act to repair and refold denatured proteins (Tomanek, 2010; Tomanek et al., 2011), and when permanently damaged, proteins are targeted and eliminated (Bond et al., 1988; Hanna et al., 2007).

Over the last few decades, an increasing body of research has accumulated on the biochemical systems of crustaceans' amphipods, mainly due to their wide geographical distribution and ecological relevance in marine food-webs (Costa and Costa, 1999). Nonetheless, most of these studies centered on amphipods responses to seasonality (Sroda and Cossu-Leguille, 2011), and their sensitivity to UV radiation (Krapp et al., 2009; Obermüller et al., 2007), hypoxia (Gorokhova et al., 2010), salinity regimes (Vereshchagina et al., 2016) and contamination (Barros et al., 2017; Correia et al., 2002a, 2002b; Gorokhova et al., 2013; Timofeyev et al., 2008), while the space for acclimation to changes in seawater chemistry (i.e. OA) were only assessed on amphipods' reproductive ecology, physiology and metabolism, without considering changes in their antioxidant machinery (Cardoso et al., 2018; Egilsdottir et al., 2009; Hauton et al., 2009). It is still worth noting that those studies only evaluated the effect of OA during one lifetime (i.e. one life stage, single generation), ignoring the potential for transgenerational acclimation or even adaptation over several generations.

To fill this gap of knowledge, the aim of this study was to investigate, for the first time, the transgenerational effects of OA ($\Delta p\text{CO}_2 \sim 400\text{-}500 \mu\text{atm}$) on the biochemistry of the amphipod *Gammarus locusta* for two generations (F0 and F1), through quantification of relevant biomarkers of cellular damage, protein repair and oxidative stress. This amphipod plays key ecological relevance, being the link between lower and higher tropic levels within marine food webs (Costa and Costa, 1999). Its wide geographic distribution, combined with a short generation time (40-50 days at 15°C) (Costa and Costa, 1999; Neuparth et al., 2002) and the suitability to be captive bred (Costa et al., 2005; Neuparth et al., 2005) are some of the key features which make the species a potential climate change biological beacon. In this context, we assessed: i) oxidative damage markers (lipid peroxidation and DNA damage); ii) the HSP and Ub levels; as well as iii) oxidative stress enzymes (SOD, CAT, GPx and GST) and total antioxidant capacity (TAC). Lastly, supported by literature focusing on the target amphipod species, we discussed whether the parental environmental conditioning will have an impact in the offspring's fitness, i.e. transgenerational plasticity (TGP), and to which extent it could allow *G. locusta* to thrive in an acidified ocean.

3.1. Material and methods

3.1.1. Experimental setup

3.1.1.1. Organisms collection and maintenance

Amphipods were obtained from a well-established laboratory culture from CIIMAR (Porto, Portugal), originally collected in the Sado Estuary (38°27'N, 08°43'W, Portugal), and transported to the Laboratório Marítimo da Guia aquaculture facilities (Cascais, Portugal). Organisms were maintained under stable conditions, mimicking those found in their natural environment (temperature = 18°C, pH = 8.0, ~ 400 μatm $p\text{CO}_2$, salinity = 35, 12 h light: 12 h dark), for 60-days preceding the experimental exposure.

3.1.1.2. CO₂ exposure

Organisms (n = 25 per replicate for each generation) were randomly placed in a flow-through system (5 replicate tanks of 4L per treatment) and exposed to one of the following experimental conditions: i) Control (18°C, pH = 8.0, ~ 400 μatm $p\text{CO}_2$); or ii) High CO₂ (18°C, pH = 7.7, ~ 800 μatm $p\text{CO}_2$), according to IPCC's Representative Concentration Pathways (RCP) scenario 8.5 (IPCC, 2014). The CO₂ levels were automatically adjusted using a Profilux controlling system (Profilux 3.1, GHL, Germany), which adjusted pH values every two seconds. Solenoid valves were connected to individual pH probes (PL-0071, GHL, Germany) to downregulate seawater pH through the injection of a certified CO₂ gas mixture (Airliquide, Portugal) and upregulate through the injection of atmospheric air (Soda lime, Sigma-Aldrich). Additionally, temperature (Thermometer TFX 430, WTW GmbH, Germany), salinity (refractometer V2, TMC Iberia, Portugal), and pH (SevenGo pro SG8, Mettler Toledo, Switzerland) were monitored daily, using handheld equipment, to adjust system setpoints as necessary. Seawater carbonate system speciation (see Supplementary Table SI) was measured weekly for each generation by spectrophotometry (595 nm), through the quantification of total alkalinity according to Sarazin et al. (1999). Levels of total dissolved inorganic carbon, $p\text{CO}_2$, bicarbonate and aragonite were calculated using the CO2SYS software (Lewis et al., 1998), with dissociation constants from Dickson and Millero (1987).

Temperature values were set to mean annual values found at *G. locusta* natural environment (Rocha et al., 2013), and maintained inside each tank by a partial immersion in a water bath. Upon demand, seawater temperature was upregulated through submerged digital heaters (V2Therm 200W aquarium heater, TMC Iberia, Portugal) or downregulated using seawater chillers (Hailea, HC-250A, Guangdong, China). The tanks were illuminated with white fluorescent lamps in a 12 h: 12 h (light/dark) photoperiod. Organisms were fed daily ad libitum on *Ulva* sp., reflecting feeding preferences reported in their natural environment (Costa and Costa, 1999)

3.1.1.3. Transgenerational exposure and reciprocal transplant design

The experimental design is described in Fig. 1. After 60 days acclimating, stock new-borns were allowed to reach maturity (~ 30 days), after which, fifteen mate-guarding couples were randomly allocated (60L tanks) and gradually acclimated to one of the experimental conditions (Control or High CO₂), with pH decreases of 0.1 units per day. Consequently, the first generation (F0) was conceived and allowed to develop under the respective treatment. After reaching sexual maturity, couples were allowed to mate, and upon couple's separation, new-borns were removed from the parental population. New-borns were indiscriminately sorted into independent 4-L replicate tanks (25 new-borns per replicate). The resulting F0 progeny (F1) was divided and exposed to: i) the same treatment as their progenitors [Control (C-C) or High CO₂ (H-H)]; or ii) the opposing treatment [cross treatments: High CO₂ – Control (H-C) or Control – High CO₂ (C-H)] (see Fig. 1). Each generation, F0 and F1, were reared from juvenile to sexual maturity, after which fifteen organisms per treatment (n=3 per each of the 5 replicates) were collected and immediately frozen at -80 °C for posterior biochemical analyses.

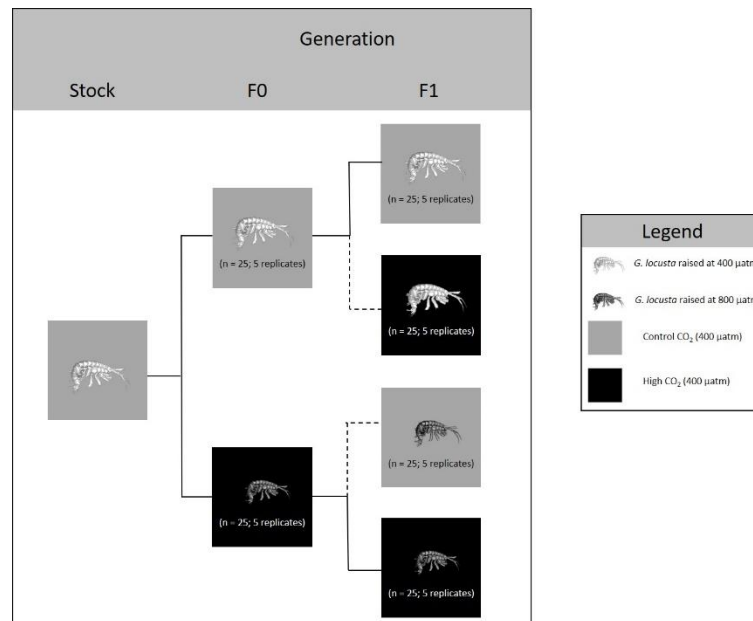


Figure 1 - Diagram of the experimental design. Parental generation (F0): C - amphipods reared under control $p\text{CO}_2$ levels; H - amphipods reared under elevated $p\text{CO}_2$ levels. Offspring generation (F1): offspring reared under the same treatment as their progenitors (continues line) [Control (C-C) or High CO₂ (H-H)]; or reared on the opposing treatment (dotted line) [High CO₂ - Control (H-C) or Control - High CO₂ (C-H)].

3.1.2. Biochemical Analyses

3.1.2.1. Sample preparation

Samples (n=3 per each of the 5 replicates, n=15 per treatment) were homogenized using an Ultra-Turrax (Staufen, Germany), in 2 mL of phosphate buffered saline solution (PBS: 0.14 M NaCl, 2.7 mM KCl, 8.1 mM Na₂HPO₄ and 1.47 mM KH₂PO₄, pH 7.4). Homogenates were centrifuged at 10.000 x g for 15 min at 4°C and frozen (-80°C) until further analyses. Each sample was run in triplicate (technical replicates), and the results were normalized to total protein content, as described by Bradford (1976).

3.1.2.2. Cellular and DNA damage

Lipid peroxidation (LPO), was determined through the quantification of a specific end product of lipid damage, i.e. malondialdehyde (MDA), according to the thiobarbituric acid reactive substances (TBARS) assay (Uchiyama and Mihara, 1978). A total of 5 μL of each sample was added to a new microtube, as well as 45 μL of monobasic sodium phosphate buffer (50 mM), 12.5 μL of sodium dodecyl sulphate (8.1 %), 93.5 μL of trichloroacetic acid (20 %, pH 3.5), 93.5 μL of thiobarbituric acid (1 %), and 50.5 μL of Milli-Q ultrapure water. Subsequently each tube was mixed, punctured and then placed in boiling water (100 °C) for 10 min. Afterwards, microtubes were placed on ice to cool and 62.5 μL of Milli-Q ultrapure water was added to each microtube. Finally, 150 μL of each sample was added to 96-well microplates, and the absorbance read at 532 nm in a microplate reader (Asys UVM 340, Biochrom, USA). Malondialdehyde concentrations were calculated based on a calibration curve (0 - 0.3 μM) using MDA bis (dimethyl acetal) standards, and results expressed as nmol mg^{-1} total protein.

DNA damage was measured according to Maclouf et al. (1987) and Shen et al. (2007) assessed through an ELISA method, via the quantification of 8- hydroxy- 2'- deoxyguanosine (8-OHdG). Each sample (100 μL) was added to each well in a 96-well microplate and allowed to incubate overnight at 4°C. On the subsequent day, plates were washed (3x) with PBS-TWEEN 20 and 200 μL of the blocking solution (BSA) was added to each well and allowed to incubate for 90 min at room temperature. After another washing procedure, microplates were incubated overnight with a primary antibody (anti-OHdG, clone 15 A3, Sigma-Aldrich, Germany) by adding 50 μL to each well at a concentration of 0.5 $\mu\text{g mL}^{-1}$. Subsequently, microplates were washed to remove non-linked antibody and allowed to incubate for 90 min at 37°C with the secondary antibody (alkaline phosphatase-conjugated anti-mouse IgG, Fab specific, Sigma-Aldrich, USA), by adding 50 μL to each well at a concentration of 1 $\mu\text{g mL}^{-1}$. After a final washing procedure, 50 μL of substrate (SIGMA FAST™ p-Nitrophenyl Phosphate Tablets, Sigma-Aldrich, USA) were added to each well and micrplates were incubated at room temperature for 30 min. Then the reaction was stopped by adding 100 μL of 3M NaOH. The absorbance was read at 405 nm using a microplate reader (Asys UVM 340, Biochrom, USA), and results expressed according to sample protein (abs mg^{-1} total protein).

3.1.2.3. Protein Repair and removal mechanisms

Heat Shock Protein 70 (HSP70) levels were determined through an ELISA according to Njemini et al. (2005). Briefly, 10 μL of each sample was diluted in 980 μL phosphate-buffered saline (PBS). Subsequently, 100 μL of each diluted sample was added to 96-well microplates (Microloan 600, Greiner, Germany) and allowed to incubate overnight at 4°C. On the subsequent day, microplates were washed (3x) using PBS containing 0.05 % TWEEN-20. Afterwards, 100 μL of blocking solution [1 % bovine serum albumin (BSA)] was added to each well, and microplates were incubated for 90 min at 37°C. Afterwards, 50 μL of primary antibody (5 $\mu\text{g mL}^{-1}$ in 1% BSA: anti-HSP70/HSC70, Acris, USA) was added to each well. After another incubation period (overnight at 4°C), microplates were washed (3x) to remove non-linked antibodies and a second antibody [alkaline phosphatase-conjugated anti-mouse IgG (Fab specific, Sigma-Aldrich, USA)] was added (50 μL of 1 $\mu\text{g mL}^{-1}$) to each well, and microplates allowed to incubate at 37°C for 90 min. After an additional washing procedure, 100 μL of substrate (2.7 mM p-Nitrophenyl Phosphate, 100 mM trizma hydrochloride, 100 mM sodium chloride, 5 mM magnesium chloride in deionized ultrapure water, pH 8.5) was added to each well and incubated for 30 min at room temperature. Afterwards, 50 μL of stop solution (3 M NaOH) was added to each well and the absorbances read at 405 nm (Asys UVM 340, Biochrom, USA). HSP content was calculated from the calibration curve, based on serial dilutions of purified HSP70 active protein (0 – 2,000 $\mu\text{g mL}^{-1}$, Acris, USA) and results normalized to sample protein ($\mu\text{g mg}^{-1}$ total protein).

Ubiquitin (Ub) content was assessed through a direct ELISA, according to Lopes et al. (2018). Each sample (100 μL) was added to 96-well microplates (Microloan 600, Greiner, Germany) and incubated overnight at 4°C. On the next day microplates were washed (3x) with PBS-TWEEN. Afterwards, 100 μL of blocking solution [1 % bovine serum albumin (BSA)] was added to each well and microplates were allowed to incubate for 90 min at 37°C. Subsequently, 50 μL of primary antibody at a concentration of 200 $\mu\text{g mL}^{-1}$ (P4D1, sc-8017, HRP conjugate, Santa Cruz, USA) was added to each well, and after another incubation period (overnight at 4°C), microplates were washed (3x) to remove non-linked antibodies. Afterwards, 100 μL of TMB/E substrate (Temecula California, Merck Millipore) was added to each well and incubated for 30 min at room temperature. Finally, 100 μL of stop solution (1M HCL) was added to each well and the absorbances were read at 415 nm, using a microplate reader (Asys UVM 340, Biochrom,

USA). The Ub content was assessed based on a serial dilution of purified ubiquitin (0 - 1 $\mu\text{g mL}^{-1}$, UbqBio, E-1100, USA) and results expressed according to total sample protein ($\mu\text{g mg}^{-1}$ total protein).

3.1.2.4. Enzymatic activities and total antioxidant capacity

Superoxide dismutase (SOD: EC 1.15.1.1) inhibition was determined through an adaptation of the method described by McCord and Fridovich (1969) to 96-well microplates. Each sample (10 μL) as well as 180 μL of the reaction mix, consisting of deionized ultrapure water, 50 mM potassium phosphate, 0.1 mM ethylenediaminetetraacetic acid, 0.01 mM cytochrome c and 0.05 mM xanthine, were added to a 96-well microplate. Subsequently the reaction was initiated by adding 10 μL of xanthine oxidase (0.005 units). The absorbance was read at 550 nm using a microplate reader (Asys UVM 340, Biochrom, USA), and results normalized according to sample protein levels (% Inhibition $\text{min}^{-1} \text{mg}^{-1}$ total protein).

Catalase (CAT) activity was measured based on the method described by Johansson and Borg (1988). Each sample (20 μL), as well as 100 mM potassium phosphate (100 μL) and methanol (30 μL) were added to a 96-well microplate, and plates incubated for 20 minutes and continuously shaken. Afterwards, 10 M potassium hydroxide (30 μL) and 34.2 mM purpald in 0.5 M HCl (30 μL) were added to each well, and plates shaken and incubated for another 10 minutes. Subsequently, 10 μL of potassium periodate (65.2 mM in 0.5 M KOH) was added to each well, and a final incubation was performed for 5 minutes. The absorbance was read at 540 nm, using a microplate reader (Asys UVM 340, Biochrom, USA). Formaldehyde concentration of the samples was calculated based on a calibration curve (from 0 to 75 μM formaldehyde), followed by the calculation of the CAT activity of each sample, where one unit of catalase is defined as the amount that will cause the formation of 1.0 nmol of formaldehyde per minute at 25°C. The results were expressed in relation to total protein content ($\text{nmol min}^{-1} \text{mg}^{-1}$ total protein).

Glutathione peroxidase (GPx: EC 1.11.1.9) activity was determined according to Lawrence and Burk (1976), through an adaptation to 96-well microplates. Briefly, 20 μL of each sample, 50 mM phosphate buffer (pH 7.6), co-substrate mixture (0.8 mM β -NADPH, 4 mM Glutathione, 4 U/mL glutathione reductase, and 4 mM sodium azide) and 15 mM cumene hydroperoxide ($\text{C}_9\text{H}_{12}\text{O}_2$) were added to each well, and the absorbance was read at 340 nm (Asys UVM 340,

Biochrom, USA), every minute for 6 min. The GPx activity was determined using the β -NADPH coefficient extinction, and results given $\text{nmol min}^{-1} \text{mg}^{-1}$ total protein.

Glutathione S-transferase (GST) was determined following the method described by Habig et al. (1974), optimized for 96-well microplates. Specifically, 180 μL of substrate solution (100 mM 1-chloro-2,4-dinitrobenzene (CDNB), 200 mM L-glutathione and Dulbecco's PBS) were added to 20 μL sample in each well and the absorbance was read at 340 nm (Asys UVM 340, Biochrom, USA) every minute for 6 min. Equine liver GST (Sigma-Aldrich) was used as positive control to validate the assay and GST activity calculated using the molar extinction coefficient for CDNB of 5.3 ϵmM . The results were expressed according to total protein of the sample ($\text{nmol min}^{-1} \text{mg}^{-1}$ total protein).

Total antioxidant capacity (TAC) was determined according to Kambayashi et al. (2009). Each sample (10 μL) was added to each well in a 96-well microplate. Subsequently, 90 μM myoglobin (10 μL), 600 μM 2,2'-azino-bis (3-ethylbenzothiazoline-6-sulphonic acid) (150 μL) and 500 μM hydrogen peroxide (40 μL) were added to the wells. Microplates were incubated at room temperature for 5 min and the absorbance was read at 410 nm (Asys UVM 340, Biochrom, USA). TAC was calculated from a calibration curve, based on a series of Trolox (0 – 0.3 Mm) and expressed according to samples total protein (mM Trolox mg^{-1} total protein).

3.1.3. Statistical analysis

In order to infer intra- and inter-generational differences, generalized linear models (GLM) analyses were implemented. Mixed models were used to ascertain significant differences between replicates within each group, for all variables used, and ruled unnecessary whenever the analysis did not show significant differences. Our data was fitted using gamma family models, and model residuals were checked for homogeneity of variances, while independence and leverage were used to perform model validation. Treatment (4 levels: Control, High CO_2 , and the two cross-treatments), Generation (2 levels: F0 and F1) and Replicates (5 levels for each treatment) were used as explanatory variables according to each dependent variable (LPO, DNA damage, HSP, Ub, SOD, CAT, GPx, GST and TAC). All statistical analyses were performed in R Studio (R Development Core Team 2017).

3.2. Results

3.2.1. Parental generation (F0)

Following exposure of *G. locusta* to the upcoming high CO₂ conditions, survival rates decreased significantly from 75-80% in the F0 control treatment to 60-65% when exposed to high CO₂ (please see Borges et al., 2018b).

Focusing strictly in the first generation, from all the biomarkers investigated, only ubiquitin (Ub), glutathione peroxidase (GPx) and the total antioxidant capacity (TAC) differ significantly between treatments (GLM analysis in tables SV, SVIII, SX; Figs. 3B, 4C, E, respectively). Furthermore, biomarkers of cellular injury, such as LPO and DNA damage, revealed no significant differences between control organisms and those reared under high CO₂ conditions (GLM analysis in tables SII and SIII, Fig. 2A and Fig. 2B, respectively). Likewise, HSP levels, indicative of protein repair mechanisms, did not vary between treatments (GLM analysis in table SIV, Fig. 3A) as well as the enzymatic activities of SOD, CAT and GST (GLM analysis in tables SVI, SVII, SIX; Figs. 4A, B, D).

3.2.2. Offspring generation (F1)

In contrast with the parental generation, no survival differences were found between control and high CO₂ treatments, nor between generations (F0 versus F1). Furthermore, cross-treatment groups (H-C and C-H) displayed the lowest survival rates, below 50% (please see Borges et al., 2018a).

In general, the levels of all biomarkers boosted significantly from the parental generation (F0) to the offspring (F1), with exception of SOD (i.e. control organisms had similar values to their equivalent ones in the first generation; GLM analysis in table SVI, Fig. 4A), CAT (i.e. F1 amphipods reared under high CO₂ displayed similar values to their counterparts in F0; GLM analysis in table SVII, Fig. 4B) and TAC, which followed the same trend described for CAT (GLM analysis in table SX, Fig. 4E). Additionally, levels of LPO were maximum in the H-C treatment (GLM analysis in table SII; Fig. 2A), indicative of higher cellular damage when amphipods were reared under this condition, while damage in nucleic acids was found in both cross treatments (GLM analysis in table SIII, Fig. 2B). Regarding indicators of protein repair and removal mechanisms (i.e. HSP and Ub) no significant differences were observed among

treatments (GLM analysis in tables SIV and V; Fig. 3A, B). The values of biomarkers measured in cross treatments (i.e. H-C and C-H) were generally higher than the control and high CO₂-reared F1 amphipods. This was particularly evident for cellular injury indicators, including LPO (Fig. 2A) and DNA damage (Fig. 2B), as well as for oxidative stress biomarkers, such as SOD (Fig. 4A), CAT (Fig. 4B), GPx (Fig. 4C) and TAC (Fig. 4E).

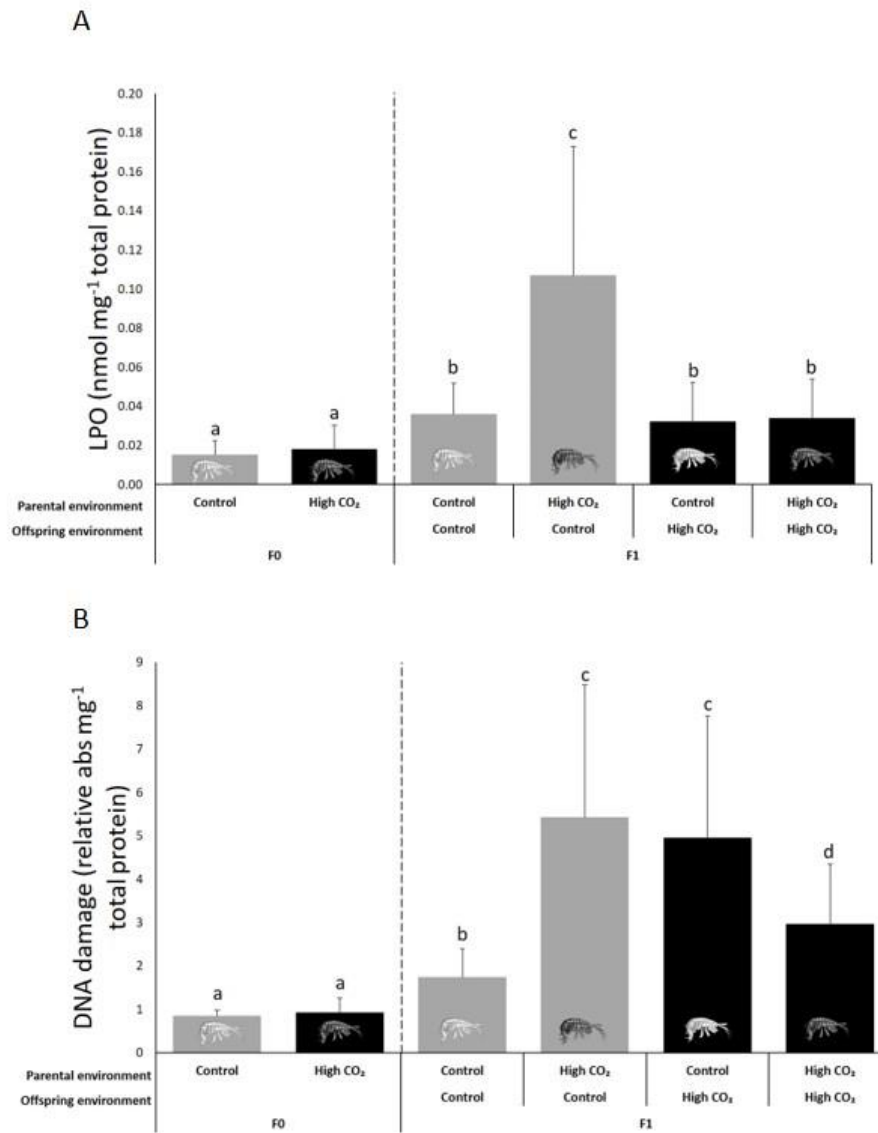


Figure 2 – Impact of high CO₂ exposure on: A) LPO (nmol mg⁻¹ total protein); and B) DNA damage (relative abs mg⁻¹ total protein) levels in *G. locusta* parents and offspring's. Values represent mean \pm SD. Different letters represent significant differences between treatments identified by GLM analyses which are described in Supplemental Tables SII and SIII.

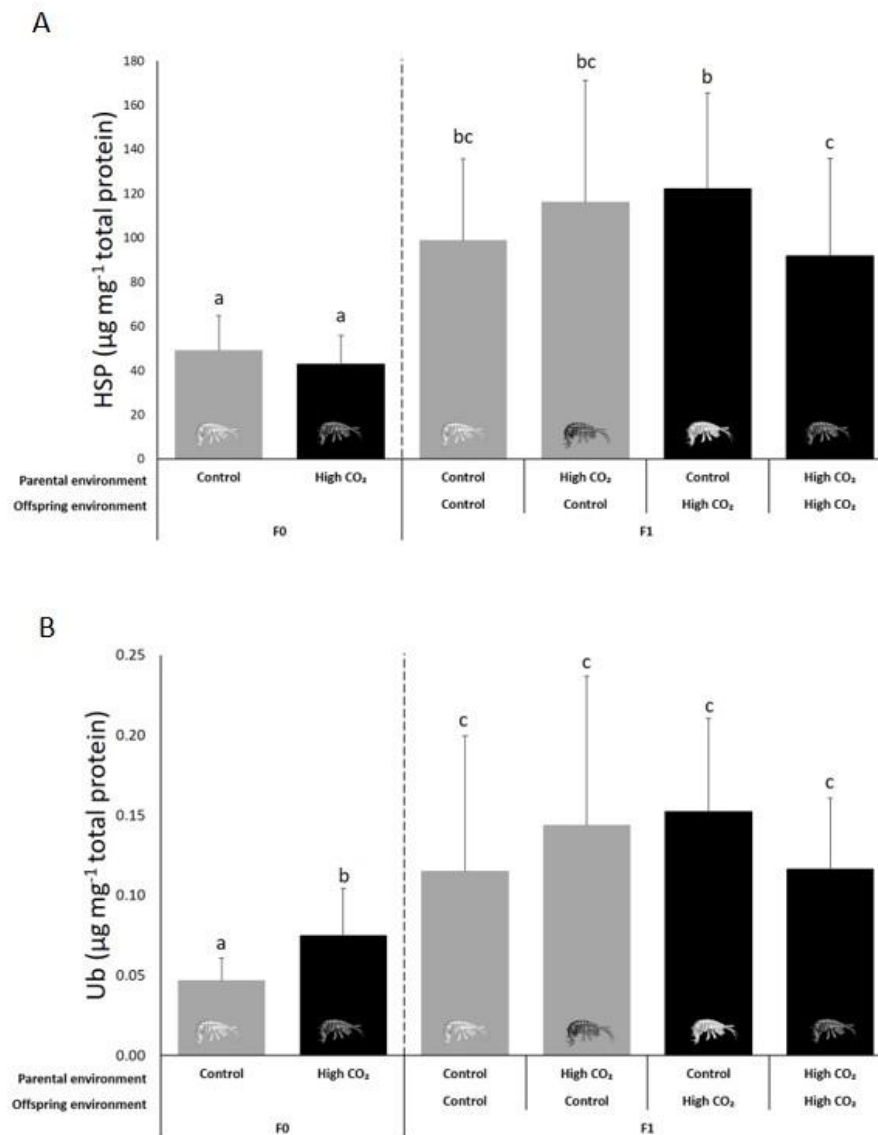


Figure 3 – Impact of high CO₂ exposure on: A) HSP (µg mg⁻¹ total protein); and B) Ub (µg mg⁻¹ total protein) levels in *G. locusta* parents and offspring's. Values represent mean ± SD. Different letters represent significant differences between treatments identified by GLM analyses which are described in Supplemental Tables SIV and SV.

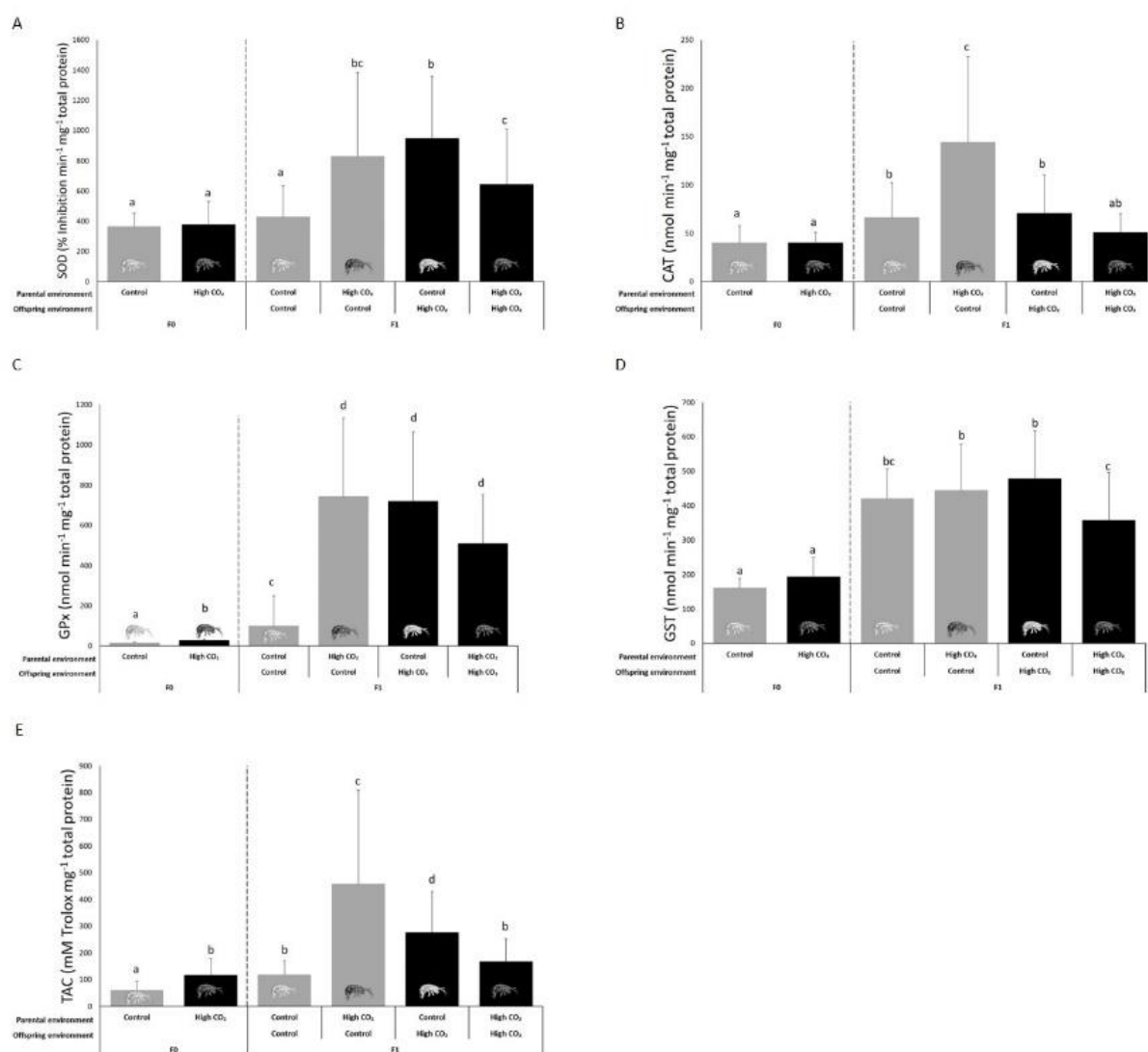


Figure 4 – Impact of high CO₂ exposure on: A) SOD (% Inhibition min⁻¹ mg⁻¹ protein); B) CAT (nmol min⁻¹ mg⁻¹ total protein); C) GPx (nmol min⁻¹ mg⁻¹ total protein); D) GST (nmol min⁻¹ mg⁻¹ total protein) activities; and E) TAC (mM Trolox mg⁻¹ total protein) levels in *G. locusta* parents and offspring's. Values represent mean ± SD. Different letters represent significant differences between treatments identified by GLM analyses which are described in Supplemental Tables SVI-SXI.

Table I – Summary table of the oxidative damage (LPO and DNA), protein repair and removal mechanisms (HSP and Ub) and antioxidant response (SOD, CAT, GPx and GST activities and TAC) in *G. locusta* following within- and transgenerational exposure to ocean acidification

		F0 High CO ₂	Control	F0 vs F1			F1			
				High CO ₂	C- CH	H- HC	High CO ₂	CC- CH	HH- HC	HC- CH
Oxidative damage	LPO	=	↑	↑	↑	↑	=	=	↑	↓
	DNA	=	↑	↑	↑	↑	↑	↑	↑	=
Protein repair and removal	HSP	=	↑	↑	↑	↑	=	=	=	=
	Ub	↑	↑	↑	↑	↑	=	=	=	=
Antioxidant response	SOD	=	=	↑	↑	↑	↑	↑	=	=
	CAT	=	↑	=	↑	↑	=	=	↑	↓
	GPx	↑	↑	↑	↑	↑	↑	↑	=	=
	GST	=	↑	↑	↑	↑	=	=	↑	=
	TAC	↑	↑	=	↑	↑	=	↑	↑	↓

3.3. Discussion

In the present study, we assessed for the first time the biochemical strategies (see summary Table I) developed by the amphipod *G. locusta* facing a future acidified ocean, over two generations (F0 and F1). Specifically, even though exposure to OA decreased survival rates in the parental generation (Borges et al., 2018a), it did not elicit lipid peroxidation nor DNA damage in the parents. Nonetheless, there was an increase in both damage levels from the progenitors to the progeny (F0 versus F1). In fact, in the present study we observed a persistent transgenerational increase for all the biomarkers tested, i.e. oxidative damage, antioxidant response and protein repair and elimination, concomitant with evidence of metabolic depression reported in Borges et al. (2018b). This is in line with findings in a marine polychaete (*Ophryotrocha labronica*), where specific traits (e.g. fecundity and growth rates) increased over three generations until reaching a cap level, after which both traits remained constant over multiple generations (from F3 to F7) (Rodríguez-Romero et al., 2016), without representing a direct negative response to the CO₂ exposure. Additionally, while survival rates and lipid peroxidation levels remained unchanged between control and high CO₂ in F1 (C-C versus H-H), a surprising increase in lipid damage occurred when offspring raised under high CO₂ was grown under control conditions (H-C),

which was also coincident with increased mortality rates (Borges et al., 2018b). We reason that parents exposed to OA conditions were able to produce offspring capable to withstand seawater acidification – through positive parental effects – without undergoing lipid peroxidation, i.e. transgenerational plasticity (TGP), as observed in other marine organisms (Miller et al., 2012; Parker et al., 2012; Thor and Dupont, 2015). Nonetheless when conditions were reversed, these new phenotypes could act as a bottleneck for this species, as they have developed to cope better with the prior environment. In fact, even increased SOD, CAT and GPx activities and TAC levels in this treatment were not sufficient to circumvent lipid damage.

Furthermore, DNA damage levels almost doubled with acidification. Carry-over effects (H-C) were also observed, suggesting that even though no DNA damage was evident in the parental generation, negative effects of CO₂ exposure are being inherited by the offspring, and persist even if exposure conditions are reversed. Moreover, a first exposure to high CO₂ in a second generation (C-H) also led to high levels of DNA damage. This increase in DNA damage levels in F1 due to high CO₂ exposure could be related to increased Ub levels in the parents' generation. In fact, Ub is considered an indirect measure of protein damage, since it targets irreversibly oxidized proteins so they can be permanently eliminated (Bond et al., 1988; Hanna et al., 2007), and it is consensual that the proteome is intrinsically related to the quality of an individual's genome (Gueranger et al., 2014; Krisko and Radman, 2013). Specifically, DNA repair mechanisms involve key proteins that act to avoid DNA strand breaks or base pair mismatch (Hoeijmakers, 2009; Sejersted et al. 2009), and thus, protein damage severely confines the efficiency of the DNA repair proteome (Krisko and Radman, 2013; Montaner et al., 2007; Peacock et al., 2014; Polo and Jackson, 2011). We argue that the oxidative stress imposed in the proteome of the parental generation could have induced negative parental effects and impaired the capacity of genome repair and replication, which will in turn affect the capacity of subsequent generations to endure in such harsh environment.

Heat shock protein levels did not change between treatments in neither generation, as observed in a single-generation study for the same species, conducted by Hauton et al. (2009). Nonetheless, in that specific study, it was suggested that low pH exposure did not induced acid-base imbalances in *G. locusta*, from juvenile to adulthood, which contrasts with the present study, specifically looking for increased protein and DNA damage levels. In fact, OA is expected to increase the availability of the highly reactive H⁺ ions, as the CO₂ dissolves in the seawater (Caldeira and Wickett, 2003; Doney et al., 2009; Zeebe and Ridgwell, 2011). Due to its increased

reactivity and membrane permeability, H^+ ions interact with O_2^- , generating other ROS, such as H_2O_2 , which can be further reduced, through Fenton reaction into OH^\bullet , the most damaging of ROS. Subsequently, this burst of ROS, will culminate in oxidative stress and, consequently, cellular damage (i.e. lipid, protein and nucleic acid damage) (Dean, 20010; Feder and Hofmann, 1999; Hu et al., 2015; Sampaio et al., 2018; Tomanek et al., 2011). Thus, the inactivation of protein repair and refold mechanisms, via molecular chaperones (i.e. HSP), under seawater acidification, may have contributed to increased protein damage and consequent elimination (i.e. high Ub levels), since these mechanisms can be complementary (Alberti et al., 2002; Finley et al., 1984).

Oxidative stress generally occurs when ROS overwhelm the organisms' antioxidant machinery (Lesser, 2006; Matozzo et al., 2013). In the present study, the predicted upsurge in ROS with high CO_2 levels led to a general increase in *G. locusta* antioxidant response, which culminated in protein and DNA damage. In more detail, elevated CO_2 increased TAC levels in the parental generation, while SOD activity increased in the offspring's and GPx activity increased for both. Comparisons of our results with published data was an arduous task, since within- or transgenerational effects of OA in the antioxidant enzyme activities of marine organisms are still unaccounted for. Nevertheless, single-generation studies conducted in other taxa, supported that OA generally causes oxidative stress. For example, in oysters (*Crassostrea virginica*), elevated CO_2 increased oxidative stress due to ROS overproduction, directly through CO_2 interaction with ROS, as described above, or through the molecular CO_2 - RNS (e.g. peroxynitrite) interplay, that often results into nitro-oxidative reactions, produced by other reactive intermediates (e.g. nitosoperoxocaroxyate), and indirectly via intracellular H^+ ions increase (intracellular acidosis), ultimately affecting the cytoskeleton-related proteins (Dean, 20010; Tomanek et al., 2011). Moreover, studies conducted in marine fishes (larvae and adults stages) also showed a similar increasing trend in the antioxidant enzymatic activity (i.e. SOD, CAT and GST) with OA, but again insufficient in avoiding lipid damage (i.e. lipid peroxidation through MDA quantification) (Pimentel et al., 2015; Sampaio et al., 2018).

Adding to the information that marine calcifying organisms are one of the most sensitive groups to seawater acidification - due to the elevated costs in exoskeleton formation that frequently render high mortality rates (Duquette et al., 2017; Taylor et al., 2015) - the results reported in the present study support, for the first time, that predicted end-century CO_2 levels can cause within-generational oxidative stress and damage in *G. locusta*, along with metabolic

depression (Borges et al. 2018b), and that a transgenerational exposure to seawater acidification could further increase their vulnerability to OA. Nonetheless, to fully access the effects of seawater acidification in this species, it is important to unravel age-related changes in the antioxidant status - that are known to change even under natural conditions (Correia et al., 2003) - since early stages may be at greater risk and possibly compromise the species' resilience in an acidifying ocean. Moreover, it is central to increase the number of studies comprising further generations - through multigenerational studies - to accurately predict how marine amphipods will respond to future $p\text{CO}_2$ levels.

3.4. Acknowledgements

This work was supported by the Portuguese Foundation for Science and Technology (FCT), through the project CLIMATOXEEL (PTDC/AAG-GLO/3795/2014) awarded to TFG, the strategic project (UID/MAR/04292/2013) granted to MARE, and the Programa Investigador FCT 2013 to RR. FCT also supported this work through a post-doctoral grant attributed to TFG (SFRH/BPD/98590/2013) and PhD grants attributed to ARL (SFRH/BD/97070/2013), CF (SFRH/BD/130023/2017) and ES (SFRH/BD/131771/2017).

3.5. Conflict of Interest

The authors declare no conflict of interest.

3.6. References

- Alberti S, Demand J, Esser C, Emmerich N, Schild H, Höhfeld J (2002) Ubiquitylation of BAG-1 Suggests a novel regulatory mechanism during the sorting of chaperone substrates to the proteasome. *Journal of Biological Chemistry* 277: 45920-45927
- Barros S, Montes R, Quintana JB, Rodil R, Oliveira JMA, Santos MM, Neuparth T (2017) Chronic effects of triclocarban in the amphipod *Gammarus locusta*: Behavioural and biochemical impairment. *Ecotoxicology and Environmental Safety* 135: 276-283
- Bartosz G (2003) Total antioxidant capacity, in: Spiegel HE, Nowacki G, Hsiao K-J (eds.) *Advances in clinical chemistry*. Academic press, California, USA, pp. 220-272
- Baumann H, Talmage SC, Gobler CJ (2012) Reduced early life growth and survival in a fish in direct response to increased carbon dioxide. *Nature Climate Change* 2: 38-41
- Borges et al. (2018a). Hypercapnia-induced disruption of long-distance mate-detection and reduction of energy expenditure in a coastal keystone crustacean. *Physiology and Behavior*
- Borges FO, Figueiredo C, Sampaio E, Rosa R, Grilo TF (2018b) Transgenerational deleterious effects of ocean acidification on the reproductive success of a keystone crustacean (*Gammarus locusta*). *Marine Environmental Research* 138: 55-64
- Bond UNA, Haas AL, Redman K, Schlesinger MJ (1988) Ubiquitin in stressed chicken embryo fibroblast. *Journal of Biological Chemistry* 263: 2384-2388
- Bradford MM (1976) A rapid and sensitive method for the quantitation of microgram quantities of protein utilizing the principle of protein-dye binding. *Analytical Biochemistry* 72: 248-254
- Burnett LE (1997) The Challenges of living in hypoxic and hypercapnic aquatic environments. *Integrative and Comparative Biology* 37: 633-640
- Caldeira K, Wickett ME (2003) Anthropogenic carbon and ocean pH. *Nature* 425: 365-365
- Cardoso PG, Loganimoce EM, Neuparth T, Rocha MJ, Rocha E, Arenas F (2018) Interactive effects of increased temperature, pCO₂ and the synthetic progestin levonorgestrel on the fitness and breeding of the amphipod *Gammarus locusta*. *Environmental Pollution* 236:937-947
- Correia AD, Costa MH, Luis OJ, Livingstone DR (2003) Age-related changes in antioxidant enzyme activities, fatty acid composition and lipid peroxidation in whole body *Gammarus*

- locusta* (Crustacea: Amphipoda). Journal of Experimental Marine Biology and Ecology 289: 83–101
- Correia AD, Lima G, Costa MH, Livingstone DR (2002a) Studies on biomarkers of copper exposure and toxicity in the marine amphipod *Gammarus locusta* (Crustacea): I. Induction of metallothionein and lipid peroxidation. Biomarkers 7:422-437
- Correia AD, Livingstone DR, Costa MH (2002b) Effects of water-borne copper on metallothionein and lipid peroxidation in the marine amphipod *Gammarus locusta*. Marine Environmental Research 54:357-360
- Costa FO, Costa MH (1999) Life history of the amphipod *Gammarus locusta* in the Sado estuary (Portugal). Acta Oecologica 20: 305–314
- Costa FO, Neuparth T, Correia AD, Costa MH (2005) Multi-level assessment of chronic toxicity of estuarine sediments with the amphipod *Gammarus locusta*: II. Organism and population-level endpoints. Marine Environmental Research 60:93-110
- Dean JB (2010) Hypercapnia causes cellular oxidation and nitrosation in addition to acidosis: implications for CO₂ chemoreceptor function and dysfunction. Journal of Applied Physiology 108:1786–1795
- Dickson AG, Millero FJ (1987) A comparison of the equilibrium constants for the dissociation of carbonic acid in seawater media. Deep Sea Research Part A - Oceanographic Research Papers 34:1733-1743
- Doney SC, Fabry VJ, Feely RA, Kleypas JA (2009) Ocean acidification: The other CO₂ problem. Annual Review of Marine Science 1:169-192
- Duquette A, McClintock JB, Amsler CD, Pérez-Huerta A, Milazzo M, Hall-Spencer JM (2017) Effects of ocean acidification on the shells of four Mediterranean gastropod species near a CO₂ seep. Marine Pollution Bulletin 124: 917–928.
- Egilsdottir H, Spicer JJ, Rundle SD (2009) The effect of CO₂ acidified sea water and reduced salinity on aspects of the embryonic development of the amphipod *Echinogammarus marinus* (Leach). Marine Pollution Bulletin 58:1187-1191
- Feder ME, Hofmann GE (1999) Heat-shock proteins, molecular chaperones, and the stress response: evolutionary and ecological physiology. Annual Review of Physiology 61:243-282
- Finley D, Ciechanover A, Varshavsky A (1984) Thermolability of ubiquitin-activating enzyme from the mammalian cell cycle mutant ts85. Cell 37:43-55

- Gattuso J-P, Hansson L (2011) Ocean Acidification: background and history, in: Gattuso J-P, Hansson L (eds.). Ocean Acidification. Oxford University Press, Oxford, New York, pp.1-17
- Gorokhova E, Löf M, Halldórsson HP, Tjärnlund U, Lindströmd M, Elfving T, Sundelin B (2010) Single and combined effects of hypoxia and contaminated sediments on the amphipod *Monoporeia affinis* in laboratory toxicity bioassays based on multiple biomarkers. Aquatic Toxicology 99:263-274
- Gorokhova E, Löf M, Reutgard M, Lindström M, Sundelin B (2013) Exposure to contaminants exacerbates oxidative stress in amphipod *Monoporeia affinis* subjected to fluctuating hypoxia. Aquatic Toxicology 127:46-53
- Gueranger Q, Li F, Peacock M, Larnicol-Fery A, Brem R, Macpherson P, Egly J-MPK (2014) Protein oxidation and DNA repair inhibition by 6-Thioguanine and UVA radiation. Journal of Investigative Dermatology 134:1408-1417
- Habig WH, Pabst MJ, Jakoby WB (1974) Glutathione S-transferases. The first enzymatic step in mercapturic acid formation. Journal of Biological Chemistry 249:7130-7139
- Hanna J, Meides A, Zhang DP, Finley D (2007) A ubiquitin stress response induces altered proteasome composition. Cell 129:747-759
- Hauton C, Tyrrell T, Williams J (2009) The subtle effects of sea water acidification on the amphipod *Gammarus locusta*. Biogeosciences 6:1479-1489
- Heuer RM, Grosell M (2014) Physiological impacts of elevated carbon dioxide and ocean acidification on fish. American Journal of Physiology. Regulatory, Integrative and Comparative Physiology 307:R1061-1084
- Hoeijmakers JHJ (2009) DNA Damage, Aging, and Cancer. New England Journal of Medicine 361: 1475-1485
- Hu M, Li L, Sui Y, Li J, Wang Y, Lu W, Dupont S (2015) Effect of pH and temperature on antioxidant responses of the thick shell mussel *Mytilus coruscus*. Fish and Shellfish Immunology 46:573-583
- IPCC (2014) Climate change 2014: impacts, adaptation, and vulnerability. In: Part A: Global and Sectoral Aspects. Contribution of Working Group II to the Fifth Assessment Report of the Intergovernmental Panel on Climate Change. Cambridge University Press, Cambridge, United Kingdom and New York, NY, USA.

- Johansson LH, Borg LA (1988) A spectrophotometric method for determination of catalase activity in small tissue samples. *Analytical Biochemistry* 174:331-336
- Kambayashi Y, Binh NT, Asakura HW, Hibino Y, Hitomi Y, Nakamura H, Ogino K (2009) Efficient assay for total antioxidant capacity in human plasma using a 96-well microplate. *Journal of Clinical Biochemistry and Nutrition* 44:46-51
- Krapp RH, Bassinet T, Berg J, Pampanin DM, Camus L (2009) Antioxidant responses in the polar marine sea-ice amphipod *Gammarus wilkitzkii* to natural and experimentally increased UV levels. *Aquatic Toxicology* 94:1-7
- Krisko A, Radman M (2013) Phenotypic and genetic consequences of protein damage. *Plos Genetics* 9:e1003810
- Kroecker KJ, Kordas RL, Crim RN, Singh GG (2010) Meta-analysis reveals negative yet variable effects of ocean acidification on marine organisms. *Ecology Letters* 13:1419-1434
- Lawrence RA, Burk RF (1976) Glutathione peroxidase activity in selenium-deficient rat liver. *Biochemical and Biophysical Research Communications* 71:952-958
- Lesser MP (2006) Oxidative stress in marine environments: biochemistry and physiological ecology. *Annual Review of Physiology* 68:253-278
- Lewis E, Wallace D, Allison LJ (1998) Program developed for CO₂ system calculations. Carbon Dioxide Information Analysis Center, managed by Lockheed Martin Energy Research Corporation for the US Department of Energy Tennessee.
- Lopes AR, Sampaio E, Santos C, Couto A, Pegado MR, Diniz M, Munday PL, Rummer JL, Rosa R (2018) Absence of cellular damage in tropical newly hatched sharks (*Chiloscyllium plagiosum*) under ocean acidification conditions. *Cell Stress and Chaperones*
- Lüthi D, Le Floch M, Bereiter B, Blunier T, Barnola J-M (2008) High-resolution carbon dioxide concentration record 650,000-800,000 years before present. *Nature* 453:379-382
- Macclouf J, Grassi J, Pradelles P (1987) Development of enzyme-immunoassay techniques for measurement of eicosanoids, in: Walden TL, Hughes HN (eds.), *Prostaglandin and Lipid Metabolism in Radiation Injury*. Springer, US, pp. 355-364
- Matozzo V, Chinellato A, Munari M, Bressan M, Marin MG (2013) Can the combination of decreased pH and increased temperature values induce oxidative stress in the clam *Chamelea gallina* and the mussel *Mytilus galloprovincialis*? *Marine Pollution Bulletin* 72:34-40

- McCord JM, Fridovich I (1969) Superoxide dismutase an enzymic function for erythrocyte hemocuprein (hemocuprein). *Journal of Biological Chemistry* 244:6049-6055
- Michaelidis B, Ouzounis C, Paleras A, Pörtner H-O (2005) Effects of long-term moderate hypercapnia on acid-base balance and growth rate in marine mussels *Mytilus galloprovincialis*. *Marine Ecology Progress Series* 293:109-118
- Miller GM, Watson S-A, Donelson JM, McCormick MI, Munday PL (2012) Parental environment mediates impacts of increased carbon dioxide on a coral reef fish. *Nature Climate Change* 2, 858–861
- Montaner B, O'Donovan P, Reelfs O, Perrett CM, Zhang X, Xu Y-Z, Ren X, Macpherson P, Frith D, Karran P (2007) Reactive oxygen-mediated damage to a human DNA replication and repair protein. *Scientific Report* 8:1074-1079
- Neuparth T, Correia AD, Costa FO, Lima G, Costa MH (2005) Multi-level assessment of chronic toxicity of estuarine sediments with the amphipod *Gammarus locusta*: I. Biochemical endpoints. *Marine Environmental Research* 60:69-91
- Neuparth T, Costa FO, Costa MH (2002) Effects of temperature and salinity on life history of the marine amphipod *Gammarus locusta*. Implications for ecotoxicological testing. *Ecotoxicology* 11:61-73
- Njemini R, Demanet C, Mets T (2005) Comparison of two ELISAs for the determination of Hsp70 in serum. *Journal of Immunological Methods* 306:176-182
- Obermüller B, Puntarulo S, Abele D (2007) UV-tolerance and instantaneous physiological stress responses of two Antarctic amphipod species *Gondogeneia antarctica* and *Dierboea furcipes* during exposure to UV radiation. *Marine Environmental Research* 64:267-285
- Pane EF, Barry JP (2007) Extracellular acid-base regulation during short-term hypercapnia is effective in a shallow-water crab, but ineffective in a deep-sea crab. *Marine Ecology Progress Series* 334:1-9
- Parker LM, Ross PM, O'Connor WA, Borysko L, Raftos DA, Pörtner H-O (2012) Adult exposure influences offspring response to ocean acidification in oysters. *Global Change Biology* 18:82–92
- Peacock M, Brem R, Macpherson P, Karran P (2014) DNA repair inhibition by UVA photoactivated fluoroquinolones and vemurafenib. *Nucleic Acids Research* 42:13714-13722

- Pimentel MS, Faleiro F, Diniz M, Machado J, Pousão-Ferreira P, Peck MA, Pörtner H-O, Rosa R (2015) Oxidative stress and digestive enzyme activity of flatfish larvae in a changing ocean. *PLoS ONE* 10:e0134082
- Polo SE, Jackson SP (2011) Dynamics of DNA damage response proteins at DNA breaks: a focus on protein modifications. *Genes and Development* 25:409-433
- Pörtner H-O, Karl DM, Boyd PW, Cheung WW, Lluch-Cota SE, Nojiri Y, Schmidt DN, Zavialov PO, Alheit J, Aristegui J (2014) Ocean systems. In: Field CB, Barros VR, Dokken DJ, Mach KJ, Mastrandrea MD et al., editors. *Climate Change 2014: Impacts, Adaptation, and Vulnerability Part A: Global and Sectoral Aspects Contribution of Working Group II to the Fifth Assessment Report of the Intergovernmental Panel on Climate Change*. Cambridge University Press, 411-484
- Pörtner H-O, Langenbuch M, Reipschlager A (2004) Biological impact of elevated ocean CO₂ concentrations: Lessons from animal physiology and earth history. *J. Ocean.* 60:705-718
- Pörtner H-O, Reipschläger A (1996) Ocean disposal of anthropogenic CO₂: physiological effects on tolerant and intolerant animals, in: Ormerod, B., Angel, M.V. (Eds.), *Ocean Storage of Carbon Dioxide. Workshop 2 - Environmental Impact*. IEA Greenhouse Gas R&D Programme, Cheltenham, UK, pp. 57-81
- Rocha MJ, Cruzeiro C, Reis M, Rocha E, Pardal MA (2013) Determination of 17 endocrine disruptor compounds and their spatial and seasonal distribution in the Sado River Estuary (Portugal). *Toxicological and Environmental Chemistry* 95:237-253
- Rodriguez-Romero A, Jarrold MD, Massamba-N'Siala G, Spicer JL, Calosi P (2016) Multi-generational responses of a marine polychaete to a rapid change in seawater pCO₂. *Evolutionary Applications* 9:1082-1095
- Rosa R, Rummer JL, Munday PL (2017) Biological responses of sharks to ocean acidification. *Biology Letters* 13:20160796
- Rosa R, Seibel BA (2008) Synergistic effects of climate-related variables suggest future physiological impairment in a top oceanic predator. *Proceedings of the National Academy of Sciences of the United States of America* 105:20776-20780
- Sampaio E, Lopes AR, Francisco S, Paula JR, Pimentel M, Maulvault AL, Repolho T, Grilo TF, Pousão-Ferreira P, Marques A, Rosa R (2018) Ocean acidification dampens physiological stress response to warming and contamination in a commercially-important fish (*Argyrosomus regius*). *Science of the Total Environment* 618:388-398

- Sarazin G, Michard G, Prevot FMP (1999) A rapid and accurate spectroscopic method for alkalinity measurements in sea water samples. *Water Research* 33:290-294
- Sejersted Y, Hildrestrand GA, Kunke D, Rolseth V, Krokeide SZ, Neurauter CG, Suganthan R, Atneosen-Asegg M, Fleming AM, Saugstad OD, et al., 2011. Endonuclease VIII-like 3 (Neil3) DNA glycosylase promotes neurogenesis induced by hypoxia-ischemia. *Proceedings of the National Academy of Sciences USA* 108:18802–18807
- Shen J, Deininger P, Hunt JD, Zhao H (2007) 8-Hydroxy-2'-deoxyguanosine (8-OH-dG) as a potential survival biomarker in patients with nonsmall-cell lung cancer. *Cancer* 109:574-580
- Sroda S, Cossu-Leguille C (2011) Seasonal variability of antioxidant biomarkers and energy reserves in the freshwater gammarid *Gammarus roeseli*. *Chemosphere* 83:538-544
- Taylor JRA, Gilleard JM, Allen MC, Deheyn DD (2015) Effects of CO₂ -induced pH reduction on the exoskeleton structure and biophotonic properties of the shrimp *Lysmata californica*. *Nature Scientific Reports* 5:10608
- Timofeyev MA, Shatilina ZM, Bedulina DS, Protopopova MV, Pavlichenko VV, Grabelnykh OI, Kolesnichenko AV (2008) Evaluation of biochemical responses in Palearctic and Lake Baikal endemic amphipod species exposed to CdCl₂. *Ecotoxicology and Environmental Safety* 70:99-105
- Tomanek L (2010) Variation in the heat shock response and its implication for predicting the effect of global climate change on species' biogeographical distribution ranges and metabolic costs. *Journal of Experimental Biology* 213:971-979
- Tomanek L, Zuzow MJ, Ivanina AV, Beniash E, Sokolova IM (2011) Proteomic response to elevated pCO₂ level in eastern oysters, *Crassostrea virginica*: evidence for oxidative stress. *Journal of Experimental Biology* 214:1836-1844
- Uchiyama M, Mihara M (1978) Determination of malonaldehyde precursor in tissues by thiobarbituric acid test. *Analytical Biochemistry* 86:271-278
- Vereshchagina KP, Lubyaga YA, Shatilina Z, Bedulina D, Gurkov A, Axenov-Gribanov DV, Baduev B, Kondrateva ES, Gubanov M, Zadereev E, Sokolova E, Timofeyev M (2016) Salinity modulates thermotolerance, energy metabolism and stress response in amphipods *Gammarus lacustris*. *Biochemistry, Biophysics and Molecular Biology* PerrJ4:e2657

Zeebe RE, Ridgwell A (2011) Past changes in ocean carbonate chemistry, in: Gattuso J-P, Hansson L (Eds.), Ocean Acidification. Oxford University Press, Oxford, New York, pp. 21-37

Part Two

Biochemical Responses Under a Multiple Stressor
Environment

4 Physiological resilience of a temperate soft coral to ocean warming and acidification

Ana R Lopes^{1,2}, Filipa Faleiro¹, Inês C Rosa¹, Marta Pimentel¹, Katja Trübenbach¹, Tiago Repolho¹, Mário Diniz², Rui Rosa¹

¹MARE- Marine Environmental Sciences Centre & Laboratório Marítimo da Guia, Faculdade de Ciências, Universidade de Lisboa, Av. Nossa Senhora do Cabo 939, 2750-374 Cascais, Portugal

²UCIBIO, REQUIMTE, Departamento de Química, Faculdade de Ciências e Tecnologia, Universidade Nova de Lisboa, Quinta da Torre, 2829-516 Caparica, Portugal

Published in: *Cell Stress and Chaperones* (DOI: 10.1007/s12192-018-0919-9)

Abstract

Atmospheric concentration of carbon dioxide (CO₂) is increasing at an unprecedented rate and subsequently leading to ocean acidification. Concomitantly, ocean warming is intensifying, leading to serious and predictable biological impairments over marine biota. Reef-building corals have proven to be very vulnerable to climate change, but little is known about the resilience of non- reef-building species. In this study, we investigated the effects of ocean warming and acidification on the antioxidant enzyme activity (CAT - catalase, and GST - glutathione S-transferase), lipid peroxidation (using malondialdehyde - MDA - levels as a biomarker) and heat shock response (HSP70/HSC70 content) of the octocoral *Veretillum cynomorium*. After 60 days of acclimation, no mortalities were registered in all treatments. Moreover, CAT and GST activities, as well as MDA levels, did not change significantly under warming and/or acidification. Heat shock response was significantly enhanced under warming, but high CO₂ did not have a significant effect. Contrasting to many of their tropical coral-reef relatives, our findings suggest that temperate shallow-living octocorals may be able to physiologically withstand future conditions of increased temperature and acidification.

Keywords: Climate change, Heat shock proteins, Antioxidant enzymes, Lipid peroxidation, *Veretillum cynomorium*

Since the start of the industrial revolution, atmospheric concentrations of carbon dioxide (CO₂) have been rising, reaching for the first time levels above 400 ppm (Lüthi et al. 2008) and being expected to reach 730-1020 ppm by the end of the century (Pörtner et al. 2014). Nearly 30 % of atmospheric CO₂ is absorbed by the oceans (Hoegh-Guldberg et al. 2014), resulting in a change in seawater chemistry that is expected to prompt a 0.13-0.42 pH unit drop in seawater pH by the year 2100 (Pörtner et al. 2014). Increasing atmospheric CO₂ concentration is also increasing global temperature, with future projections pointing out to a rise up to 4 °C in sea surface temperature until the end of the century (Collins et al. 2013). Additionally, the frequency and extent of extreme weather events, such as heat waves, are expected to increase at a global scale (Pörtner et al. 2014). These changes are expected to cause major shifts in species distribution, phenology and physiology (e.g. Edwards and Richardson 2004; Harvey et al. 2013b; Kroeker et al. 2013; Parmesan and Yohe 2003), which can ultimately lead to worldwide extinction events (Thomas et al. 2004).

Important constituents of coral reef ecosystems in tropical regions and abundant components of shallow-water habitats in temperate environments, corals harbour an overwhelming complexity of species and play an essential ecological role within benthic communities (Carpenter et al. 2008; Freiwald et al. 2004). Considering their ecological relevance, large efforts have been undertaken in order to study the effects of climate change on corals worldwide (e.g. Baker et al. 2008; Hofmann et al. 2008). In fact, temperature and CO₂ levels have been proven to affect several life-history processes of reef-building corals (e.g. development and reproduction), besides damaging several key physiological functions, such as calcification, photosynthesis and respiration (Ateweberhan et al. 2013; Pandolfi et al. 2011). Moreover, increased seawater temperature is also threatening the symbiosis between corals and zooxanthellae, in a phenomenon known as coral bleaching (Glynn 1996). In contrast to reef-building corals, studies targeted to non-reef-building corals are still scarce. In fact, investigations addressing the effects of climate change on soft corals are mainly focused on community spatial distribution rather than in understanding the effects upon species ecophysiology (e.g. Gómez et al. 2015; Inoue et al. 2013; Ruzicka et al. 2013).

In order to avoid deleterious effects caused by environmental disturbances, marine organisms display a diverse set of physiological regulatory defence mechanisms, which include heat shock and antioxidant responses (Feder and Hofmann 1999; Lesser 2006). Heat shock

response involves the synthesis of heat shock proteins (HSP), which possess an important role by promoting stabilization and refolding of denatured proteins (Dong et al. 2008; Tomanek 2010). On the other hand, antioxidant response is characterized by a powerful set of enzymatic antioxidants [e.g. catalase (CAT) and glutathione S-transferase (GST)], which act against toxic effects of reactive oxygen species [ROS, i.e. superoxide radicals (O_2^-), hydrogen peroxides (H_2O_2), singlet oxygens (1O_2) and hydroxyl radicals (HO^\bullet)] (Apel and Hirt 2004). Under environmental stress, high levels of ROS production may cause cellular damage through lipid peroxidation, one of the most frequent cellular injury processes where ROS react with membrane-associated lipids (Lesser 2011).

Over the last few decades, the effects of increasing temperature and hypercapnia on the physiological defence mechanisms of corals have been extensively studied (see Supplementary Table SI). However, the bulk of these studies are focused on hexacorals species (e.g. Agostini et al. 2016; Downs et al. 2013; Downs et al. 2000; Griffin and Bhagooli 2004; Griffin et al. 2006), while studies on octocorals remain scarce (Madeira et al. 2015; Mydlarz and Jacobs 2006; Wiens et al. 2000). Moreover, most of the above-mentioned studies focus on the effects of temperature alone, without considering the effect of ocean acidification or the interaction between stressors.

The finger-shaped sea pen, *Veretillum cynomorium* (Pallas, 1766), is a colonial octocoral belonging to the order Pennatulacea. This species is widely distributed in the eastern Atlantic Ocean (Vander Land 2008), and it is found on coastal shallow waters, inhabiting the soft sediment of beaches and sand plains (Cornelius et al. 1995), with a bathymetric distribution between 0 and circa 200 m (López-González et al. 2001). Previous studies have already addressed the great tolerance of this species to deal with the extreme abiotic conditions of the intertidal environment, as they are fitted with an anticipatory response to cope with oxidative stress during air exposure at low tide conditions (Teixeira et al. 2013). Additionally, it was also seen that they tolerate well the seasonal variation in temperature regimes, being able to withstand low tide conditions during summer without undergoing cellular damage (Madeira et al. 2015). Nevertheless, this species resilience towards climate change-related conditions remains unknown. To that end, the aim of the present study was to investigate the physiological mechanisms that may enable *V. cynomorium* to withstand future ocean warming and acidification conditions. More specifically, we analysed: i) antioxidant enzyme activities (GST and CAT), ii) lipid peroxidation (malondialdehyde – MDA), and iii) heat shock response (HSP70/HSC70).

4.1. Materials and Methods

4.1.1. Coral collection and laboratory acclimation

Twenty-four *V. cynomorium* colonies were hand-collected near the mouth of the Sado estuary (38°29'11" N, 8°53'13" W, Setúbal, Portugal) in March 2014. After field collection, organisms were immediately transported to the aquatic facilities of Laboratório Marítimo da Guia (Cascais, Portugal).

Octocorals were maintained in twelve 50-L holding tanks coupled to recirculation aquaculture systems filled with 0.35 µm-filtered (Harmsco, USA) and UV-irradiated (V²ecton 600, TMC Iberia, Portugal) natural seawater, directly pumped from the sea. Each system was fitted with mechanical (Glass wool, Fernando Ribeiro Lda, Portugal), biological (Ouriço®, Fernando Ribeiro Lda, Portugal) and physico-chemical filtration (V²Skim Pro 450, TMC Iberia, Portugal), with additional UV-irradiation (V²ecton 300, TMC Iberia, Portugal). A 10 % seawater renewal was daily performed. Ammonia, nitrite and nitrate levels were daily monitored by means of colorimetric tests (Profi Test, Salifert, Holland) and kept below detectable levels. During the experimental exposure, a photoperiod of 14 h:10 h (light:dark cycle) was performed. All colonies were fed (twice a day) with a mixture of frozen *Artemia* spp. and *Mysis* spp. (TMC Iberia, Portugal).

Upon arrival, colonies were acclimated for 15 days to the prevailing natural conditions of the collection site (temperature 19 ± 1 °C, pH 8.0 ± 0.1 , pCO₂ ~ 500 µatm, salinity 35 ± 1). Subsequently, organisms were exposed for 60 days to different experimental conditions (3 tanks per treatment): i) control temperature and normocapnia (19 °C, pH 8.0, pCO₂ ~ 460 µatm); ii) control temperature and hypercapnia (19 °C, pH 7.7, pCO₂ ~ 1020 µatm); iii) warming and normocapnia (26 °C, pH 8.0, pCO₂ ~ 430 µatm); and iv) warming and hypercapnia (26 °C, pH 7.7, pCO₂ ~ 1060 µatm). The warming condition was chosen based on the temperature values observed during heat events in the collection site (see Supplementary Figure S1). Regarding the pCO₂ scenarios, one should keep in mind that this species inhabits the Western Iberian Upwelling Ecosystem, part of the Canary Current Upwelling System. In these regions, actual pCO₂ levels may reach up to 500 µatm (Álvarez-Salgado et al. 1997; Perez et al. 1999) and are thus expected to exceed the level of 420-940 µatm projected for 2100 (Pörtner et al. 2014).

Water temperature and pH were continuously controlled and adjusted by means of an automatic monitoring device (Profilux 3.1, GHL, Germany), connected to temperature and pH

probes (PL-0094 and PL-0071, respectively, GHL, Germany). Upon demand, seawater temperature was upregulated using submerged digital heaters (V²Therm 200 W, TMC Iberia, Portugal) or downregulated using seawater chillers (HC-250A, Hailea, China). Adjustment of pH levels was performed automatically via solenoid valves connected to the Profilux system. Reduction of pH values was accomplished by the injection of a certified CO₂ gas (Airliquide, Portugal), while upregulation was achieved by the injection of CO₂-filtered atmospheric air (using soda lime, Sigma-Aldrich, Portugal). Additionally, a daily monitoring of seawater temperature (thermometer TFX 430, WTW GmbH, Germany), salinity (V² Refractometer, TMC Iberia, Portugal) and pH (pH/ion meter SG8, Mettler-Toledo, Switzerland) was performed using handheld equipment. Seawater carbonate system speciation (see Supplementary Table SII) was calculated weekly from total alkalinity (determined according to Sarazin et al. 1999) and pH measurements, using the CO2SYS software, with dissociation constants from Mehrbach (1973) as refitted by Dickson and Millero (1987).

At the end of the experimental exposure, colonies were collected, immediately placed in liquid nitrogen and stored at -80 °C for subsequent biochemical analyses.

4.1.2. Biochemical Analyses

4.1.2.1. Preparation of tissue extracts

Tissue samples from different colonies (n = 2 per tank, n = 6 per treatment) were individually homogenized in phosphate saline buffer (PBS), according to Lopes et al. (2013). Homogenates were centrifuged at 14000 x g for 20 min at 4 °C. Antioxidant enzyme activity, lipid peroxidation and the heat shock response were quantified in the supernatant fraction. Each sample was run in triplicate (technical replicates) and results were normalized to total protein content, as described by Bradford (1976).

4.1.2.2. Antioxidant enzymes

CAT activity was determined following Aebi (1984). A total of 100 µL of each sample was added to 2.9 mL of substrate solution [50 mM potassium phosphate buffer (pH 7.0) and 12.1 mM H₂O₂], into quartz cuvettes. Absorbance was measured at 240 nm (Helios spectrophotometer, Unicam, UK), during 15-s intervals across a 180-s incubation period. Bovine

CAT solution was used as a positive control to validate the assay. CAT activity was calculated based on the absorbance increase per minute, using the H_2O_2 extinction coefficient (0.04 EmM).

GST activity was determined according to Habig et al. (1974b). A total of 180 μL of substrate solution [200 mM L-glutathione reduced, Dulbecco phosphate-buffered saline and 100 mM 1-chloro-2,4-dinitrobenzene (CDNB) solution] was added to 96-well microplates, alongside with 20 μL of GST standard or sample. Equine liver GST was used as a positive control to validate the assay. Enzyme activity was determined spectrophotometrically at 340 nm (Bio-Rad, Benchmark, USA), every minute during a 6-min time frame. GST activity was calculated based on the absorbance increase per minute, using the CDBN extinction coefficient (5.3 EmM).

4.1.2.3. Lipid peroxidation

Lipid peroxidation was determined by MDA quantification, according to the thiobarbituric acid reactive substances (TBARS) protocol (Uchiyama and Mihara 1978a). Briefly, 10 μL of each sample was added to 50 mM of monobasic sodium phosphate buffer (45 μL), followed by the addition of 8.1 % of sodium dodecyl sulphate (12.5 μL), 20 % of trichloroacetic acid (93.5 μL) and 1 % of thiobarbituric acid (93.5 μL). A volume of 50.5 μL of Milli-Q ultrapure water was added to this mixture, being subsequently mixed for 30 s and incubated in boiling water for 10 min. The resulting mixture was placed on ice for 3 min to lower temperature. Afterwards, 62.5 μL of Milli-Q ultrapure water and 312.5 μL of n-butanol pyridine (15:1 v/v) were added and microtubes centrifuged at 2000 x g for 5 min. The supernatant fraction (150 μL) was added to 96-well microplates and absorbance was read at 532 nm (Bio-Rad, Benchmark, USA). MDA concentrations were calculated based on a calibration curve (0 - 0.3 μM) using MDA bis (dimethyl acetal) standards.

4.1.2.4. Heat shock response

The HSP70/HSC70 content was assessed through enzyme-linked immunosorbent assay (ELISA), according to an adaptation of the method described by Njemini et al. (2005a). Each sample (10 μL) was diluted in 990 μL of PBS. Afterwards, 50 μL of each diluted sample was added to 96-well microplates (Microloan 600, Greiner, Germany) and incubated overnight at 4 °C. After 24 h, microplates were washed (4 times) using PBS containing 0.05 % Tween-20. Then, 100 μL of blocking solution (1 % bovine serum albumin) was added to each well and microplates

were incubated in darkness for 2 h at room temperature. Consequently, 50 μL of primary antibody HSP70/HSC70 (5 $\mu\text{g mL}^{-1}$, Acris, USA) was added to each well. Microplates were incubated overnight at 4 °C and washed 24 h afterwards to remove non-linked antibodies. The alkaline phosphatase-conjugated anti-mouse IgG (Fab specific, Sigma-Aldrich, USA) was used as a secondary antibody, by adding 50 μL (1 $\mu\text{g mL}^{-1}$) to each well, and microplates were incubated for 90 min at 37 °C. After an additional washing procedure, 100 μL of substrate p-nitrophenyl phosphate tablets were added to each well and incubated for 30 min at room temperature. Lastly, 50 μL of stop solution (3 M NaOH) were added to each well, with absorbance being read at 405 nm in a microplate reader (BIO-RAD, Benchmark, USA). Heat shock protein content was calculated from the calibration curve, based on serial dilutions (0 - 2000 $\mu\text{g mL}^{-1}$) of purified HSP70 active protein (Acris, USA).

4.1.3. Statistical analyses

Generalized linear models (GLM) analysis was used to ascertain significant differences between temperature and pH treatments. For each dependent variable (CAT, GST, MDA and HSP70/HSC70), temperature (2 levels: 19 and 26 °C) and pH (2 levels: 8.0 and 7.7) were used as explanatory variables, as well as their interaction. Mixed models were used to infer significant differences between replicate tanks within each treatment. Since there were no significant differences, the random effect of the tank was removed from the models. Our data was fitted using Gaussian family models. Model residuals were checked for departures from the assumed distributions and no significant deviations were found. Homogeneity and normality assumptions were checked through Levene and Shapiro tests, respectively. The most parsimonious models were selected based on the Akaike Information Criterion (Quinn and Keough, 2002). Independence and leverage of the residuals were used to perform model validation. All statistical analyses were performed on R Studio (R Development Core Team, 2017), using the lme4 and nlme packages.

4.2. Results

After 60 days of exposure to upcoming ocean warming and acidification conditions, no colony mortality was observed in all experimental treatments.

The activity of the antioxidant enzymes CAT and GST (Fig. 1) did not change significantly under warming and/or acidification ($p > 0.05$, GLM analysis in Supplementary Table SIII).

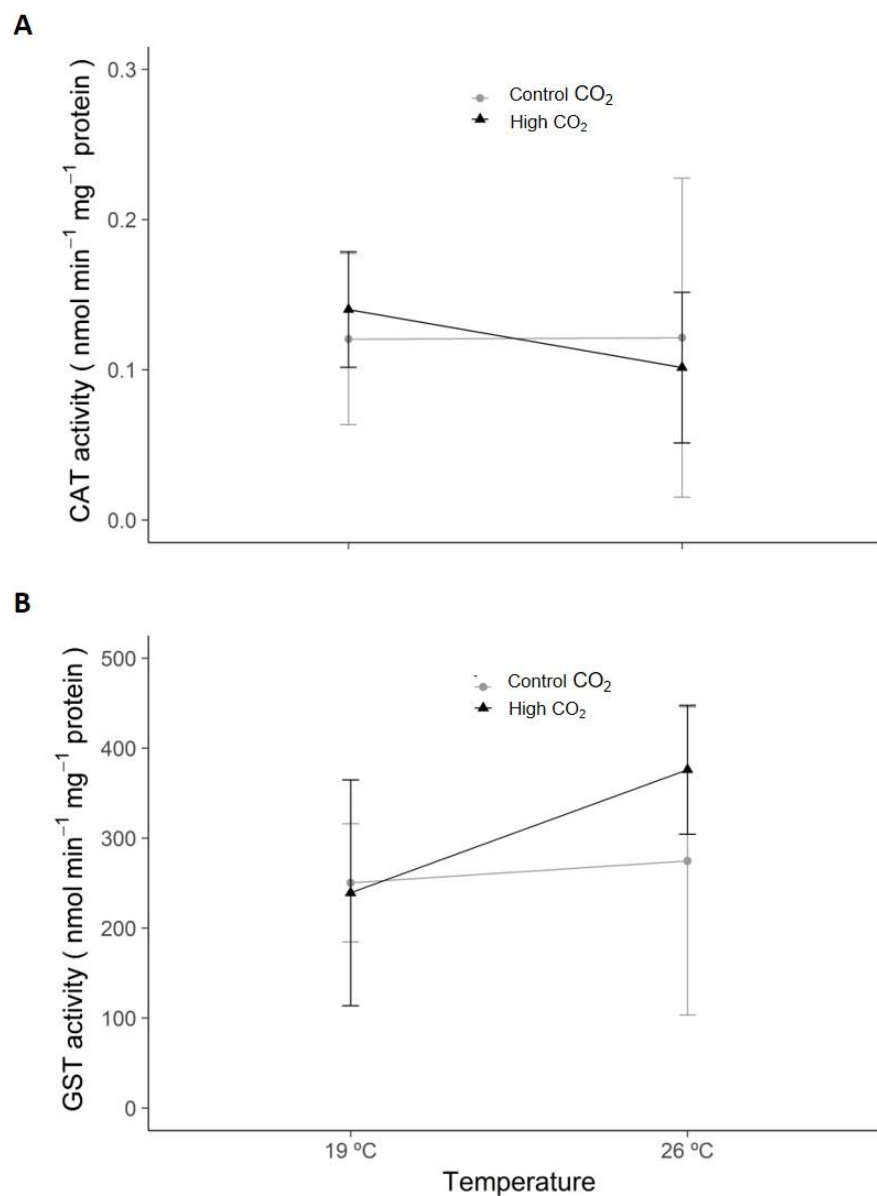


Figure 1 – Antioxidant enzyme activities in *Veretillum cynomorium* under ocean warming and acidification conditions: **(A)** Catalase (CAT) and **(B)** Glutathione S-transferase (GST). Values represent mean \pm standard deviation.

MDA levels (Fig. 2), a specific end-product of lipid peroxidation, also did not change significantly after exposure to ocean warming and/or acidification conditions ($p > 0.05$, GLM analysis in Supplementary Table SIII).

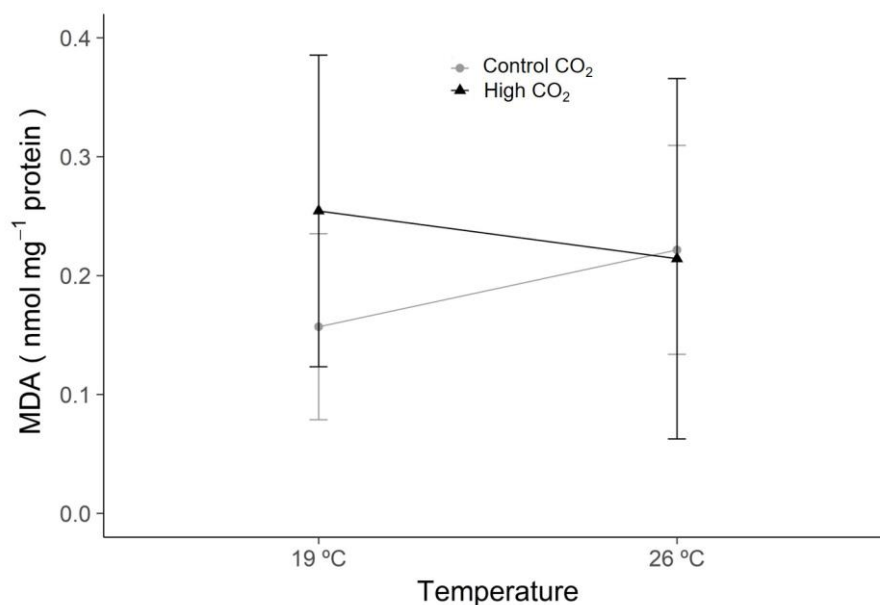


Figure 2 – Lipid peroxidation (MDA - malondialdehyde) levels in *Veretillum cynomorium* under ocean warming and acidification conditions. Values represent mean \pm standard deviation.

In contrast, the heat shock response (HSP70/HSC70, Fig. 3) was significantly enhanced under warming ($p = 0.009$, GLM analysis in Supplementary Table SIII), increasing from 210.1 ± 131.6 to 588.6 ± 271.9 $\mu\text{g mg}^{-1}$ protein under normocapnia, and from 158.6 ± 179.1 to 349.0 ± 190.2 $\mu\text{g mg}^{-1}$ protein under hypercapnia. Neither the effect of acidification, nor the interaction between warming and acidification, were significant ($p > 0.05$, GLM analysis in Supplementary Table SIII).

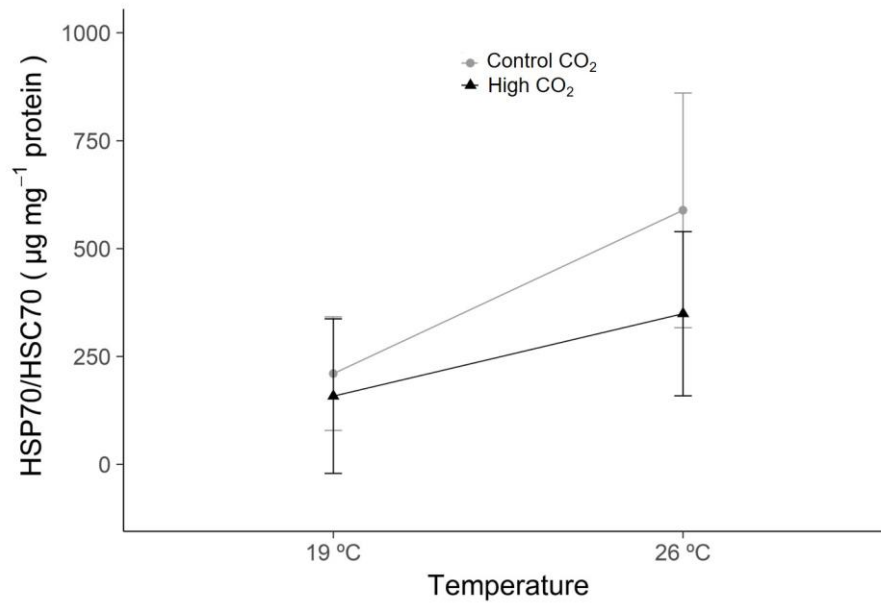


Figure 3 – Heat shock protein (HSP70/HSC70) concentrations in *Veretillum cynomorium* under ocean warming and acidification conditions. Values represent mean \pm standard deviation.

4.3. Discussion

In the last decade, a significant body of research has been accumulated on the impact of climate change on coral ecophysiology, mainly on reef-building species (see Supplementary Table SI). Nonetheless, the impact of future ocean conditions on soft corals remains poorly known. To the best of our knowledge, only three studies were conducted so far in order to infer the impact of rising sea temperature on octocorals (Madeira et al. 2015; Mydlarz and Jacobs 2006; Wiens et al. 2000), and none of these studies have evaluated the effect of ocean acidification or the combination between increasing temperature and acidification.

Increased seawater temperature is known for enhancing ROS production and activating antioxidant enzymes, which are essential to eliminate ROS and prevent cellular damage such as lipid peroxidation (Lesser 2011). In most hard corals, the heat shock and antioxidant defence mechanisms are triggered under warming and/or acidified conditions (see Supplementary Table SI). However, in many cases, they are not able to avoid cellular damage in coral tissues (e.g. Downs et al. 2000; Flores-Ramírez and Liñán-Cabello 2007; Ritson-Williams et al. 2016; Soriano-Santiago et al. 2013; Yakovleva et al. 2009). Contrarily to reef-building corals, the present study showed that in the octocoral *V. cynomorium* CAT and GST activities were not significantly affected

by warming and/or acidification, and neither was cellular damage caused by lipid peroxidation. On the other hand, heat shock proteins, which play an important role in thermotolerance by helping denatured proteins to stabilize and refold (Tomanek 2010), were activated as a defence mechanism against high temperature, i.e. increasing significantly under warming conditions.

It is worth mentioning that the observed high tolerance of *V. cymorium* to such abiotic conditions is not surprising, since this species can be found in coastal shallow habitats that are daily subject to extreme abiotic fluctuations (e.g. temperature, salinity, oxygen). Indeed, this species proved to tolerate rapid cyclical fluctuations of the intertidal environment, by presenting integrated heat shock and antioxidant responses that allow them to cope with the underlying oxidative stress to which they are frequently exposed during the emersion stage (Teixeira et al. 2013) and across thermal gradients (Madeira et al. 2015). In both studies, *V. cymorium* proved to be equipped with powerful defence mechanisms that enable them to avoid peroxidative damage under stressful conditions. Thus, in a time when climate change threatens coral reefs all over the world, the octocoral *V. cymorium* stands out for its great resilience to warming and acidification.

Comparative studies between symbiotic and non-symbiotic corals clearly showed that symbiotic corals are more vulnerable to high temperatures and are at greater risk (Baker et al. 2008; Pandolfi et al. 2011). This may be due to the fact that increased seawater temperature leads to coral bleaching and mortality, which is primarily initiated with an overproduction of ROS in the symbionts (Downs et al. 2002; Lesser 2006; Mydlarz et al. 2009), impairing the association between corals and zooxanthellae (Glynn 1996). In contrast, octocorals such as *V. cymorium*, instead of an endosymbiotic algae assemblage, harbour microbial communities within their tissues (Baptista et al. 2012), which might confer broader tolerance to heat and chemical stress. In fact, recent studies have brought to light that the resistance of a coral is not only determined by the coral itself, but rather to the association between all its parts, i.e. coral, zooxanthellae and associated microorganisms (Grottoli et al. 2018; Roche et al. 2018), and that a shift in coral symbiosis elements to specific microorganisms could eventually enhance their thermal resistance (Torda et al. 2017).

On the other hand, hard corals have also shown to be quite vulnerable to ocean acidification, since hypercapnia is reducing ocean carbonate ion availability and compromising the capacity of hard corals to build their skeletons (Carpenter et al. 2008). In contrast, *V. cymorium* lacks an external calcium carbonate body. Instead, it presents a central axial skeleton

composed by a fibrillar collagenous matrix calcified with calcite (Ledger and Franc 1978) and covered by an external tissue that may act as a barrier against decreased seawater pH, as previously observed in another octocoral species (Gabay et al. 2014).

In conclusion, the present study shows that exposure to ocean warming and acidification conditions did not have a negative impact on *V. cynomorium* physiology. Warmer conditions enhanced the heat shock response, a defence mechanism that allows them to tolerate higher temperatures, while the antioxidant response and cellular damage were not significantly affected. In contrast to reef-building corals that have shown to be particularly sensitive to climate-induced changes (Baker et al. 2008), the present findings show that *V. cynomorium* is a resilient species in the face of warming and acidified conditions and is expected to be able to withstand predicted future ocean conditions associated with climate change. Nevertheless, further studies are essential to evaluate the impact of future ocean scenarios on octocoral larvae, since the greater vulnerability of the early stages of development may become the bottleneck for species persistence in a changing ocean.

4.4. Acknowledgments

This project was supported by the Portuguese Foundation for Science and Technology (FCT), through financial support to MARE (UID/MAR/04292/2013), a doctoral grant to Ana Rita Lopes (SFRH/BD/97070/2013), postdoctoral grants to Filipa Faleiro (SFRH/BPD/79038/2011), Marta Pimentel (SFRH/BPD/117533/2016) and Tiago Repolho (SFRH/BPD/94523/2013), and an Investigador FCT consolidation grant to Rui Rosa.

4.5. Competing of interests

The authors declare that there are no conflicts of interest.

4.6. References

- Aebi H (1984) Catalase. In: Packer L (ed) *Methods in Enzymology*. Academic Press, Orlando, 121-126
- Agostini S, Fujimura H, Hayashi H, Fujita K (2016) Mitochondrial electron transport activity and metabolism of experimentally bleached hermatypic corals. *Journal of Experimental Marine Biology and Ecology* 475:100-107
- Álvarez-Salgado XA, Castro CG, Pérez FF, Fraga F (1997). Nutrient mineralisation patterns in shelf waters of the western Iberian Upwelling. *Continental Shelf Research* 17:1247-1270
- Apel K, Hirt H (2004) Reactive oxygen species: metabolism, oxidative stress, and signal transduction. *Annual Review of Plant Biology* 55:373-399
- Ateweberhan M, Feary DA, Keshavmurthy S, Chen A, Schleyer MH, Sheppard CR (2013) Climate change impacts on coral reefs: Synergies with local effects, possibilities for acclimation, and management implications. *Marine Pollution Bulletin* 74:526-539
- Baker AC, Glynn PW, Riegl B (2008) Climate change and coral reef bleaching: An ecological assessment of long-term impacts, recovery trends and future outlook. *Estuarine, Coastal and Shelf Science* 80:435-471
- Baptista M, Lopes VM, Pimentel MS, Bandarra N, Narciso L, Marques A, Rosa R (2012) Temporal fatty acid dynamics of the octocoral *Veretillum cynomorium*. *Comparative Biochemistry and Physiology Part B: Biochemistry and Molecular Biology* 161:178-187
- Bradford MM (1976) A rapid and sensitive method for the quantitation of microgram quantities of protein utilizing the principle of protein-dye binding. *Analytical Biochemistry* 72:248-254
- Carpenter KE et al. (2008) One-third of reef-building corals face elevated extinction risk from climate change and local impacts. *Science* 321:560-563
- Collins M, Knutti R, Arblaster J, Dufresne J-L, Fichefet T, Friedlingstein P, Gao X, Gutowski WJ, Johns T, Krinner G, Shongwe M, Tebaldi C, Weaver AJ, Wehner M (2013) Long-term Climate Change: Projections, Commitments and Irreversibility. In: Stocker TF, Qin D, Plattner G-K, Tignor M, Allen SK, Boschung J, Nauels A, Xia Y, Bex V, Midgley PM (eds.). *Climate Change 2013: The Physical Science Basis. Contribution of Working Group I to the Fifth Assessment Report of the Intergovernmental Panel on Climate*

- Change Cambridge University Press, Cambridge, United Kingdom and New York, NY, USA
- Cornelius PFS, Manuel RL, Ryland JS (1995) Hydroids, sea anemones, jellyfish, and comb jellies. In: Hayward, P.J., Ryland, J.S. (Eds.), Handbook of the Marine fauna of North-West Europe. Oxford University Press, Oxford, pp. 62–135
- Császár N, Seneca F, Van Oppen M (2009) Variation in antioxidant gene expression in the scleractinian coral *Acropora millepora* under laboratory thermal stress. Marine Ecology Progress Series 392:93-102
- Deschaseaux ESM, Jones GB, Deseo MA, Shepherd KM, Kiene RP, Swan HB, Harrison PL, Eyre BD (2014) Effects of environmental factors on dimethylated sulfur compounds and their potential role in the antioxidant system of the coral holobiont Limnology and Oceanography 59:758-768
- Dickson A, Millero FJ (1987) A comparison of the equilibrium constants for the dissociation of carbonic acid in seawater media. Deep Sea Research Part A Oceanographic Research Papers 34:1733-1743
- Dong Y, Miller LP, Sanders JG, Somero GN (2008) Heat-shock protein 70 (Hsp70) expression in four limpets of the genus *Lottia*: interspecific variation in constitutive and inducible synthesis correlates with in situ exposure to heat stress. The Biological Bulletin 215:173-181
- Downs CA, McDougall KE, Woodley CM, Fauth JE, Richmond RH, Kushmaro A, Gibb SW, Loya Y, Ostrander GK, Kramarsy-Winter E (2013) Heat-stress and light-stress induce different cellular pathologies in the symbiotic dinoflagellate during coral bleaching. PLoS One 8:e77173
- Downs CA, Fauth JE, Halas JC, Dustan P, Bemiss J, Woodley CM (2002) Oxidative stress and seasonal coral bleaching. Free Radical Biology and Medicine 33:533-543
- Downs CA, Mueller E, Phillips S, Fauth JE, Woodley CM (2000) A molecular biomarker system for assessing the health of coral (*Montastraea faveolata*) during heat stress. Marine Biotechnology 2:533-544
- Duckworth CG, Picariello CR, Thomason RK, Patel KS, Bielmyer-Fraser GK (2017) Responses of the sea anemone, *Exaiptasia pallida*, to ocean acidification conditions and zinc or nickel exposure. Aquatic Toxicology 182:120-128

- Edwards M, Richardson AJ (2004) Impact of climate change on marine pelagic phenology and trophic mismatch. *Nature* 430:881-884
- Fang L-S, Huang S-P, Lin K-L (1997) High temperature induces the synthesis of heat-shock proteins and the elevation of intracellular calcium in the coral *Acropora grandis*. *Coral Reefs* 16:127-131
- Feder ME, Hofmann GE (1999) Heat-shock proteins, molecular chaperones, and the stress response: evolutionary and ecological physiology. *Annual Review of Physiology* 61:243-282
- Flores-Ramírez LA, Liñán-Cabello MA (2007) Relationships among thermal stress, bleaching and oxidative damage in the hermatypic coral, *Pocillopora capitata*. *Comparative Biochemistry and Physiology Part C: Toxicology and Pharmacology* 146:194-202
- Freiwald A, Fosså JH, Grehan A, Koslow T, Roberts JM (2004) Cold-water coral reefs. UNEP-WCMC, Cambridge, UK 84
- Gabay Y, Fine M, Barkay Z, Benayahu Y (2014) Octocoral Tissue Provides Protection from Declining Oceanic pH. *PLoS ONE* 9:e91553
- Glynn PW (1996) Coral reef bleaching: facts, hypotheses and implications. *Global Change Biology* 2:495-509
- Gómez CE, Paul VJ, Ritson-Williams R, Muehllehner N, Langdon C, Sánchez JA (2015) Responses of the tropical gorgonian coral *Eumicea fusca* to ocean acidification conditions. *Coral Reefs* 34:451-460
- Griffin SP, Bhagooli R (2004) Measuring antioxidant potential in corals using the FRAP assay. *Journal of Experimental Marine Biology and Ecology* 302:201-211
- Griffin SP, Bhagooli R, Weil E (2006) Evaluation of thermal acclimation capacity in corals with different thermal histories based on catalase concentrations and antioxidant potentials. *Comparative Biochemistry and Physiology Part A: Molecular and Integrative Physiology* 144:155-162
- Grottoli AG, Martins PD, Wolkins MJ, Johnston MD, Warner ME, Cai W-J, Melman TF, Hoadley KD, Pettay DT, Levas S, Schoepf V (2018) Coral physiology and microbiome dynamics under combined warming and ocean acidification *PLoS ONE* 13:e0191156
- Habig WH, Pabst MJ, Jakoby WB (1974) Glutathione S-transferases: the first enzymatic in mercapturic acid formation. *Journal of Biological Chemistry* 249:7130-7139

- Harvey BP, Gwynn-Jones D, Moore PJ (2013) Meta-analysis reveals complex marine biological responses to the interactive effects of ocean acidification and warming. *Ecology and Evolution* 3:1016-1030
- Hawkins TD, Krueger T, Wilkinson SP, Fisher PL, Davy SK (2015) Antioxidant responses to heat and light stress differ with habitat in a common reef coral. *Coral Reefs* 34:1229-1241
- Higuchi T, Agostini S, Casareto BE, Suzuki Y, Yuyama I (2015) The northern limit of corals of the genus *Acropora* in temperate zones is determined by their resilience to cold bleaching. *Scientific Reports* 5:18467
- Hoegh-Guldberg O, Cai R, Poloczanska ES, Brewer PG, Sundby S, Hilmi K, Fabry VJ, Jung S (2014) The Ocean. In: Barros VR, Field CB, Dokken DJ, Mastrandrea MD, Mach KJ, Bilir TE, Chatterjee M, Ebi KL, Estrada YO, Genova RC, Girma B, Kissel ES, Levy AN, MacCracken S, Mastrandrea PR, White LL (eds). *Climate Change 2014: Impacts, Adaptation, and Vulnerability. Part B: Regional Aspects. Contribution of Working Group II to the Fifth Assessment Report of the Intergovernmental Panel on Climate Change* Cambridge University Press, Cambridge, United Kingdom and New York, NY, USA:1655-1731
- Hofmann GE, O'Donnell MJ, Todgham AE (2008) Using functional genomics to explore the effects of ocean acidification on calcifying marine organisms. *Marine Ecology Progress Series* 373:219-225
- Howells EJ, Abrego D, Meyer E, Kirk NL, Burt JA (2016) Host adaptation and unexpected symbiont partners enable reef-building corals to tolerate extreme temperatures. *Global Change Biology* 22: 2702-2714
- Inoue S, Kayanne H, Yamamoto S, Kurihara H (2013) Spatial community shift from hard to soft corals in acidified water. *Nature Climate Change* 3:683-687
- Kroeker KJ, Kordas RL, Crim R, Hendriks IE, Ramajo L, Singh GS, Duarte CM, Gattuso G-P (2013) Impacts of ocean acidification on marine organisms: quantifying sensitivities and interaction with warming. *Global Change Biology* 19:1884-1896
- Ledger PW, Franc S (1978) Calcification of the collagenous axial skeleton of *Veretillum cymorium* Pall. (Cnidaria: Pennatulacea). *Cell and Tissues Research* 192:249-266
- Lesser MP (2006) Oxidative stress in marine environments: biochemistry and physiological ecology. *Annual Review of Physiology* 68:253-278

- Lesser MP (2011) Oxidative stress in tropical marine ecosystems. In: Abele D, Zenteno-Savín T, Vazquez-Medina J (eds) *Oxidative Stress in Aquatic Ecosystems*. John Wiley & Sons, Ltd, Chichester, UK, pp 7-19
- Liñán-Cabello MA, Flores-Ramírez LA, Zenteno-Savín T, Olguín-Monroy NO, Sosa-Avalos R, Patiño-Barragan M, Olivos-Ortiz A (2010) Seasonal changes of antioxidant and oxidative parameters in the coral *Pocillopora capitata* on the Pacific coast of Mexico. *Marine Ecology* 31:407-417
- Lopes AR, Trübenbach K, Teixeira T, Lopes VM, Pires V, Baptista M, Repolho, T, Calado R, Diniz M, Rosa R (2013) Oxidative stress in deep scattering layers: Heat shock response and antioxidant enzymes activities of myctophid fishes thriving in oxygen minimum zones. *Deep Sea Research Part I: Oceanographic Research Papers* 82:10-16
- López-González PJ, Gili JM, Williams GC (2001) New records of Pennatulacea (Anthozoa: Octocorallia) from the African Atlantic coast, with description of a new species and a zoogeographic analysis. *Scientia Marina* 65: 59-74
- Louis YD, Kaullysing D, Gopeechund A, Mattan-Moorgawa S, Bahorun T, Dyll SD, Bhagooli R (2016) In hospite Symbiodinium photophysiology and antioxidant responses in *Acropora muricata* on a coast-reef scale: implications for variable bleaching patterns. *Symbiosis* 68:61-72
- Lüthi D, Le Floch M, Bereiter B, Blunier T, Barnola J-M (2008) High-resolution carbon dioxide concentration record 650,000-800,000 years before present. *Nature* 453:379-382
- Lutz A, Raina J-B, Motti CA, Miller DJ, van Oppen MJ (2015) Host coenzyme Q redox state is an early biomarker of thermal stress in the coral *Acropora millepora*. *PloS one* 10:e0139290
- Madeira C, Madeira D, Vinagre C, Diniz M (2015) Octocorals in a changing environment: Seasonal response of stress biomarkers in natural populations of *Veretillum cynomorium*. *Journal of Sea Research* 103:120-128
- Mehrbach C, Culberson CH, Hawley JE, Pytkowicz RM (1973) Measurement of the apparent dissociation constants of carbonic acid in seawater at atmospheric pressure. *Limnology and Oceanography* 18: 897-907
- Mydlarz LD, Jacobs RS (2006) An inducible release of reactive oxygen radicals in four species of gorgonian corals. *Marine and Freshwater Behaviour and Physiology* 39:143-152

- Mydlarz LD, McGinty ES, Harvell D (2009) What are the physiological and immunological responses of coral to climate warming and disease? *Journal of Experimental Biology* 213:934-945
- Njemini R, Demanet C, Mets T (2005) Comparison of two ELISAs for the determination of Hsp70 in serum *Journal of Immunological Methods* 306:176-182
- Olsen K, Paul VJ, Ross C (2015) Direct effects of elevated temperature, reduced pH, and the presence of macroalgae (*Dictyota spp.*) on larvae of the Caribbean coral *Porites astreoides*. *Bulletin of Marine Science* 91:255-270
- Olsen K, Ritson-Williams R, Ochrietor J, Paul V, Ross C (2013) Detecting hyperthermal stress in larvae of the hermatypic coral *Porites astreoides*: the suitability of using biomarkers of oxidative stress versus heat-shock protein transcriptional expression. *Marine Biology* 160:2609-2618
- Pandolfi JM, Connolly SR, Marshall DJ, Cohen AL (2011) Projecting Coral Reef Futures Under Global Warming and Ocean Acidification. *Science* 333:418-422
- Parmesan C, Yohe G (2003) A globally coherent fingerprint of climate change impacts across natural systems. *Nature* 421:37-42
- Perez FF, Rios AF, Roson G (1999) Sea surface carbon dioxide off the Iberian Peninsula (North Eastern Atlantic Ocean). *Journal of Marine Systems* 19 (1-3): 27-46
- Pörtner H-O, Karl DM, Boyd PW, Cheung WWL, Lluh-Cota SE, Nojiri Y, Schmidt DN, Zavialov PO (2014) Ocean systems. In: *Climate Change 2014: Impacts, Adaptation, and Vulnerability. Part A: Global and Sectoral Aspects. Contribution of Working Group II to the Fifth Assessment Report of the Intergovernmental Panel on Climate Change* [Field CB, Barros VR, Dokken DJ, Mach KJ, Mastrandrea MD, Bilir TE, Chatterjee M, Ebi KL, Estrada YO, Genova RC, Girma B, Kissel ES, Levy AN, MacCracken S, Mastrandrea PR, and White LL (eds.)]. Cambridge University Press, Cambridge, United Kingdom and New York, NY, USA, pp. 411-484
- Richier S, Furla P, Plantivaux A, Merle P-L, Allemand D (2005) Symbiosis-induced adaptation to oxidative stress. *Journal of Experimental Biology* 208:277-285
- Ritson-Williams R, Ross C, Paul VJ (2016) Elevated Temperature and allelopathy impact coral recruitment. *PloS one* 11:e0166581

- Roche RC, Williams GJ, Turner JR (2018) Towards developing a mechanistic understanding of coral reef resilience to thermal stress across multiple scales. *Current Climate Change Reports* 4:51-64
- Rodriguez-Troncoso A, Carpizo-Ituarte E, Cupul-Magana A (2013) Oxidative damage associated with thermal stress in *Pocillopora verrucosa* from the Mexican Pacific. *International Journal of marine Sciences* 39: 113-118
- Ross C, Ritson-Williams R, Olsen K, Paul V (2013) Short-term and latent post-settlement effects associated with elevated temperature and oxidative stress on larvae from the coral *Porites astreoides*. *Coral Reefs* 32:71-79
- Ruzicka RR, Colella MA, Porter JW, Morrison JM, Kidney JA, Brinkhuis V, Lunz KS, Macaulay KA, Bartlett LA, Meyers MK, Colee J (2013) Temporal changes in benthic assemblages on Florida Keys reefs 11 years after the 1997/1998 El Niño. *Marine Ecology Progress Series* 489:125-141
- Sarazin G, Michard G, Prevot FMP (1999) A rapid and accurate spectroscopic method for alkalinity measurements in sea water samples. *Water Research* 33:290-294
- Seveso D, Montano S, Strona G, Orlandi I, Galli P, Vai M (2014) The susceptibility of corals to thermal stress by analyzing Hsp60 expression. *Marine environmental research* 99:69-75
- Sharp VA, Brown BE, Miller D (1997) Heat shock protein (hsp 70) expression in the tropical reef coral *Goniopora djiboutiensis*. *Journal of Thermal Biology* 22:11-19
- Siddiqui S, Bielmyer-Fraser GK (2015) Responses of the sea anemone, *Exaiptasia pallida*, to ocean acidification conditions and copper exposure. *Aquatic Toxicology* 167:228-239
- Soriano-Santiago OS, Liñán-Cabello MA, Delgadillo-Nuño MA, Ortega-Ortiz C, Cuevas-Venegas S (2013) Physiological responses to oxidative stress associated with pH variations in host tissue and zooxanthellae of hermatypic coral *Pocillopora capitata*. *Marine and Freshwater Behaviour and Physiology* 46:275-286
- Strahl J, Francis D, Doyle J, Humphrey C, Fabricius KE (2015) Biochemical responses to ocean acidification contrast between tropical corals with high and low abundances at volcanic carbon dioxide seeps. *ICES Journal of Marine Science* 73: 897-909
- Teixeira T, Diniz M, Calado R, Rosa R (2013) Coral physiological adaptations to air exposure: Heat shock and oxidative stress responses in *Veretillum cynomorium*. *Journal of Experimental Marine Biology and Ecology* 439:35-41

- Thomas CD, Cameron A, Green RE, Bakkenes M, Beaumont LJ, Collingham YC, Erasmus BFN, Siqueira MF, Grainger A, Hannah L, Hughes L, Huntley B, Jaarsveld ASV, Midgley GF, Miles L, Ortega-Huerta MA, Peterson AT, Phillips OL, Williams SE (2004) Extinction risk from climate change. *Nature* 427:145-148
- Tomanek L (2010) Variation in the heat shock response and its implication for predicting the effect of global climate change on species' biogeographical distribution ranges and metabolic costs. *Journal of Experimental Biology* 213:971-979
- Torda G, Donelson JM, Aranda M, Barshis DJ, Bay L, Berumen ML, Bourne DG, Cantin N, Foret S, Matz M, Miller DJ, Moya A, Putnam HM, Ravasi T, Oppen MJHV, Thurber RV, Vidal-Dupiol J, Voolstra CR, Watson S-A, Whitelaw E, Willis BL, Munday PL (2017) Rapid adaptive responses to climate change in corals. *Nature Climate Change* 7:627-636
- Uchiyama M, Mihara M (1978) Determination of malonaldehyde precursor in the tissues by thiobarbituric acid test. *Analytical Biochemistry* 86:271-278
- Vander Land J, 2008. UNESCO IOC Register of Marine Organisms.
- Wiens M et al. (2000) Induction of heat-shock (stress) protein gene expression by selected natural and anthropogenic disturbances in the octocoral *Dendronephthya klunzingeri*. *Journal of Experimental Marine Biology and Ecology* 245:265-276
- Yakovleva I, Bhagooli R, Takemura A, Hidaka M (2004) Differential susceptibility to oxidative stress of two scleractinian corals: antioxidant functioning of mycosporine-glycine. *Comparative Biochemistry and Physiology Part B: Biochemistry and Molecular Biology* 139:721-730
- Yakovleva IM, Baird AH, Yamamoto HH, Bhagooli R, Nonaka M, Hidaka M (2009) Algal symbionts increase oxidative damage and death in coral larvae at high temperatures. *Marine Ecology Progress Series* 378:105-112

5

Encased in troubled waters: Oxidative damage in shark embryos under ocean warming and the protective role of the capsule against contamination

Ana R Lopes^{1,2}, Catarina Santos^{1,3}, Mário Diniz², Rui Rosa¹

¹MARE- Marine Environmental Sciences Centre & Laboratório Marítimo da Guia, Faculdade de Ciências, Universidade de Lisboa, Av. Nossa Senhora do Cabo 939, 2750-374 Cascais, Portugal

²UCIBIO, REQUIMTE, Departamento de Química, Faculdade de Ciências e Tecnologia, Universidade Nova de Lisboa, Quinta da Torre, 2829-516 Caparica, Portugal

³IGC - Instituto Gulbenkian de Ciência, R. Quinta Grande, 6, 2780-156 Oeiras, Portugal

Abstract

Carbon dioxide levels (CO₂) have been increasing since pre-industrial times, triggering the rise in seawater temperature, with predictions pointing out to a 3-4 °C increase until the end of the century. Concomitantly, the anthropogenic load of heavy metals released in coastal areas is increasing contamination, with mercury (Hg) as one of the most harmful contaminants for marine organisms. Both warming and Hg contamination are expected to increase the naturally occurring amount of reactive oxygen species (ROS), inactivating key enzymes, ultimately causing lipid, protein and DNA damage. The purpose of the present study was to evaluate, for the first time, the combined impact of Hg exposure (HgCl₂: 50 µg L⁻¹) and environmental warming (Δ 4°C) in the embryos of the small-spotted catshark (*Scyliorhinus canicula*). More specifically, we determine the oxidative stress-related responses [protein repair and removal mechanisms (HSP and Ub); oxidative damage markers: lipid peroxidation (LPO) and DNA damage; oxidative stress enzymes: SOD, CAT, GPx, GST and AChE and total antioxidant capacity (TAC)]. After 6-days exposure the combined contamination and temperature treatment acted synergistically, causing a 100% mortality. Additionally, and as expected, Hg total levels increased with contamination, with capsule exhibiting the highest levels. Furthermore, within the embryo the highest Hg concentration was found in the gills, followed by the liver, muscle and brain. Elevated temperatures increased HSP levels, nonetheless, insufficient in avoiding protein damage (indirectly measured by through Ub levels) and lipid peroxidation. Moreover, both warming and contamination elicited an up-regulation of the embryos antioxidant defense mechanisms, with the warmer conditions exhibiting a greater effect than contamination. Overall, the antioxidant defense system of *S. canicula* embryos seems to be triggered with increasing temperatures, leading to increased HSP production, nonetheless ineffective in avoiding oxidative damage. Moreover, we argue that the capsule may have a crucial role in protecting the embryos from contamination, especially at earlier embryonic stages (i.e. when the capsule is closed).

Key-words: Mercury chloride, ocean warming, shark eggs, biochemical analysis, oxidative stress, contamination

Atmospheric carbon dioxide levels (CO₂) have been rising since the industrial revolution and are expected to reach ~ 900 ppm until the end of the twenty first century (Pörtner et al. 2014). Considered one of the main greenhouse gases, CO₂ is triggering the rise in global temperature, with a concomitant rise in mean seawater temperature of about 0.7°C since pre-industrial values, and a further increase of 3-4 °C foreseen until the end of the century (Pörtner et al. 2014). This changes in seawater temperature are expected to increase metabolic demands, reducing species aerobic scope (Pörtner and Farrell 2008; Portner and Knust 2007), which will in turn decrease the energy available for growth and reproduction (Donelson et al. 2010; Pankhurst and Munday 2011). Ocean warming will also affect organisms foraging behavior, leading to changes in prey-predator interactions (Malavasi et al. 2013; Nagelkerken and Munday 2015), and species distribution (Perry et al. 2005), leading to worldwide migrations and extinctions (Cahill et al. 2013; Thomas et al. 2004), affecting ecosystems structure and function and consequently species biodiversity (Cheung et al. 2009).

Additionally, marine organisms will be dealing with contamination, due to the high anthropogenic loads of pollutants (i.e. heavy metals and organic chemicals) into the ocean. Mercury (Hg) is one of the most hazardous contaminants for all living organisms and is often found in natural environments as a result of geogenic (i.e. mining processes), industrial (i.e. coal burning, petroleum combustion, power plants), pharmaceutical (i.e. medical wastes) and domestic (i.e. sewage discharge) sources (He et al. 2005; Tchounwou et al. 2012). Inorganic Hg (Hg^{II}) is delivered to the seawater and can either be reduced into elemental Hg (Hg⁰) and released to the atmosphere or methylated by bacteria into organic mercury [methylmercury (MeHg)]. The later greatly increases Hg bioavailability, bioaccumulation and biomagnification in marine food webs (Braune et al. 2015; Jaishankar et al. 2014). Mercury (Hg) can negatively affect marine organisms due to its high toxicity. Specifically, Hg can block ion channels or be transported along the central nervous system, causing neurotoxicity (Clarkson et al. 2003; Lüring 2015), or impair behavior patterns, such as predator avoidance (Boyd 2010; Sloman 2007).

Furthermore, warming and Hg contamination can further increase the naturally occurring amount of reactive oxygen species (ROS), damaging lipids, proteins and nucleic acids. Specifically, increasing temperatures lead to protein denaturation, causing the loss of activity in key enzymes that are temperature-specific (Somero 1995; Tomanek 2010). On the other hand, Hg has a high affinity for the thiol group of proteins, affecting key cellular protection

mechanisms, resulting in an increase in ROS accumulation within the cell (Tchounwou et al. 2012). This increase in ROS will in turn trigger the antioxidant defense mechanisms in the organism, consisting of enzymatic and non-enzymatic (e.g. vitamins, ascorbic and uric acids) antioxidants (Bartosz 2003). As a first line of defense, superoxide dismutase (SOD) converts superoxide ions (O_2^-) into hydrogen peroxide (H_2O_2), which is further transformed into water (H_2O) and oxygen (O_2) by catalase (CAT) and glutathione peroxidase (GPx) (Lesser 2006). Additionally, glutathione S-transferase (GST) plays a key role in the second phase of the detoxification process, enabling the excretion of xenobiotics (Wang et al. 2000). Acetylcholinesterase (AChE), an enzyme responsible for the breakdown of acetylcholine (neurotransmitter responsible for the nervous impulses), ensures the optimal neuronal function (Durieux et al. 2011; Quinn 1987). Furthermore, heat shock proteins will be triggered with increasing temperatures (Repolho et al. 2014; Rosa et al. 2012; Rosa et al. 2014) and contamination (Rajeshkumar and Munuswamy 2011; Williams et al. 1996), in order to repair and refold denatured proteins (Tomanek 2010; Tomanek 2011), and when irreversibly damaged, ubiquitin (Ub) targets proteins to be eliminated (Bond et al. 1988; Hanna et al. 2007). Nevertheless, when the organism's physiological response fails to balance the antioxidant-prooxidant levels, ROS excess will instigate oxidative damage (i.e. lipid peroxidation, protein degradation and DNA strand breaks).

As top-predators, sharks are known to accumulate high levels of Hg in their tissues through bioaccumulation processes (Barrera-García et al. 2012; 2013). In fact, high contamination levels are proven to cause lipid, protein and DNA damage in the blue shark (*Prionace glauca*), due to enzymatic inhibition (Alves et al. 2016). Additionally, mako sharks (*Isurus oxyrinchus*) also undergo oxidative damage, even if SOD and glutathione reductase (GR) activities increase (Vélez-Alavez et al. 2013). Nonetheless, most research has focused on adult stages, while this effects in early life stages, namely in oviparous species which are directly exposed to environmental stressors since laid, have received less attention. To the best of our knowledge, to date no studies addressed the protective role of the shark's capsule in protecting the embryo from toxicity, oxidative stress and damage caused by warming and Hg contamination. In fact, it is known that the capsule has an important role in protecting the embryo, especially if we take into account that contaminant exposure poses a major threat during early life stages, particularly if the embryonic development occurs near contaminated areas (Boening 2000; Rosa et al. 2015). *Scyliorhinus canicula* (Linnaeus, 1758) is a bottom-dwelling shark, with a wide geographic

distribution (from the northeast Atlantic to the Mediterranean), that deposits eggs on macroalgae in shallow coastal waters, with a gestation period of approximately 5-11 months, depending on water temperature (Capapé et al. 2008; Ellis and Shackley 1997).

The aim of the present study was to evaluate, for the first time, the accumulation of Hg in *S. canicula* capsule and embryos (i.e. brain, gills, muscle, liver and stomach tissues). Moreover, we determined the oxidative stress-related responses under mercury chloride (HgCl_2 : $50 \mu\text{g L}^{-1}$) contamination and warming ($\Delta 4^\circ\text{C}$) conditions. Specifically, after 1-week exposure to HgCl_2 and warming we measured: i) oxidative damage markers [lipid peroxidation (LPO) and DNA damage], ii) oxidative stress enzymes (SOD, CAT, GPx, GST and AChE) as well as total antioxidant capacity (TAC), and iii) protein repair and removal mechanisms (HSP and Ub).

5.1. Material and methods

5.1.1. Experimental setup and incubation

Scyliorhinus canicula eggs, derived from wild-caught mothers from Figueira da Foz, Portugal, were reared during the entire embryogenesis in 600L tanks, in the Laboratório Marítimo da Guia aquaculture facilities (Cascais, Portugal), where they were maintained under stable control conditions, representing those found in their natural habitat (temperature = 18°C , pH = 8.0, salinity = 35), until they reach stage 33 (according to Ballard et al. 1993). After 90-110 days (corresponding to stage 33 at 18°C) eggs ($n = 5$ per treatment) were individually transferred and suspended in 200 mL cups and acclimated to ocean warming ($\Delta T = 4^\circ\text{C}$) conditions expected for 2100 (Pörtner et al. 2014) and HgCl_2 contamination ($50 \mu\text{g L}^{-1}$; limit for residual water discharges, Diário da República – I Série A, nº 176, 1-8-1988) for 7 days. More specifically, embryos were incubated to one of the following experimental conditions: i) Control (18°C , non-contaminated); ii) Contamination (18°C , HgCl_2 contaminated), iii) Warming (22°C , non-contaminated) and iv) Warming and Contamination (22°C , HgCl_2 contaminated). Temperature and contamination values were maintained inside each cup through a continuous flow (3 mL/min) of aerated seawater from pre-treated 20L header tanks, corresponding to a 100% seawater renovation, twice a day. Additionally, water temperature was also ensured by a partial immersion in a water bath, automatically upregulated, through submerged digital heaters (V²Therm 200W aquarium heater, TMC Iberia, Portugal), or downregulated, using seawater chillers (Hailea, HC-250A, Guangdong,

China). Contamination levels were warranted through a manual addition of HgCl_2 in the corresponding header tank, in each new 0.35 μm filtered (Hamsco, USA) and UV-irradiated (V²ecton 600, TMC Iberia, Portugal) natural seawater renewal. Furthermore, a daily monitoring of seawater temperature (Thermometer TFX 430, WTW GmbH, Germany) and salinity (refractometer V2, TMC Iberia, Portugal) was performed using handheld equipment. Tanks were illuminated with white fluorescent lamps in a 12 h: 12 h (light/dark) photoperiod.

5.1.2. Total mercury accumulation

The total mercury (Hg) was determined in *S. canicula* tissue (brain, gills, muscle, liver and stomach), as well as in capsules and water samples by inductively coupled plasma atomic emission spectrometry (ICP-EAS) using a Horiba-Jobin Yvon, model Ultima) apparatus. Tissues samples were dried, weighed, and subsequently digested with 1.0 mL HNO_3 (Merk, Darmstadt, Germany). The water samples were acidified with HNO_3 and analyzed. Accuracy was checked by analysis of certified biological material (Standard Reference Material, ERM CE278k—Mussel tissue). The total Hg ($\mu\text{g g}^{-1}$) measured in digested samples of reference material (Hg 0.082 ± 0.009) showed a good agreement with the certified values (Hg 0.071 ± 0.007).

5.1.3. Biochemical Analyses

5.1.3.1. Sample preparation

Brain, gills, liver, muscle and stomach samples ($n = 4$ per treatment) were homogenized using a Teflon grinder, in 0.5 mL (brain), 0.7 mL (stomach) and 1 mL (remaining tissues) of phosphate buffered saline solution (PBS: 0.14 M NaCl, 2.7 mM KCl, 8.1 mM Na_2HPO_4 and 1.47 mM KH_2PO_4 , pH 7.4). Homogenates were centrifuged at $10.000 \times g$ for 15 min at 4°C and frozen (-80°C) until further analyses. Each sample was run in triplicate (technical replicates), and the enzyme results were normalized to total protein content, as described by Bradford (1976).

5.1.3.2. Heat shock response

Heat Shock Protein 70 (HSP70) and **Ubiquitin (Ub)** levels were determined in *S. canicula* tissues brain, gills, liver, muscle and stomach, through an ELISA, as described by Lopes et al. (2018). Briefly, 100 μL of each sample (HSP: 10 μL sample diluted in 980 μL PBS; Ub: 100 μL non-diluted sample) was added to 96-well microplates (Microlon 600, Greiner, Germany) and allowed to incubate overnight at 4°C . On the subsequent day, microplates were washed (3x) with PBS TWEEN-20. Subsequently, 100 μL of BSA was added to each well, and microplates incubated for 90 min at 37°C . Then, 50 μL of primary antibody (HSP: 5 $\mu\text{g mL}^{-1}$ of anti-HSP70/HSC70 in 1% BSA, Acris, USA; Ub: 200 $\mu\text{g mL}^{-1}$ of P4D1 in 1% BSA, sc-8017, Santa Cruz, USA) was added to each well. After another incubation period (overnight at 4°C), microplates were washed (3x) and allowed to incubate for 90 min at 37°C with the second antibody [50 μL of 1 $\mu\text{g mL}^{-1}$; alkaline phosphatase-conjugated anti-mouse IgG (Fab specific, Sigma-Aldrich, USA)]. Afterward, and following an additional washing procedure, 100 μL of substrate (SIGMA FAST™ p-Nitrophenyl Phosphate Tablets, Sigma-Aldrich, USA) was added to each well and incubated for 30 min at room temperature. Finally, 50 μL of stop solution (3 M NaOH) was added to each well and the absorbances read at 405 nm (Asys UVM 340, Biochrom, USA). HSP content was calculated from the calibration curve, based on serial dilutions of purified HSP70 active protein (0 - 2.000 $\mu\text{g mL}^{-1}$, ACRIS, USA) and results normalized to sample protein ($\mu\text{g mg}^{-1}$ protein). The Ub content was assessed based on serial dilutions of purified ubiquitin (0 - 1 $\mu\text{g mL}^{-1}$, UbpBio, E-1100, USA).

5.1.3.3. Oxidative damage

Lipid peroxidation (LPO), was determined in the *S. canicula* tissues (brain, gills, liver, muscle and stomach) according to the thiobarbituric acid reactive substances (TBARS) assay (Uchiyama and Mihara 1978b), as described by Lopes et al, 2018, through the quantification of malondialdehyde (MDA), a specific end product of lipid damage. Briefly, 5 μL of each sample, as 45 μL of monobasic sodium phosphate buffer (50 mM), 12.5 μL of sodium dodecyl sulphate (8.1 %), 93.5 μL of trichloroacetic acid (20 %, pH 3.5), 93.5 μL of thiobarbituric acid (1 %), and 50.5 μL of Milli-Q ultrapure water were added to a new microtube. Afterward each microtube was mixed and placed in boiling water (100°C) for 10 min. After those 10 min, microtubes were

placed on ice until cool and an additional addition of 62.5 μL of Milli-Q ultrapure water performed. Finally, 150 μL of each sample was added to 96-well microplates, and the absorbance read at 532 nm (Asys UVM 340, Biochrom, USA). MDA concentrations were calculated based on a calibration curve (0 - 0.3 μM MDA bis (dimethyl acetal)).

DNA/RNA damage was measured according to Lopes et al (2018), in the gills, liver, muscle and stomach of *S. canicula*, through 8-hydroxy-2'-deoxyguanosine (8-OHdG) quantification. A total of 100 μL of each sample was added to 96-well microplates and allowed to incubate overnight at 4°C. On the next day, plates were washed 3 times with PBS-TWEEN, and microplates incubated for 90 min at room temperature with 200 μL of 1 % bovine serum albumin (BSA). After another washing procedure, microplates were incubated overnight with primary antibody (anti-OHdG, clone 15 A3, Sigma-Aldrich, Germany). Subsequently, and after another washing procedure, microplates were incubated for 90 min at 37°C with the secondary antibody (alkaline phosphatase-conjugated anti-mouse IgG, Fab specific, Sigma-Aldrich, USA). After a final washing procedure, plates were incubated for 30 min at room temperature with the substrate (SIGMA FAST™ p-Nitrophenyl Phosphate Tablets, Sigma-Aldrich, USA), after 30 min the reaction was stopped by adding 100 μL of 3M NaOH. The absorbance was read at 405 nm using a microplate reader (Asys UVM 340, Biochrom, USA).

5.1.3.4. Enzymatic activities and total antioxidant capacity

Superoxide dismutase (SOD: EC 1.15.1.1) inhibition was determined in the gills, liver, muscle and stomach samples, as described by Lopes et al. (2018), through an adaptation of the method described by McCord and Fridovich (1969) to 96-well microplates. Each sample (10 μL) was added to a 96-well microplate, as well as 180 μL of the reaction mix [50 mM potassium phosphate, 0.1 mM ethylenediaminetetraacetic acid, 0.01 mM cytochrome c and 0.05 mM xanthine]. Afterwards, the reaction was started by adding 10 μL of xanthine oxidase (0.005 units), and the absorbance read at 550 nm (Asys UVM 340, Biochrom, USA).

Catalase (CAT) activity was measured in gills, liver, muscle and stomach tissues based on the method described by Johansson and Borg (1988). Briefly, 20 μL of each sample, 100 μL potassium phosphate (100 mM) and 30 μL methanol were added to a 96-well microplate. Afterwards, plates were incubated for 20 minutes with continuous agitation. Subsequently, 30 μL potassium hydroxide (10 M) and 30 μL purpald (34.2 mM in 0.5 M HCl) were added to each well,

and plates shaken and incubated for another 10 minutes. Finally, 10 μL of potassium periodate (65.2 mM in 0.5 M KOH) was added to each well, and plates incubated for 5 more minutes. The absorbance was read at 540 nm, using a microplate reader (Asys UVM 340, Biochrom, USA). Formaldehyde concentration was calculated based on a calibration curve (from 0 to 75 μM formaldehyde), followed by the calculation of the CAT activity of each sample, where one unit of catalase is defined as the amount that will cause the formation of 1.0 nmol of formaldehyde per minute at 25°C. The results were expressed in relation to total protein content ($\text{nmol min}^{-1} \text{mg}^{-1} \text{protein}$).

Glutathione peroxidase (GPx: EC 1.11.1.9) activity was determined in gills, liver, muscle and stomach samples according to Lawrence and Burk (1976), through an adaptation to 96 well microplates as described by Lopes et al. (2018). Briefly, 20 μL of each sample, 50 mM phosphate buffer (pH 7.6), co-substrate mixture (0.8 mM β -NADPH, 4 mM Glutathione, 4 U/mL glutathione reductase, and 4 mM sodium azide) and 15 mM cumene hydroperoxide ($\text{C}_9\text{H}_{12}\text{O}_2$) were added to each well, and the absorbance was read at 340 nm (Asys UVM 340, Biochrom, USA), every minute for 6 min. The GPx activity was determined using the β -NADPH coefficient extinction, and results given in $\text{nmol min}^{-1} \text{mg}^{-1} \text{protein}$.

Glutathione S-transferase (GST) was determined in gills, liver, muscle and stomach tissues following the method described by Habig et al. (1974a), optimized for 96-well microplates as described by Lopes et al. (2018). Specifically, 180 μL of substrate solution (100 mM 1-chloro-2,4-dinitrobenzene (CDNB), 200 mM L-glutathione and Dulbecco's PBS) were added to 20 μL sample in each well and the absorbance was read at 340 nm (Asys UVM 340, Biochrom, USA) every minute for 6 min. Equine liver GST (Sigma-Aldrich) was used as positive control to validate the assay and GST activity calculated using the molar extinction coefficient for CDBN of 5.3 ϵmM . Result were expressed according to total protein of the sample ($\text{nmol min}^{-1} \text{mg}^{-1} \text{protein}$).

Acetylcholinesterase (AChE) activity was determined in brain and muscle samples, according to an adaptation of the Ellman et al. (1961) method to 96-well microplates, as described by Sampaio et al. (2016). Briefly, 25 μL of each sample was added to a 96-well microplate, with the subsequent addition of 250 μL of a mix solution (50 mM of sodium phosphate, 75 mM acetylthiocholine iodide and 1 mM of 5,5'-dithio-bis-2-nitrobenzoic acid). Subsequently, microplates were read at 415 nm (Asys UVM 340, Biochrom, USA) every minute for 10 min. AChE measurements were standardized to protein concentration ($\text{nmol min}^{-1} \text{mg}^{-1} \text{protein}$).

Total antioxidant capacity (TAC) was determined in gills, liver, muscle and stomach tissues according to Kambayashi et al. (2009). Each sample (10 μ L) was added to each well in a 96-well microplate. Subsequently, 10 μ L myoglobin (90 μ M), 150 μ L 2,2'-azino-bis (3-ethylbenzothiazoline-6-sulphonic acid) (600 μ M) and 40 μ L hydrogen peroxide (500 μ M) were added to the wells. Microplates were incubated at room temperature for 5 min and the absorbance was read at 410 nm (Asys UVM 340, Biochrom, USA). TAC was calculated from a calibration curve, based on a series of Trolox (0 – 0.3 Mm) and expressed according to samples total protein (mM Trolox mg^{-1} protein).

5.1.4. Statistical analysis

Generalized linear models (GLM) were used to infer significant differences between temperature and contamination treatments, and across the tissues analyzed. Data was fitted using Gaussian family and model residuals checked for homogeneity of variances, normality, independence and leverage to validate final models. Whenever the assumptions were violated, we fitted our data with Gamma models, and proceed with the same measurements to validate the model. In a first approach, tissue (five levels for LPO, HSP and Ub: brain, muscle, liver, gills and stomach; four levels for DNA damage, SOD, CAT, GPx, GST and TAC: muscle, liver, gills and stomach; two levels for AChE: brain and muscle) was used as an explanatory variable to find organ-specific patterns for each specific dependent variable (Oxidative damage: LPO and DNA damage; Oxidative Stress: SOD, CAT, GPx, GST, AChE and TAC; Protein repair and removal: HSP and Ub). Afterwards, a second approach where temperature (two levels: 18 °C and 22 °C) and HgCl contamination (two levels: Non-contaminated and Contaminated) were used as explanatory variable was performed to find patterns within each tissue. Tukey post-hoc tests were applied to better scrutinize the effect of explanatory variables on each measured endpoint. All statistical analyses were performed using R Studio (R Development Core Team 2017).

5.2. Results

After seven days of exposure, survival (Fig. 1) decreased by 20% in the control, contaminated and warming treatments, while a 100% mortality was observed in the combined warming and contaminated treatment ($p < 0.001$, GLM analysis in table SI).

Regarding total mercury (HgT) concentrations in the capsule (Fig. 2), Hg accumulation increased from levels of 0.5 ± 0.2 to 35.8 ± 14.0 mg kg⁻¹ dw from control to contaminated scenarios at 18 °C, and levels of 0.8 ± 0.5 to 21.5 ± 3.4 mg kg⁻¹ dw from control to contaminated scenarios at 22 °C ($p < 0.001$, GLM analysis in table SII). As for HgT accumulation in each tissue (Fig. 3), gills were the tissue with the highest Hg accumulation ($p < 0.05$, GLM analysis in table SIII), while the stomach was the tissue exhibiting lowest levels of HgT ($p < 0.05$, GLM analysis in table SIII).

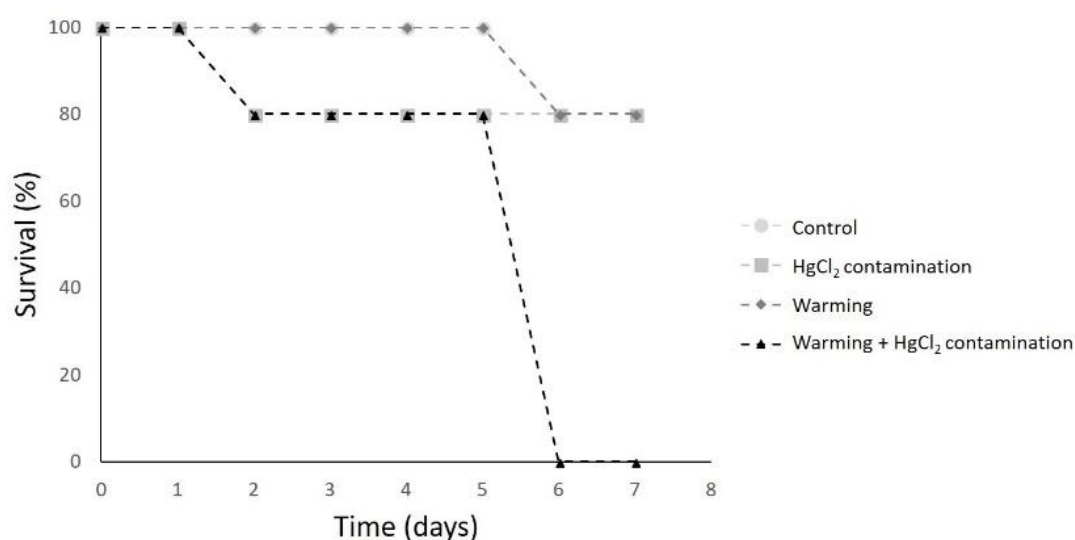


Figure 1 – Survival (%) of *S. canicula* exposed to different combinations of temperature and HgCl₂ contamination for seven days. GLM analyses described in Supplemental Table SI.

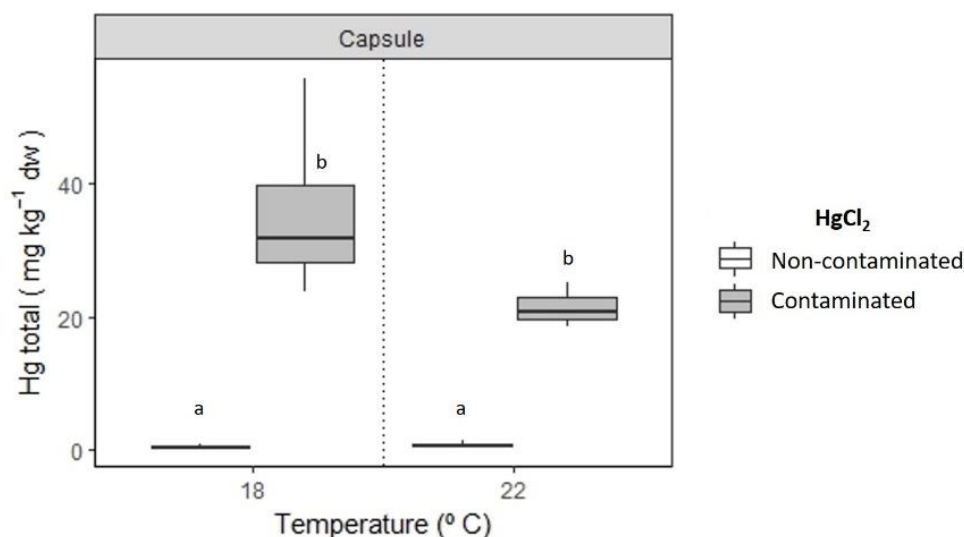


Figure 2 – Total mercury (HgT) accumulation in *S. canicula* capsule. The horizontal line within the box indicates the median, boundaries of the box indicate the 25th and 75th percentiles, and the whiskers indicate the highest and lowest values of the results. Different letters represent significant differences between treatments. GLM analyses described in Supplemental Table SII.

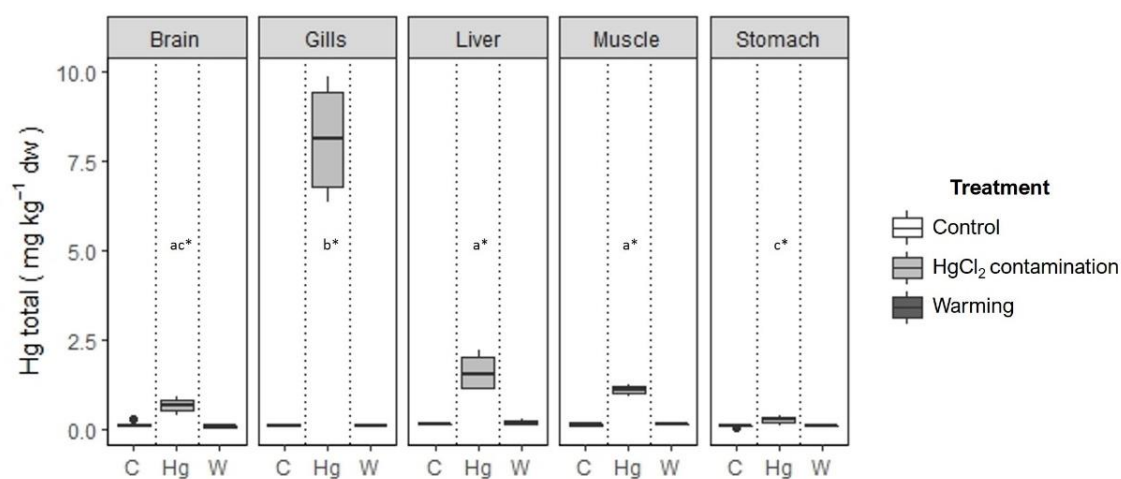


Figure 3 – Total mercury (HgT) accumulation in *S. canicula* tissues. The horizontal line within the box indicates the median, boundaries of the box indicate the 25th and 75th percentiles, and the whiskers indicate the highest and lowest values of the results. Different letters represent significant differences between tissues, while asterisks (*) represent significant differences between contamination treatments. GLM analyses described in Supplemental Table SIII.

HSP levels (Fig. 4A) were higher in the stomach ($p < 0.001$, GLM analysis in table SIV) and lower in the gills and muscle (both $p < 0.05$, GLM analysis in table SIV). Increasing temperatures significantly increased HSP levels within the brain ($p < 0.001$, GLM analysis in table SIV) and gills ($p < 0.05$, GLM analysis in table SIV), while no differences were found with contamination. As for Ub levels (Fig. 4B), significantly higher levels were found in the stomach ($p < 0.05$, GLM analysis in table SV). Contamination led to increased levels in both brain ($p < 0.05$, GLM analysis in table SV) and liver ($p < 0.05$, GLM analysis in table SV) and decreased levels in the stomach ($p < 0.05$, GLM analysis in table SV). Temperature led to increasing Ub levels in the brain, gills, liver and muscle (all $p < 0.05$, GLM analysis in table SV).

Lipid peroxidation (LPO, Fig. 5A) exhibited significant higher levels in the muscle compared with the other tissues investigated ($p < 0.05$, GLM analysis in table SVI). Furthermore, significantly higher LPO levels were observed with temperature within the gills ($p < 0.05$, GLM analysis in table SVI) and muscle ($p < 0.05$, GLM analysis in table SVI), while no differences were found across contamination levels. Moreover, DNA/RNA damage (Fig. 5B) also significantly differ among the tissues analyzed, displaying higher levels in the stomach, and lower in the liver ($p < 0.05$, GLM analysis in table SVII), nonetheless, neither contamination nor increased temperature rendered significant differences within each tissue ($p > 0.05$, GLM analysis in table SVII).

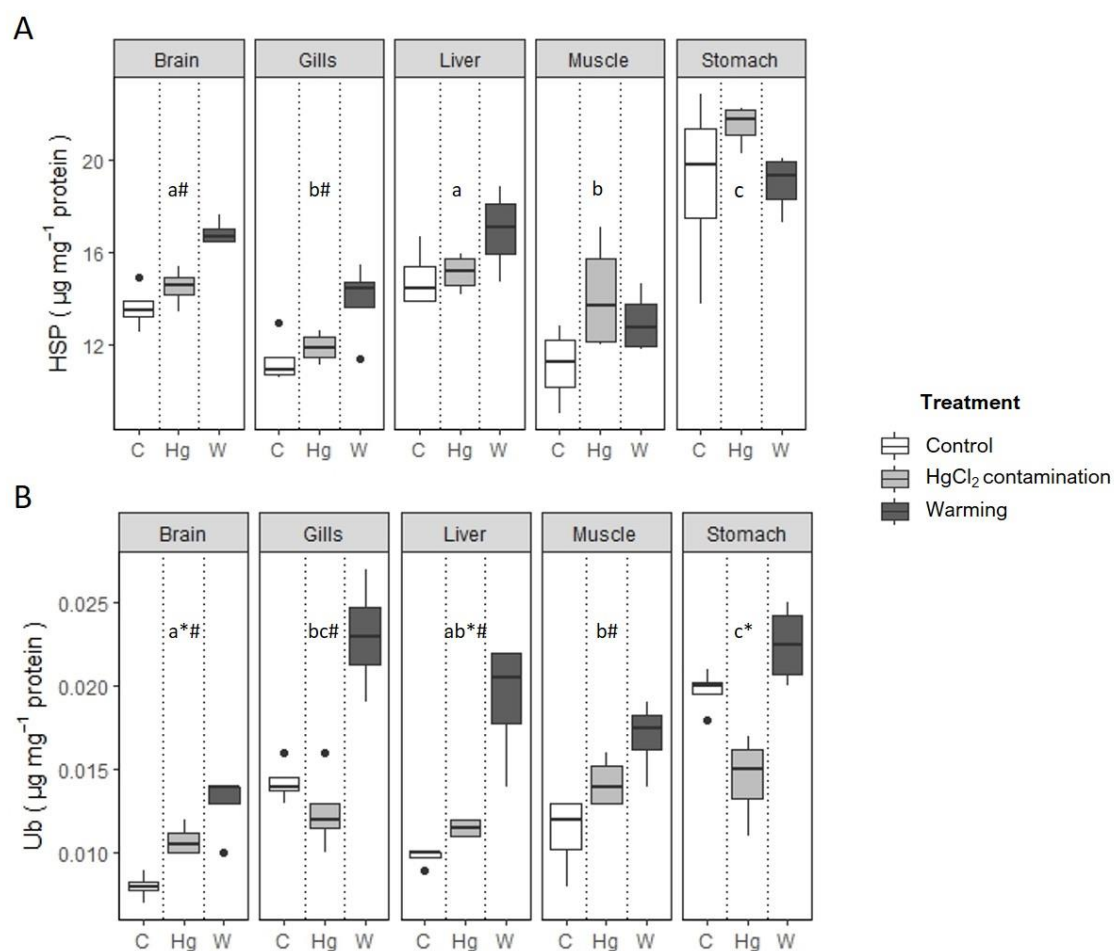


Figure 4 - Impact of HgCl₂ and warming exposure on levels of: A) Heat shock proteins (HSP) and B) Ubiquitin (Ub) in *S. canicula* tissues. The horizontal line within the box indicates the median, boundaries of the box indicate the 25th and 75th percentiles, and the whiskers indicate the highest and lowest values of the results. Different letters represent significant differences between tissues, while asterisks (*) and cardinals (#) represent significant differences between contamination and temperatures, respectively. GLM analyses described in Supplemental Tables SIV and SV.

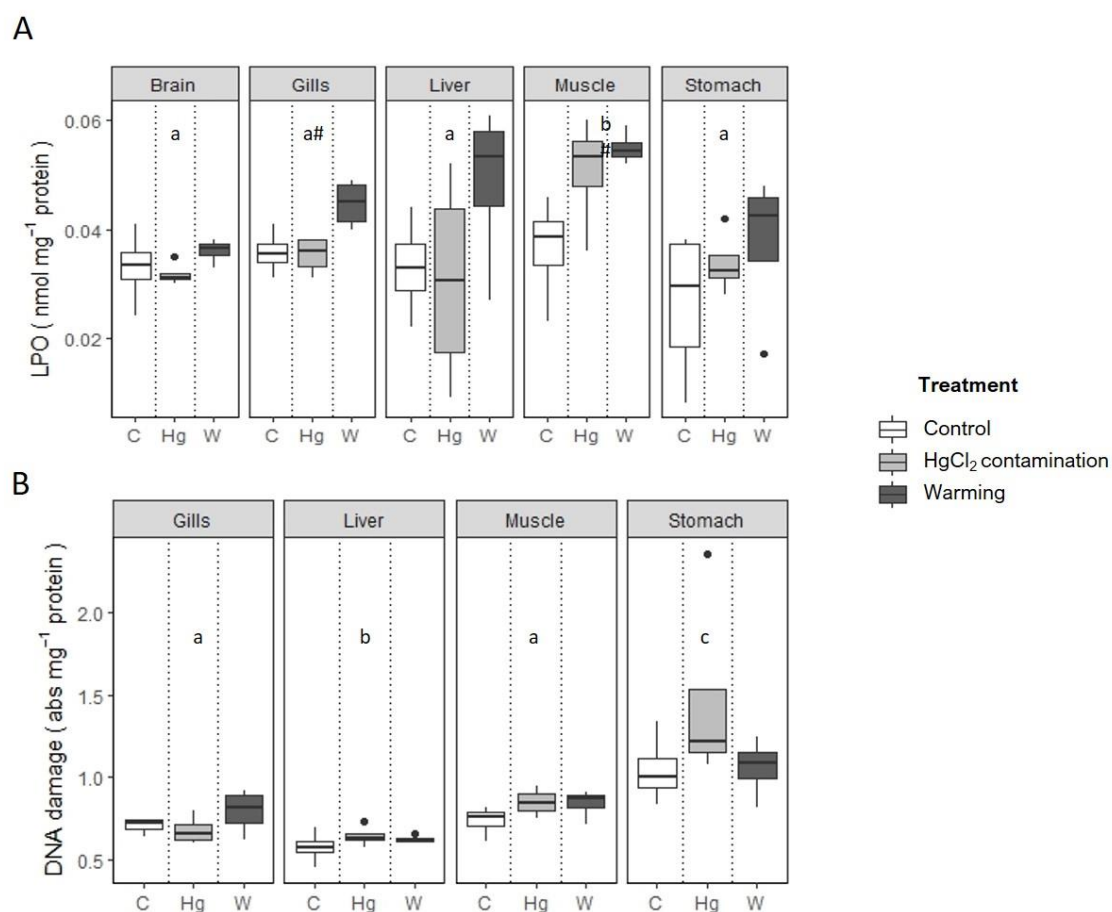


Figure 5 – Impact of HgCl₂ and warming exposure on levels of: A) Lipid peroxidation (LPO) and B) DNA/RNA damage levels in *S. canicula* tissues. The horizontal line within the box indicates the median, boundaries of the box indicate the 25th and 75th percentiles, and the whiskers indicate the highest and lowest values of the results. Different letters represent significant differences between tissues, while cardinals (#) represent significant differences between temperatures. GLM analyses described in Supplemental Tables SVI and SVII.

Regarding the antioxidant enzymatic machinery, SOD activity (Fig. 5A) varied among tissues, with higher activity levels in the stomach ($p < 0.001$, GLM analysis in table SVIII). Within tissues, SOD activity increased with contamination, in the liver and muscle (both $p < 0.001$, GLM analysis in table SVIII), and with temperature, in the gills ($p < 0.05$, GLM analysis in table SVIII), liver ($p < 0.001$, GLM analysis in table SVIII), muscle ($p < 0.001$, GLM analysis in table SVIII) and stomach ($p < 0.05$, GLM analysis in table SVIII). As for CAT activity (Fig. 5B), the highest levels were observed in the gills ($p < 0.001$, GLM analysis in table SIX) and lowest in the muscle and stomach (both $p < 0.001$, GLM analysis in table SIX). Additionally, Hg contamination led to a decrease in CAT activity in the gills ($p < 0.001$, GLM analysis in table SIX) and muscle ($p < 0.001$, GLM analysis in table SIX), and an increase in the liver ($p < 0.05$, GLM analysis in table SIX). Furthermore, temperature decreased CAT activity in the gills ($p < 0.05$, GLM analysis in table SIX). Moreover, GPx activity (Fig. 5C) did not changed significantly among tissues ($p > 0.05$, GLM analysis in table SX), nonetheless decreased with contamination in the liver ($p < 0.05$, GLM analysis in table SX) and increased with temperature in the muscle ($p < 0.001$, GLM analysis in table SX). GST activity (Fig. 5D) displayed higher levels for the liver ($p < 0.05$, GLM analysis in table SXI) and lower in gills and muscle ($p < 0.05$, GLM analysis in table SXI). Moreover, GST activity increased with temperature within the gills ($p < 0.05$, GLM analysis in table SXI), liver ($p < 0.001$, GLM analysis in table SXI) and stomach ($p < 0.05$, GLM analysis in table SXI), but no differences with contamination. Finally, AChE activity (Fig. 5E) did not differ among tissues ($p > 0.05$, GLM analysis in table SXII), although increasing in the muscle with both contamination ($p < 0.05$, GLM analysis in table SXII) and temperature ($p < 0.001$, GLM analysis in table SXII). As for TAC levels (Fig. 5F), stomach displayed the highest values ($p < 0.001$, GLM analysis in table SXIII) and significant decrease was found in the liver with increased temperature ($p < 0.05$, GLM analysis in table SXIII).

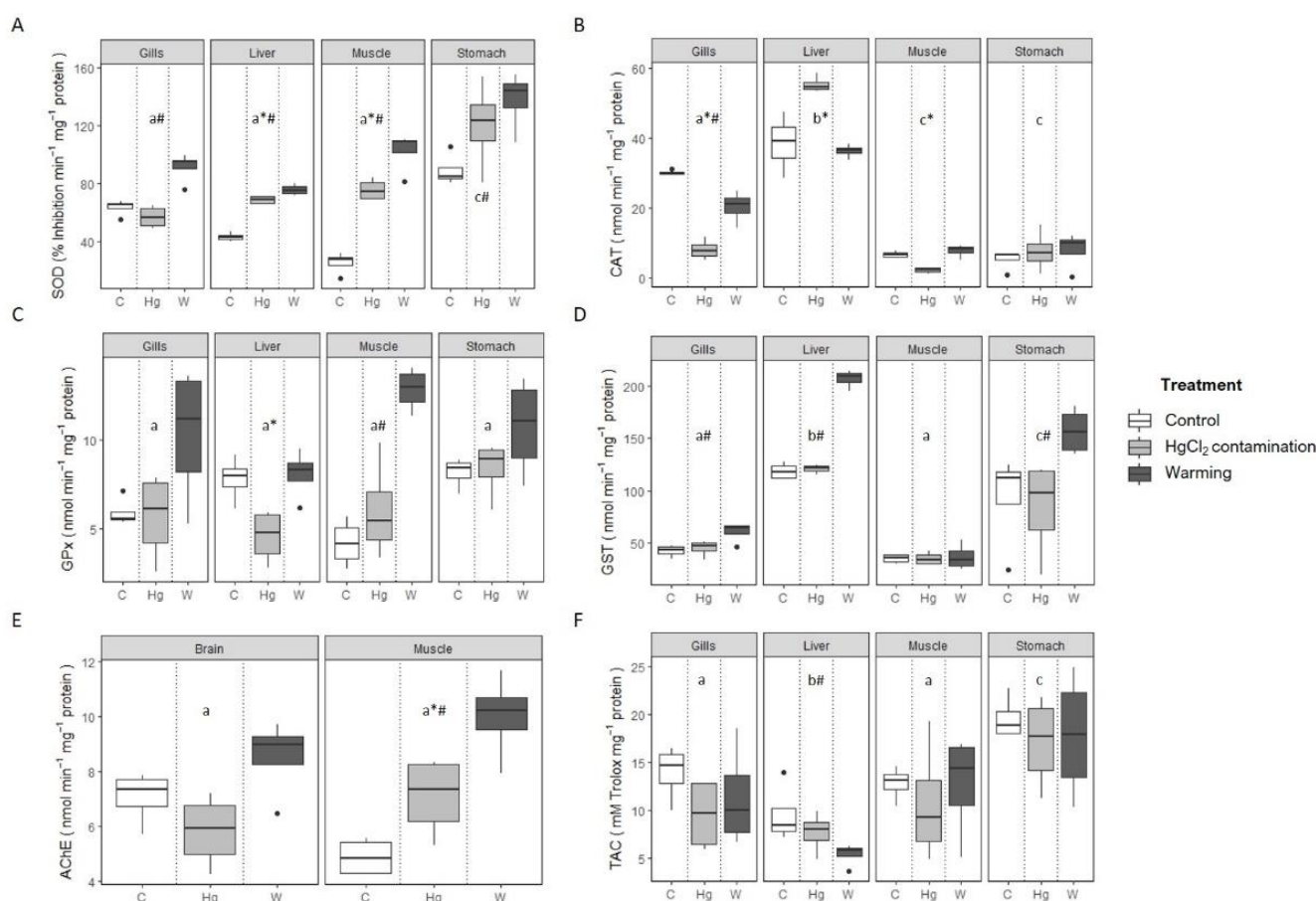


Figure 6 - Impact of HgCl_2 and warming exposure on: A) Superoxide dismutase (SOD), B) Catalase (CAT), C) Glutathione peroxidase (GPx), D) Glutathione S-Transferase (GST), E) Acetylcholinesterase (AChE) activities and F) Total antioxidant capacity (TAC) in *S. canicula* tissues. The horizontal line within the box indicates the median, boundaries of the box indicate the 25th and 75th percentiles, and the whiskers indicate the highest and lowest values of the results. Different letters represent significant differences between tissues, while asterisks (*) and cardinals (#) represent significant differences between contamination and temperatures, respectively. GLM analyses described in Supplemental Tables SVI-SXI.

5.4. Discussion

Coastal areas endure an ever-growing anthropogenic pressure, both directly (e.g. contamination through industrial effluents and sewage discharges) and indirectly (e.g. increased temperatures due to CO_2 -driven warming). The input of heavy metals through natural and anthropogenic sources (He et al. 2005; Tchounwou et al. 2012) often results in deleterious effects on wildlife, ecosystems and ultimately human health (Caeiro et al. 2005; Fung et al. 2004), while

warmer temperatures render changes in ecosystems structure (Cheung et al. 2009). Hence, considering that *S. canicula* use coastal areas as nursery (Capapé et al. 2008; Ellis and Shackley 1997), it should be expected that contamination and warming would play an important role during embryogenesis and early life stages (Boening 2000). In the present study, both inorganic Hg (HgCl_2) contamination and increased temperatures led to a 20% mortality of *S. canicula* embryos. It is known that Hg toxicity increases with temperature (Boening 2000), and in the present study, the combination between contamination and temperature acted synergistically, leading to 100% mortality after 6-days exposure. This synergistic interaction between contamination and rising temperatures has been previously reported in other freshwater and marine species (Jones 1973; MacLeod and Pessah 1973). Moreover, this effect may have been further exacerbated by the greater sensitivity of embryo and larval stages to HgCl_2 toxicity (Boening 2000), which may be due to a temperature-driven increase in the rate of Hg uptake and accumulation (Jezierska and Witeska 2006; MacLeod and Pessah 1973; Maulvault et al. 2016). Additionally, oxygen consumption also tends to rise with temperature, which can further increase the water passage through the gills, resulting in a higher Hg exposure and accumulation (Pimentel et al. 2014). Nonetheless, one should bear in mind that the high mortality (i.e. 100%) observed under the combined warming and HgCl_2 scenario forestall us to quantify the Hg concentration and the physiological state of those embryos, hindering our ability to deliver a reliable assumption.

Contamination led to 20-35 times higher Hg total levels in the capsule when compared with non-contaminated conditions, without exhibiting significant differences with temperature. Furthermore, the highest Hg concentration within the embryo was found in the gills, with an eightyfold increase when compared with the non-contaminated treatment. Affinity for metal accumulation is known to be tissue-specific, and as reported in previous studies, gills tend to show the highest Hg levels, since contaminated water is directly pumped over the gills, they are the main site for metal entry into the body (Cairns et al. 1975; Jezierska and Witeska 2006). Additionally, inorganic Hg accumulation also tends to occur in lipid-rich tissues such as the liver, which has an important role in the metabolism and excretion of metals (Jezierska and Witeska 2006; Vergilio et al. 2012). Furthermore, the lowest levels of Hg accumulation were found in *S. canicula* muscle and brain. In fact, the muscle is known to have a low inorganic Hg affinity (Jezierska and Witeska 2006; Ribeiro et al. 1996; Vergilio et al. 2012), moreover the blood-brain

barrier is less permeable to inorganic Hg than to MeHg, which typically results in a lower neurotoxicity (Korbas et al. 2012; Maulvault et al. 2016).

Elevated temperature is known to disrupt the balance between stability and lability of proteins, leading to protein unfolding and subsequent structural and function loss (Dong et al. 2008). Therefore, when exposed to warming conditions, specialized molecular chaperones (i.e. HSP) are triggered to stabilize and refold denatured proteins (Tomanek 2010). Indeed, in the present study, HSP levels increased in the brain and gills, after 7-days exposure to warmer conditions. Notwithstanding, proteins can occasionally reach a denatured level in which its stabilization and recovery is impossible. In fact, increasing temperatures boosted Ub levels, an indirect marker of protein damage that targets irreversibly damaged proteins to be eliminated (Bond et al. 1988; Hanna et al. 2007). Additionally, and despite no patterns observed for HSP levels with HgCl₂ contamination, Ub levels increased in the brain and liver tissues of shark embryos, reaffirming the potential of Ub as a biochemical marker of protein oxidation when exposed to warming and HgCl₂. Furthermore, and even though warmer temperatures increased gills and muscle HSP levels, this was not sufficient to circumvent lipid peroxidation (i.e. MDA build-up). Lipid peroxidation is known to increase with warming, due to an overproduction of ROS and its consequent action in cell membranes (Lesser 2006; Pimentel et al. 2015; Repolho et al. 2014; Rosa et al. 2016a; Rosa et al. 2012). On the other hand, no lipid damage was observed with HgCl₂ contamination. Concomitantly, no DNA damage was found with higher temperatures or contamination.

To cope with temperature- and contamination-related ROS overproduction, marine organisms exhibit an effective antioxidant defense system encompassing antioxidant enzymes known to be intrinsically dependent upon one another (Cooper et al. 2002; Lesser 2006). Both increasing temperatures and contamination elicited an up-regulation of antioxidant defense mechanisms, with the former exhibiting a greater effect than the latter. Specifically, SOD and GST activities showed a general increase in all the tissues analyzed, while TAC levels and GPx activity decreased in the liver with warming and contamination, respectively. Nonetheless the enhanced antioxidative response to warming was insufficient in avoiding protein (within the brain, gills, liver and muscle tissues) and lipid (gills and muscle) damage. Moreover, we also detected a decreased CAT activity within the gills, with warming and contamination, which can be explained by one of two hypotheses: i) increasing GST activity acted more promptly within this tissue and was enough to diminish H₂O₂ levels, reducing CAT activity (Wang et al. 2000); or

ii) high ROS concentration was removed through H_2O_2 diffusion in the gills, a distinctive feature often found in sharks (López-Cruz et al. 2012). Additionally, GPx activity decreased with contamination, as previously reported by Alves et al. (2016) for the blue shark (*Prionace glauca*), nonetheless, and in contrast with said study, our results showed no signs of oxidative damage.

Increased AChE activity within the muscle, may act in order to block the overflow of nervous impulses, due to neurotransmitter excess (i.e. acetylcholine) to ensure the ideal neuronal function, and to warn of the increased neurotoxicity commonly associated with Hg contamination (Durieux et al. 2011; Quinn 1987). In contrast to previous studies, where AChE activity increased within the brain with warmer temperatures (Rosa et al. 2016a), in the present study the AChE activity did not change. Moreover, the fact that AChE activity did not change with contamination may be related with the fact that inorganic Hg, in contrast with organic Hg (MeHg), has a greater difficulty passing the blood-brain barrier, and thus, does not directly affect the brain (Korbas et al. 2012; Maulvault et al. 2016).

Overall, the antioxidant defense system of *S. canicula* embryos seems to be triggered with increasing temperatures, leading to increased HSP production, nonetheless ineffective in avoiding oxidative damage (lipid peroxidation and protein oxidation). The fact that the sharks' capsule retained the largest Hg concentration could suggest a potential protective role towards metal contamination. Nonetheless, and considering the embryonic duration, the capsule could have a crucial role in protecting *S. canicula* embryos from contamination and high temperature levels encountered in the surrounding environment, particularly during the first stages of embryogenesis, when the capsule is fully-sealed. Additionally, shark capsules also bear an effective oxidative power, scavenging for heavy metals to produce toxic external coats, and also as a function site of ROS production, through the Fenton reaction, providing effective antifouling and anti-predatory strategies (Thomason et al. 1996). It would be of extreme relevance to understand the mechanisms behind the possible Hg scavenging process, and to understand if increasing temperatures could further increase or reduce the production of highly reactive ROS by the capsule. Additionally, since the whole warming and contaminated treatment died, it would be interesting to recreate this study, with more than one Hg contamination level, to understand the lethal concentration of this species and the physiological mechanisms that may or may not allow them to thrive under the combination of stressors (with low Hg levels). Furthermore, to understand the true role of the capsule as a shield against Hg contamination, we should expose *S. canicula* eggs throughout the entire embryogenesis, as the eggs remain closed until it reaches

stage 30 (Ballard et al. 1993). Nonetheless by the time the embryo is 40 mm long, the capsule opens allowing a continuous flow of the external water within the egg (Ballard et al. 1993). Moreover, and from a conservation point of view, the legal Hg levels allowed in sewage discharges should be reconsidered, as ocean warming is expected to increase Hg toxicity and uptake.

5.5. Acknowledgments

We would like to thank Maria Rita Pegado and Marta Pimentel for the fundamental technical support during adult and embryo shark acclimation preceding the present experiment.

5.6. Funding

The Portuguese Foundation for Science and Technology (FCT) supported this work through the Programa Investigador FCT 2013 to R.R. FCT also supported this work through: i) the strategic project UID/MAR/04292/2013 granted to MARE, and ii) PhD grants to ARL (SFRH/BD/97070/2013) and CS (SFRH/BD/117890/2016).

5.7. Conflict of Interest

The authors declare that there are no conflicts of interest.

5.8. References

- Alves LMF, Nunes M, Marchand P, Bizec BL, Mendes S, Correia JPS, Lemos MFL, Novais SC (2016) Blue sharks (*Prionace glauca*) as bioindicators of pollution and health in the Atlantic Ocean: Contamination levels and biochemical stress responses. *Science of the Total Environment* 563-564:282-292
- Ballard WW, Mellinger J, Lechenault H (1993) A series of normal stages for development of *Scyliorhinus canicula*, the Lesser Spotted Dogfish (*Chondrichthyes: Scyliorhinidae*). *Journal of Experimental Zoology* 267:318-336
- Barrera-García A, O'Hara T, Galván-Magaña F, Méndez-Rodríguez LC, Castellini JM, Zenteno-Savín T (2012) Oxidative stress indicators and trace elements in the blue shark (*Prionace glauca*) off the east coast of the Mexican Pacific Ocean. *Comparative Biochemistry and Physiology C - Toxicology and Pharmacology* 156:59-66
- Barrera-García A, O'Hara T, Galván-Magaña F, Méndez-Rodríguez LC, Castellini JM, Zenteno-Savín T (2013) Trace elements and oxidative stress indicators in the liver and kidney of the blue shark (*Prionace glauca*). *Comparative Biochemistry and Physiology A - Molecular and Integrative Physiology* 165:483-490
- Bartosz G (2003) Total antioxidant capacity. In: Spiegel HE, Nowacki G, Hsiao K-J (eds) *Advances in clinical chemistry*, vol 37. Academic press, California, USA, pp 220-272
- Boening DW (2000) Ecological effects, transport, and fate of mercury: a general review. *Chemosphere* 40:1335-1351
- Bond U, N A, Haas AL, Redman K, Schlesinger MJ (1988) Ubiquitin in stressed chicken embryo fibroblast. *Journal of Biological Chemistry* 263:2384-2388
- Boyd RS (2010) Heavy metal pollutants and chemical ecology: exploring new frontiers. *Journal of Chemical Ecology* 36:46-58
- Bradford MM (1976) A rapid and sensitive method for the quantitation of microgram quantities of protein utilizing the principle of protein-dye binding. *Analytical Biochemistry* 72:248-254
- Braune B, Chételat J, Amyot M, Brown T, Clayden M, Evans M, Fisk A, Gadenh A, Girard C, Hare A, Kirk J, Lehnher I, Letcher R, Loseto L, Macdonald R, Mann E, McMeans B, Muir D, O'Driscoll N, Poulain A, Reimer K, Stern G (2015) Mercury in the marine

- environment of the Canadian Arctic: Review of recent findings. *Science of the Total Environment* 509-510:67-90
- Caeiro S, Costa MH, Ramos TB, Fernandes F, Silveira N, Coimbra A, Medeiros G, Painho M (2005) Assessing heavy metal contamination in Sado Estuary sediment: An index analysis approach. *Ecological Indicators* 5:151-169
- Cahill AE, Aiello-Lammens ME, Fisher-Reid MC, Hua X, Karanewsky CJ, Ryu HY, Sbeglia GC, Spagnolo F, Waldron JB, Warsi O, Wiens JJ (2013) How does climate change cause extinction? *Proceedings of the Royal Society B - Biological Sciences* 280:20121890
- Cairns JJ, Heath AG, Parker BC (1975) The effects of temperature upon the toxicity of chemicals to aquatic organisms. *Hydrobiologia* 41:135-171
- Capapé C, Reynaus C, Vergne Y, Quignard J-P (2008) Biological observations on the smallspotted catshark *Scyliorhinus canicula* (Chondrichthyes: Scyliorhinidae) off the Languedocian coast (southern France, northern Mediterranean). *Pan-American Journal of Aquatic Sciences* 3:282-289
- Cheung WWL, Lam VWY, Sarmiento JL, Kearney K, Watson R, Pauly D (2009) Projecting global marine biodiversity impacts under climate change scenarios. *Fish and Fisheries* 10:235-251
- Clarkson TW, Magos L, Myers GJ (2003) The toxicology of mercury – current exposures and clinical manifestations. *New England Journal of Medicine* 349:1731-1737
- Cooper RU, Clough LM, Farwell MA, West TL (2002) Hypoxia-induced metabolic and antioxidant enzymatic activities in the estuarine fish *Leiostomus xanthurus*. *Journal of Experimental Marine Biology and Ecology* 279:1-20
- Donelson J, Munday P, McCormick M, Pankhurst N, Pankhurst P (2010) Effects of elevated water temperature and food availability on the reproductive performance of a coral reef fish. *Marine Ecology Progress Series* 401:233-243
- Dong Y, Miller LP, Sanders JG, Somero GN (2008) Heat-shock protein 70 (Hsp70) expression in four limpets of the genus *Lottia*: interspecific variation in constitutive and inducible synthesis correlates with in situ exposure to heat stress. *The Biological Bulletin* 215:173-181
- Durieux EDH, Farver TB, Fitzgerald PS, Eder KJ, Ostrach DJ (2011) Natural factors to consider when using acetylcholinesterase activity as neurotoxicity biomarker in Young-Of-Year striped bass (*Morone saxatilis*). *Fish Physiology and Biochemistry* 37:21-29

- Ellis JR, Shackley SE (1997) The reproductive biology of *Scyliorhinus canicula* in the Bristol Channel, U.K.. *Journal of Fish Biology* 51:361-372
- Ellman GL, Courtney KD, Andres V, Featherstone RM (1961) A new and rapid colorimetric determination of acetylcholinesterase activity. *Biochemical Pharmacology* 7:88-90
- Fung CN, Lam JCW, Zheng GJ, Connell DW, Monirith I, Tanabe S, Richardson BJ, Lam PK (2004) Mussel-based monitoring of trace metal and organic contaminants along the east coast of China using *Perna viridis* and *Mytilus edulis*. *Environmental Pollution* 127:203-216
- Habig WH, Pabst MJ, Jakoby WB (1974) Glutathione S-transferases. The first enzymatic step in mercapturic acid formation. *Journal of Biological Chemistry* 249:7130-7139
- Hanna J, Meides A, Zhang DP, Finley D (2007) A ubiquitin stress response induces altered proteasome composition. *Cell* 129:747-759
- He ZL, Yang XE, Stoffella PJ (2005) Trace elements in agroecosystems and impacts on the environment. *Journal of Trace Elements in Medicine and Biology* 19:125-140
- Jaishankar M, Tseten T, Anbalagan N, Mathew BB, Beeregowda KN (2014) Toxicity, mechanism and health effects of some heavy metals. *Interdisciplinary Toxicology* 7:60-72
- Jezierska B, Witeska M (2006) The metal uptake and accumulation in fish living in polluted waters. In: Twardowska I, Allen HE, Häggblom MM, Stefaniak S (eds) *Soil and Water Pollution Monitoring, Protection and Remediation*. NATO Sciences Series, vol 69. Springer, Dordrecht
- Johansson LH, Borg LA (1988) A spectrophotometric method for determination of catalase activity in small tissue samples. *Analytical Biochemistry* 174:331-336
- Jones MB (1973) Influence of salinity and temperature on the toxicity of mercury to marine and brackish water isopods (Crustacea). *Estuarine and Coastal Marine Science* 1:425-431
- Kambayashi Y, Binh NT, Asakura HW, Hibino Y, Hitomi Y, Nakamura H, Ogino K (2009) Efficient assay for total antioxidant capacity in human plasma using a 96-well microplate. *Journal of Clinical Biochemistry and Nutrition* 44:46-51
- Korbas M, MacDonald TC, Pickering I, George G, Krone P (2012) Chemical form matters: different accumulation of mercury following inorganic and organic mercury exposures in zebrafish larvae. *ACS Chemical Biology* 7:411-420
- Lawrence RA, Burk RF (1976) Glutathione peroxidase activity in selenium-deficient rat liver. *Biochemical and Biophysical Research Communications* 71:952-958

- Lesser MP (2006) Oxidative stress in marine environments: biochemistry and physiological ecology. *Annual Review of Physiology* 68:253-278
- López-Cruz RI, Dafre AL, Filho DW (2012) Oxidative stress in sharks and rays. In: D. A, Vázquez-Medina JP, Zenteno-Savín T (eds) *Oxidative stress in aquatic ecosystems*. Wiley-Blackwell, Oxford, pp 157-163
- Lürling M (2015) Infodisruption: pollutants interfering with the natural chemical information conveyance in aquatic systems In: Brönmark C, Hansson L-A (eds) *Chemical Ecology in Aquatic Systems*. pp 250-271
- MacLeod JC, Pessah E (1973) Temperature effects on mercury accumulation, toxicity and metabolic rate in Rainbow Trout (*Salmo gairdneri*). *Journal of the Fisheries Research Board of Canada* 30:485-492
- Malavasi S, Cipolatto G, Cioni C, Torricelli P, Allea E, Manciooco A, Toni M (2013) Effects of temperature on the antipredator behaviour and on the cholinergic expression in the European Sea Bass (*Dicentrarchus labrax* L.) Juveniles. *Ethology* 119:592-604
- Maulvault AL, Custódio A, Anacleto P, Repolho T, Pousão P, Nunes ML, Diniz M, Rosa R, Marques A (2016) Bioaccumulation and elimination of mercury in juvenile seabass (*Dicentrarchus labrax*) in a warmer environment. *Environmental Research* 149:77-85
- McCord JM, Fridovich I (1969) Superoxide dismutase an enzymic function for erythrocyte hemocuprein. *Journal of Biological Chemistry* 244:6049-6055
- Nagelkerken I, Munday PL (2015) Animal behaviour shapes the ecological effects of ocean acidification and warming: moving from individual to community-level responses. *Global Change Biology* 22:974-989
- Pankhurst N, Munday P (2011) Effects of climate change on fish reproduction and early life history stages. *Marine and Freshwater Research*, 62 1015-1026
- Perry AL, Low PJ, Ellis JR, Reynolds JD (2005) Climate change and distribution shifts in marine fishes. *Science* 308:1912-1915
- Pimentel MS, Faleiro F, Diniz M, Machado J, Pousão-Ferreira P, Peck MA, Pörtner H-O, Rosa R (2015) Oxidative stress and digestive enzyme activity of flatfish larvae in a changing ocean. *PLoSOne* 10:e0134082
- Pimentel MS, Faleiro F, Dionísio G, Repolho T, Pousão-Ferreira P, Machado J, Rosa R (2014) Defective skeletogenesis and oversized otoliths in fish early stages in a changing ocean. *The Journal of Experimental Biology* 217:2062-2070

- Pörtner H-O, Karl DM, Boyd PW, Cheung WWL, Lluch-Cota SEL, Nojiri Y, Schmidt DN, Zavalov PO, Alheit J, Aristegui J (2014) Ocean systems. In: Field CB, Barros VR, Dokken DJ, Mach KJ, Mastrandrea MD et al. (eds) Climate Change 2014: Impacts, Adaptation, and Vulnerability Part A: Global and Sectoral Aspects Contribution of Working Group II to the Fifth Assessment Report of the Intergovernmental Panel on Climate Change Cambridge University Press:411-484
- Pörtner H-O, Farrell AP (2008) Physiology and climate change. *Science* 322:690-692
- Pörtner H-O, Knust R (2007) Climate change affects marine fishes through the oxygen limitation of thermal tolerance. *Science* 315:95-97
- Quinn DM (1987) Acetylcholinesterase: enzyme structure, reaction dynamics, and virtual transition states. *Chemical Reviews* 87:955-979
- Rajeshkumar S, Munuswamy N (2011) Impact of metals on histopathology and expression of HSP 70 in different tissues of Milk fish (*Chanos chanos*) of Kaattuppalli Island, South East Coast, India. *Chemosphere* 83:415-421
- Repolho T, Baptista M, Pimentel MS, Dionisio G, Trubenbach K, Lopes VM, Lopes AR, Calado R, Diniz M, Rosa R (2014) Developmental and physiological challenges of octopus (*Octopus vulgaris*) early life stages under ocean warming. *Journal of Comparative Physiology B - Biochemical, Systems and Environmental Physiology* 184:55-64
- Ribeiro CAO, Guimarães JRD, Pfeiffer WC (1996) Accumulation and distribution of inorganic mercury in a tropical fish (*Trichomycterus zonatus*). *Ecotoxicology and Environmental Safety* 34:190-195
- Rosa IC, Raimundo J, Lopes VM, Brandão C, Couto A, Santos C, Cabecinhas AS, Cereja R, Calado R, Caetano M, Rosa R (2015) Cuttlefish capsule: An effective shield against contaminants in the wild. *Chemosphere* 135:7-13
- Rosa R, Paula JR, Sampaio E, Pimentel M, Lopes AR, Baptista M, Guerreiro M, Santos C, Campos D, Almeida-Val VMF (2016) Neuro-oxidative damage and aerobic potential loss of sharks under elevated CO₂. *Marine Biology* 163:119
- Rosa R, Pimentel MS, Boavida-Portugal J, Teixeira T, Trübenbach K, Diniz M (2012) Ocean warming enhances malformations, premature hatching, metabolic suppression and oxidative stress in the early life stages of a keystone squid. *PLoS ONE* 7(6): e38282
- Rosa R, Trübenbach K, Pimentel MS, Boavida-Portugal J, Faleiro F, Baptista M, Dionisio G, Calado R, Pörtner H-O (2014) Differential impacts of ocean acidification and warming

- on winter and summer progeny of a coastal squid (*Loligo vulgaris*) The Journal of Experimental Biology 217:518-525
- Sampaio E, Maulvault AL, Lopes VM, Paula JR, Barbosa V, Alves R, Pousão-Ferreira P, Repolho T, Marques A, Rosa R (2016) Habitat selection disruption and lateralization impairment of cryptic flatfish in a warm, acid, and contaminated ocean. Marine Biology 163:217
- Sloman KA (2007) Effects of trace metals on salmonid fish: The role of social hierarchies. Applied Animal Behaviour Science 104:326-345
- Somero GN (1995) Proteins and temperature. Annual Reviews of Physiology 57:43-68
- Tchounwou PB, Yedjou CG, Patlolla AK, Sutton DJ (2012) Heavy metal toxicity and the environment. In: Luch A (ed) Molecular, Clinical and Environmental Toxicology vol 101. Springer, Basel, pp 133-164
- Thomas CD, Cameron A, Green RE, Bakkenes M, Beaumont LJ, Collingham YC, Erasmus BFN, de Siqueira MF, Grainger A, Hannah L, Hughes L, Huntley B, van Jaarsveld AS, Midgley GF, Miles L, Ortega-Huerta MA, Peterson AT, Phillips OL, Williams SE (2004) Extinction risk from climate change. Nature 427:145-148
- Thomason JC, Marrs SJ, Davenport J (1996) Antibacterial and antisettlement activity of the dogfish (*Scyliorhinus canicula*) eggcase. Journal of the Marine Biological Association of the United Kingdom 76:777-792
- Tomanek L (2010) Variation in the heat shock response and its implication for predicting the effect of global climate change on species' biogeographical distribution ranges and metabolic costs. Journal of Experimental Biology 213:971-979
- Tomanek L (2011) Environmental proteomics: changes in the proteome of marine organisms in response to environmental stress, pollutants, infection, symbiosis, and development. Annual Review of Marine Science 3:373-399
- Uchiyama M, Mihara M (1978) Determination of malonaldehyde precursor in tissues by thiobarbituric acid test. Analytical Biochemistry 86:271-278
- Vélez-Alavez M-, Labrada-Martagón V, Méndez-Rodríguez LC, Galván-Magaña F, Zenteno-Savín T (2013) Oxidative stress indicators and trace element concentrations in tissues of mako shark (*Isurus oxyrinchus*). Comparative Biochemistry and Physiology A - Molecular and Integrative Physiology 165:508-514

- Vergilio CS, Carvalho CEV, Melo EJT (2012) Accumulation and histopathological effects of mercury chloride after acute exposure in tropical fish *Gymnotus carapo*. *Journal of Chemical and Health Risks* 2:1-8
- Wang L, Groves MJ, Hepburn MD, Bowen DT (2000) Glutathione S-transferase enzyme expression in hematopoietic cell lines implies a differential protective role for T1 and A1 isoenzymes in erythroid and for M1 in lymphoid lineages. *Haematologica* 85 573-579
- Williams JH, Petersen NS, Young PA, Stansbury MA, Farag AM, Bergman HL (1996) Accumulation of hsp70 in juvenile and adult rainbow trout gill exposed to metalcontaminated water and/or diet. *Environmental Toxicology and Chemistry* 15 1324-1328

6

Ocean acidification dampens physiological stress response to warming and contamination in a commercially-important fish (*Argyrosomus regius*)

Eduardo Sampaio^{1#*}, Ana R Lopes^{1,2#}, Sofia Francisco¹, Jose R Paula¹, Marta Pimentel¹, Ana L Maulvault^{1,3,4}, Tiago Repolho¹, Tiago F Grilo¹, Pedro Pousão-Ferreira³, António Marques^{3,4}, Rui Rosa¹

equally contributed

¹MARE- Marine Environmental Sciences Centre & Laboratório Marítimo da Guia, Faculdade de Ciências, Universidade de Lisboa, Av. Nossa Senhora do Cabo 939, 2750-374 Cascais, Portugal

²UCIBIO, REQUIMTE, Departamento de Química, Faculdade de Ciências e Tecnologia, Universidade Nova de Lisboa, Quinta da Torre, 2829-516 Caparica, Portugal

³Divisão de Aquacultura e Valorização (DivAV), Instituto Português do Mar e da Atmosfera (IPMA, I.P.), Av. Brasília, 1449-006 Lisboa, Portugal

⁴Interdisciplinary Centre of Marine and Environmental Research (CIIMAR), University of Porto, Rua das Bragas, 289, 4050-123 Porto, Portugal

Published in: Science of Total Environment (Doi: 10.1016/j.scitotenv.2017.11.059)

Abstract

Increases in carbon dioxide (CO₂) and other greenhouse gases emissions are changing ocean temperature and carbonate chemistry (warming and acidification, respectively). Moreover, the simultaneous occurrence of highly toxic and persistent contaminants, such as methylmercury, will play a key role in further shaping the ecophysiology of marine organisms. Despite recent studies reporting mostly additive interactions between contaminant and climate change effects, the consequences of multi-stressor exposure are still largely unknown. Here we disentangled how *Argyrosomus regius* physiology will be affected by future stressors, by analyzing organ-dependent mercury (Hg) accumulation (gills, liver and muscle) within isolated/combined warming ($\Delta T = 4\text{ }^{\circ}\text{C}$) and acidification ($\Delta p\text{CO}_2 = 1100\text{ }\mu\text{atm}$) scenarios, as well as direct deleterious effects and phenotypic stress response over multi-stressor contexts. After 30 days of exposure, although no mortalities were observed in any treatments, Hg concentration was enhanced under warming conditions, especially in the liver. On the other hand, elevated CO₂ decreased Hg accumulation and consistently elicited a dampening effect on warming and contamination-elicited oxidative stress (catalase, superoxide dismutase and glutathione-S-transferase activities) and heat shock responses. Thus, potentially unpinned on CO₂-promoted protein removal and ionic equilibrium between hydrogen and reactive oxygen species, we found that co-occurring acidification decreased heavy metal accumulation and contributed to physiological homeostasis. Although this indicates that fish can be physiologically capable of withstanding future ocean conditions, additional experiments are needed to fully understand the biochemical repercussions of interactive stressors (additive, synergistic or antagonistic).

Keywords: Ocean acidification, methylmercury, warming, oxidative stress, antagonistic effects, *Argyrosomus regius*

Atmospheric carbon dioxide (CO₂) concentrations have been increasing since the preindustrial era (recently surpassing 400 CO₂ µatm), and are expected to reach approximately 1000 CO₂ µatm by the year 2100 (IPCC, 2014). Moreover, conjointly with other “greenhouse” gases, increased CO₂ has triggered a continuous rise in mean ocean temperatures (nowadays increased by 0.76 °C from pre-industrial values), with predictions pointing to a further 0.3-4.8 °C increase by the end of the century (IPCC, 2014). Atmospheric CO₂ dissolves in the ocean, shifting seawater carbonate chemistry equilibrium. Carbon dioxide uptake increases hydrogen ion (H⁺) availability, leading to a concomitant decrease of 0.13-0.42 units in mean ocean pH by the year 2100, i.e. ocean acidification (IPCC, 2014). Due to naturally frequent variations in seawater physicochemical properties (e.g. upwelling events, significant carbon input from river basins), a more accentuated CO₂ input will occur in coastal areas, easily reaching pCO₂ values beyond 1500 µatm (Melzner, 2013). The combined occurrence of ocean warming and acidification imposes ecophysiological challenges to marine organisms, eliciting interactive negative effects on survival, growth and overall physiological fitness (Harvey et al., 2013; Kroeker et al., 2010; Pimentel et al., 2015).

Concurrently to ocean warming and acidification, marine biota will also deal with another major stressor: contamination. One of the most concerning and persistent metal contaminants is mercury (Hg) and its ubiquitous environmental compound, methylmercury (MeHg) (Korbas et al., 2012). Often a by-product of fossil fuel combustion and unfiltered industrial processes (e.g. chloralkaline), inorganic Hg is transported to the sediments of estuaries and coastal areas, and methylated into organic MeHg by bacteria (Dijkstra et al., 2013), augmenting Hg bioavailability, bioaccumulation and biomagnification in organisms throughout the marine food web (Campbell et al., 2005; Evers et al., 2011). In teleost fish, MeHg accumulates preferentially in soft organ tissues, producing site-specific structural and functional damage (Gonzalez et al., 2005), and comprises around 90–95% of total mercury (HgT) in the organism (Burger et al., 2003; Gray et al., 2000). Due to its high affinity for thiol groups (present in key peptides and proteins), Hg accumulation can cause deleterious effects, including physiological distress, i.e. activation of antioxidant and xenobiotic defenses (Gonzalez et al., 2005; Mieiro et al., 2010), behavioural and organ functionality impairments (Berntssen et al., 2003; Sampaio et al., 2016) and ultimately mortality (Coccini et al., 2000).

Contaminant uptake and its impacts are potentially shaped by increased temperature or CO₂ and vice-versa (Noyes et al., 2009). Specifically, interactions between temperature and heavy metal contamination influence the physiological tolerance to both stress factors (Sokolova and Lannig, 2008) while exacerbating biological responses (Dorts et al., 2014; Lapointe et al., 2011; Sappal et al., 2014). Consequently, MeHg accumulation is augmented and propagation throughout the food chain is strengthened, until metabolic thresholds are reached (Dijkstra et al., 2013). In parallel, severe acidification (pH < 7) increases metal availability (Wiener et al., 1990) and toxicity (Han et al., 2014). However, such effect may be offset by CO₂-linked decreases in mercury accumulation (Sampaio et al., 2016; Schiedek et al., 2007; Wang et al., 2017). Under environmental stress, a general deleterious biochemical pathway triggered is the formation of reactive oxygen species (ROS) in organism cells. Although there is some proof linking ROS production to hypercapnic scenarios (Pimentel et al., 2015), such is particularly true for increased temperature and mercury contamination (Berntssen et al., 2003; Portner, 2002). The presence of ROS causes ion-based protein damage and lipid peroxidation in cellular membranes, i.e. oxidative stress, from which the reactive and mutagenic compound malondialdehyde (MDA) is an end-product (Lesser, 2006). As a physiological defense response, ROS production elicits antioxidant activity in the organism. Specifically, a battery of enzymes is activated to eliminate ROS and prevent MDA build-up: superoxide dismutase (SOD), which converts superoxide (O₂⁻) into hydrogen peroxide (H₂O₂); catalase (CAT) which converts H₂O₂ into water (H₂O) and oxygen (O₂); and glutathione S-transferase (GST), which is involved in the protection against xenobiotics and linked to antioxidant defense (Lesser, 2006; Wang et al., 2000). Moreover, tissue-specific heat shock protein (Hsp70) production is also correlated with thermal stress, i.e. high temperatures (Repolho et al., 2014; Rosa et al., 2012, 2014a) and metal contamination (Rajeshkumar and Munuswamy, 2011; Williams et al., 1996). Heat shock proteins help repair, refold and eliminate damaged or denatured proteins, as well as protect and control ROS formation (Sokolova et al., 2011). Given their wide scope, these constituents of the antioxidant enzymatic and protein chaperone machineries are widely used as biomarkers in ecotoxicology to assess fish physiological stress responses (e.g. Anacleto et al., 2014; Fonseca et al., 2011; Rosa et al., 2014b; Maulvault et al. 2016).

Despite the inevitability of marine organisms having to cope with simultaneous effects of ocean warming, acidification and persistent contamination (MeHg), no studies have focused on how the interactive effects between these three stressors will challenge fish ecophysiology. The

meagre (*Argyrosomus regius*) is an oceanodromous teleost fish dispersed across the eastern Atlantic, with increasing economic value within fisheries and aquaculture activities. Due to its nearshore distribution, this species is particularly susceptible to MeHg accumulation, especially when adults migrate towards estuaries to spawn (Durrieu et al., 2005). Understanding how this commercially important species will deal with the forecasted future scenarios may provide valuable information on future stock population conditions and potential impacts on coastal food-webs. To fill these knowledge gaps, we performed a 30-day acclimation experiment under future ocean conditions, in which we investigated how interacting stressors modulate physiological impacts and elicited responses on the commercially important *A. regius*. To this end, we gauged how organ-dependent Hg accumulation (gills, liver and muscle) was modulated by warming ($\Delta T = 4\text{ }^{\circ}\text{C}$) and acidification ($\Delta p\text{CO}_2 = 1100\text{ }\mu\text{atm}$), and measured the direct consequences of isolated and combined stressor exposure at organism (survival rates and condition index) and cellular (lipid peroxidation, i.e. MDA) levels. Moreover, in order to provide a comprehensive depiction of physiological state, the phenotypic responses of antioxidant enzymatic (SOD, CAT and GST) and molecular chaperone (Hsp70) machineries were also evaluated.

6.1. Material and Methods

6.1.1. Experimental setup and incubation

Juvenile *A. regius* ($n \approx 100$) (mean \pm SD; total weight: $4.26 \pm 2.8\text{ g}$; total length: $6.30 \pm 1.2\text{ cm}$) were acquired from EPPO - IPMA (Estação Piloto de Piscicultura de Olhão - Instituto Português do Mar e da Atmosfera, Portugal), where standard summer season environmental parameters were maintained ($\text{pH} = 8.0$ and $19\text{ }^{\circ}\text{C}$). In August 2014, fish were transported via land for 3 hours, in tanks containing seawater and oxygen-saturated air, to the facilities of Laboratório Marítimo da Guia (LMG, MARE, Faculdade de Ciências, Universidade de Lisboa). Upon arrival, fish were randomly placed and acclimated for two weeks in twenty-four 50 l tanks ($n = 3\text{-}4$ per tank) with individual recirculating aquaculture systems (RAS) equipped with glass wool (physical filtration), bio-balls (Fernando Ribeiro Lda) and protein skimmers (biological filtration, ReefSkimPro 850, TMC Iberia), as well as additional UV disinfection (Vecton 120, TMC Iberia) to maintain superior water quality. Natural seawater was pumped directly from the ocean into an 8 m^3 storage tank, and subsequently filtered ($0.35\text{ }\mu\text{m}$ filters, Fernando Ribeiro

Lda) and UV-sterilized (Vecton600, TMC Iberia), before pumping into mixing ($n = 24$) and respective experimental ($n = 24$, 50 l) tanks/RAS. To prevent fluctuations in environmental parameters, each RAS worked as a semi-closed system, with constant low flow external water input (flux $> 2 \text{ l h}^{-1}$; 50 l tank turnover rate = 24 h). Consequently, ammonia ($\text{NH}_3/\text{NH}_4^+$), nitrite (NO_2^-) and nitrate (NO_3^-) concentrations were daily checked (Colourimetric kits, Aquamark, Germany), and kept below detectable levels (i.e. $\text{NH}_3/\text{NH}_4^+ < 0.25 \text{ mg l}^{-1}$; $\text{NO}_2^- < 0.10 \text{ mg l}^{-1}$; $\text{NO}_3^- < 0.20 \text{ mg l}^{-1}$), and salinity was kept at 35.0 ± 1.0 (V2 Refractometer, TMC Iberia, Portugal). Temperature and pH (multiparametric probe, Multi3420 SET G, WTW) were measured daily, directly in the holding tanks. Photoperiod was fixed at 12 h light : 12 h dark.

As per experimental conditions, temperature in the tanks was down-regulated using chillers ($\pm 0.1 \text{ }^\circ\text{C}$, Frimar, Fernando Ribeiro Lda), and up-regulated by submerged 200 W heaters (V2Therm, TMC Iberia). Seawater carbonate chemistry was altered through CO_2 -enriched air input, with pH (8.0 and 7.5) used as proxy measurement. We used a Profilux system (± 0.1 , Profilux 3.1N, GHL) as pH controller, connected to each tank by individual pH probes. Within each RAS, pH was down-regulated by injection of certified CO_2 -enriched air (Air Liquide), and up-regulated by injection of atmospheric air. Seawater carbonate system speciation (Table S1) was calculated once every week from $\text{pH}_{\text{total scale}}$ (pH_T) and total alkalinity. pH_T was quantified via a Metrohm pH meter (826 pH mobile, Metrohm, Filderstadt, Germany) connected to a glass electrode (Schott IoLine, SI analytics, ± 0.001) and calibrated against TRIS-HCl (TRIS) and 2-aminopyridine-HCl (AMP; Mare, Liège, Belgium) seawater buffers (Dickson et al., 2007). Total alkalinity was measured spectrophotometrically (wavelength = 595 nm; UV-1800 Shimadzu, Japan) through base neutralization by formic acid and a pH sensitive dye (bromophenol blue), following Sarazin et al. (1999). Total dissolved inorganic carbon (C_T), pCO_2 and aragonite saturation were calculated using CO2SYS software (Lewis and Wallace, 1998), with dissociation constants from Mehrbach et al. (1973) as refitted by Dickson and Millero (1987). The non-contaminated and contaminated fish were fed similar diets, differing only on MeHg content. Contaminated diet was fortified with MeHg (inserted in the form of MeHg(II) chloride, CH_3ClHg , 99.8 %, Sigma-Aldrich, solubilized previously in ethanol). Given our dietary option, ecologically relevant MeHg concentrations (low contamination, $\sim 0.12 \text{ mg kg}^{-1}$ wet weight (ww); and high contamination, $\sim 1.6 \text{ mg kg}^{-1}$ ww) were chosen based on levels found in common juvenile *A. regius* prey species (mainly gastropods and crustaceans, particularly *Crangon crangon*) from contaminated coastal areas (Cabral and Ohmert, 2001; Cardoso et al., 2014; Nunes et al., 2008).

The pellets given to fish allocated to non-contaminated and contaminated treatments had approximately $0.06 \pm 0.01 \text{ mg kg}^{-1}$ dry weight (dw) and $8.02 \pm 0.01 \text{ mg kg}^{-1}$ dw of MeHg, respectively, which were considered to mimic concentrations found in the field (see Maulvault et al., 2016, 2017). Feed composition, manufacturing and MeHg spiking processes were executed as described by Maulvault et al. (2016). Fish were fed two to three times a day and total feed quantity provided per day was approximately 1% (standard calculation for aquaculture) of animal weight (at the end of 30 days, each fish was given approximately 0.0106 mg of HgT). Selected feed quantity also minimized food remains, which, in case of existing, were siphoned together with fish feces after feeding. Water samples were not taken as previous use of this feed showed no MeHg/Hg leakage into the water column (Maulvault et al. 2016).

After 15 days of lab acclimation (control conditions: 19°C , $\text{CO}_2 \approx 400 \text{ }\mu\text{atm}$), fish were kept during 30 days under crossed-treatments of ocean warming ($\Delta T = 4^\circ\text{C}$), acidification ($\Delta\text{pH} = 0.5$ units, i.e. $\Delta\text{pCO}_2 = 1100 \text{ }\mu\text{atm}$) and MeHg contamination (contaminated and non-contaminated) in a full-factorial design, simulating predicted “business-as-usual” scenarios for the year 2100 (IPCC, 2014; Melzner et al., 2013; Schiedek et al., 2007). The experimental setup mimicked the design elaborated by Cornwall and Hurd (Fig. 3d, 2015). More specifically, the setup was divided in eight treatments ($n = 3$ tanks per treatment): i) 19°C , $400 \text{ pCO}_2 \text{ }\mu\text{atm}$ (control conditions) and non-contaminated feed (MeHg: 0.06 mg kg^{-1} ; HgT: 0.07 mg kg^{-1}), ii) 19°C , $400 \text{ pCO}_2 \text{ }\mu\text{atm}$ and contaminated feed (MeHg: 8.02 mg kg^{-1} ; HgT: 8.28 mg kg^{-1}), iii) 19°C , $1500 \text{ pCO}_2 \text{ }\mu\text{atm}$ (control temperature and hypercapnic scenario) and non-contaminated feed (MeHg: 0.06 mg kg^{-1} ; HgT: 0.07 mg kg^{-1}), iv) 19°C , $1500 \text{ pCO}_2 \text{ }\mu\text{atm}$ and contaminated feed (MeHg: 8.02 mg kg^{-1} ; HgT: 8.28 mg kg^{-1}); v) 23°C , $400 \text{ pCO}_2 \text{ }\mu\text{atm}$ (warming and normocapnic scenario) and non-contaminated feed (MeHg: 0.06 mg kg^{-1} ; HgT: 0.07 mg kg^{-1}); vi) 23°C , $400 \text{ pCO}_2 \text{ }\mu\text{atm}$ and contaminated feed (MeHg: 8.02 mg kg^{-1} ; HgT: 8.28 mg kg^{-1}); vii) 23°C , $1500 \text{ pCO}_2 \text{ }\mu\text{atm}$ (warming and hypercapnic scenario) and non-contaminated feed (MeHg: 0.06 mg kg^{-1} ; HgT: 0.07 mg kg^{-1}); and viii) 23°C , $1500 \text{ pCO}_2 \text{ }\mu\text{atm}$ and contaminated feed (MeHg: 8.02 mg kg^{-1} ; HgT: 8.28 mg kg^{-1}).

Survival rates were monitored throughout the experiment, and after 30 days fish were measured (total length) and weighed. Health status was assessed through the widely used Fulton’s condition factor K ($n = 6-8$ per treatment), described by the following formula: $K = 100 \times (\text{Weight} / \text{Length}^3)$. Individuals were anesthetized with MS-222 and euthanized by swift spinal cord

severing. Sample tissues of three organs (muscle, liver and gills) were harvested and frozen (-80 °C) until further analysis.

6.1.2. Total mercury and Methylmercury accumulation

Methylmercury extraction from samples (fish and different feeds, $n = 3-6$) was performed as described by Scerbo and Barghigiani (1998), i.e. freeze-dried samples (~200 mg) were hydrolyzed in 10 ml of hydrobromic acid (47 % w/w, Merck), following addition of 35 ml toluene (99.8 % w/w, Merck) to allow MeHg extraction and removal with 6 ml cysteine solution (1 % L-cysteinium chloride in 12.5 % anhydrous sodium sulfate and 0.775 % sodium acetate, Merck). Afterwards, HgT (all samples) and MeHg (feed samples) were determined (10-15 mg for solids or 100-200 μl for liquids) by atomic absorption spectrometry (AAS), following EPA (2007) by means of an automatic Hg analyser (AMA 254, LECO, USA). Mercury concentrations were calculated through linear calibration (using > 5 standard concentrations), with a Hg(II) nitrate standard solution (1000 mg l^{-1} , Merck) dissolved in nitric acid (0.5 mol l^{-1} , Merck), reporting $\sim 0.01 \text{ mg kg}^{-1}$ and $\sim 0.04 \text{ mg kg}^{-1}$ as detection and quantification limits. Accuracy was further checked by analysing certified reference material DORM-4, and framing results obtained within the certified range of values (Table S2). A minimum of three measurements were performed per sample. Blanks were always tested in the same conditions as the samples and measurements were taken in triplicate. All laboratory ware was previously cleaned using nitric acid (20 % v/v) for 24h and ultrapure water, in that order. All standards and reagents were of analytical (pro analysis) or superior grade.

6.1.3. Enzymatic assays

6.1.3.1. Preparation of tissue extracts

Muscle, liver and gill samples ($n = 4-6$) were homogenized (Ultra-Turrax, Staufen, Germany) in accordance to body mass of each sample in homogenization buffer, 300 mg tissue per 1 ml phosphate buffered saline solution (PBS, pH 7.4: 0.14 M NaCl, 2.7 mM KCl, 8.1 mM Na_2HPO_4 , 1.47 mM KH_2PO_4). Homogenates were centrifuged (20 min at 14000 rpm at 4 °C) and antioxidant enzyme activities, as well as lipid peroxidation and heat shock response concentrations, quantified in the supernatant fraction. All enzyme assays were tested with

commercial enzymes obtained from Sigma rpm Aldrich (St. Louis, USA), and each sample was run in triplicate (technical replicates). The enzyme results were normalized with total protein content following the Bradford method (Bradford, 1976).

6.1.3.2. Lipid peroxides assay (malondialdehyde concentration)

As an end-product of oxidative stress, malondialdehyde (MDA) concentration was used as a proxy to assess extent of lipid peroxidation in the muscle. We used the thiobarbituric acid reactive substances (TBARS) protocol described by Uchiyama and Mihara (1978). A total of 10 μ l of each sample were added to 45 μ l of monobasic sodium phosphate buffer (50 mM), followed by addition of 12.5 μ l of sodium dodecyl sulfate (8.1%), 93.5 μ l of trichloroacetic acid (20%, pH = 3.5) and 93.5 μ l of thiobarbituric acid (1%) to each microtube. Then, 50.5 μ l of ultrapure water were added to this mixture and placed in a vortex for 30 s. A needle was used to puncture the lids and microtubes were incubated in boiling water (10 min) followed by ice cooling. Subsequently, 62.5 μ l of ultrapure water and 312.5 μ l of n-butanol pyridine (15:1, v/v) (Sigma-Aldrich, Hamburg, Germany) were added and microtubes centrifuged (5000 rpm; 5 min.). Afterwards, 150 μ l of the supernatant's reaction were introduced into a 96-well microplate in duplicate and absorbance was read at 530 nm. Lipid peroxides (i.e., MDA concentration) were determined using malondialdehyde (dimethylacetal) (MDA) (Merck, Switzerland) standards in an eight-point calibration curve (0–0.3 μ M). Results were expressed in relation to the sample total protein (nmol mg^{-1} total protein).

6.1.3.3. Catalase (CAT) activity

Catalase activity in the muscle was assessed through an adaptation of the method described by Johansson and Borg (1988). In this assay, 20 μ l of each sample, 100 μ l of 100 mM potassium phosphate and 30 μ l of methanol were added to a 96-well microplate, which was promptly shaken and incubated for 20 minutes. Afterwards, 30 μ l of potassium hydroxide (10 M KOH) and 30 μ l of purpald (34.2 mM in 0.5 M HCl) were added to each well, and the plate shaken and incubated for another 10 minutes. Subsequently, 10 μ l of potassium periodate (65.2 mM in 0.5 M KOH) was added to each well and a final incubation was performed for 5 minutes. Using a microplate reader (Asys UVM 340, Biochrom, USA), enzymatic activity was determined

spectrophotometrically at 540 nm. Formaldehyde concentration of the samples was calculated based on a calibration curve (from 0 to 75 μM formaldehyde), followed by the calculation of CAT activity for each sample, where one unit of CAT is defined as the amount that will cause the formation of 1.0 nmol of formaldehyde per minute at 25 °C. The results are expressed in relation to total protein content (nmol min mg^{-1} protein).

6.1.3.4. Superoxide Dismutase (SOD) activity

SOD activity in the muscle was determined following the nitro blue tetrazolium (NBT) method adapted from Sun et al. (1988). Superoxide radicals (O_2^-) are generated by xanthine oxidation, and simultaneous reduction of NBT to formazan. SOD competes with NBT for the dismutation of O_2^- into hydrogen peroxide (H_2O_2) and molecular oxygen, and this is used to determine enzyme activity. Briefly, the assay was performed using a 96-well microplate (Nunc-Roskilde), adding to each well 200 μl of 50 mM phosphate buffer (pH 8.0) (Sigma-Aldrich), 10 μl of 3 mM EDTA (Riedel-de Haën, Seelze, Germany), 10 μl of 3 mM xanthine (Sigma-Aldrich), 10 μl of 0.75 mM NBT (Sigma-Aldrich) and 10 μl of SOD standard or sample. Reaction began by adding 10 μl of 100 mU xanthine-oxidase (XOD, Sigma-Aldrich) and absorbance (560 nm) was recorded every 5 minutes for 25 minutes, using a plate reader (Asys UVM 340, Biochrom, USA). SOD from bovine erythrocytes (Sigma-Aldrich) was used as standard and positive control, and a negative control included all components except SOD or sample. The latter yielded a maximum threshold in absorbance, which allowed the assessment of inhibition percentage per minute (averaged from 25 minutes), which is caused by SOD activity. Thus, SOD activity percentage was expressed in % inhibition mg^{-1} of total protein.

6.1.3.5. Glutathione S-Transferase (GST) activity

GST activity in the muscle was determined according to the procedure described by Habig et al. (1974) and optimized for 96-well microplate (Sigma Technical Bulletin, GST Assay Kit CS0410). In this assay, 1-Chloro-2,4-dinitrobenzene (CDNB) is used as substrate and, upon conjugation of the thiol group of glutathione to the CDNB absorbance is proportionally increased, enabling spectrophotometric determination. The assay included 200 mM L-glutathione (reduced), 100 mM 1-chloro-2,4-dinitrobenzene (CDNB) solution and Dulbecco's PBS. Equine liver GST (Sigma-Aldrich) was used as positive control to validate the assay. Briefly,

180 μl of substrate solution were added to 20 μl sample in each well of a 96-well microplate (Nunc-Roskilde) and absorbance (at 340 nm) was registered every minute during 6 minutes, through a plate reader (Asys UVM 340, Biochrom, USA). Finally, GST activity was calculated using a molar extinction coefficient for CDNB of 5.3 ϵmM (Sigma Technical Bulletin, CS0410), as follows: $\text{GST activity} = (\Delta A_{340\text{min}} / 0.0053) \times (\text{Total volume} / \text{Sample volume}) \times \text{dilution factor}$. Results were expressed in relation to total protein of the sample ($\text{nmol min}^{-1} \text{mg}^{-1}$ total protein).

6.1.3.6. Heat shock proteins

Heat shock protein (Hsp70/Hsc70) content in the muscle, liver and gills was assessed by Enzyme-Linked Immunoabsorbent Assay (ELISA) protocol adapted from Njemini et al. (2005). Specifically, 10 μl of the supernatant was diluted in 990 μl of PBS and 50 μl of that sample were added to a 96-well microplate (Microloan 600, Greiner) and allowed to incubate overnight at 4 °C. On the next day, microplates were washed (three times) in 0.05 % PBS-Tween-20. 100 μl of blocking solution (1 % bovine serum albumin (BSA) Sigma-Aldrich) were added to each well and left to incubate for 2 h at room temperature. After washing the 96-well plates, we introduced 50 μl of 5 $\mu\text{g ml}^{-1}$ primary antibody (Mouse anti-Hsp70/Hsc70, Acris, San Diego, CA, USA), and again left incubating overnight at 4 °C. According to manufacturer details, this primary antibody (AM12032PU-N) possesses broad range reactivity, e.g. in varied fish species, making it suitable for our analysis. On the next day, the non-linked antibody was removed by washing the microplates, and 50 μl of 1 $\mu\text{g ml}^{-1}$ of the secondary antibody, antimouse IgG, Fab specific, alkaline phosphatase conjugate (Sigma-Aldrich) were added and incubated for 2 h at room temperature. After three additional washes, 100 μl of substrate (SIGMA FASTTM p-Nitrophenyl Phosphate Tablets, Sigma-Aldrich) was added to each well and incubated 10-30 minutes at room temperature. Stop solution (50 μl ; 3 N NaOH) was added in each well, and absorbance was read at 405 nm in a 96-well microplate reader (Asys UVM 340, Biochrom, USA). The amount of Hsp70/Hsc70 present in the samples was calculated from an absorbance/concentration calibration curve based on serial dilutions of purified Hsp70 active protein (Acris), ranging from 0 to 2000 ng ml^{-1} . The coefficients of variation were below 2.5% and results were expressed in relation to the sample total protein (ng mg^{-1} total protein).

6.1.4. Statistics

All statistical analyses were performed on R Studio (R Development Core Team, 2016). We used Generalized Linear Models (GLM) analysis to infer significant differences between sampled groups (see R script provided in the Supplemental Data for a step-by-step protocol). Mix models, e.g. tank as random factor, were ruled unnecessary as previous analysis (using 'lme4' and 'nlme' packages) showed no significant differences between tanks, within each group treatment, for all variables used. Best model selection fit for our data was found using the Akaike Information Criterion (AIC), a widespread indicator that balances model complexity with model quality of fitness (Quinn and Keough, 2002). Thus, models were simplified and factors that did not influence data variation were removed. Data was fitted using gaussian family and model residuals were checked for homogeneity of variances, independence and leverage to validate final models. When assumptions were not met, we turned to gamma family models to fit our data, and model validation was assessed following the same procedure. Temperature (T, 2 levels: 19 °C, 23 °C) CO₂ (CO₂, 2 levels: 400 µatm, 1500 µatm), MeHg exposure (MeHg, 2 levels: Non-contaminated, 0.06 mg kg⁻¹; Contaminated, 8.02 mg kg⁻¹) and organ tissue sampled (Tissue, 3 levels: Muscle, Gills, Liver) were generally used as explanatory variables or factors, according to each specific dependent variable. Finally, ANOVA tests were used to provide F and p values for factors with more than two levels.

6.2. Results

After 30 days of exposure, no mortalities were registered in any treatment. Moreover, Fulton condition (K) did not show any significant differences between treatments (MeHg, $p > 0.05$, GLM analysis in Table 1). Regarding total mercury (Hg) concentrations, contaminated and non-contaminated scenarios were significantly different (GLM analysis, $t = 9.079$, $p < 0.001$, see Supplemental Data) and Hg accumulation was also tissue-specific (ANOVA F test, $F = 14.015$, $p < 0.001$, see Supplemental Data). Among tissues, Hg concentration was lower in the muscle than in other organs analyzed (Muscle & Liver / Muscle & Gills, $p < 0.001$, GLM Analysis in Table 1, Figure 1a). In addition, consistent in all tissues tested, temperature and high CO₂ interactively affected MeHg accumulation (T x CO₂, $p < 0.001$ for all tissues, GLM analysis in Table 2, Figure

1b-d), showing an antagonistic relation. That is, while temperature increased Hg accumulation, this stimulating effect was offset by high CO₂.

Table 1. GLM analysis of *A. regius* Fulton's K and total mercury (HgT) concentration in tissues (3 levels within contaminated treatments: liver, muscle and gills) exposed to MeHg contamination (2 levels: non-contaminated and contaminated) for 30 days. Model formula on top, family and respective model AIC in the bottom. Est – Estimates; Std Error – Standard Error. Bold values indicate $p < 0.05$. For more details please see the R script in Supplemental Data.

GLM: Fulton's K in function of MeHg

	Est	Std Error	t value	p value
(Intercept)	1.602	0.041	39.09	0.001
MeHg	-0.072	0.057	0.057	0.213

Family = Gaussian

AIC = -8.6

GLM: HgT in function of MeHg * Tissues

	Est	Std Error	t value	p value
(Intercept)	1.576	0.082	19.11	0.001
Muscle & Gills	0.470	0.128	3.665	0.001
Muscle & Liver	0.660	0.130	5.063	0.001
Gills & Liver	0.191	0.141	1.355	0.181

Family = Gamma

AIC = 270.3

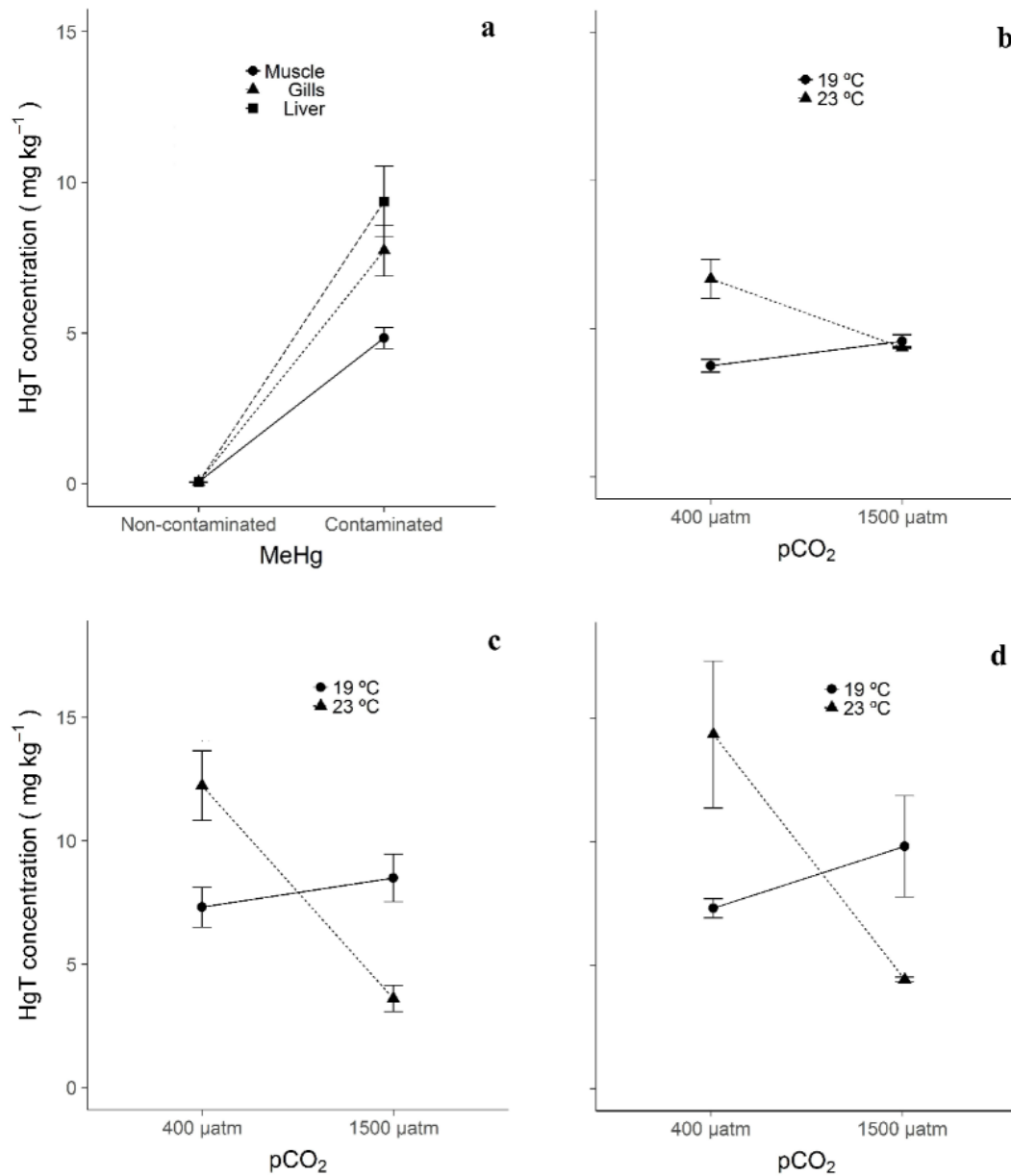


Figure 1. Total mercury (HgT) accumulation (mean \pm SE) in *A. regius*: **a**) Differences among tissues (muscle, gills and liver); and shaped by interactions between temperature (19 and 23 °C) and CO₂ (400 and 1500 μ atm) within **b**) muscle, **c**) gills and **d**) liver, respectively. Graphs were plotted according to significant factors yielded by GLM analysis described in Table 1 and 2, respectively.

Table 2. GLM analysis of total mercury concentration (HgT) within each sampled tissue (liver, muscle and gills) of *A. regius* exposed to MeHg for 30 days, under crossed treatments of temperature (T, 2 levels: 19 °C and 23 °C) and CO₂ (CO₂, 2 levels: 400 µatm and 1500 µatm). Model formula on top, family and respective model AIC in the bottom. Est – Estimates; Std Error – Standard Error. Bold values indicate $p < 0.05$. For more details please see the R script in Supplemental Data.

	<i>GLM: Liver HgT in function of T * CO₂</i>				<i>GLM: Muscle HgT in function of T * CO₂</i>				<i>GLM: Gills HgT in function of T * CO₂</i>			
	Est	Std Error	t value	p value	Est	Std Error	t value	p value	Est	Std Error	t value	p value
(Intercept)	2.287	0.151	15.18	< 0.001	1.520	0.063	24.31	< 0.001	2.059	0.125	16.74	< 0.001
T	0.794	0.261	-3.043	0.010	0.579	0.088	6.551	< 0.001	-0.917	0.191	-4.792	< 0.001
CO ₂	-0.295	0.195	-1.514	0.156	-0.201	0.088	-2.268	0.035	-0.157	0.162	-0.970	0.350
T * CO ₂	1.468	0.326	4.508	< 0.001	0.627	0.125	5.017	< 0.001	1.452	0.251	5.799	< 0.001
Family = Gamma (all)				AIC = 82.0	AIC = 59.8				AIC = 73.3			

Lipid peroxidation and oxidative stress response were measured in the muscle, the largest tissue. A significant additive effect between increasing temperature and MeHg contamination was detected, causing MDA build-up ($T \times \text{MeHg}$, $p < 0.05$, GLM analysis in Table 3, Figure 2). Regarding the antioxidant enzyme machinery response, CAT activity was only increased by MeHg contamination (MeHg, $p < 0.05$, GLM analysis in Table 4, Figure 3a). On the other hand, isolated high temperature- or CO_2 -related increases in SOD activity were reversed when both stressors co-occurred ($T \times \text{CO}_2$, $p < 0.001$, GLM analysis in Table 4, Figure 3b). Finally, GST activity was modelled by two interactions between CO_2 and temperature ($T \times \text{CO}_2$, $p < 0.05$, GLM analysis in Table 4, Figure 4a), and between CO_2 and MeHg contamination ($\text{CO}_2 \times \text{MeHg}$, $p < 0.01$, GLM analysis in Table 4, Figure 4b). In both cases, increased CO_2 inhibited GST activity when combined with warming (Figure 4a) or MeHg contamination (Figure 4b).

Table 3. GLM analysis of malondialdehyde (MDA) build-up in *A. regius* after 30 days exposed to crossed treatments of MeHg contamination (MeHg, 2 levels, non-contaminated and contaminated) and temperature (T, 2 levels: 19 °C and 23 °C). Model formula on top, family and respective model AIC in the bottom. Est – Estimates; Std Error – Standard Error. Bold values indicate $p < 0.05$. For more details please see the R script in Supplemental Data.

GLM: MDA in function of $T * \text{MeHg}$

	Est	Std Error	t value	<i>p</i>
(Intercept)	0.026	0.003	8.055	< 0.001
T	-0.010	0.005	2.163	0.036
MeHg	-0.004	0.005	0.954	0.345
$T * \text{MeHg}$	0.014	0.007	2.174	0.035

Family = Gaussian

AIC = -277.2

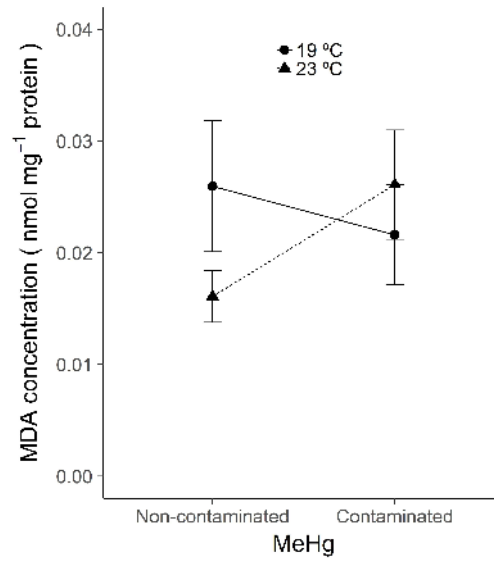


Figure 2. Malondialdehyde (MDA) build-up concentrations (mean \pm SE) in *A. regius* muscle driven by an interaction between MeHg contamination (Non-contaminated and contaminated) and temperature (19 and 23 °C). Graphs were plotted according to significant factors yielded by GLM analysis described in Table 3 and 4, respectively.

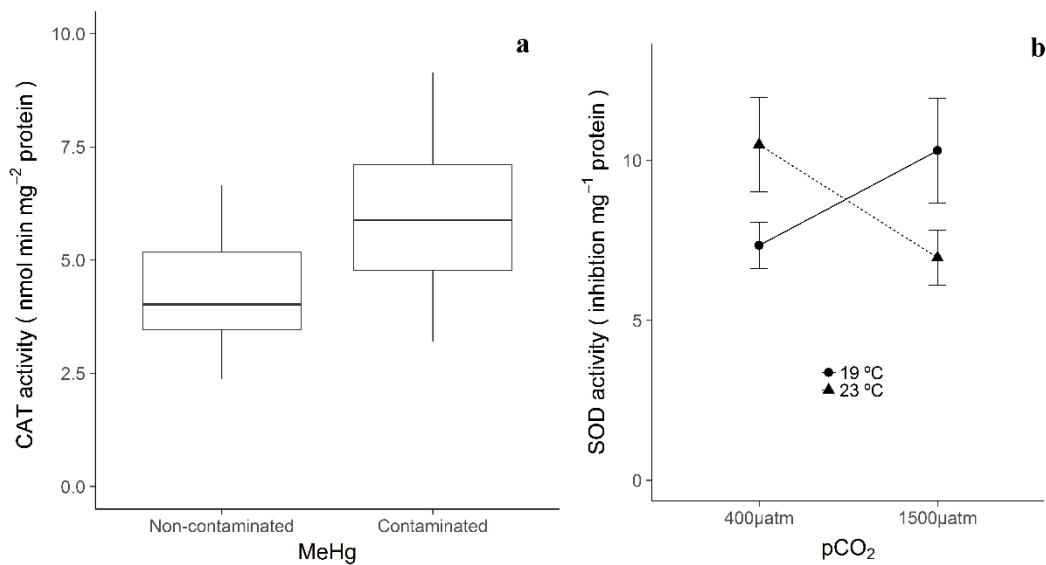


Figure 3. a) Catalase (CAT) enzyme activities (mean \pm SE) driven by MeHg contamination (Non-contaminated and Contaminated). **b)** Superoxide dismutase (SOD) activities (mean \pm SE) in *A. regius* muscle driven by an interaction temperature (19 and 23 °C) and CO₂ (400 and 1500 µatm). Graphs were plotted according to significant factors yielded by GLM analysis described in Table 4.

Table 4. GLM analysis of oxidative stress response (CAT, SOD and GST) in *A. regius* after 30 days exposed to crossed treatments of MeHg exposure (MeHg, 2 levels: non-contaminated and contaminated), temperature (T, 2 levels: 19°C and 23°C) and CO₂ (CO₂, 2 levels: 400 µatm and 1500 µatm). Model formula on top, family and respective model AIC in the bottom. Est – Estimates; Std Error – Standard Error. Bold values indicate $p < 0.05$. For more details please see the R script in Supplemental Data.

GLM: CAT in function of CO₂ * MeHg

	Est	Std Error	t value	<i>p</i>
(Intercept)	4.375	0.399	10.96	< 0.001
CO ₂	-0.454	0.564	-0.804	0.426
MeHg	1.482	0.564	2.625	0.012
CO ₂ * MeHg	1.313	0.818	1.605	0.116
Family = Gaussian				AIC = 166.2

GLM: SOD in function of CO₂ * T + CO₂ * MeHg

(Intercept)	9.496	1.040	9.135	< 0.001
T	3.346	1.200	-2.787	0.008
CO ₂	-1.264	1.484	-0.852	0.399
MeHg	1.614	1.200	1.344	0.186
T * CO ₂	6.319	1.744	3.623	< 0.001
CO ₂ * MeHg	-3.399	1.744	-1.949	0.058
Family = Gaussian				AIC = 237.3

GLM: GST in function of T * CO₂ * MeHg

(Intercept)	7.561	0.676	11.19	< 0.001
T	-1.174	0.955	-1.229	0.227
CO ₂	-2.320	0.955	-2.428	0.020
MeHg	-2.054	0.955	-2.150	0.038
T * CO ₂	4.076	1.351	3.017	0.005
T * MeHg	2.375	1.351	1.758	0.087
CO ₂ * MeHg	4.427	1.351	3.277	0.002
T * CO ₂ * MeHg	-3.422	1.970	-1.737	0.090
Family = Gaussian				AIC = 186.1

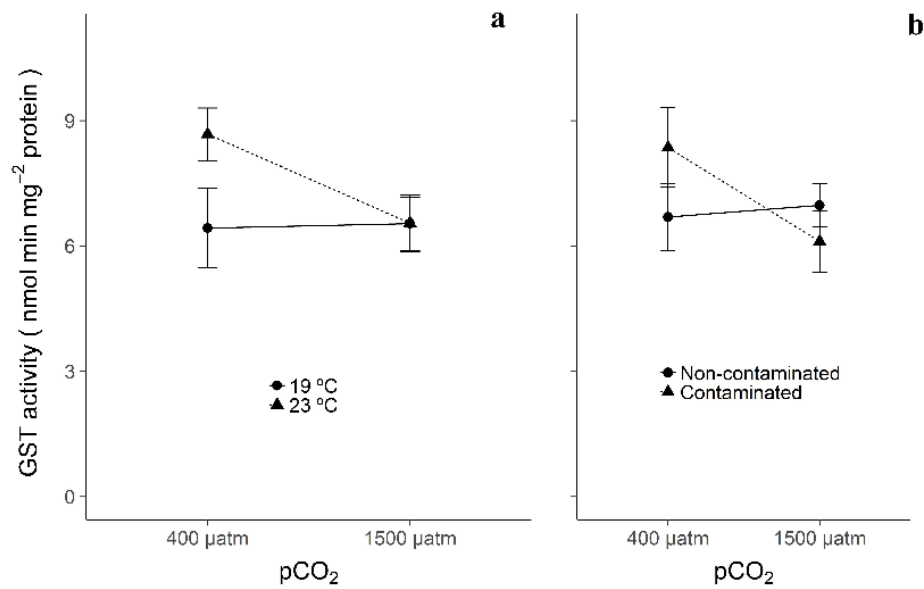


Figure 4. Glutathione S-Transferase (GST) activities (mean \pm SE) in *A. regius* muscle driven by: **a)** an interaction between temperature (19 and 23 °C) and CO₂ (400 and 1500 µatm); and **b)** an interaction between MeHg contamination (Non-contaminated and contaminated) and CO₂ (400 and 1500 µatm). Graphs were plotted according to significant factors yielded by GLM analysis (triple interaction) described in Table 4.

Heat shock response was differently affected by stressors within tissues (ANOVA F test, $F = 11.732$, $p < 0.001$, see Supplemental Data). Hsp70 production reported higher levels in the liver and lower in the gills (liver > muscle > gills; see GLM analysis in Table 5 for p values, Figure 5a). Looking at tissue-specific effects, Hsp70 concentration was positively affected by MeHg contamination within the gills (Gills, $p < 0.05$, GLM analysis in Table 5, Figure 5b). On the other hand, temperature and CO₂ interactively modulated Hsp70 production in the muscle (T x CO₂, $p < 0.001$, GLM analysis in Table 5, Figure 5c), with temperature-stimulated Hsp70 production being dampened by co-occurring high CO₂. Likewise in the liver, MeHg contamination increased Hsp70 production, but this effect was countered by increased CO₂ (CO₂ x MeHg, $p < 0.01$, GLM analysis in Table 5, Figure 5d).

Table 5. GLM analysis of heat shock protein 70 (Hsp70) production in *A. regius* tissues (gills, muscle and liver) and, posteriorly within tissues, under crossed treatments of MeHg exposure (MeHg, 2 levels, non-contaminated and contaminated), temperature (T, 2 levels: 19°C and 23°C) and CO₂ (CO₂, 2 levels: 400 µatm and 1500 µatm). Model formula on top, family and respective model AIC in the bottom. Est – Estimates; Std Error – Standard Error. Bold values indicate $p < 0.05$. For more details please see the R script in Supplemental Data.

GLM: Hsp70 in function of Tissues

	Est	Std Error	t value	<i>p</i>
(Intercept)	3.605	0.235	15.32	< 0.001
Gills & Liver	1.607	0.335	4.804	< 0.001
Gills & Muscle	0.975	0.333	2.929	0.004
Muscle & Liver	0.633	0.335	1.890	0.061
Family = Gaussian				AIC = 481.5

GLM: Gills Hsp70 in function of T + MeHg

(Intercept)	3.561	0.255	13.99	< 0.001
T	-0.530	0.299	-1.775	0.083
MeHg	0.622	0.299	2.085	0.043
Family = Gaussian				AIC = 146.4

GLM: Muscle Hsp70 in function of T * CO₂

(Intercept)	4.671	0.291	16.07	< 0.001
T	-0.294	0.411	-0.715	0.479
CO ₂	-0.955	0.411	-2.323	0.025
T * CO ₂	-2.331	0.596	3.913	< 0.001
Family = Gaussian				AIC = 137.0

GLM: Liver Hsp70 in function of T + CO₂

(Intercept)	5.376	0.593	9.064	< 0.001
CO ₂	-0.588	0.839	-0.702	0.487
MeHg	1.315	0.839	-1.567	0.125
CO ₂ * MeHg	3.627	1.235	2.938	0.005
Family = Gaussian				AIC = 73.3

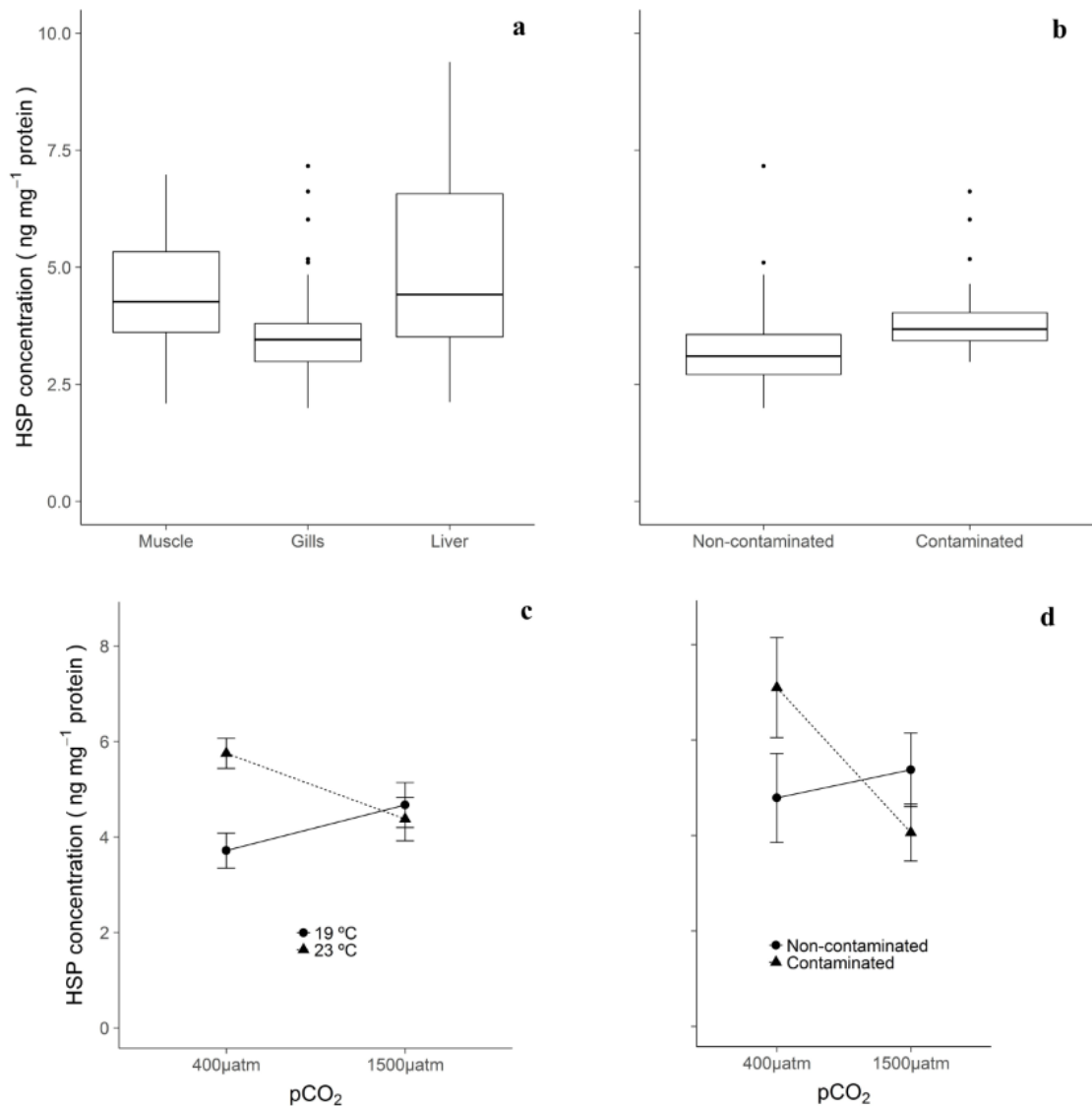


Figure 5. Heat shock protein70 (Hsp70) concentrations (mean \pm SE) in *A. regius*: **a)** tissues; **b)** in the gills shaped by MeHg contamination (Non-contaminated and Contaminated) and CO₂ (400 and 1500 μ atm); in the **c)** muscle shaped by an interaction between temperature (19 and 23 °C) and CO₂ (400 and 1500 μ atm); and in the **d)** liver shaped by an interaction between MeHg contamination (Non-contaminated and Contaminated) and CO₂ (400 and 1500 μ atm). Graphs were plotted according to significant factors yielded by GLM analysis described in Table 5.

6.3. Discussion

6.3.1. Non-lethal preferential accumulation

The present study showed that Hg contamination, ocean warming and acidification interactively affected fish physiology at sublethal levels, i.e. zero mortality and no effects on Fulton condition were registered. The fact that the meagre (*A. regius*) is a very resilient species and easily adapts to environmental change (Monfort, 2010) may explain the absence of effects at these specific levels, after a short-term acclimation.

After 30 days of exposure to MeHg contaminated feed, mean levels of Hg accumulation (HgT concentrations up to 12-13 mg kg⁻¹ dry weight) found in *A. regius* were similar to those reported in other coastal teleost fish under similar experimental conditions, such as in the temperate sole *Solea senegalensis* (Sampaio et al., 2016) and the seabass *Dicentrarchus labrax* (Maulvault et al., 2016). Affinity for metal accumulation varied between fish tissues with increasing Hg accumulation as follows: muscle < gills < liver, which is in line with previous reports on mercury tissue preferential accumulation (Gonzalez et al., 2005; Korbas et al., 2012). Specifically, due to its high lipophilicity, Hg accumulates preferentially in lipid-rich organs, such as the brain or the liver (Guzzi and La Porta, 2008). Thus, the muscle is a tissue generally characterized for its low metal affinity (Jezierska and Witeska, 2006) compared to, e.g. the liver, where metals also accumulate at higher levels, due to its key role in metal accumulation and detoxification (Gbem et al., 2001; Gonzalez et al., 2005; Wagner and Boman, 2003). Furthermore, as a consequence of increased blood supply, the gills are organs likewise known to possess higher Hg affinity than the muscle (Jezierska and Witeska, 2006; Vergilio et al., 2012).

6.3.2. Environmental influence on mercury accumulation

Mercury accumulation in fish is known to depend on the water physicochemical properties (e.g. temperature, pH, alkalinity) (Harris and Bodaly, 1998; Ponce and Bloom, 1991; Wren et al., 1991). Confirming previous reports (Dijkstra et al. 2013; Maulvault et al., 2016), our results showed a consistent increase in Hg accumulation under the warming scenario. Most likely, temperature increases Hg bioaccumulation in fish due to enhanced

metabolism and consequent higher intake of MeHg-contaminated prey (Dijkstra et al., 2013; MacLeod and Pessah, 1973). However, when both temperature and CO₂ stressors were present, Hg accumulation was decreased. Despite previous evidence that lowered pH (< 7.0 units) increases Hg accumulation in freshwater fish (Haines et al., 1992; Ponce and Bloom, 1991), the current findings do not reflect this pattern, arguably due to the magnitude of pH decrease (here we used pH 7.5). Instead, our results support recent studies demonstrating that hypercapnia dampens Hg accumulation in marine organisms (Li et al., 2017; Sampaio et al., 2016; Wang et al., 2017). There are several possible reasons which may mechanistically explain how an increase of H⁺/CO₂ could lead to slower Hg accumulation rates via digestive system, mainly encompassing direct molecular mechanisms (competition between Hg and H⁺ ions for binding sites, impacts on Hg plasma transport, lower phospholipidic membrane permeability, etc) and alterations in the digestive system (reduced digestive efficiency, reduced uptake through the gut membrane, increased Hg depuration, among others) (Li et al., 2017). Indirectly, taking into account that the occurrence of both warming and acidification changes physiological thresholds (Christensen et al., 2011; Harley et al., 2006; Rosa et al., 2013; Rosa and Seibel, 2008; Sampaio et al., 2017), a degree of metabolic depression, and consequently less feed intake, is likely to play a role in decreased HgT accumulation (Dijkstra et al., 2013; Sampaio et al., 2016). Whatever the proximate mechanisms, CO₂-decreased Hg accumulation rates (and possibly the respective toxic effects; Li et al., 2017) in a pelagic predator, may translate into lower Hg transference and overall diminished biomagnification through the trophic chain in coastal ecosystems. From a consumer perspective, the counteracting CO₂ effect (hampering warming-stimulated Hg accumulation) was consistent in the muscle, the main tissue ingested by human population. Since this is the most relevant tissue for commercialization, such results constitute an important finding in the seafood safety research area, warranting further investigation.

6.3.3. Oxidative stress under a multi-stressor environment

Exposure to MeHg contamination, ocean warming and acidification potentiated significant changes in meagre physiology. As expected from the results of previous studies in fish and other animal models (e.g. bivalves), lipid peroxidation and consequent MDA build-up was increased by the combined effects of contamination (in this case, MeHg) and

increased temperature (Lannig et al., 2006; Pimentel et al., 2015; Sokolova and Lannig, 2008). Despite the capability of *A. regius* to overcompensate for temperature-elicited ROS, the further crippling of antioxidant defenses induced by contaminants, leads to oxidative damage (Sokolova and Lannig, 2008). However, the fact that simultaneous contamination and warming elicited only a small MDA build-up relatively to what has been reported for *Salmo salar* or *Dicentrarchus labrax* (Berntssen et al., 2003; Lannig et al., 2006; Pimentel et al., 2015), may be attributed to *A. regius* being a highly resilient estuarine species, i.e. possessing great tolerance to environmental stressors (Monfort, 2010). Further proof of *A. regius* resilience can be extracted from the fact that CO₂ did not elicit MDA production, in opposition to what has been verified for other temperate and tropical fish, albeit in different life stages (Pimentel et al., 2015; Rosa et al., 2016). Moreover, to cope with oxidative stress prompted by mercury contamination and warming, *A. regius* upregulated activities of the antioxidant enzymes CAT, SOD and GST, which is in line with previous studies reporting an overall enhanced antioxidative stress response to these stressors, in coastal fish (Maulvault et al., 2017; Pimentel et al., 2015; Vieira et al., 2009). While it is worth mentioning that increased CO₂ played a minor role in CAT activity (non-significant, MeHg * CO₂ ,p = 0.116), regarding the other enzymes, hypercapnia as a sole stressor generally provoked slight increases of antioxidant activity, as has been physiologically predicted (Dean, 2010) and empirically reported in, e.g. *Solea senegalensis* (Pimentel et al., 2015). However, when combined with other stressors, elevated CO₂ antagonized the co-occurring stressor effect (i.e. contamination and/or warming). In copepods, increased CO₂ (co-occurring with Hg contamination) upregulates the lysosome-autophagy pathway, which is responsible for removing damaged proteins and organelles, and effectively reduces oxidative stress (Li et al., 2017; Wang et al., 2017). Given that lysosomes and this biochemical pathway are conserved in nearly all animal cells (e.g. Kroemer and Jäätelä, 2005), this removal mechanism can potentially be activated in teleost fish, and may contribute to alleviate not only Hg induced stress, but also warming-related oxidative stress. Moreover, this antagonistic relation can also be explained by a CO₂-related increase of H⁺ ion concentrations in the blood and cellular surroundings, counterbalanced by bicarbonate increase (acid-base compensation) to normalize pH levels (Heuer and Grosell, 2014; Michaelidis et al., 2007). By itself, the presence of excessive H⁺ ions activate free radical neutralizing defenses (Tiedke et al., 2013), which is in line with the present findings when

hypercapnia acted as a sole stressor. However, the production of O_2^- and other ROS free radicals (e.g. OH^\cdot) by other stressors may result in facilitated H_2O and H_2O_2 formation, due to chemical reactions balancing equilibrium (e.g. $H^+ + OH^- \rightleftharpoons H_2O$), thus eliminating free radicals and decreasing activity of antioxidant enzymes to basal standards.

6.3.4. Protein chaperone functioning under a multi-stressor environment

Hsp70 response was tissue-dependent, showing a pattern similar to HgT tissue preferential accumulation (liver showing higher levels, see first section), and what has been reported in other studies in marine organisms (Maulvault et al., 2017; Sokolova and Lanning, 2008). Comparatively to other tissues, high liver expression is to be expected given the fact that this organ plays a key role in metal accumulation and detoxification (Gbem et al., 2001; Wagner and Boman, 2003). Conversely, lower Hsp70 production verified in the gills may reflect the fact that exposure to contamination was not performed via water, but via feed, since this tissue is usually reactive to waterborne contaminants (see Feder and Hofmann, 1999). According to previous studies, protein chaperone functioning was activated under warming or Hg contamination, simultaneously with upregulation of antioxidant enzymes, which confirms that Hsp70 expression is closely correlated with other forms of antioxidative response (CAT, SOD, and GST) (Lesser, 2006; Iwama et al., 1998; Rosa et al., 2012, 2014a; Pimentel et al., 2015). More importantly, regarding interactions among stressors, and as observed for the antioxidant stress enzymatic machinery, hypercapnia revealed the same antagonistic relationship with other stressor's effects: increased CO_2 down-regulated heat shock response in the liver of contaminated fish and in the muscle of temperature-elevated fish. More so than for oxidative stress, the enhanced removal of damaged proteins and enzymes indirectly promoted by increased CO_2 (via up-regulated lysosome-autophagy) may have especially contributed to subside protein chaperone production. Given that Hsp70 production can also be stimulated by high ionic (e.g. H^+) concentrations (see Dean, 2010; Feder and Hofmann, 1999), we reason that the same additional mechanism by which hypercapnia potentially modulates oxidative stress can be applied for heat shock response. Enhanced CO_2 leads to increased H^+ concentration triggering physiological stress responses, while the facilitated conversion of free ions and

radicals (H^+ and O-associated molecules) into H_2O and H_2O_2 leads to reduced stress input by warming, contamination, and hypercapnia (itself). Such regulation of key components of fish physiological stress response (antioxidant and protein chaperone responses), indicates that ocean acidification potentially suppresses the deleterious effects caused by co-occurring stressors, as has been reported for other marine organisms (e.g. copepods; Li et al., 2017).

6.3.5. Conclusions

In this study, we observed that sublethal MeHg contamination is organ selective (accumulating preferentially in the liver, across the organs analyzed) and found that future abiotic conditions modulate its accumulation throughout the organism. In general, warming conditions enhanced MeHg accumulation but CO_2 -linked impacts countered this effect. Likewise, despite negative effects as a sole stressor, acidification consistently elicited antagonistic responses to temperature and contamination impacts on oxidative stress (including heat shock response). These responses are potentially underpinned on stimulated removal of damaged proteins and organelles (Wang et al., 2017), as well as by the coinciding increase of hydrogen (H^+) and reactive oxygen species (e.g. O_2^- , OH^-) due to the spontaneous equilibrium of chemical reactions (e.g. $H^+ + OH^- \rightleftharpoons H_2O$) and consequent ROS elimination. Thus, for the first time in teleost fish, we found evidence that, when co-occurring with other stressors, ocean acidification can simultaneously diminish heavy metal (Hg specifically) accumulation and its toxic effects, as well as the physiological stress response elicited by both Hg and ocean warming. Ultimately, not only may these dampening effects translate into diminished contaminant biomagnification within the trophic chain, but also contribute to balancing fish physiology and promote homeostasis.

In the future, it is important to deepen our understanding on the mechanisms underlying this antagonistic relationship between acidification and other stressors, and evaluate its presence in other species, particularly less-resilient ones. Further knowledge on climate change and contamination impacts on fish ecophysiology (specifically, biochemical stress-coping mechanisms and response-activated pathways) will help towards better comprehension of future fish stock health conditions and forecasting socio-ecological consequences in the oceans of tomorrow. Further multi-stressor studies on seafood safety and biochemical changes should follow, with the intent of assisting stakeholders and

regulatory authorities to define future consumption recommendations and preventive legislation.

6.4. Acknowledgments

We thank Kenneth Storey for the helpful discussion and IPMA-Olhão for providing juvenile meagre specimens for the trials. This work was supported by Fundação para a Ciência e Tecnologia (FCT): PhD (ES, SFRH/BD/131771/2017; ARL, SFRH/BD/97070/2013; JRP, SFRH/BD/111153/2015; ALM, SFRH/BD/103569/2014) and post-doctoral (TFG, SFRH/BPD/98590/2013; TR, SFRH/BPD/98590/2013) grants, as well as RR and AM in the framework of the IF2013 and IF2014 programs.

6.5. References

- Anacleto P, Luísa A, Lopes V M, Repolho T, Diniz M, Leonor M, Marques A, Rosa R (2014) Ecophysiology of native and alien-invasive clams in an ocean warming context. *Comparative Biochemistry and Physiology, Part A* 175:28–37
- Berntssen MHG, Aatland A, Handy RD (2003) Chronic dietary mercury exposure causes oxidative stress, brain lesions, and altered behaviour in Atlantic salmon (*Salmo salar*) parr. *Aquatic Toxicology* 65(1):55–72
- Bradford, MM (1976) A rapid and sensitive method for the quantitation of microgram quantities of protein utilizing the principle of protein-dye binding. *Analytical Biochemistry* 72:248–254
- Burger J, Dixon C, Boring S, Gochfeld M (2003) Effect of deep-frying fish on risk from mercury. *Journal of Toxicology and Environmental Health Part A* 66(9):817–828
- Cabral HN, Ohmert B (2001) Diet of juvenile meagre, *Argyrosomus regius*, within the Tagus estuary. *Cahiers de Biologie Marine* 42(3):289–293
- Cardoso PG, Pereira E, Duarte AC, Azeiteiro UM (2014) Temporal characterization of mercury accumulation at different trophic levels and implications for metal biomagnification along a coastal food web. *Marine Pollution Bulletin* 87(1):39–47
- Campbell LM, Norstrom RJ, Hobson KA, Muir DCG, Backus S, Fisk AT (2005) Mercury and other trace elements in a pelagic Arctic marine food web (Northwater Polynya, Baffin Bay). *Science of the Total Environment* 351:247–263
- Christensen AB, Nguyen HD, Byrne M (2011) Thermotolerance and the effects of hypercapnia on the metabolic rate of the ophiuroid *Ophionereis schayeri*: Inferences for survivorship in a changing ocean. *Journal of Experimental Marine Biology and Ecology* 403(1–2):31–38
- Coccini T, Randine G, Candura SM, Nappi RE, Prockop LD, Manzo L (2000) Low-level exposure to methylmercury modifies muscarinic cholinergic receptor binding characteristics in rat brain and lymphocytes: physiologic implications and new opportunities in biologic monitoring. *Environmental Health Perspectives* 108(1):29–33
- Cornwall CE, Hurd CL (2015) Experimental design in ocean acidification research: problems and solutions. *ICES Journal of Marine Sciences* 73:572–581

- Dean JB (2010) Hypercapnia causes cellular oxidation and nitrosation in addition to acidosis: implications for CO₂ chemoreceptor function and dysfunction. *Journal of Applied Physiology* 108(6):1786–95
- Dickson AG, Sabine CL, Christian JR (2007) Guide to best practices for ocean CO₂ measurements. PICES Special Publication 3
- Dickson A, Millero F (1987) A comparison of the equilibrium constants for the dissociation of carbonic acid in seawater media. *Deep Sea Research* 34:1733–1743
- Dijkstra JA, Buckman KL, Ward D, Evans DW, Dionne M, Chen CY (2013) Experimental and natural warming elevates mercury concentrations in estuarine fish. *PLoS One* 8(3):1–9
- Dorts J, Kestemont P, Thézenas M-L, Raes M, Silvestre F (2014) Effects of cadmium exposure on the gill proteome of *Cottus gobio*: Modulatory effects of prior thermal acclimation. *Aquatic Toxicology* 154:87–96
- Durrieu G, Maury-Brachet R, Girardin M, Rochard E and Boudou A (2005) Contamination by heavy metals (Cd, Zn, Cu, and Hg) of eight fish species in the Gironde estuary (France). *Estuaries*, 28(4):581–591
- EPA (2007) Method 7473 Mercury in solids and solutions by thermal decomposition, amalgamation, and atomic absorption spectrophotometry, U.S. Environmental Protection Agency
- Evers DC, Wiener JG, Basu N, Bodaly RA, Morrison HA, Williams KA (2011) Mercury in the Great Lakes region: bioaccumulation, spatiotemporal patterns, ecological risks, and policy. *Ecotoxicology* 20(7):1487–1499
- Feder ME, Hofmann GE (1999) Heat-shock proteins, molecular chaperones, and the stress response: Evolutionary and ecological physiology. *Annual Reviews in Physiology* 61:243–282
- Fonseca VF, França S, Serafim A, Company R, Lopes B, Bebianno MJ, Cabral HN (2011) Multi-biomarker responses to estuarine habitat contamination in three fish species: *Dicentrarchus labrax*, *Solea senegalensis* and *Pomatoschistus microps*. *Aquatic Toxicology* 102(3–4):216–227
- Gbem TT, Balogun JK, Lawal FA, Annune PA (2001) Trace metal accumulation in *Clarias gariepinus* (Teugels) exposed to sublethal levels of tannery effluent. *Science of the Total Environment* 271(1):1–9

- Gonzalez P, Dominique Y, Massabuau JC, Boudou A, Bourdineaud JP (2005) Comparative effects of dietary methylmercury on gene expression in liver, skeletal muscle, and brain of the Zebrafish (*Danio rerio*). *Environmental Science and Technology* 39:3972–3980
- Gray JE, Theodorakos PM, Bailey EA, Turner RR (2000) Distribution, speciation, and transport of mercury in stream-sediment, stream-water, and fish collected near abandoned mercury mines in southwestern Alaska, USA. *Science of the Total Environment* 260(1):21–33
- Guzzi G, La Porta CAM (2008) Molecular mechanisms triggered by mercury. *Toxicology* 244(1):1–12
- Habig WH, Pabst MJ, Jakoby WB (1974) Glutathione S-transferases the first enzymatic step in mercapturic acid formation. *Journal of Biological Chemistry* 249(22):7130–7139
- Han Z-X, Wu D-D, Wu J, Lv C-X, Liu Y-R (2014) Effects of ocean acidification on toxicity of heavy metals in the bivalve *Mytilus edulis* L. *Synthesis and Reactivity in Inorganic, Metal-Organic, and Nano-Metal Chemistry* 44(1):133–139
- Harley CDG, Hughes AR, Kristin M, Miner BG, Sorte CJB, Carol S (2006) The impacts of climate change in coastal marine systems. *Ecology Letters* 9:228–241
- Harris RC, Bodaly RAD (1998) Temperature, growth and dietary effects on fish mercury dynamics in two Ontario lakes. *Biogeochemistry* 40(2–3):175–187
- Harvey BP, Gwynn-Jones D, Moore PJ (2013) Meta-analysis reveals complex marine biological responses to the interactive effects of ocean acidification and warming. *Ecology and Evolution* 3(4):1016–1030
- Heuer RM, Grosell M (2014) Physiological impacts of elevated carbon dioxide and ocean acidification on fish. *AJP Regulatory, Integrative and Comparative Physiology* 307(9):R1061–R1084
- IPCC (2014) *Climate Change 2014: Impacts, Adaptation, and Vulnerability. Part A: Global and Sectoral Aspects. Contribution of Working Group II to the Fifth Assessment Report of the Intergovernmental Panel on Climate Change*, Cambridge University Press, Cambridge, United Kingdom and New York, NY, USA.
- Iwama GK, Thomas PT, Forsyth RB, Vijayan MM (1998) Heat shock protein expression in fish. *Reviews in Fish Biology and Fisheries* 8:35–36

- Jezierska B, Witeska M (2006) The metal uptake and accumulation in fish living in polluted waters, in Soil and water pollution monitoring, protection and remediation, pp. 107–114, Springer
- Johansson LH, Borg LAH (1988) A spectrophotometric method for determination of catalase activity in small tissue samples. *Analytical Biochemistry* 174(1):331–336
- Kannan K, Smith Jr RG, Lee RF, Windom HL, Heitmuller PT, Macauley JM, Summers JK (1998) Distribution of total mercury and methyl mercury in water, sediment, and fish from South Florida Estuaries. *Archives of Environmental Contamination and Toxicology* 34:109–118
- Korbas M, MacDonald TC, Pickering IJ, George GN, Krone PH (2012) Chemical form matters: differential accumulation of mercury following inorganic and organic mercury exposures in zebrafish larvae. *ACS Chemical Biology* 7(2):411–420
- Kroeker KJ, Kordas RL, Crim RN, Singh GG (2010) Meta-analysis reveals negative yet variable effects of ocean acidification on marine organisms. *Ecology Letters* 13(11):1419–34
- Kroemer G, Jäättelä M (2005) Lysosomes and autophagy in cell death control. *Nature Reviews in Cancer* 5(11):886–897
- Lannig G, Flores JF, Sokolova IM (2006) Temperature-dependent stress response in oysters, *Crassostrea virginica*: Pollution reduces temperature tolerance in oysters. *Aquatic Toxicology* 79(3):278–287
- Lapointe D, Pierron F, Couture P (2011) Individual and combined effects of heat stress and aqueous or dietary copper exposure in fathead minnows (*Pimephalespromelas*) *Aquatic Toxicology* 104(1):80–85
- Lesser MP (2006) Oxidative stress in marine environments: biochemistry and physiological ecology. *Annual Reviews in Physiology* 68(3):253–278
- Lewis E, Wallace DWR (1998) Program developed for the CO₂ system calculations, Brookhaven National Lab., Dept. of Applied Science, Upton, NY (United States); Oak Ridge National Lab., Carbon Dioxide Information Analysis Center, TN (United States), Report ORNL/CDIAC-105
- Li Y, Wang W-X, Wang M (2017) Alleviation of mercury toxicity to a marine copepod under multigenerational exposure by ocean acidification, *Scientific Reports* 7(1):324
- Maulvault AL, Custodio A, Anacleto P, Repolho T, Pousao P, Nunes ML, Diniz M, Rosa

- R, Marques A (2016) Bioaccumulation and elimination of mercury in juvenile seabass (*Dicentrarchus labrax*) in a warmer environment. *Environmental Research* 149:77–85
- Maulvault AL, Barbosa V, Alves R, Custódio A, Anacleto P, Repolho T, Pousão-Ferreira P, Rosa R, Marques A, Diniz M (2017) Ecophysiological responses of juvenile seabass (*Dicentrarchus labrax*) exposed to increased temperature and dietary methylmercury. *Science of the Total Environment* 586:551–558
- Mehrbach C, Culbertson CH, Hawley JE, Pytkowicz RM (1973) Measurement of the apparent dissociation constants of carbonic acid in seawater at atmospheric pressure, *Limnology and Oceanography* 18:897–907
- Melzner F, Thomsen J, Koeve W, Oschlies A, Gutowska MA, Bange HW, Hansen HP, Kortzinger A (2013) Future ocean acidification will be amplified by hypoxia in coastal habitats. *Marine Biology* 160(8):1875–1888
- Michaelidis B, Spring A, Pörtner H-O (2007) Effects of long-term acclimation to environmental hypercapnia on extracellular acid-base status and metabolic capacity in Mediterranean fish *Sparus aurata*. *Marine Biology* 150(6):1417–1429
- Mieiro CL, Ahmad I, Pereira ME, Duarte AC, Pacheco M (2010) Antioxidant system breakdown in brain of feral golden grey mullet (*Liza aurata*) as an effect of mercury exposure. *Ecotoxicology* 19(6):1034–1045
- Monfort MC (2010) Present market situation and prospects of meagre (*Argyrosomus regius*), as an emerging species in Mediterranean aquaculture, FAO
- Njemini R, Demanet C, Mets T (2005) Comparison of two ELISAs for the determination of Hsp70 in serum. *Journal of Immunological Methods* 306(1):176–182
- Noyes PD, McElwee MK, Miller HD, Clark BW, Van Tiem LA, Walcott KC, Erwin KN, Levin ED (2009) The toxicology of climate change: Environmental contaminants in a warming world. *Environment International* 35(6):971–986
- Nunes M, Coelho JP, Cardoso PG, Pereira ME, Duarte AC, Pardal MA (2008) The macrobenthic community along a mercury contamination in a temperate estuarine system (Ria de Aveiro, Portugal). *Science of the Total Environment* 405(1–3):186–194
- Perry SF, Walsh PJ, Mommsen TP, Moon TW (1988) Metabolic consequences of hypercapnia in the rainbow trout *Salmo airdneri*: B-adrenergic effects. *General and Comparative Endocrinology* 69:439–447

- Pimentel MS, Faleiro F, Diniz M, Machado J, Pousão-Ferreira P, Peck MA, Pörtner H-O, Rosa R (2015) Oxidative stress and digestive enzyme activity of flatfish larvae in a changing ocean. *PLoS One* 10(7):e0134082
- Ponce RA, Bloom NS (1991) Effect of pH on the bioaccumulation of low level, dissolved methylmercury by rainbow trout (*Oncorhynchus mykiss*). *Water Air Soil Pollution* 56(1):631–640
- Pörtner H-O (2002) Climate variations and the physiological basis of temperature dependent biogeography: Systemic to molecular hierarchy of thermal tolerance in animals. *Comparative Biochemistry and Physiology - A Molecular and Integrative Physiology* 132(4):739–761
- Pyle GG, Rajotte JW, Couture P (2005) Effects of industrial metals on wild fish populations along a metal contamination gradient. *Ecotoxicology and Environmental Safety* 61(3):287–312
- Quinn GP, Keough MJ (2002) *Experimental Design and Data Analysis for Biologists*, Cambridge University Press
- R Development Core Team (2016) *R: A Language and Environment for Statistical Computing*, [online] Available from: www.R-project.org
- Rajeshkumar S, Munuswamy N (2011) Impact of metals on histopathology and expression of HSP 70 in different tissues of Milk fish (*Chanoschanos*) of Kaattuppalli Island, South East Coast, India. *Chemosphere* 83(4):415–421
- Repolho T, Baptista M, Pimente, MS, Dionisio G, Trubenbach K, Lopes VM, Lopes AR, Calado R, Diniz M, Rosa R (2014) Developmental and physiological challenges of octopus (*Octopus vulgaris*) early life stages under ocean warming. *Journal of Comparative Physiology B Biochemistry, Systematics and Environmental Physiology* 184(1):55–64
- Rosa R, Seibel BA (2008) Synergistic effects of climate-related variables suggest future physiological impairment in a top oceanic predator. *Proceedings of the National Academy of Sciences* 105(52):20776–20780
- Rosa R, Pimentel MS, Boavida-Portugal J, Teixeira T, Trübenbach K, Diniz M (2012) Ocean warming enhances malformations, premature hatching, metabolic suppression and oxidative stress in the early life stages of a keystone squid. *PLoS One* 7(6):e38282–e38282

- Rosa R, Trübenbach K, Repolho T, Pimentel M, Faleiro F, Boavida-Portugal J, Baptista M, Lopes VM, Dionísio G, Leal MC, Calado R, Pörtner H-O (2013) Lower hypoxia thresholds of cuttlefish early life stages living in a warm acidified ocean. *Proceeding of the Biological Sciences* 280(1768):20131695
- Rosa R, Trübenbach K, Pimentel MS, Boavida-Portugal J, Faleiro F, Baptista M, Dionísio G, Calado R, Pörtner H-O, Repolho T (2014a) Differential impacts of ocean acidification and warming on winter and summer progeny of a coastal squid (*Loligo vulgaris*). *Journal of Experimental Biology* 217:518–25
- Rosa R, Lopes AR, Pimentel M, Faleiro F, Baptista M, Trubenbach K, Narciso L, Dionísio G, Pegado MR, Repolho T, Calado R, Diniz M (2014b) Ocean cleaning stations under a changing climate: Biological responses of tropical and temperate fish-cleaner shrimp to global warming. *Global Change Biology*., 20(10):3068–3079
- Rosa R, Paula JR, Sampaio E, Pimentel M, Lopes AR, Baptista M, Guerreiro M, Santos C, Campos D, Almeida-Val VMF, Calado R, Diniz M, Repolho T (2016) Neuro-oxidative damage and aerobic potential loss of sharks under elevated CO₂ and warming. *Marine Biology* 163(5)
- Sampaio E, Maulvault AL, Lopes VM, Paula JR, Barbosa V, Alves R, Pousão-Ferreira P, Repolho T, Marques A, Rosa R (2016) Habitat selection disruption and lateralization impairment of cryptic flatfish in a warm, acid, and contaminated ocean. *Marine Biology* 163(10):217
- Sampaio E, Rodil IF, Vaz-Pinto F, Fernández A, Arenas F (2017) Interaction strength between different grazers and macroalgae mediated by ocean acidification over warming gradients, *Marine Environmental Research* 125:25–33
- Sappal R, MacDonald N, Fast M, Stevens D, Kibenge F, Siah A, Kamunde C (2014) Interactions of copper and thermal stress on mitochondrial bioenergetics in rainbow trout, *Oncorhynchus mykiss*. *Aquatic Toxicology* 157:10–20
- Sarazin G, Michard G, Prevot F (1999) A rapid and accurate spectroscopic method for alkalinity measurements in sea water samples. *Water Research* 33(1):290–294
- Scerbo R, Barghigiani C (1998) Organic mercury determination in fish samples using an automatic mercury analyser. *Environmental Technology* 19(3):339–342
- Schiedek D, Sundelin B, Readman JW, Macdonald RW Interactions between climate change and contaminants. *Marine Pollution Bulletin* 54:1845–1856

- Sokolova I, Lannig G (2008) Interactive effects of metal pollution and temperature on metabolism in aquatic ectotherms: implications of global climate change. *Climate Research* 37:181–201
- Sokolova IM, Sukhotin AA, Lannig G (2011) Stress effects on metabolism and energy budgets in mollusks, *Oxidative Stress. Aquatic Ecosystems* 261–280
- Sun YI, Oberley LW, Li Y (1988) A simple method for clinical assay of superoxide dismutase. *Clinical Chemistry* 34(3):497–500
- Tiedke J, Cubuk C, Burmester T (2013) Environmental acidification triggers oxidative stress and enhances globin expression in zebrafish gills. *Biochemical and Biophysical Research Communications* 441(3):624–629
- Uchiyama M, Mihara M (1978) Determination of malonaldehyde precursor in tissues by thiobarbituric acid test. *Analytical Biochemistry* 86(1):271–278
- Vergilio CS, Carvalho CEV, Melo EJT (2012) Accumulation and Histopathological Effects of Mercury Chloride after Acute Exposure in Tropical Fish *Gymnotus carapo*. *Journal of Chemical Health Risks* 2(4):1–8
- Vieira LR, Gravato C, Soares AMVM, Morgado F, Guilhermino L (2009) Acute effects of copper and mercury on the estuarine fish *Pomatoschistus microps*: Linking biomarkers to behavior. *Chemosphere* 76:1416–1427
- Wagner A, Boman J (2003) Biomonitoring of trace elements in muscle and liver tissue of freshwater fish. *Spectrochimica Acta Part B Atomic Spectroscopy* 58(12):2215–2226
- Wang L, Groves MJ, Hepburn MD, Bowen DT (2000) Glutathione S-transferase enzyme expression in hematopoietic cell lines implies a differential protective role for T1 and A1 isoenzymes in erythroid and for M1 in lymphoid lineages. *Haematologica* 85(6):573–579
- Wang M, Lee J-S, Li Y (2017b) Global Proteome Profiling of a Marine Copepod and the Mitigating Effect of Ocean Acidification on Mercury Toxicity after Multigenerational Exposure. *Environmental and Science Technology* 51:5820–5831
- Wiener JG, Fitzgerald WF, Watras CJ, Rada RG (1990) Partitioning and bioavailability of mercury in an experimentally acidified wisconsin lake. *Environmental Toxicology and Chemistry* 9:909–918
- Williams JH, Petersen NS, Young PA, Stansbury MA, Farag AM, Bergman HL (1996) Accumulation of hsp70 in juvenile and adult rainbow trout gill exposed to metal-

contaminated water and/or diet. *Environmental Toxicology and Chemistry* 15(8):1324–1328

Wren CD, Scheider WA, Wales DL, Muncaster BW, Gray IM (1991) Relation between mercury concentrations in walleye (*Stizostedion vitreum vitreum*) and northern pike (*Esox lucius*) in Ontario lakes and influence of environmental factors. *Canadian Journal of Fisheries and Aquatic Science* 48(1):132–139

7

General Discussion

The present thesis entails a comprehensive and comparative analysis of the biochemical strategies, encompassing the antioxidant defense mechanisms - both enzymatic and non-enzymatic antioxidants - as well as the protein repair and removal mechanisms, of marine organisms - octocorals, amphipods, teleost and elasmobranch fishes - to climate change-related variables, such as ocean warming and/or acidification, as well as the combination with contamination (see main results showed in summary table I).

It is widely known that the tolerance towards climate change-related stressors is species-specific, thus it is utterly important to understand the biochemical mechanisms of marine organisms - encompassing different life stages (i.e. new-born, juvenile, adult) and life strategies - to accurately predict those effects on marine communities, and ultimately the whole marine biodiversity.

7.1. Biochemical responses under a multi-stressor environment

Ocean warming and acidification are among the most significant environmental challenges to which marine organisms will be exposed in the ocean of tomorrow (Pörtner et al. 2014). Additionally, and allied to these challenges growing human pressures are also causing seawater contamination, increasing organisms' susceptibility and limiting their stress tolerance (Bryan and Darracott 1979; Clarkson et al. 2003; Fung et al. 2004; Holmstrup et al. 2010; Tchounwou et al. 2012). When exposed to increasing temperatures and decreased pH marine organisms need to perform metabolic adjustments in order to maintain the acid-base balance and consequently optimal cell functioning, to avoid potential noxious cascading effects on their fitness responses (i.e. growth, development and reproduction) (Pimentel et al. 2015; Rosa et al. 2016; 2012).

The results obtained in the present dissertation showed that single effects of warming and acidification are usually responsible for the burst in ROS production, ultimately causing oxidative stress, through increased enzymatic activity and protein repair mechanisms activation, with the latter responding primarily to increasing temperatures

than to ocean acidification. Nonetheless this upsurge in the biochemical defense mechanisms were usually ineffective in avoiding oxidative damage through lipid, protein (either measure directly through PC or indirectly via Ub levels) and nucleic acid damage. Specifically, warming was responsible for the activation of the HSR, via increased HSP production, which play an important role in thermotolerance, by helping to maintain optimal protein function and conformation (Tomanek 2010).

The negative effects of OA are usually related to increasing H^+ ions availability. Directly through H^+ interaction with ROS (i.e. O_2^-), that will in turn generate H_2O_2 , that can be further reduced, through Fenton reaction into OH^\bullet - the most damaging of ROS - or through the reaction of molecular CO_2 with RNS, such as peroxynitrite, that often results into nitro-oxidative reactions (Tiedke et al. 2013). Furthermore, intracellular H^+ ions are also causing intracellular acidosis, which will in turn affect pH-dependent protein function. Thus, and even though this increases in ROS production are followed by increased protective mechanisms, they do not seem to be efficient in avoiding oxidative stress and consequently damage.

However, when the abovementioned stressors acted synergistically, those effects seemed to be reversed, specifically elevated CO_2 usually dampens the effect of the co-occurring stressor effect (i.e. warming). This “buffer” effect can be explained by the elimination of ROS produced by warming (e.g. O_2^- and OH^\bullet), via chemical reactions balancing equilibrium, through the conversion of H^+ and OH^\bullet into H_2O , thus eliminating free radicals and decreasing the enzymatic activity to basal standards, ultimately culminating into decreased cellular damage (Dean 20010; Heuer and Grosell 2014; Li et al. 2017).

Regarding contamination, it played a minor role as a sole stressor when compared with the abovementioned stressors. In fact, and even though Hg contamination - either administered via feed (i.e. MeHg) or dissolved in seawater (i.e. $HgCl_2$) - resulted in increased enzymatic activity, it did not seem to cause any sort of oxidative damage (i.e. lipid or DNA damage). Additionally, we also observed that the affinity for metal accumulation is tissue-specific, accumulating preferentially in lipid-rich organs such as the liver for *A. regius*. With an important role in metal metabolism and excretion, the liver is more prone to accumulate organic Hg (i.e. MeHg), contributing for metal biomagnification through the food chain (Gonzalez et al. 2005; Jezierska and Witeska 2006; Vergilio et al. 2012). Furthermore, the highest Hg concentration in *S. canicula* embryo was found in the gills, the main organ for

inorganic Hg (i.e. HgCl_2) entry in the body, once the contaminated water is directly pumped over the gills (Cairns et al. 1975; Jezierska and Witeska 2006).

Increasing temperatures enhanced Hg accumulation in *A. regius* tissues. Even though we could not measure Hg accumulation in *S. canicula* embryos exposed to high temperatures, the elevated mortality rate observed under the combination of stressors (i.e. warming and Hg) leads us to assume that increasing temperatures are also increasing Hg toxicity, as already stated in previous works (Boening 2000; Cairns et al. 1975; MacLeod and Pessah 1973; Maulvault et al. 2017). We reason that temperature increases Hg bioaccumulation in marine organisms due to enhanced metabolism (increasing inorganic Hg diffusion through the gills) and higher intake of MeHg-contaminated prey (Dijkstra et al. 2013; MacLeod and Pessah 1973). Nonetheless, when both temperature and CO_2 were present, Hg accumulation decreased, demonstrating that hypercapnia - as observed when combined with temperature - is also dampening Hg accumulation in marine organisms, as proven in recent studies (Li et al., 2017; Sampaio et al., 2016; Wang et al., 2017). The slower MeHg accumulation in *A. regius* can be explained through: i) the direct competition between Hg and H^+ ions for binding sites; ii) the loss of membrane permeability; and iii) alterations in the digestive system (reduced digestive efficiency, increased Hg depuration, etc.) (Li et al., 2017). Furthermore, and taking into account that the simultaneous exposure to OW and OA is expected to change organisms' physiological thresholds (Christensen et al., 2011; Harley et al., 2006; Rosa et al., 2013; Rosa and Seibel, 2008; Sampaio et al., 2017), decaying metabolic processes (i.e. metabolic depression), and consequently less feed intake (due to slow metabolism), is also likely to play a key-role in decreased Hg accumulation (Dijkstra et al. 2013; Sampaio et al. 2016). Taking into account the results obtained in the present dissertation and considering that Hg toxicity and availability are more likely to increase under OW conditions, we argue that the legal Hg levels allowed in sewage discharges should be reconsidered, and that stakeholders and regulatory authorities should also define future consumption recommendations and preventive legislation.

Table I- Summary of the major findings in the present dissertation (n.a. – not available)

					 <i>Veretillum cynomorium</i>	 <i>Gammarus locusta</i>	 <i>Argyrosomus regius</i>	 <i>Scyliorhinus canicula</i>	 <i>Chiloscyllium plagiosum</i>
					F0	F1			
Antioxidant Defense	SOD	n.a.	n.a.	n.a.	=	↑	↑ = = ↓ = = =	↑ ↓	=
	CAT	=	=	=	=	=	= = ↑ = = = =	= ↓	=
	GPx	n.a.	n.a.	n.a.	↑	↑	n.a. n.a. n.a. n.a. n.a. n.a. n.a.	↑ =	↓
	GST	=	=	=	=	=	= ↓ ↑ ↓ = ↓ =	↑ =	n.a.
	Aconitase	n.a.	n.a.	n.a.	n.a.	n.a.	n.a. n.a. n.a. n.a. n.a. n.a. n.a.	n.a. n.a.	=
	AChE	n.a.	n.a.	n.a.	n.a.	n.a.	n.a. n.a. n.a. n.a. n.a. n.a. n.a.	↑ ↓	n.a.
	TAC	n.a.	n.a.	n.a.	↑	=	n.a. n.a. n.a. n.a. n.a. n.a. n.a.	= =	↑
Protein Repair/ Removal	HSP	↑	=	=	=	=	= = = ↓ = ↓ =	↑ =	↓
	Ub	n.a.	n.a.	n.a.	↑	=	n.a. n.a. n.a. n.a. n.a. n.a. n.a.	↑ ↑	↑
Oxidative Damage	LPO	=	=	=	=	=	↓ = = = ↑ = =	↑ =	=
	PC	n.a.	n.a.	n.a.	n.a.	n.a.	n.a. n.a. n.a. n.a. n.a. n.a. n.a.	n.a. n.a.	=
	DNA	n.a.	n.a.	n.a.	=	↑	n.a. n.a. n.a. n.a. n.a. n.a. n.a.	= =	↑

7.2. Biochemical responses across taxa

Understanding the ability of species to cope with climate-related stressors is of upmost concern if we ought to predict phenology and biogeography, as well as extinction rates of marine organisms (Parmesan 2006; Perry et al. 2005; Thomas et al. 2004). The findings of the present dissertation showed that species inhabiting highly variable environments in terms of abiotic parameters (i.e. temperature, salinity, oxygen, etc.) – e.g. temperate intertidal zone and estuaries – have usually a broader tolerance to climate change-related conditions than organisms occupying relatively more stable environments – e.g. tropical waters (Stillman 2003; Tewksbury et al. 2008; Tomanek 2014; Wright et al. 2009). This is mainly due to the fact that the former usually induces their antioxidant defense systems and HSR more frequently, to respond to the range of abiotic stressors that they usually experience on a daily basis. For example, in Chapter 4 we found that the octocoral *V. cynomorium*, which is usually found in coastal shallow habitats, subject to daily fluctuation in abiotic parameters, are usually equipped with a powerful defence mechanism⁸ – HSR and antioxidant responses - that allow them to avoid oxidative damage under stressful conditions (i.e. emersion-immersion, across thermal gradients) (Madeira et al. 2015; Teixeira et al. 2013). Thus, and contrarily to reef-building corals, that have shown to be particularly sensitive to climate-induced changes (Baker et al. 2008; Downs et al. 2002; Glynn 1996; Pandolfi et al. 2011), it seems that this anticipatory mechanisms found in *V. cynomorium* play also a crucial role in defining its resilience towards OW and OA. Additionally, and contrarily to hard corals, *V. cynomorium* instead of an external calcium carbonate body, it has a central calcite skeleton covered by an external tissue that may act as a physical barrier against decreased seawater pH, thus helping the species to be more resilient towards the chemical chain of reactions under hypercapnic scenarios (i.e. reduced carbonate ions).

In fact, and when considering marine calcifying organisms such as the amphipod *G. locusta* (Chapter 3), the predicted increase of ROS and RNS with OA (as explained in the previous section) seemed to overwhelm amphipod antioxidant machinery, increasing GPx and TAC levels, nonetheless insufficient in circumventing protein damage. Specifically, high levels of H⁺ ions (due to ocean acidification) are expected to cause intracellular acidosis, which could ultimately

⁸ Also known as the preparation for oxidative stress (POS), first proposed by Hermes-Lima et al. (1998), and proved for this species by Teixeira et al. (2013)

affect cytoskeleton-related proteins (i.e. proteins responsible for cell structure) (Dean 20010; Tomanek et al. 2011).

Following the line of thought that marine organisms inhabiting highly variable environments are predicted to perform better in relation to abiotic variables, in Chapter 6, we also found that *A. regius* tolerance towards OW and OA conditions, as well as Hg contamination, is most likely based on its estuarine life habitat (Monfort 2010), which confers greater tolerance for climate-induced changes when compared with other temperate and tropical fish species (e.g. Pimentel et al. 2015; Rosa et al. 2016).

Nonetheless, and even though marine tropical species are known to be at a greater risk than their congeneric species in temperate environments, it does not seem to be the case of the tropical whitespotted bamboo shark (*C. plagiosum*, Chapter 2). In fact, newly-hatched *C. plagiosum* seemed to be resilient to OA-induced ROS due to their conserved antioxidant systems based on non-enzymatic antioxidants. Indeed, the antioxidant system of marine organisms can be associated with their phylogenetic position in the tree of life (Rudneva 1997). Thus, ancient cartilaginous fishes' have antioxidant systems strongly based on molecular-based antioxidants, such as urea, ascorbic acid and TMAO, while relatively newly evolved teleost fishes possess an enzyme-based antioxidant system (Filho and Boveris 1993; Solé et al. 2009). Furthermore, and considering the negative effects of elevated CO₂ in some teleost fishes (Baumann et al. 2012; Pimentel et al. 2014; Stiasny et al. 2016), the findings presented in Chapter 2 could suggest that molecules rather than complex enzymatic proteins) are more effective in dealing with OA-elicited ROS formation, at least in elasmobranch species.

Marine organisms defense mechanisms are species-specific and dependent upon individual life-stage and life-strategy, as well as the stressor to which they are exposed. Therefore, and even though OA seems to play a minor role in instigating oxidative damage (only observed increased DNA damage within the liver) in *C. plagiosum* offspring, exposure to warming and inorganic Hg (i.e. HgCl₂) contamination resulted in 100% mortality in *S. canicula* embryos after 6-days exposure. Unfortunately, the high mortality observed under these conditions hinder us to quantify the Hg concentration, as well as the defense mechanisms of those embryos. Nonetheless, we assume that the great sensitivity of embryos and larval stages to HgCl₂ toxicity (Boening 2000), may be further exacerbated with increasing temperatures due to increased metabolic demand, which will in turn increase Hg uptake and accumulation (Jezierska and Witeska 2006; MacLeod and Pessah 1973; Maulvault et al. 2016). Furthermore, while looking into the individual

contribution of each stressor, OW played a major role in triggering the antioxidant defense mechanisms (i.e. antioxidant enzymes and HSR), when compared with contamination, however it was insufficient to avoid protein (i.e. indirectly quantified via Ub levels) and lipid damage. Additionally, the minor role of Hg contamination in *S. canicula* embryos (i.e. absence of LPO and DNA damage) could be related to the fact that sharks' capsule retained the largest Hg concentration, possibly suggesting a potential protective role towards metal contamination.

7.3. Within- and trans-generational biochemical responses

Over the last few decades there has been an increasing interest to understand the effects of climate change on marine organisms. Nonetheless, the bulk of these studies focus mainly on those effects during a single lifetime - i.e. within-generation effects (Dupont and Portner 2013; Michaelidis et al. 2007; Orr et al. 2005; Rosa et al. 2017), while the transgenerational effects have received less attention. Furthermore, to the best of our knowledge, none have evaluated the carry-over effects on the organisms' defense mechanisms after parenting conditioning to the upcoming conditions.

To that end, in the present dissertation, we evaluated the biochemical responses of the amphipod *G. locusta* to a future acidified ocean over two generations (F0 and F1). As abovementioned, OA conditions are expected to overwhelm *G. locusta* antioxidant machinery, culminating into protein damage in the parent generation. Thus, and considering the findings present in Chapter 3, it seems that the negative effects of OA are potentially being inherited by the offspring. Specifically, the oxidative stress imposed in the parent proteome - i.e. decreased HSP and increased Ub levels - is probably confining the efficiency of the DNA repair proteome (i.e. damaging key proteins that act in order to avoid DNA strand breaks or base pair mismatch) (Hoeijmakers 2003; Sejersted et al. 2011). Therefore, we reason that the oxidative stress imposed in the parents' proteome could have induced negative parental effects, impairing the offspring capacity of genome repair and replication, thus increasing *G. locusta* vulnerability towards OA. Furthermore, and if we combine the present findings to the information that marine calcifying organisms are one of the most sensitive to OA (Michaelidis et al. 2005a; Michaelidis et al. 2005b; Orr et al. 2005), it is expected that the capacity of subsequent generations to endure in such harsh environment might be compromised.

7.4. Final Remarks

The findings of the present dissertation provide valuable insights on how marine organisms will respond to the foreseen warming and acidification conditions. Specifically, the present work is the first addressing a comparative analysis of the biochemical strategies developed by marine organisms, across taxa – from invertebrate to vertebrate species– to face climate change-related variables.

In conclusion, organisms' response was mostly underpinned by temperature, either by acting as a sole stressor or in combination with Hg contamination, while ocean acidification as a sole stressor usually played a minor role in defining species vulnerability, being responsible for increased oxidative stress, especially in marine calcifying organisms (i.e. *G. locusta*). Nonetheless when co-occurring with warming and contamination scenarios, hypercapnia was usually responsible for: i) reduction of heavy metal accumulation and toxicity; and ii) diminished physiological stress response elicited by both Hg and warming.

Marine organism's responses were species-specific, with organisms typical of variable environments (i.e. in terms of abiotic conditions) being more tolerant towards environmental change - absence of oxidative damage - than organisms that usually inhabit more stable environments. Additionally, early life stages seem to be more vulnerable to environmental stress, especially those that use coastal areas as nursery, and with long embryonic development. But again, we should bear in mind that species responses are dependent upon the (magnitude of the) stressor to which they are exposed to. Moreover, those responses are also reliant on the individuals life-stage that may play a major role in defining species vulnerability – i.e. even though sharks species seem to bear a powerful non-enzymatic antioxidant system, it seems that shark embryos are at a greater risk than new-born. Furthermore, transgenerational studies are extremely important if we ought to have a more reliable analysis of the marine organisms' response in the ocean of tomorrow.

7.5. Future Directions

As reinforced by this dissertation, unraveling the biochemical responses of marine organisms is unquestionably important in order to better understand the processes occurring

throughout different trophic levels and ultimately the whole marine ecosystem functioning. In a constantly changing ocean it is of utmost importance to understand how marine biota will respond across all levels of organization, nonetheless in most cases the molecular challenges of marine organisms remain unknown. Furthermore, trans- and multi-generational studies to understand the biochemical responses of marine organisms are of utmost concern to understand how parental conditioning could affect future generations, and if it will be translated into positive or negative carry-over effects, and to infer the resilience of the upcoming generations. Additionally, ocean warming and acidification are just two pieces of a bigger picture. In a future ocean, marine organisms will also have to deal with low oxygen availability (i.e. hypoxia) - increasing ocean stratification and expansion of OMZs - which is also responsible for increased ROS and consequently damage.

7.6. References

- Baker AC, Glynn PW, Riegl B (2008) Climate change and coral reef bleaching: An ecological assessment of long-term impacts, recovery trends and future outlook. *Estuarine, Coastal and Shelf Science* 80:435-471
- Boening DW (2000) Ecological effects, transport, and fate of mercury: a general review. *Chemosphere* 40:1335-1351
- Bryan GW, Darracott A (1979) Bioaccumulation of marine pollutants. *Philosophical Transactions of the Royal Society B* 286:483-505
- Cairns JJ, Heath AG, Parker BC (1975) The effects of temperature upon the toxicity of chemicals to aquatic organisms. *Hydrobiologia* 41:135-171
- Clarkson TW, Magos L, Myers GJ (2003) The toxicology of mercury – current exposures and clinical manifestations. *New England Journal of Medicine* 349:1731-1737
- Dean JB (2010) Hypercapnia causes cellular oxidation and nitrosation in addition to acidosis: implications for CO₂ chemoreceptor function and dysfunction. *Journal of Applied Physiology* 108 1786-1795
- Dijkstra JA, Buckman KL, Ward D, Evans DW, Dionne M, Chen CY (2013) Experimental and natural warming elevates mercury concentrations in estuarine fish. *PLoSOne* 8:e58401
- Downs CA, Fauth JE, Halas JC, Dustan P, Bemiss J, Woodley CM (2002) Oxidative stress and seasonal coral bleaching. *Free Radical Biology and Medicine* 33:533-543
- Dupont S, Portner H (2013) Marine science: Get ready for ocean acidification. *Nature* 498:429-429
- Fung CN, Lam JC, Zheng GJ, Connell DW, Monirith I, Tanabe S, Richardson BJ, Lam PK (2004) Mussel-based monitoring of trace metal and organic contaminants along the east coast of China using *Perna viridis* and *Mytilus edulis*. *Environmental Pollution* 127:203-216
- Glynn PW (1996) Coral reef bleaching: facts, hypotheses and implications. *Global Change Biology* 2:495-509
- Gonzalez P, Dominique Y, Massabuau JC, Boudou A, Bourdineaud JP (2005) Comparative effects of dietary methylmercury on gene expression in liver, skeletal muscle, and brain of the zebrafish (*Danio rerio*). *Environmental Science and Technology* 39:3972-3980

- Hermes-Lima M, Storey JM, Storey KB (1998) Antioxidant defenses and metabolic depression. the hypothesis of preparation for oxidative stress in land snails. *Comparative Biochemistry and Physiology, Part B: Biochemistry and Molecular Biology* 120:437-448
- Heuer RM, Grosell M (2014) Physiological impacts of elevated carbon dioxide and ocean acidification on fish. *American Journal of Physiology Regulatory, Integrative and Comparative Physiology* 307:R1061-1084
- Hoeijmakers JHJ (2003) DNA Damage, Aging, and Cancer. *New England Journal of Medicine* 361:1475-1485
- Holmstrup M et al. (2010) Interactions between effects of environmental chemicals and natural stressors: A review. *Science of the Total Environment* 408:3746-3762
- Jezierska B., Witeska M. (2006) The metal uptake and accumulation in fish living in polluted waters. In: Twardowska I., Allen H.E., Häggblom M.M., Stefaniak S. (eds) *Soil and Water Pollution Monitoring, Protection and Remediation*. NATO Science Series, vol 69. Springer, Dordrecht
- Li Y, Wang W-X, Wang M (2017) Alleviation of mercury toxicity to a marine copepod under multigenerational exposure by ocean acidification. *Scientific Reports* 7:324
- MacLeod JC, Pessah E (1973) Temperature effects on mercury accumulation, toxicity and metabolic rate in Rainbow Trout (*Salmo gairdneri*). *Journal of the Fisheries Research Board of Canada* 30:485-492
- Madeira C, Madeira D, Vinagre C, Diniz M (2015) Octocorals in a changing environment: Seasonal response of stress biomarkers in natural populations of *Veretillum cynomorium*. *Journal of Sea Research* 103:120-128
- Michaelidis B, Haas D, Grieshaber MK (2005a) Extracellular and intracellular acid-base status with regard to the energy metabolism in the oyster *Crassostrea gigas* during exposure to air. *Physiological and Biochemical Zoology* 78:373-383
- Michaelidis B, Ouzounis C, Palaras A, Pörtner HO (2005b) Effects of long-term moderate hypercapnia on acid-base balance and growth rate in marine mussels *Mytilus galloprovincialis*. *Marine Ecology Progress Series* 293:109-118
- Michaelidis B, Spring A, Portner HO (2007) Effects of long-term acclimation to environmental hypercapnia on extracellular acid-base status and metabolic capacity in Mediterranean fish *Sparus aurata*. *Marine Biology* 150:1417-1429

- Monfort MC (2010) Present market situation and prospects of meagre (*Argyrosomus regius*), as an emerging species in mediterranean aquaculture. FAO
- Orr JC et al. (2005) Anthropogenic ocean acidification over the twenty-first century and its impact on calcifying organisms. *Nature* 437:681-686
- Pandolfi JM, Connolly SR, Marshall DJ, Cohen AL (2011) Projecting Coral Reef Futures Under Global Warming and Ocean Acidification. *Science* 333:418-422
- Parmesan C (2006) Ecological and evolutionary responses to recent climate change. *Annual Review of Ecology, Evolution, and Systematics* 37:637-669
- Perry AL, Low PJ, Ellis JR, Reynolds JD (2005) Climate change and distribution shifts in marine fishes. *Science* 308:1912-1915
- Pimentel MS et al. (2015) Oxidative Stress and Digestive Enzyme Activity of Flatfish Larvae in a Changing Ocean. *PloS one* 10:e0134082
- Pörtner H-O et al. (2014) Ocean systems. In: Field CB, Barros VR, Dokken DJ, Mach KJ, Mastrandrea MD et al., editors. *Climate Change 2014: Impacts, Adaptation, and Vulnerability Part A: Global and Sectoral Aspects Contribution of Working Group II to the Fifth Assessment Report of the Intergovernmental Panel on Climate Change* Cambridge University Press:411-484
- Rosa R, Paula JR, Sampaio E, Pimentel M, Lopes AR, Baptista M, Guerreiro M, Santos C, Campos D, Almeida-Val VMF, Calado R, Diniz M, Repolho T (2016) Neuro-oxidative damage and aerobic potential loss of sharks under elevated CO₂ and warming. *Marine Biology* 163:1-10
- Rosa R, Pimentel MS, Boavida-Portugal J, Teixeira T, Trubenbach K, Diniz M (2012) Ocean Warming Enhances Malformations, Premature Hatching, Metabolic Suppression and Oxidative Stress in the Early Life Stages of a Keystone Squid. *PlosOne* 7(6): e38282
- Rosa R, Rummer JL, Munday PL (2017) Biological responses of sharks to ocean acidification. *Biology Letters* 13:20160796
- Sampaio E, Maulvault AL, Lopes VM, Paula JR, Barbosa V, Alves R, Pousão-Ferreira P, Repolho T, Marques A, Rosa R (2016) Habitat selection disruption and lateralization impairment of cryptic flatfish in a warm, acid, and contaminated ocean. *Marine Biology* 163:217
- Sejersted Y et al. (2011) Endonuclease VIII-like 3 (Neil3) DNA glycosylase promotes neurogenesis induced by hypoxia-ischemia *Proceedings of the National Academy of Sciences of the United States of America* 108:18802-18807

- Stillman JH (2003) Acclimation capacity underlies susceptibility to climate change. *Science* 301:65
- Tchounwou PB, Yedjou CG, Patlolla AK, Sutton DJ (2012) Heavy Metal Toxicity and the Environment. In: Luch A (ed) *Molecular, Clinical and Environmental Toxicology* vol 101. Springer, Basel, pp 133-164
- Teixeira T, Diniz M, Calado R, Rosa R (2013) Coral physiological adaptations to air exposure: Heat shock and oxidative stress responses in *Veretillum cynomorium*. *Journal of Experimental Marine Biology and Ecology* 439:35-41
- Tewksbury JJ, Huey RB, Deutsch CA (2008) Putting heat on tropical animals. *Science* 320:1296-1297
- Thomas CD et al. (2004) Extinction risk from climate change. *Nature* 427:145-148
- Tiedke J, Cubuk C, Burmester T (2013) Environmental acidification triggers oxidative stress and enhances globin expression in zebrafish gills. *Biochemical and Biophysical Research Communications* 441:624-629
- Tomanek L (2010) Variation in the heat shock response and its implication for predicting the effect of global climate change on species' biogeographical distribution ranges and metabolic costs. *Journal of Experimental Biology* 213:971-979
- Tomanek L (2014) Proteomics to study adaptations in marine organisms to environmental stress. *Journal of Proteomics* 105:92-106
- Tomanek L, Zuzow MJ, Ivanina AV, Beniash E, Sokolova IM (2011) Proteomic response to elevated P_{CO_2} level in eastern oysters, *Crassostrea virginica*: evidence for oxidative stress. *Journal of Experimental Biology* 214:1836-1844
- Vergilio CS, Carvalho CEV, Melo EJT (2012) Accumulation and histopathological effects of mercury chloride after acute exposure in tropical fish *Gymnotus carapo*. *Journal of Chemical and Health Risks* 2:1-8
- Wright SJ, Muller-Landau HC, Schipper J (2009) The future of tropical species on warmer planet. *Conservation Biology* 23:1418-1426

Supplemental Material

Chapter 2

Table S1. Seawater physicochemical parameters in all experimental conditions. Temperature, pH (pH_T), and total alkalinity (A_T) were used to calculate carbonate system parameters [pCO₂ (carbon dioxide partial pressure), C_T (total inorganic carbon), and Ω Arg (aragonite saturation state)]. Values represent means ± standard deviation.

Table S2. GLM analyses of oxidative damage (LPO, Protein Carbonyl and 8-OHdG) in *C. plagiosum* tissues (muscle, gills and liver) after 50 days. Est – Estimates; Std Error – Standard Error. Bold values indicate $p < 0.05$.

Table S3. GLM analyses of oxidative stress enzyme activities (SOD, CAT, GPx, and Aconitase) and total antioxidant capacity (TAC) in *C. plagiosum* tissues (muscle, gills, and liver) after 50 days. Est – Estimates; Std Error – Standard Error. Bold values indicate $p < 0.05$.

Table S4. GLM analyses of protein repair and removal levels (HSP and Ub) in *C. plagiosum* tissues (muscle, gills, and liver) after 50 days. Est – Estimates; Std Error – Standard Error. Bold values indicate $p < 0.05$.

Table S5. GLM analyses of oxidative damage (LPO, Protein Carbonyl, and 8-OHdG) in *C. plagiosum* tissues (muscle, gills and liver) after 50 days exposed to CO₂ (Control, High CO₂). Est – Estimates; Std Error – Standard Error. Bold values indicate $p < 0.05$.

Table S6. GLM analyses of oxidative stress enzyme activities (SOD, CAT, GPx, and Aconitase) and total antioxidant capacity (TAC) in *C. plagiosum* tissues (muscle, gills and liver) after 50 days exposed to CO₂ (Control, High CO₂). Est – Estimates; Std Error – Standard Error. Bold values indicate $p < 0.05$.

Table S7. GLM analyses of protein repair and removal levels (HSP and Ub) in *C. plagiosum* tissues (muscle, gills, and liver) after 50 days exposed to CO₂ (Control, High CO₂). Est – Estimates; Std Error – Standard Error. Bold values indicate $p < 0.05$.

Chapter 3

Table S1. Seawater physicochemical parameters in all experimental conditions, for each generation. Temperature, pH (pH_T) and total alkalinity (A_T) were used to calculate carbon dioxide partial pressure (pCO₂), total inorganic carbon (C_T) and aragonite saturation state (Ω Arg). Values represent mean ± standard deviation.

Table S2. GLM analysis of LPO levels in *G. locusta* after CO₂ exposure. Comparisons within the parental generation (C * H), between generations for each treatment (C * C-C; H * H-H; F0 * F1) and cross-treatments (C-H * H-C; Offspring crosses: C-C * C-H; H-H * H-C; and Parental crosses: C * C-H; H * H-C). Est – Estimates; Std Error – Standard Error. Statistical differences ($p < 0.05$) are indicated in bold.

Table S3. GLM analysis of DNA damage levels in *G. locusta* after CO₂ exposure. Comparisons within the parental generation (C * H), between generations for each treatment (C * C-C; H * H-H; F0 * F1) and cross-treatments (C-H * H-C; Offspring crosses: C-C * C-H; H-H * H-C; and Parental crosses: C * C-H; H * H-C). Est – Estimates; Std Error – Standard Error. Statistical differences ($p < 0.05$) are indicated in bold.

Table S4. GLM analysis of HSP levels in *G. locusta* after CO₂ exposure. Comparisons within the parental generation (C * H), between generations for each treatment (C * C-C; H * H-H; F0 * F1) and cross-treatments (C-H * H-C; Offspring crosses: C-C * C-H; H-H * H-C; and Parental crosses: C * C-H; H * H-C).

| Supplemental material

Est – Estimates; Std Error – Standard Error. Statistical differences ($p < 0.05$) are indicated in bold.

Table S5. GLM analysis of Ub levels in *G. locusta* after CO₂ exposure. Comparisons within the parental generation (C * H), between generations for each treatment (C * C-C; H * H-H; F0 * F1) and cross-treatments (C-H * H-C; Offspring crosses: C-C * C-H; H-H * H-C; and Parental crosses: C * C-H; H * H-C). Est – Estimates; Std Error – Standard Error. Statistical differences ($p < 0.05$) are indicated in bold.

Table S6. GLM analysis of SOD activity in *G. locusta* after CO₂ exposure. Comparisons within the parental generation (C * H), between generations for each treatment (C * C-C; H * H-H; F0 * F1) and cross-treatments (C-H * H-C; Offspring crosses: C-C * C-H; H-H * H-C; and Parental crosses: C * C-H; H * H-C). Est – Estimates; Std Error – Standard Error. Statistical differences ($p < 0.05$) are indicated in bold.

Table S7. GLM analysis of CAT activity in *G. locusta* after CO₂ exposure. Comparisons within the parental generation (C * H), between generations for each treatment (C * C-C; H * H-H; F0 * F1) and cross-treatments (C-H * H-C; Offspring crosses: C-C * C-H; H-H * H-C; and Parental crosses: C * C-H; H * H-C). Est – Estimates; Std Error – Standard Error. Statistical differences ($p < 0.05$) are indicated in bold.

Table S8. GLM analysis of GPx activity in *G. locusta* after CO₂ exposure. Comparisons within the parental generation (C * H), between generations for each treatment (C * C-C; H * H-H; F0 * F1) and cross-treatments (C-H * H-C; Offspring crosses: C-C * C-H; H-H * H-C; and Parental crosses: C * C-H; H * H-C). Est – Estimates; Std Error – Standard Error. Statistical differences ($p < 0.05$) are indicated in bold.

Table S9. GLM analysis of GST activity in *G. locusta* after CO₂ exposure. Comparisons within the parental generation (C * H), between generations for each treatment (C * C-C; H * H-H; F0 * F1) and cross-treatments (C-H * H-C; Offspring crosses: C-C * C-H; H-H * H-C; and Parental crosses: C * C-H; H * H-C). Est – Estimates; Std Error – Standard Error. Statistical differences ($p < 0.05$) are indicated in bold.

Table S10. GLM analysis of TAC in *G. locusta* after CO₂ exposure. Comparisons within the parental generation (C * H), between generations for each treatment (C * C-C; H * H-H; F0 * F1) and cross-treatments (C-H * H-C; Offspring crosses: C-C * C-H; H-H * H-C; and Parental crosses: C * C-H; H * H-C). Est – Estimates; Std Error – Standard Error. Statistical differences ($p < 0.05$) are indicated in bold.

Chapter 4

Figure S1. Temperature variations from January 2011 to June 2015 in the sampling area. Box and whisker plots for annual, summer and heat wave temperatures. The horizontal line within the box indicates the median, boundaries of the box indicate the 25th and 75th percentiles, and the whiskers indicate the highest and lowest values of the results.

Table S1. Summary table of the available studies on the impact of warming and acidification on the antioxidant machinery in corals, including soft corals (order Alcyonacea), sea anemones (order Actiniaria) and hard corals (order Scleractinia).

Table S2. Seawater physicochemical parameters in all experimental conditions. Temperature, pH and total alkalinity (A_T) were used to calculate carbonate system parameters (pCO_2 - carbon dioxide partial pressure, C_T - total inorganic carbon, and Ω_{Arg} - aragonite saturation state). Values represent mean \pm standard deviation.

Table S3 – Generalized Linear Models analyses for each dependent variable (catalase -CAT, glutathione S-transferase - GST, malondialdehyde - MDA, and heat shock protein - HSP), using both temperature and pH as explanatory variables, as well as their interaction. Est – Estimates; Std Error – Standard Error. Bold values indicate $p < 0.05$.

Chapter 5

Table S1. GLM analysis of survival (%) of *S. canicula* exposed to different combinations of temperature and HgCl₂ contamination for 7 days. Est – Estimates; Std Error – Standard Error. Bold values indicate $p < 0.05$.

Table S2. GLM analysis of total mercury (HgT) accumulation in *S. canicula* capsule after 7 days exposure. Est – Estimates; Std Error – Standard Error. Bold values indicate $p < 0.05$.

Table S3. GLM analysis of total mercury (HgT) accumulation in *S. canicula* tissues, and within each sampled tissue regarding different contamination and temperature conditions, after 7 days exposure. Est – Estimates; Std Error – Standard Error. Bold values indicate $p < 0.05$.

Table S4. GLM analysis of heat shock protein (HSP) levels in *S. canicula* tissues, and within each sampled tissue regarding different contamination and temperature conditions, after 7 days exposure. Est – Estimates; Std Error – Standard Error. Bold values indicate $p < 0.05$.

Table S5. GLM analysis of ubiquitin (Ub) levels in *S. canicula* tissues, and within each sampled tissue regarding different contamination and temperature conditions, after 7 days exposure. Est – Estimates; Std Error – Standard Error. Bold values indicate $p < 0.05$.

Table S6. GLM analysis of lipid peroxidation levels in *S. canicula* tissues, and within each sampled tissue regarding different contamination and temperature conditions, after 7 days exposure. Est – Estimates; Std Error – Standard Error. Bold values indicate $p < 0.05$.

Table S7. GLM analysis of DNA damage levels in *S. canicula* tissues, and within each sampled tissue regarding different contamination and temperature conditions, after 7 days exposure. Est – Estimates; Std Error – Standard Error. Bold values indicate $p < 0.05$.

Table S8. GLM analysis of superoxide dismutase (SOD) activity in *S. canicula* tissues, and within each sampled tissue regarding different contamination and temperature conditions, after 7 days exposure. Est – Estimates; Std Error – Standard Error. Bold values indicate $p < 0.05$.

Table S9. GLM analysis of catalase (CAT) activity in *S. canicula* tissues, and within each sampled tissue regarding different contamination and temperature conditions, after 7 days exposure. Est – Estimates; Std Error – Standard Error. Bold values indicate $p < 0.05$.

Table S10. GLM analysis of glutathione peroxidase (GPx) activity in *S. canicula* tissues, and within each sampled tissue regarding different contamination and temperature conditions, after 7 days exposure. Est – Estimates; Std Error – Standard Error. Bold values indicate $p < 0.05$.

Table S11. GLM analysis of glutathione s-transferase (GST) activity in *S. canicula* tissues, and within each sampled tissue regarding different contamination and temperature conditions, after 7 days exposure. Est – Estimates; Std Error – Standard Error. Bold values indicate $p < 0.05$.

Table S12. GLM analysis of acetylcholinesterase (AChE) activity in *S. canicula* tissues, and within each sampled tissue regarding different contamination and temperature conditions, after 7 days exposure. Est – Estimates; Std Error – Standard Error. Bold values indicate $p < 0.05$.

Table S13. GLM analysis of total antioxidant capacity (TAC) in *S. canicula* tissues, and within each sampled tissue regarding different contamination and temperature conditions, after 7 days exposure. Est – Estimates; Std Error – Standard Error. Bold values indicate $p < 0.05$.

Chapter 2

Table S1. Seawater physicochemical parameters in all experimental conditions. Temperature, pH (pH_T), and total alkalinity (A_T) were used to calculate carbonate system parameters [*p*CO₂ (carbon dioxide partial pressure), C_T (total inorganic carbon), and Ω Arg (aragonite saturation state)]. Values represent means ± standard deviation.

	26°C	
	pH 8.0	pH 7.7
<i>Measured</i>		
Temperature (°C)	26 ± 0.1	26 ± 0.1
pH _T (total scale)	8.0 ± 0.11	7.7 ± 0.01
Salinity	35 ± 0.1	35 ± 0.1
A _T (μmol kg ⁻¹ SW)	2280.2 ± 302.0	2374.8 ± 246.0
<i>Calculated</i>		
<i>p</i> CO ₂ (ppm)	414.7 ± 70.5	894.4 ± 116.6
C _T (μmol kg ⁻¹ SW)	1983.0 ± 270.2	2199.8 ± 227.3
Ω Arg	3.4 ± 0.6	2.1 ± 0.3

Table S2. GLM analyses of oxidative damage (LPO, Protein Carbonyl and 8-OHdG) in *C. plagiosum* tissues (muscle, gills and liver) after 50 days. Est – Estimates; Std Error – Standard Error. Bold values indicate *p* < 0.05.

GLM: LPO in function of Tissues

	Est	Std Error	t value	p
Muscle-Liver	0.029	0.008	4.142	< 0.001
Muscle-Gills	-0.004	0.007	-0.606	0.550
Gills-Liver	0.034	0.007	4.748	< 0.001

GLM: Protein Carbonyl in function of Tissues

	Est	Std Error	t value	p
Muscle-Liver	-0.041	0.019	-2.155	0.041
Muscle-Gills	0.008	0.019	-0.422	0.677
Gills-Liver	-0.033	0.019	-1.734	0.095

GLM: 8-OHdG in function of Tissues

	Est	Std Error	t value	p
Muscle-Liver	-0.083	0.021	-3.904	< 0.001
Muscle-Gills	0.019	0.021	0.875	0.390
Gills-Liver	-0.102	0.021	-4.915	< 0.001

Table S3. GLM analyses of oxidative stress enzyme activities (SOD, CAT, GPx, and Aconitase) and total antioxidant capacity (TAC) in *C. plagiosum* tissues (muscle, gills, and liver) after 50 days. Est – Estimates; Std Error – Standard Error. Bold values indicate $p < 0.05$.

GLM: SOD in function of Tissues

	Est	Std Error	t value	p
Muscle-Liver	0.213	7.288	0.029	0.977
Muscle-Gills	9.558	7.288	1.312	0.201
Gills-Liver	-9.346	7.288	-1.282	0.211

GLM: CAT in function of Tissues

	Est	Std Error	t value	p
Muscle-Liver	-2.385	2.547	-0.937	0.358
Muscle-Gills	-10.558	2.547	-4.146	< 0.001
Gills-Liver	8.173	2.547	3.210	0.004

GLM: GPx in function of Tissues

	Est	Std Error	t value	p
Muscle-Liver	0.219	0.160	1.370	0.182
Muscle-Gills	-0.109	0.160	-0.682	0.501
Gills-Liver	0.328	0.160	2.052	0.503

GLM: Aconitase in function of Tissues

	Est	Std Error	t value	p
Muscle-Liver	-4.673	0.468	-9.976	< 0.001
Muscle-Gills	-4.203	0.468	-8.973	< 0.001
Gills-Liver	-0.470	0.468	-1.004	0.325

GLM: TAC in function of Tissues

	Est	Std Error	t value	p
Muscle-Liver	-12.502	1.426	-8.768	< 0.001
Muscle-Gills	3.949	1.426	2.770	0.012
Gills-Liver	-16.451	1.426	-11.537	< 0.001

Table S4. GLM analyses of protein repair and removal levels (HSP and Ub) in *C. plagiosum* tissues (muscle, gills, and liver) after 50 days. Est – Estimates; Std Error – Standard Error. Bold values indicate $p < 0.05$.

GLM: HSP in function of Tissues

	Est	Std Error	t value	p
Muscle-Liver	-12.502	1.426	-8.768	< 0.001
Muscle-Gills	3.949	1.426	2.770	0.010
Gills-Liver	-16.451	1.426	-11.537	< 0.001

GLM: Ub in function of Tissues

	Est	Std Error	t value	p
Muscle-Liver	-0.016	0.007	-2.106	0.046
Muscle-Gills	-0.023	0.008	-3.047	0.006
Gills-Liver	0.007	0.007	0.998	0.328

Table S5. GLM analyses of oxidative damage (LPO, Protein Carbonyl, and 8-OHdG) in *C. plagiosum* tissues (muscle, gills and liver) after 50 days exposed to CO₂ (Control, High CO₂). Est – Estimates; Std Error – Standard Error. Bold values indicate $p < 0.05$.

GLM: LPO in function of CO₂

	Est	Std Error	t value	p
Gills	-0.023	0.015	-1.473	0.179
Liver	-0.007	0.006	-1.095	0.306
Muscle	-0.007	0.005	-1.372	0.207

GLM: Protein Carbonyl in function of CO₂

	Est	Std Error	t value	p
Gills	-0.267	0.077	-3.484	0.008
Liver	-0.022	0.023	-0.980	0.356
Muscle	0.032	0.035	0.913	0.388

GLM: 8-OHdG in function of CO₂

	Est	Std Error	t value	p
Gills	-0.041	0.025	-1.661	0.135
Liver	0.074	0.019	3.850	< 0.005
Muscle	-0.048	0.027	-1.796	0.116

Table S6. GLM analyses of oxidative stress enzyme activities (SOD, CAT, GPx, and Aconitase) and total antioxidant capacity (TAC) in *C. plagiosum* tissues (muscle, gills and liver) after 50 days exposed to CO₂ (Control, High CO₂). Est – Estimates; Std Error – Standard Error. Bold values indicate $p < 0.05$.

GLM: SOD in function of CO₂

	Est	Std Error	t value	p
Gills	17.282	8.295	2.084	0.071
Liver	-14.570	4.941	-2.949	0.019
Muscle	38.453	8.597	4.473	0.002

GLM: CAT in function of CO₂

	Est	Std Error	t value	p
Gills	-0.719	1.788	-0.402	0.698
Liver	-0.256	0.065	-3.952	0.004
Muscle	-0.459	1.395	-0.329	0.747

GLM: GPx in function of CO₂

	Est	Std Error	t value	p
Gills	-2.367	0.870	-2.721	0.026
Liver	-2.801	0.458	-6.118	< 0.001
Muscle	3.818	1.177	3.243	0.012

GLM: Aconitase in function of CO₂

	Est	Std Error	t value	p
Gills	-0.639	0.203	-3.149	0.014
Liver	-0.406	0.351	-1.155	0.281
Muscle	-0.143	1.009	-0.142	0.891

GLM: TAC in function of CO₂

	Est	Std Error	t value	p
Gills	-1.169	1.804	-0.648	0.535
Liver	-0.243	0.478	-0.509	0.625
Muscle	0.380	0.095	3.997	0.004

Table S7. GLM analyses of protein repair and removal levels (HSP and Ub) in *C. plagiosum* tissues (muscle, gills, and liver) after 50 days exposed to CO₂ (Control, High CO₂). Est – Estimates; Std Error – Standard Error. Bold values indicate $p < 0.05$.

GLM: HSP in function of CO₂

	Est	Std Error	t value	p
Gills	-0.423	0.113	-3.751	0.006
Liver	0.107	0.139	0.771	0.463
Muscle	-4.634	6.467	-0.717	0.494

GLM: Ub in function of CO₂

	Est	Std Error	t value	p
Gills	0.619	0.234	2.643	0.030
Liver	-0.021	0.004	-4.753	0.001
Muscle	-0.110	-0.179	-0.617	0.560

Chapter 3

Table S1 - Seawater physicochemical parameters in all experimental conditions, for each generation. Temperature, pH (pH_T) and total alkalinity (A_T) were used to calculate carbon dioxide partial pressure (pCO₂), total inorganic carbon (C_T) and aragonite saturation state (Ω Arg). Values represent mean \pm standard deviation.

	F0			F1		
	C	H	C-C	H-C	C-H	H-H
<i>Measured</i>						
Temperature (°C)	18.3 \pm 1.3	18.4 \pm 1.4	18.8 \pm 0.8	18.7 \pm 0.6	18.8 \pm 0.6	18.8 \pm 0.6
pH _T (total scale)	8.1 \pm 0.1	7.7 \pm 0.1	8.0 \pm 0.1	8.0 \pm 0.1	7.7 \pm 0.1	7.7 \pm 0.1
Salinity	35	35	35	35	35	35
A _T (μ mol kg ⁻¹ SW)	1932.2 \pm 109.8	1971.5 \pm 64.3	2126.5 \pm 112.3	2105.7 \pm 108.9	1943.6 \pm 88.4	2044.1 \pm 140.4
<i>Calculated</i>						
pCO ₂ (μ atm)	375.9 \pm 67.7	827.5 \pm 73.2	354.2 \pm 28.7	366.8 \pm 20.5	803.2 \pm 27.8	825.5 \pm 71.5
C _T (μ mol kg ⁻¹ SW)	1727.9 \pm 80.5	1925.4 \pm 122.4	2104.4 \pm 259.5	2002.3 \pm 231.6	1970.6 \pm 145.1	1939.8 \pm 131.5
Ω Arg	1.1 \pm 0.3	1.1 \pm 0.4	1.4 \pm 0.4	1.8 \pm 0.4	1.4 \pm 0.2	1.3 \pm 0.2

Table S2 – GLM analysis of LPO levels in *G. locusta* after CO₂ exposure. Comparisons within the parental generation (C * H), between generations for each treatment (C * C-C; H * H-H; F0 * F1) and cross-treatments (C-H * H-C; Offspring crosses: C-C * C-H; H-H * H-C; and Parental crosses: C * C-H; H * H-C). Est – Estimates; Std Error – Standard Error. Statistical differences (p < 0.05) are indicated in bold.

	Est	Std Error	t value	p
Model: GLMM (Gamma)				
Response variable: Lipid peroxidation levels				
Final model term(s): CO ₂ effects in each generation and comparison between generations and cross-treatments, with replicates as random effects				
C * H	0.126	0.195	0.643	0.520
C * C-C	0.791	0.195	4.055	< 0.001
H * H-H	0.603	0.195	3.088	0.002
C-C * H-H	-0.062	0.194	-0.321	0.748
C-H * H-C	1.226	0.193	6.351	< 0.001
C-C * C-H	-0.090	0.194	-0.466	0.641
H-H * H-C	1.198	0.194	6.186	< 0.001
C * C-H	0.701	0.194	3.610	< 0.001
H * H-C	1.801	0.196	9.194	< 0.001
F0 * F1	1.135	0.155	7.300	< 0.001

| Supplemental material

Table S3 – GLM analysis of DNA damage levels in *G. locusta* after CO₂ exposure. Comparisons within the parental generation (C * H), between generations for each treatment (C * C-C; H * H-H; F0 * F1) and cross-treatments (C-H * H-C; Offspring crosses: C-C * C-H; H-H * H-C; and Parental crosses: C * C-H; H * H-C). Est – Estimates; Std Error – Standard Error. Statistical differences ($p < 0.05$) are indicated in bold.

	Est	Std Error	t value	<i>p</i>
Model: GLM (Gamma)				
Response variable: DNA damage levels				
Final model term(s): CO ₂ effects in each generation and comparison between generations and cross-treatments				
C * H	0.081	0.162	0.501	0.618
C * C-C	0.719	0.162	4.449	< 0.001
H * H-H	1.175	0.162	7.264	< 0.001
C-C * H-H	0.536	0.162	3.316	0.001
C-H * H-C	0.091	0.162	0.563	0.575
C-C * C-H	1.049	0.162	6.484	< 0.001
H-H * H-C	0.603	0.162	3.730	< 0.001
C * C-H	1.768	0.162	10.932	< 0.001
H * H-C	1.778	0.162	10.994	< 0.001
F0 * F1	1.454	0.134	10.885	< 0.001

Table S4 – GLM analysis of HSP levels in *G. locusta* after CO₂ exposure. Comparisons within the parental generation (C * H), between generations for each treatment (C * C-C; H * H-H; F0 * F1) and cross-treatments (C-H * H-C; Offspring crosses: C-C * C-H; H-H * H-C; and Parental crosses: C * C-H; H * H-C). Est – Estimates; Std Error – Standard Error. Statistical differences ($p < 0.05$) are indicated in bold.

	Est	Std Error	t value	<i>p</i>
Model: GLM (Gamma)				
Response variable: HSP levels				
Final model term(s): CO ₂ effects in each generation and comparison between generations and cross-treatments				
C * H	-0.129	0.143	-0.906	0.368
C * C-C	0.703	0.143	4.919	< 0.001
H * H-H	0.759	0.143	5.314	< 0.001
C-C * H-H	-0.073	0.143	-0.511	0.611
C-H * H-C	-0.050	0.143	-0.352	0.726
C-C * C-H	0.213	0.143	1.492	0.140
H-H * H-C	0.236	0.143	1.650	0.103
C * C-H	0.865	0.143	6.058	< 0.001
H * H-C	0.995	0.143	6.964	< 0.001
F0 * F1	0.848	0.088	9.598	< 0.001

Table S5 – GLM analysis of Ub levels in *G. locusta* after CO₂ exposure. Comparisons within the parental generation (C * H), between generations for each treatment (C * C-C; H * H-H; F0 * F1) and cross-treatments (C-H * H-C; Offspring crosses: C-C * C-H; H-H * H-C; and Parental crosses: C * C-H; H * H-C). Est – Estimates; Std Error – Standard Error. Statistical differences ($p < 0.05$) are indicated in bold.

	Est	Std Error	t value	<i>p</i>
Model: GLM (Gamma)				
Response variable: Ub levels				
Final model term(s): CO ₂ effects in each generation and comparison between generations and cross-treatments				
C * H	0.470	0.183	2.564	0.012
C * C-C	0.901	0.183	4.916	< 0.001
H * H-H	0.444	0.183	2.423	0.018
C-C * H-H	0.013	0.183	0.071	0.944
C-H * H-C	-0.060	0.183	-0.327	0.745
C-C * C-H	0.283	0.183	1.547	0.126
H-H * H-C	0.211	0.183	1.149	0.254
C * C-H	1.184	0.183	6.463	< 0.001
H * H-C	0.654	0.183	3.572	< 0.001
F0 * F1	0.776	0.116	6.674	< 0.001

Table S6 – GLM analysis of SOD activity in *G. locusta* after CO₂ exposure. Comparisons within the parental generation (C * H), between generations for each treatment (C * C-C; H * H-H; F0 * F1) and cross-treatments (C-H * H-C; Offspring crosses: C-C * C-H; H-H * H-C; and Parental crosses: C * C-H; H * H-C). Est – Estimates; Std Error – Standard Error. Statistical differences ($p < 0.05$) are indicated in bold.

	Est	Std Error	t value	<i>p</i>
Model: GLM (Gamma)				
Response variable: Superoxide Dismutase activity				
Final model term(s): CO ₂ effects in each generation and comparison between generations and cross-treatments				
C * H	0.030	0.178	0.166	0.868
C * C-C	0.165	0.178	0.929	0.356
H * H-H	0.542	0.178	3.046	0.003
C-C * H-H	0.406	0.178	2.283	0.025
C-H * H-C	-0.133	0.178	-0.749	0.456
C-C * C-H	0.792	0.178	4.452	< 0.001
H-H * H-C	0.253	0.178	1.420	0.159
C * C-H	0.958	0.178	5.380	< 0.001
H * H-C	0.795	0.178	4.465	< 0.001
F0 * F1	0.658	0.121	5.415	< 0.001

| Supplemental material

Table S7 – GLM analysis of CAT activity in *G. locusta* after CO₂ exposure. Comparisons within the parental generation (C * H), between generations for each treatment (C * C-C; H * H-H; F0 * F1) and cross-treatments (C-H * H-C; Offspring crosses: C-C * C-H; H-H * H-C; and Parental crosses: C * C-H; H * H-C). Est – Estimates; Std Error – Standard Error. Statistical differences (p < 0.05) are indicated in bold.

	Est	Std Error	t value	p
Model: GLM (Gamma)				
Response variable: Catalase activity				
Final model term(s): CO ₂ effects in each generation and comparison between generations and cross-treatments				
C * H	-0.002	0.178	-0.010	0.992
C * C-C	0.504	0.178	2.830	0.006
H * H-H	0.240	0.178	1.350	0.181
C-C * H-H	-0.265	0.178	-1.490	0.140
C-H * H-C	0.715	0.178	4.014	< 0.001
C-C * C-H	0.064	0.178	0.361	0.719
H-H * H-C	1.044	0.178	5.866	< 0.001
C * C-H	0.568	0.178	3.191	0.002
H * H-C	1.285	0.178	7.216	< 0.001
F0 * F1	0.658	0.121	5.415	< 0.001

Table S8 – GLM analysis of GPx activity in *G. locusta* after CO₂ exposure. Comparisons within the parental generation (C * H), between generations for each treatment (C * C-C; H * H-H; F0 * F1) and cross-treatments (C-H * H-C; Offspring crosses: C-C * C-H; H-H * H-C; and Parental crosses: C * C-H; H * H-C). Est – Estimates; Std Error – Standard Error. Statistical differences (p < 0.05) are indicated in bold.

	Est	Std Error	t value	p
Model: GLMM (Gamma)				
Response variable: Glutathione Peroxidase activity				
Final model term(s): CO ₂ effects in each generation and comparison between generations and cross-treatments, with replicates as random effects				
C * H	0.684	0.270	2.535	0.013
C * C-C	1.937	0.270	7.174	< 0.001
H * H-H	2.892	0.270	10.711	< 0.001
C-C * H-H	1.639	0.270	6.072	< 0.001
C-H * H-C	0.033	0.270	0.123	0.902
C-C * C-H	1.984	0.270	7.3497	< 0.001
H-H * H-C	0.378	0.270	1.401	0.165
C * C-H	3.921	0.270	14.523	< 0.001
H * H-C	3.270	0.270	12.112	< 0.001
F0 * F1	3.193	0.183	17.430	< 0.001

Table S9 – GLM analysis of GST activity in *G. locusta* after CO₂ exposure. Comparisons within the parental generation (C * H), between generations for each treatment (C * C-C; H * H-H; F0 * F1) and cross-treatments (C-H * H-C; Offspring crosses: C-C * C-H; H-H * H-C; and Parental crosses: C * C-H; H * H-C). Est – Estimates; Std Error – Standard Error. Statistical differences ($p < 0.05$) are indicated in bold.

	Est	Std Error	t value	<i>p</i>
Model: GLM (Gamma)				
Response variable: Glutathione S-Transferase activity				
Final model term(s): CO ₂ effects in each generation and comparison between generations and cross-treatments				
C * H	0.184	0.104	1.773	0.080
C * C-C	0.960	0.104	9.244	< 0.001
H * H-H	0.613	0.104	5.901	< 0.001
C-C * H-H	-0.163	0.104	-1.570	0.120
C-H * H-C	-0.075	0.104	-0.718	0.475
C-C * C-H	0.129	0.104	1.240	0.218
H-H * H-C	0.217	0.104	2.092	0.039
C * C-H	1.089	0.104	10.484	< 0.001
H * H-C	0.830	0.104	7.993	< 0.001
F0 * F1	0.874	0.066	13.257	< 0.001

Table S10 – GLM analysis of TAC in *G. locusta* after CO₂ exposure. Comparisons within the parental generation (C * H), between generations for each treatment (C * C-C; H * H-H; F0 * F1) and cross-treatments (C-H * H-C; Offspring crosses: C-C * C-H; H-H * H-C; and Parental crosses: C * C-H; H * H-C). Est – Estimates; Std Error – Standard Error. Statistical differences ($p < 0.05$) are indicated in bold.

	Est	Std Error	t value	<i>p</i>
Model: GLM (Gamma)				
Response variable: Total antioxidant capacity				
Final model term(s): CO ₂ effects in each generation and comparison between generations and cross-treatments				
C * H	0.660	0.208	3.171	0.002
C * C-C	0.671	0.208	3.222	0.002
H * H-H	0.360	0.208	1.731	0.087
C-C * H-H	0.350	0.208	1.680	0.097
C-H * H-C	0.509	0.208	2.445	0.017
C-C * C-H	0.848	0.208	4.072	< 0.001
H-H * H-C	1.007	0.208	4.837	< 0.001
C * C-H	1.518	0.208	7.294	< 0.001
H * H-C	1.367	0.208	6.568	< 0.001
F0 * F1	1.057	0.187	5.642	< 0.001

Chapter 4

Figure S1 – Temperature variations from January 2011 to June 2015 in the sampling area. Box and whisker plots for annual, summer and heat wave temperatures. The horizontal line within the box indicates the median, boundaries of the box indicate the 25th and 75th percentiles, and the whiskers indicate the highest and lowest values of the results.

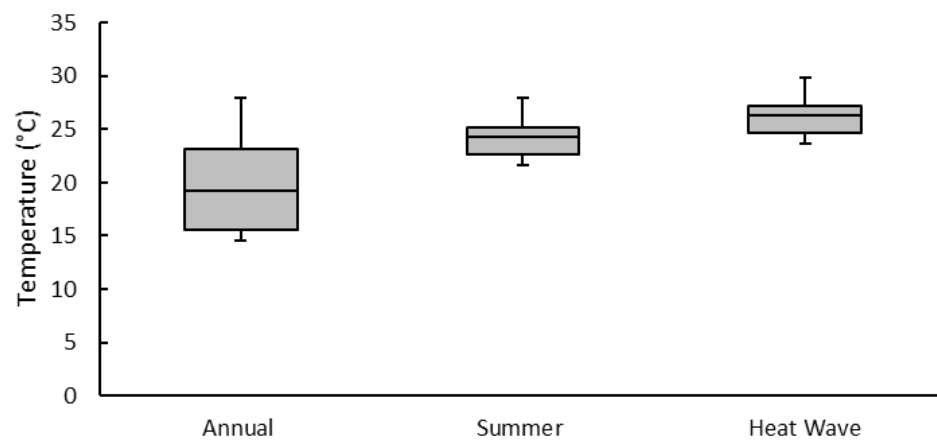


Table S1 – Summary table of the available studies on the impact of warming and acidification on the antioxidant machinery in corals, including soft corals (order Alcyonacea), sea anemones (order Actiniaria) and hard corals (order Scleractinia).

Subclass	Order	Species	Region	pCO2 (µatm)		pH		Temperature (°C)		Acclimation period (days)		Biomarkers used	Effects	Reference
				C	T	C	T	C	T	C	T			
Octocorallia														
	Alcyonacea													
		Eunicea fusca	Tropical	NA	NA	NA	NA	27	33	3-6	1	Net ROS efflux, % Inhibition of H ₂ O ₂	= net ROS efflux	Mydlarz and Jacobs (2006)
		Pseudopterogorgia americana	Tropical	NA	NA	NA	NA	27	33	3-6	1	Net ROS efflux, % Inhibition of H ₂ O ₂	↑ net ROS efflux	Mydlarz and Jacobs (2006)
		Pseudopterogorgia elisabethae	Tropical	NA	NA	NA	NA	27	33	3-6	1	Net ROS efflux, % Inhibition of H ₂ O ₂	↑ net ROS efflux	Mydlarz and Jacobs (2006)
		Dendronephthya klunzingeri	Tropical	NA	NA	NA	NA	25	21- 29	< 1	< 1	Hsp90	↑ Hsp90 expression	Wiens et al. (2000)
		Veretillum cynomorium	Temperate	NA	NA	NA	NA	20	27	NA	NA	Hsp70, Ub, SOD, CAT, GST, LPO	↓ Hsp70 and Ub levels, ↓ cellular damage, ↓ GST and CAT activities, = SOD activity	Madeira et al. (2015)
Hexacorallia														
	Actiniaria													
		Actinia schmidtii	Temperate	NA	NA	NA	NA	17	24	5	5	SOD, LPO, PC	↑ antioxidant defence (SOD), ↑ carbonyl content, = cellular damage	Richier et al. (2005)

| Supplemental material

<i>Scleractinia</i>	<i>Anemonia viridis</i>	Temperate	NA	NA	NA	NA	17	24	5	5	SOD, LPO, PC	↑ antioxidant defence (SOD), ↑ carbonyl content, ↑ cellular damage	Richier et al. (2005)
	<i>Exaiptasia pallida</i>	Tropical	400	1000	8.1	7.8	NA	NA	26	NA	CAT, GPx, GR, CA	↑ CAT, GPx and GR activities, = CA activity	Siddiqui and Bielmyer-Fraser (2015)
	<i>Exaiptasia pallida</i>	Tropical	NA	1000	7.9	7.7	24	24	7	7	CAT, GR	= CAT activity, ↓ GR activity	Duckworth et al. (2017)
	<i>Acropora aspera</i>	Tropical	NA	NA	NA	NA	28	31	4	3	DMS, DMSP, DMSO, AOC	↑ DMS(P)(O), = AOC	Deschaseaux et al. (2014)
	<i>Acropora echinata</i>	Tropical	NA	NA	NA	NA	27	34	< 2	< 2	Hsp60	↑ Hsp60 levels in the first 12h, ↓ Hsp60 levels after 12h	Seveso et al. (2014)
	<i>Acropora grandis</i>	Tropical	NA	NA	NA	NA	25	35	< 1	< 1	Hsp	Induction of Hsp with molecular weights of 70, 60 and 35 kDa	Fang et al. (1997)
	<i>Acropora hyacinthus</i>	Temperate	NA	NA	NA	NA	18	13- 23	15	10	SOD, CAT	↓ SOD activity with decreasing temperature, = CAT activity	Higuchi et al. (2015)
	<i>Acropora intermedia</i>	Tropical	NA	NA	NA	NA	26	32	3	3	SOD, LPO	↑ SOD activity and cellular damage in individuals with symbionts	Yakovleva et al. (2009)
	<i>Acropora millepora</i>	Tropical	NA	NA	NA	NA	27	32	14	9	Hsp70, MnSOD	↑ Hsp70 and MnSOD expression	Császár et al. (2009)

Supplemental material |

<i>Acropora millepora</i>	Tropical	NA	NA	NA	NA	27	32	12	18	CoQ, PQ	↓ CoQ pool oxidation, = PQ pool	Lutz et al. (2015)
<i>Acropora millepora</i>	Tropical	323	803	8.1	7.8	29.5	NA	NA	NA	AOC, PC	= total antioxidant capacity, = Protein carbonylation	Strahl et al. (2015)
<i>Acropora muricata</i>	Tropical	NA	NA	NA	NA	23-25	27-30	NA	NA	TEAC, FRAP, DPPH	↑ Antioxidant capacity, ↑ Trolox antioxidant capacity, ↑ DPPH	Louis et al. (2016)
<i>Acropora pruinosa</i>	Temperate	NA	NA	NA	NA	18	13- 23	15	10	SOD, CAT	↓ SOD activity with decreasing temperature, = CAT activity	Higuchi et al. (2015)
<i>Acropora solitaryensis</i>	Temperate	NA	NA	NA	NA	18	13- 23	15	10	SOD, CAT	↓ SOD activity with decreasing temperature, = CAT activity	Higuchi et al. (2015)
<i>Galaxea fascicularis</i>	Tropical	NA	NA	NA	NA	22-26	32	45	7	Cu/ZnSOD, MnSOD	↑ MnSOD activity, = Cu/ZnSOD activity	Agostini et al. (2016)
<i>Goniopora djiboutiensis</i>	Tropical	NA	NA	NA	NA	28	30-40	< 1	< 1	Hsp70	↑ Hsp70 expression	Sharp et al. (1997)
<i>Montastraea faveolata</i>	Tropical	NA	NA	NA	NA	27	33	NA	< 1	LPO, GSH, Ub, Hsp60, Hsp70, αB-Crystallin, ChlpsHsp, Plant sHsp, Cu/ZnSOD, MnSOD	↑ Cu/ZnSOD, MnSOD activities, ↑ cellular damage, ↑ ub levels, ↓ GSH activity, ↑ Hsp60, Hsp70 and αB-Crystallin levels, ↑ Plant sHsp and chlpsHsp levels	Downs et al. (2000)

| Supplemental material

<i>Montipora monasteriata</i>	Tropical	NA	NA	NA	NA	27	34	< 2	< 2	Hsp60	↑ Hsp60 levels in the first 12h, ↓ Hsp60 levels after 12h	Seveso et al. (2014)
<i>Platygyra daedalea</i>	Tropical	NA	NA	NA	NA	27	33 – 36	NA	< 3	AOC	Persian Gulf corals have ↑ AOC than Sea of Osman corals	Howells et al. (2016)
<i>Platygyra ryukyuensis</i>	Tropical	NA	NA	NA	NA	26	33	< 1	12	SOD, CAT	↑ CAT activity after 12-h exposure to thermal stress, = SOD activity	Yakovleva et al. (2004)
<i>Pocillopora capitata</i>	Tropical	NA	NA	NA	NA	22	24 - 32	< 1	< 1	LPO, SOD	↑ cellular damage, ↑ SOD activity	Flores-Ramírez and Liñán-Cabello (2007)
<i>Pocillopora capitata</i>	Tropical	NA	NA	NA	NA	27	28	NA	NA	LPO, SOD, CAT, GPx, GR, GST	↑ cellular damage, ↑ SOD, CAT and GST activities, = GPx and GR activities	Liñán-Cabello et al. (2010)
<i>Pocillopora capitata</i>	Tropical	NA	NA	8.0-8.4	7.8-7.6	29	NA	7	7	LPO, SOD, CAT, AOC	↑ SOD and AOC activities, ↑ cellular damage	Soriano-Santiago et al. (2013)
<i>Pocillopora damicornis</i>	Tropical	NA	NA	NA	NA	26.5-27	28-31	< 1	< 1	FRAP assay	↑ Antioxidant capacity	Griffin and Bhagooli (2004)
<i>Pocillopora damicornis</i>	Tropical	NA	NA	NA	NA	29	32 – 33	5	5	FRAP assay, CAT	= Antioxidant capacity	Griffin et al. (2006)
<i>Pocillopora damicornis</i>	Tropical	NA	NA	NA	NA	25	32	NA	5	Protein carbonyl, Ub, Hsp70, Gpx, ChlpsHsp, MnSOD	↑ Protein Carbonylation, ↑ cellular damage, ↑ Ub, Hsp70 and ChlpsHsp levels, ↑	Downs et al. (2013)

Supplemental material |

											Gpx and MnSOD activities	
<i>Pocillopora meandrina</i>	Tropical	NA	NA	NA	NA	26.5-27	28-31	< 1	< 1	FRAP assay	↑ Antioxidant capacity	Griffin and Bhagooli (2004)
<i>Pocillopora meandrina</i>	Tropical	NA	NA	NA	NA	29	32 – 33	5	5	FRAP assay, CAT	= Antioxidant capacity	Griffin et al. (2006)
<i>Pocillopora verrucosa</i>	Tropical	NA	NA	NA	NA	28	31	8	8	Cu/ZnSOD	↑ Cu/ZnSOD activity	Rodriguez-Troncoso et al. (2013)
<i>Porites astreoides</i>	Tropical	NA	NA	NA	NA	27	30	1	1	LPO, CAT	↑ CAT activity, = cellular damage	Ross et al. (2013)
<i>Porites astreoides</i>	Tropical	NA	NA	NA	NA	27.3	30.8	2	2	LPO, CAT, Hsp16, Hsp60	= Hsp expression, ↑ cellular damage, ↑ CAT activity	Olsen et al. (2013)
<i>Porites astreoides</i>	Tropical	~537	~2608	8.1	7.6	28	31	3	3	LPO	↑ cellular damage	Olsen et al. (2015)
<i>Porites astreoides</i>	Tropical	NA	NA	NA	NA	27	30.5	< 1	< 1	SOD, CAT, Lipid Hydroperoxide, PC	↑ SOD and CAT activities, ↑ Lipid hydroperoxide levels, ↑ protein carbonylation content	Ritson-Williams et al. (2016)
<i>Porites cylindrica</i>	Tropical	NA	NA	NA	NA	24-27	32	45	7	Cu/ZnSOD, MnSOD	↑ MnSOD and Cu/ZnSOD activities	Agostini et al. (2016)
<i>Porites spp.</i>	Vent sites	323	803	8.1	7.8	29.5	NA	NA	NA	AOC, PC	= Antioxidant capacity, = Protein carbonylation	Strahl et al. (2015)
<i>Seriatopora hystrix</i>	Tropical	NA	NA	NA	NA	27	34	< 2	< 2	Hsp60	↑ Hsp60 levels in the first 12h, ↓	Seveso et al. (2014)

| Supplemental material

											Hsp60 levels after 12h	
<i>Stylophora pistillata</i>	Tropical	NA	NA	NA	NA	26	33	< 1	12	SOD, CAT	↑ CAT and SOD activities after 6-h exposure to thermal stress	Yakovleva et al. (2004)
<i>Stylophora pistillata</i>	Tropical	NA	NA	NA	NA	28	32	7	7	SOD, CAT	↑ CAT activity	Hawkins et al. (2015)

Abbreviations: C - Control; T - Treatment; ROS - Reactive oxygen species; H₂O₂ - Hydrogen peroxide; Hsp - Heat shock proteins; Ub - Ubiquitin; SOD - Superoxide dismutase; CAT - Catalase; GST - Glutathione S-Transferase; LPO - Lipid peroxidation; PC - protein carbonylation; GPx - Glutathione peroxidase; CA - carbonic anhydrase; DMS - Dimethylsulfide; DMSP - Dimethylsulfoniopropionate; DMSO - Dimethylsulfoxide; AOC - Antioxidant capacity; MnSOD - Manganese superoxide dismutase; CoQ - Host coenzyme Q; PQ - Symbiont plastoquinone; FRAP - Ferric ... ; TAEC - Trolox equivalente antioxidante capacity; DPPH - 2,2-Diphenyl-1-picrylhydrazyl; Cu/ZnSOD - Copper/Zinc superoxide dismutase; GSH - Total glutathione; sHsp - Small heat shock protein; chlpsHsp - Chloroplast small heat shock protein

Table S2 – Seawater physicochemical parameters in all experimental conditions. Temperature, pH and total alkalinity (A_T) were used to calculate carbonate system parameters (pCO_2 - carbon dioxide partial pressure, C_T - total inorganic carbon, and Ω Arg - aragonite saturation state). Values represent mean \pm standard deviation.

	19 °C		26 °C	
	pH 8.0	pH 7.7	pH 8.0	pH 7.7
<i>Measured</i>				
Temperature (°C)	19 \pm 0.5	19 \pm 0.3	25 \pm 0.5	26 \pm 0.3
pH _T (total scale)	8.0 \pm 0.02	7.8 \pm 0.2	8.0 \pm 0.02	7.7 \pm 0.2
Salinity	35 \pm 0.6	35 \pm 0.6	35 \pm 0.6	35 \pm 0.4
A_T (μ mol kg ⁻¹ SW)	2202.4 \pm 14.4	2585.5 \pm 107.0	2435.6 \pm 97.6	2307.6 \pm 141.5
<i>Calculated</i>				
pCO_2 (ppm)	466.5 \pm 19.9	1023.1 \pm 538.3	433.2 \pm 20.1	1063.3 \pm 504.6
C_T (μ mol kg ⁻¹ SW)	2202.4 \pm 14.4	2430.2 \pm 75.9	2119.6 \pm 86.6	2154.5 \pm 217.9
Ω Arg	2.7 \pm 0.1	2.1 \pm 1.1	3.6 \pm 0.3	2.0 \pm 1.0

Table SIII – Generalized Linear Models analyses for each dependent variable (catalase -CAT, glutathione S-transferase - GST, malondialdehyde – MDA, and heat shock protein - HSP), using both temperature and pH as explanatory variables, as well as their interaction. Est – Estimates; Std Error – Standard Error. Bold values indicate $p < 0.05$.

	Est	Std Error	t value	p
CAT				
Intercept	0.120	0.030	3.958	0.001
CO ₂	0.020	0.043	0.457	0.654
Temp	0.001	0.043	0.021	0.984
CO ₂ *Temp	-0.040	0.061	-0.650	0.525
GST				
Intercept	250.430	52.200	4.797	< 0.001
CO ₂	-11.230	73.820	-0.152	0.881
Temp	24.200	73.820	0.328	0.747
CO ₂ *Temp	112.610	104.400	1.079	0.297
MDA				
Intercept	0.157	0.052	3.022	0.008
CO ₂	0.097	0.073	1.325	0.204
Temp	0.065	0.073	0.879	0.392
CO ₂ *Temp	-0.105	0.104	-1.008	0.328
HSP				
Intercept	210.100	89.300	2.353	0.032
CO ₂	-52.100	126.300	-0.413	0.685
Temp	378.400	126.300	2.997	0.009
CO ₂ *Temp	-187.400	178.600	-1.049	0.310

Chapter 5

Table S1 – GLM analysis of survival (%) of *S. canicula* exposed to different combinations of temperature and HgCl₂ contamination for 7 days. Est – Estimates; Std Error – Standard Error. Bold values indicate $p < 0.05$.

	Est	Std Error	t value	<i>p</i>
Model: GLM (Gaussian)				
Response variable: Survival				
Model term(s): Temperature * Contamination				
Intercept	-4.200	1.19E-15	-3.53E+15	< 0.001
Temperature	1.291e-15	1.68E-15	-7.68E-01	0.454
Contamination	1.390e-15	1.68E-15	-8.27E-01	0.421
Temp * Cont	-8.000e-01	2.38E-15	-3.36E+14	< 0.001

Table S2 - GLM analysis of total mercury (HgT) accumulation in *S. canicula* capsule after 7 days exposure. Est – Estimates; Std Error – Standard Error. Bold values indicate $p < 0.05$.

	Est	Std Error	t value	<i>p</i>
Model: GLM (Gamma)				
Response variable: HgT total levels				
Model term(s): Temperature * Contamination				
Intercept	1.852	0.430	4.313	0.001
Temperature	-0.519	0.529	-0.981	0.348
Contamination	-1.825	0.430	-4.248	0.001
Temp * Cont	0.538	0.529	1.016	0.332

Supplemental material |

Table S3 - GLM analysis of total mercury (HgT) accumulation in *S. canicula* tissues, and within each sampled tissue regarding different contamination and temperature conditions, after 7 days exposure. Est – Estimates; Std Error – Standard Error. Bold values indicate $p < 0.05$.

	Est	Std Error	t value	p
Model: GLM (Gaussian)				
Response variable: HgT total levels				
Model term(s): Tissue				
Brain – Gills	-3.207	1.195	-2.684	0.010
Brain – Liver	-1.992	1.300	-1.533	0.131
Brain – Muscle	-1.274	1.413	-0.901	0.371
Brain – Stomach	4.384	2.904	1.510	0.137
Gills – Liver	1.215	0.539	2.254	0.028
Gills – Muscle	1.933	0.774	2.497	0.016
Gills – Stomach	7.591	2.652	2.862	0.006
Liver – Muscle	0.718	0.928	0.774	0.442
Liver – Stomach	6.376	2.701	2.361	0.022
Muscle – Stomach	5.658	2.758	2.052	0.045
Model: GLM (Gaussian)				
Response variable: HgT total levels				
Model term(s): Contamination				
Brain	0.513	0.123	4.185	0.006
Gills	8.006	0.874	9.164	< 0.001
Liver	1.477	0.271	5.453	0.002
Muscle	0.950	0.077	12.267	< 0.001
Stomach	0.160	0.061	2.623	0.039
Model: GLM (Gaussian)				
Response variable: HgT total levels				
Model term(s): Temperature				
Brain	-0.316	0.163	-1.938	0.081
Gills	-4.022	2.270	-1.772	0.107
Liver	-0.691	0.444	-1.556	0.151
Muscle	-0.482	0.266	-1.813	0.100
Stomach	-0.098	0.060	-1.630	0.134

| Supplemental material

Table S4 - GLM analysis of heat shock protein (HSP) levels in *S. canicula* tissues, and within each sampled tissue regarding different contamination and temperature conditions, after 7 days exposure. Est – Estimates; Std Error – Standard Error. Bold values indicate $p < 0.05$.

	Est	Std Error	t value	p
Model: GLM (Gaussian)				
Response variable: HSP levels				
Model term(s): Tissue				
Brain – Gills	-2.608	0.791	-3.298	0.002
Brain – Liver	0.654	0.791	0.827	0.412
Brain – Muscle	-2.248	0.791	-2.842	0.006
Brain – Stomach	4.889	0.791	6.182	< 0.001
Gills – Liver	3.262	0.791	4.125	< 0.001
Gills – Muscle	0.361	0.791	0.456	0.650
Gills – Stomach	7.497	0.791	9.480	< 0.001
Liver – Muscle	-2.902	0.791	-3.669	0.001
Liver – Stomach	4.235	0.791	5.355	< 0.001
Muscle – Stomach	7.137	0.791	9.024	< 0.001
Model: GLM (Gaussian)				
Response variable: HSP levels				
Model term(s): Contamination				
Brain	0.852	0.638	1.336	0.230
Gills	0.542	0.648	0.836	0.435
Liver	0.262	0.778	0.336	0.748
Muscle	3.049	1.490	2.046	0.087
Stomach	2.471	2.015	1.226	0.266
Model: GLM (Gaussian)				
Response variable: HSP levels				
Model term(s): Temperature				
Brain	3.205	0.558	5.739	0.001
Gills	2.592	1.045	2.481	0.048
Liver	2.107	1.118	1.885	0.108
Muscle	1.869	1.074	1.740	0.133
Stomach	-0.072	2.070	-0.035	0.973

Table S5 - GLM analysis of ubiquitin (Ub) levels in *S. canicula* tissues, and within each sampled tissue regarding different contamination and temperature conditions, after 7 days exposure. Est – Estimates; Std Error – Standard Error. Bold values indicate $p < 0.05$.

	Est	Std Error	t value	p
Model: GLM (Gaussian)				
Response variable: Ub levels				
Model term(s): Tissue				
Brain – Gills	0.006	0.002	3.622	0.001
Brain – Liver	0.003	0.002	1.761	0.084
Brain – Muscle	0.004	0.002	2.163	0.035
Brain – Stomach	0.008	0.002	5.031	< 0.001
Gills – Liver	-0.003	0.002	-1.861	0.068
Gills – Muscle	-0.002	0.002	-1.459	0.150
Gills – Stomach	0.002	0.002	1.409	0.165
Liver – Muscle	0.001	0.002	0.402	0.689
Liver – Stomach	0.005	0.002	3.270	0.002
Muscle – Stomach	0.005	0.002	2.868	0.006
Model: GLM (Gaussian)				
Response variable: Ub levels				
Model term(s): Contamination				
Brain	0.003	0.001	4.371	0.005
Gills	-0.002	0.001	-1.244	0.260
Liver	0.002	0.000	4.583	0.004
Muscle	0.003	0.001	2.144	0.076
Stomach	-0.005	0.001	-3.584	0.012
Model: GLM (Gaussian)				
Response variable: Ub levels				
Model term(s): Temperature				
Brain	0.005	0.001	4.629	0.004
Gills	0.009	0.002	4.869	0.003
Liver	0.010	0.002	4.990	0.002
Muscle	0.006	0.002	3.592	0.012
Stomach	0.003	0.001	2.043	0.087

| Supplemental material

Table S6 - GLM analysis of lipid peroxidation levels in *S. canicula* tissues, and within each sampled tissue regarding different contamination and temperature conditions, after 7 days exposure. Est – Estimates; Std Error – Standard Error. Bold values indicate $p < 0.05$.

	Est	Std Error	t value	p
Model: GLM (Gaussian)				
Response variable: Lipid peroxidation levels				
Model term(s): Tissue				
Brain – Gills	0.005	0.004	1.135	0.261
Brain – Liver	0.004	0.004	0.870	0.388
Brain – Muscle	0.014	0.004	3.140	0.003
Brain – Stomach	-0.001	0.004	-0.246	0.807
Gills – Liver	-0.001	0.004	-0.265	0.792
Gills – Muscle	0.009	0.004	2.005	0.050
Gills – Stomach	-0.006	0.004	-1.381	0.173
Liver – Muscle	0.010	0.004	2.270	0.027
Liver – Stomach	-0.005	0.004	-1.116	0.269
Muscle – Stomach	-0.015	0.004	-3.385	0.001
Model: GLM (Gaussian)				
Response variable: Lipid peroxidation levels				
Model term(s): Contamination				
Brain	-0.001	0.004	-0.342	0.744
Gills	-0.001	0.003	-0.187	0.858
Liver	-0.003	0.011	-0.232	0.824
Muscle	0.014	0.007	2.002	0.092
Stomach	0.008	0.008	0.975	0.367
Model: GLM (Gaussian)				
Response variable: Lipid peroxidation levels				
Model term(s): Temperature				
Brain	0.003	0.004	0.822	0.443
Gills	0.009	0.003	2.979	0.025
Liver	0.016	0.009	1.777	0.126
Muscle	0.019	0.005	3.634	0.011
Stomach	0.011	0.010	1.126	0.303

Table S7 - GLM analysis of DNA damage levels in *S. canicula* tissues, and within each sampled tissue regarding different contamination and temperature conditions, after 7 days exposure. Est – Estimates; Std Error – Standard Error. Bold values indicate $p < 0.05$.

	Est	Std Error	t value	p
Model: GLM (Gaussian)				
Response variable: DNA damage levels				
Model term(s): Tissue				
Gills – Liver	-0.168	0.082	-2.053	0.046
Gills – Muscle	0.106	0.082	1.294	0.202
Gills – Stomach	0.495	0.082	6.057	< 0.001
Liver – Muscle	0.274	0.082	3.347	0.002
Liver – Stomach	0.663	0.082	8.111	< 0.001
Muscle – Stomach	0.389	0.082	4.763	< 0.001
Model: GLM (Gaussian)				
Response variable: DNA damage levels				
Model term(s): Contamination				
Gills	-0.027	0.050	-0.532	0.614
Liver	-0.003	0.011	-0.232	0.824
Muscle	0.113	0.062	1.820	0.119
Stomach	0.423	0.318	1.331	0.232
Model: GLM (Gaussian)				
Response variable: DNA damage levels				
Model term(s): Temperature				
Gills	0.089	0.071	1.256	0.256
Liver	0.052	0.051	1.023	0.346
Muscle	0.107	0.064	1.675	0.145
Stomach	0.016	0.140	0.112	0.914

| Supplemental material

Table S8 - GLM analysis of superoxide dismutase (SOD) activity in *S. canicula* tissues, and within each sampled tissue regarding different contamination and temperature conditions, after 7 days exposure. Est – Estimates; Std Error – Standard Error. Bold values indicate $p < 0.05$.

	Est	Std Error	t value	<i>p</i>
Model: GLM (Gaussian)				
Response variable: SOD activity				
Model term(s): Tissue				
Gills – Liver	-8.111	10.298	-0.788	0.435
Gills – Muscle	-2.701	10.298	-0.262	0.794
Gills – Stomach	45.159	10.298	4.385	< 0.001
Liver – Muscle	5.410	10.298	0.525	0.602
Liver – Stomach	53.270	10.298	5.173	< 0.001
Muscle – Stomach	47.860	10.298	4.648	< 0.001
Model: GLM (Gaussian)				
Response variable: SOD activity				
Model term(s): Contamination				
Gills	-6.473	4.923	-1.315	0.237
Liver	25.301	2.071	12.220	< 0.001
Muscle	50.168	5.261	9.537	< 0.001
Stomach	31.240	16.010	1.951	0.099
Model: GLM (Gaussian)				
Response variable: SOD activity				
Model term(s): Temperature				
Gills	27.732	6.038	4.593	0.004
Liver	32.377	2.378	13.620	< 0.001
Muscle	76.917	7.935	9.693	< 0.001
Stomach	48.710	11.594	4.201	0.006

Table S9 - GLM analysis of catalase (CAT) activity in *S. canicula* tissues, and within each sampled tissue regarding different contamination and temperature conditions, after 7 days exposure. Est – Estimates; Std Error – Standard Error. Bold values indicate $p < 0.05$.

	Est	Std Error	t value	p
Model: GLM (Gaussian)				
Response variable: CAT activity				
Model term(s): Tissue				
Gills – Liver	23.980	3.069	7.813	< 0.001
Gills – Muscle	-14.013	3.069	-4.565	< 0.001
Gills – Stomach	-12.587	3.069	-4.101	< 0.001
Liver – Muscle	-37.993	3.069	-12.378	< 0.001
Liver – Stomach	-36.566	3.069	-11.913	< 0.001
Muscle – Stomach	1.426	3.069	0.465	0.644
Model: GLM (Gaussian)				
Response variable: CAT activity				
Model term(s): Contamination				
Gills	-22.119	1.438	-15.380	< 0.001
Liver	16.975	4.194	4.047	0.007
Muscle	-4.589	0.594	-7.727	< 0.001
Stomach	2.296	3.239	0.709	0.505
Model: GLM (Gaussian)				
Response variable: CAT activity				
Model term(s): Temperature				
Gills	-9.757	2.285	-4.270	0.005
Liver	-2.235	4.138	-0.540	0.608
Muscle	0.987	1.021	0.966	0.371
Stomach	2.779	3.028	0.918	0.394

| Supplemental material

Table S10 - GLM analysis of glutathione peroxidase (GPx) activity in *S. canicula* tissues, and within each sampled tissue regarding different contamination and temperature conditions, after 7 days exposure. Est – Estimates; Std Error – Standard Error. Bold values indicate $p < 0.05$.

	Est	Std Error	t value	p
Model: GLM (Gaussian)				
Response variable: GPx activity				
Model term(s): Tissue				
Gills – Liver	-0.478	1.266	-0.378	0.707
Gills – Muscle	0.397	1.266	0.314	0.755
Gills – Stomach	1.804	1.266	1.424	0.161
Liver – Muscle	0.875	1.266	0.691	0.493
Liver – Stomach	2.282	1.266	1.802	0.078
Muscle – Stomach	1.406	1.266	1.111	0.273
Model: GLM (Gaussian)				
Response variable: GPx activity				
Model term(s): Contamination				
Gills	-0.228	1.315	-0.173	0.868
Liver	-3.252	0.986	-3.297	0.017
Muscle	1.867	1.544	1.209	0.272
Stomach	0.215	0.919	0.234	0.823
Model: GLM (Gaussian)				
Response variable: GPx activity				
Model term(s): Temperature				
Gills	4.431	2.011	2.203	0.070
Liver	0.285	0.942	0.302	0.773
Muscle	8.728	0.905	9.645	< 0.001
Stomach	2.590	1.471	1.760	0.129

Table S11 - GLM analysis of glutathione s-transferase (GST) activity in *S. canicula* tissues, and within each sampled tissue regarding different contamination and temperature conditions, after 7 days exposure. Est – Estimates; Std Error – Standard Error. Bold values indicate $p < 0.05$.

	Est	Std Error	t value	<i>p</i>
Model: GLM (Gaussian)				
Response variable: GST activity				
Model term(s): Tissue				
Gills – Liver	99.840	13.813	7.228	< 0.001
Gills – Muscle	-13.882	13.813	-1.005	0.320
Gills – Stomach	62.123	13.813	4.497	< 0.001
Liver – Muscle	-113.721	13.813	-8.233	< 0.001
Liver – Stomach	-37.717	13.813	-2.731	0.009
Muscle – Stomach	-37.717	13.813	-2.731	0.009
Model: GLM (Gaussian)				
Response variable: GST activity				
Model term(s): Contamination				
Gills	-9.415	33.306	-0.283	0.787
Liver	1.985	4.245	0.468	0.657
Muscle	-0.387	3.646	-0.106	0.919
Stomach	-9.415	33.306	-0.283	0.787
Model: GLM (Gaussian)				
Response variable: GST activity				
Model term(s): Temperature				
Gills	18.381	5.594	3.286	0.017
Liver	88.493	5.762	15.360	< 0.001
Muscle	1.278	6.595	0.194	0.853
Stomach	63.820	25.920	2.462	0.049

| Supplemental material

Table S12 - GLM analysis of acetylcholinesterase (AChE) activity in *S. canicula* tissues, and within each sampled tissue regarding different contamination and temperature conditions, after 7 days exposure. Est – Estimates; Std Error – Standard Error. Bold values indicate $p < 0.05$.

	Est	Std Error	t value	<i>p</i>
Model: GLM (Gaussian)				
Response variable: AChE activity				
Model term(s): Tissue				
Brain – Muscle	0.178	0.859	0.207	0.838
Model: GLM (Gaussian)				
Response variable: AChE activity				
Model term(s): Contamination				
Brain	-1.253	0.822	-1.524	0.178
Muscle	2.220	0.810	2.740	0.034
Model: GLM (Gaussian)				
Response variable: AChE activity				
Model term(s): Temperature				
Brain	1.461	0.858	1.703	0.139
Muscle	5.149	0.852	6.045	0.001

Table S13 - GLM analysis of total antioxidant capacity (TAC) in *S. canicula* tissues, and within each sampled tissue regarding different contamination and temperature conditions, after 7 days exposure. Est – Estimates; Std Error – Standard Error. Bold values indicate $p < 0.05$.

	Est	Std Error	t value	p
Model: GLM (Gaussian)				
Response variable: TAC activity				
Model term(s): Tissue				
Gills – Liver	-4.053	1.656	-2.448	0.018
Gills – Muscle	0.456	1.656	0.276	0.784
Gills – Stomach	6.549	1.656	3.956	< 0.001
Liver – Muscle	4.509	1.655	2.724	0.009
Liver – Stomach	10.603	1.655	6.404	< 0.001
Muscle – Stomach	6.093	1.656	3.681	0.001
Model: GLM (Gaussian)				
Response variable: TAC activity				
Model term(s): Contamination				
Gills	-4.398	2.360	-1.863	0.112
Liver	-1.829	1.852	-0.988	0.361
Muscle	-2.134	3.252	-0.656	0.536
Stomach	-2.463	2.648	-0.930	0.388
Model: GLM (Gaussian)				
Response variable: TAC activity				
Model term(s): Temperature				
Gills	-2.605	3.008	-0.866	0.420
Liver	-4.129	1.636	-2.523	0.045
Muscle	-0.124	2.852	-0.043	0.967
Stomach	-1.759	3.468	-0.507	0.630